Unsupervised Monitoring of Machining Processes

by Thomas E. McLeay

A thesis submitted in partial fulfilment of the requirements
for the degree of Doctor of Philosophy

Advanced Manufacturing Research Centre with Boeing

The University of Sheffield

December 2016

Acknowledgements

I would like to thank my supervisor, Professor Sam Turner, for his continued guidance and support over the course of this research. I would also like to extend my thanks you to Professor Keith Worden for his support in allowing me to adopt and understand new areas of machine learning.

I would like to thank those at the AMRC that have supported this work, including the technicians and engineers that have helped make the experimental work a success.

Finally, I'd like to thank Emma for her continued support and patience outside of working hours.

Abstract

Machining processes, such as milling, drilling, turning and grinding, concern the removal of material from a workpiece using a cutting tool. These processes are sensitive to parameters such as cutting tool properties, workpiece materials, coolant application, machine selection, fixturing and cutting parameters. The focus of the work in this thesis is to devise a method to monitor the changing conditions of a machining process over time in order to detect faulty machining conditions and diagnose fault types and causes. A key aim of this thesis is to develop a monitoring regime that has minimal cost of implementation and upkeep in a production environment, therefore an unsupervised monitoring system which applies non-intrusive sensing hardware is proposed.

I EXECUTIVE SUMMARY

This thesis presents a method for machining process monitoring that uses a novel approach for feature selection and fault detection using unsupervised learning. A number of results have been published by the author that includes conference papers, journal papers and a patent (see section II Author Publications). These publications are also referenced in the following summary.

The first chapter introduces the motivation, hypothesis and objectives of the study. A literature review follows in Chapter 2, covering a wide range of published literature including sensing, signal processing and system architectures and algorithms.

Chapter 3 reflects on previous research and presents results of investigations into the monitoring system design requirements. A clear understanding of machining process faults and their interactions is gained by applying process failure mode and effect analysis (PFMEA) to a milling process. Interaction with industry experts and machine operators was required to obtain this understanding and to ensure the research followed a pathway to industrial exploitation. Previous literature has not applied PFMEA to machining monitoring system design problems, therefore these results have been published by the author in the journal paper; “Failure Mode Analysis to Define Process Monitoring Systems” [i].

With the PFMEA providing a clear understanding of the industry problem, an experimental method is proposed in Chapter 4. Two 3-axis profile milling experiments are conducted on a titanium workpiece; the first conducting a tool wear trial and the second introducing variable radial depths of cut to represent faulty operating conditions. A new sensing platform for monitoring milling operations was designed and built, ensuring that the proposed solution was quick to load to a machine and not intrusive to a production setting. The platform was presented at the Factory 2050 Conference held at the Advanced Manufacturing Research Centre in March 2015 [vii].

The first of two analysis sections are presented in Chapter 5, where several methods for sensor signal feature selection and assessment are investigated. Many of the techniques used are established in other subject areas such as structural health monitoring, however, a number of them have not been applied to machining applications. Polynomial model fitting

is used to obtain sensor signal features with high information content, and Gram-Schmidt orthogonalisation is applied to reduce redundancy in feature subsets. Several other feature selection methods are also compared.

Chapter 6 develops a novelty detection system to determine when a fault has occurred using the feature subsets selected in Chapter 5. A principled novelty threshold is applied using the Mahalanobis distance as a measure of discordancy. This approach is entirely new to machining applications given the emphasis on supervised learning in previous research. Aspects of the techniques used are established in the field of structural health monitoring and are successfully adapted and applied to the machining problem presented. Data clustering methods are also applied for fault diagnosis, including Gaussian mixture modelling and the nearest neighbour algorithm. Several methods are validated on a second data set for a ball nose milling operation on stainless steel. Some of the results from this chapter have been published in the Quality and Reliability Engineering International Journal [iv] and a further journal paper is currently being compiled.

The thesis concludes with a discussion of the results and future work in Chapter 7.

The area of fault prognosis has also been explored during this study and is detailed further in Appendix C. Two publications are of note; “Tool wear monitoring using Naïve Bayes classifiers” published in the International Journal for Advanced Manufacturing Technology entitled [ii] and a reviewed conference paper entitled “Remaining useful tool life predictions using Bayesian inference” [v].

II AUTHOR PUBLICATIONS

Journal Papers

[i] McLeay, T., and Turner, M.S., "Failure Mode Analysis to Define Process Monitoring Systems", Journal of Machine Engineering, 11.4, 2011.

[ii] Karandikar, J., McLeay T., Turner, S., and Schmitz, T., "Tool wear monitoring using Naïve Bayes classifiers", International Journal of Advanced Manufacturing Technology, 1-14, 2014.

[iii] Seemuang, N., McLeay, T., Slatter, T., "Using Spindle Noise to Monitor Tool Wear in a Turning Process", International Journal of Advanced Manufacturing Technology, 2016.

[iv] Harris, K., Triantafyllopoulos, K., Stillman, E., McLeay, T., "A Multivariate Control Chart for Autocorrelated Tool Wear Processes", Quality and Reliability Engineering International, 2016.

Reviewed Conference Papers

[v] Karandikar, J., McLeay T., Turner, S., and Schmitz, T., "Remaining useful tool life predictions using Bayesian inference", Manufacturing Science and Engineering Conference, Paper No. MSEC2013-1152, Madison, WI, June 10-14, 2013.

[vi] Ray, N., Cross, E.J., Worden, K., McLeay, T., Turner, M.S, Villain-Chastre, J-P., "Relationships between 3D tool geometry, in-process acoustic emissions and workpiece surface integrity in finish end milling", International Conference on Condition Monitoring and Machinery Failure Prevention, 2015.

Conference Presentations

[vii] McLeay, T. "In-Process Data for Part and Machine Verification", Factory 2050 Conference, March 2015.

Patents

[viii] McLeay, T., "Machining Control Methods and System", Application No 1519759.3, November 2015.

III TABLE OF CONTENTS

IV LIST OF FIGURES

V LIST OF TABLES

VI NOMENCLATURE

AE – Acoustic Emission (specifically in the ultrasonic range)
Ae – Radial Depth of Cut
AI – Artificial Intelligence
Ap – Axial Depth of Cut
CDF – Cumulative Distribution Function
CM – Condition Monitoring
DAG – Directed Acyclic Graph
FD – Frequency Domain
FFT – Fast Fourier Transform
FPM – Feed Per Minute
FPT – Feed Per Tooth
GMM – Gaussian Mixture Model
GP – Gaussian Process
HVM – High Value Manufacturing
IDSS – Intelligent Decision Support Systems
JDL – Joint Directors of Laboratories
ML – Machine Learning
PCA – Principle Component Analysis
PDF – Probability Density Function
PFMEA - Process Failure Mode and Effect Analysis
PM – Process Monitoring
RMS – Root Mean Square
RPM – Rotations Per Minute
RPN – Risk Priority Number
RUL – Remaining Useful Life
SHM – Structural Health Monitoring
SVM – Support Vector Machine
TCM – Tool Condition Monitoring
TD – Time Domain
TPF – Tooth Passing Frequency
Vc – Surface Speed

1 INTRODUCTION

In recent years, there has been a drive towards automated manufacturing processes that give a reduction in human intervention, machining times, re-work and scrap in order to stay competitive. In the high value manufacturing (HVM) sector, complex part geometries must be formed, work piece materials are expensive and difficult to machine, machine tools and cutting tools are costly and skilled manual intervention is required to control processes.

Kappmeyer [1] discussed the challenges faced in the manufacture of critical gas turbine components for aerospace and explains that the integration of multiple technologies, including process monitoring, process modelling and multi-functional machine tools play an important part in achieving automated processes. Though the investment in new technologies has brought step changes to process performance, the ability to fully automate and failure proof these complex machining operations has not been achieved.

A manufacturing engineer's role is to apply their experience and the equipment they have available to deliver cost effective and robust manufacturing processes. Key process variables can be difficult and expensive to tightly control, such as tolerances on the work piece stock geometry, variation in bulk material properties or inconsistent cutting tool integrity and life. Uncertainty in such variables leads to conservative manufacturing processes being delivered, with reliance on skilled operators and large amounts of manual intervention. Productivity is then reduced and human errors can lead to scrap and re-work.

Typically, manual intervention is required for one of two reasons. (i) The process itself has been designed in such a way that intervention is mandatory and follows a schedule. This may be due to the tooling, fixturing or machines used or it may be a result of the method of manufacture initially chosen. (ii) Input variables change over time and the process requires adjustments to be made in response to the input variation, without which the process would not maintain the required product quality.

Without the appropriate skill level and timeliness of these interventions, processes can result in failure. A number of solutions are available to the industry to avoid, detect or reduce the impact of some failure modes, such as:

- Monitoring systems to stop the machine if measured sensor signals move out of defined limits [2]-[8]
- On-machine measurement systems to determine geometric conformance of the work piece [9], [10].
- Adaptive tool offset and tool path control systems using metrology data, [11], [12]
- Control systems to adjust cutting parameters according to machine spindle load, [13] or from measured vibration frequencies [14].

Many failure modes are still observed in industry even with the use of these systems. Full automation and 'lights-out' machining is rarely achieved in aerospace manufacturing companies, and scrap and re-work costs remain to be a major issue. There is therefore a need for more robust, intelligent systems that can monitor a machining process, maintain it within defined limits, and if necessary, stop the process when the probable outcome is non-conforming products.

1.1 Motivation

Published research in the area of machining process monitoring is extensive, particularly for tool condition monitoring (TCM) and fault detection systems; however, the HVM industry has adopted few monitoring and control systems to replace manual, skill-based tasks in their machining processes. This thesis aims to address key challenges faced when extending this academic research to industrial exploitation.

Published material that describes commercial and academic monitoring systems will be reviewed to understand the capability and functionality of systems to date. In light of this knowledge, this study will go onto determine a monitoring system design; the selection of sensors, signal processing steps and computational techniques for fault detection and diagnosis.

The design and build of a system which can monitor and control machining processes will be a key part of this study, ensuring that both software and hardware used does not interfere with production tasks. This system will be applied to a milling process for hard-to-machine metallic components – an application in the aerospace sector that has relatively high scrap and non-conformance costs.

Another key enabler for the industry to adopt this technology is to allow monitoring tasks to succeed unsupervised with minimal resource efforts to install and maintain both software and hardware aspects of the systems. Practical considerations of the monitoring system developed in this research are therefore that; (i) sensing and data acquisition hardware is robust and minimally intrusive in the production environment, and (ii) monitoring software performs unsupervised with minimal resource to configure, train or maintain it.

1.2 Hypothesis

An unsupervised process monitoring system can be developed to deliver improved process robustness and reduced down time in machining processes.

The impact of machining process faults being left undetected may include costly damage to the work piece, tooling or machine. Increasing the level of skilled manning of the process is an expensive solution. Costs are also incurred when training supervised monitoring systems. An unsupervised process monitoring system for monitoring a machining process is therefore proposed.

1.3 Aims and Objectives

The main aim of this research is to design and demonstrate a method for monitoring machining processes that can reliably detect and diagnose faulty operating conditions. Delivering this aim should therefore eliminate the cautionary manual interventions often seen in production today. Furthermore, this aim should reduce the time taken to diagnose the cause of a fault, reduce the time taken to correct a process following a fault, and finally reduce equipment down time by minimising the frequency and severity of faults.

There are several objectives that work towards this overall aim, as follows:

1. The first objective is to identify the suitable sensor signal features available for describing the condition of the machining process.

2. The second objective is to incorporate a fault detection method into the proposed monitoring system. This requires a means for the system to identify fault conditions from sensor data, without the need for training data.

3. The third objective is to extend this calculation so that fault diagnosis is possible. With minimal training, the system should be able to distinguish between more than one fault type.

4. The fourth objective is for the system to be designed in a way that it does not obstruct the production environment, thus being a practical solution for industrial exploitation. There will be two elements to this; commercially available sensors will be used so the research will not develop new sensors; the system should not require a machine tool to be taken offline for training of the monitoring system software.

1.4 Brief Outline of the Thesis

The first chapter introduces the motivation, hypothesis and objectives of the study. A literature review follows in Chapter 2, covering a wide range of published literature including sensing, signal processing and system architectures and algorithms.

Chapter 3 reflects on previous research and presents results of investigations into the monitoring system design requirements. A clear understanding of machining process faults and their interactions is gained by applying process failure mode and effect analysis (PFMEA) to a milling process.

With the PFMEA providing a clear understanding of the industry problem, an experimental method is proposed in Chapter 4. Two 3-axis profile milling experiments are conducted on a titanium workpiece; the first conducting a tool wear trial and the second introducing variable radial depths of cut to represent faulty operating conditions. A new sensing platform for monitoring milling operations was designed and built.

The first of two analysis sections are presented in Chapter 5, where several methods for sensor signal feature selection and assessment are investigated. Polynomial model fitting is used to obtain sensor signal features with high information content, and Gram-Schmidt orthogonalisation is applied to reduce redundancy in feature subsets. Several other feature selection methods are also compared.

Chapter 6 develops a novelty detection system to determine when a fault has occurred using the feature subsets selected in Chapter 5. A principled novelty threshold is applied using the Mahalanobis distance as a measure of discordancy. Data clustering methods are also applied for fault diagnosis, including Gaussian mixture modelling and the nearest neighbour algorithm. Several methods are validated on a second data set for a ball nose milling operation on stainless steel.

The thesis concludes with a discussion of the results and future work in Chapter 7.

2 LITERATURE REVIEW

This chapter provides a brief history in process monitoring research and highlights the relevance of the subject today. The author summarises the components of a monitoring system in section 2.1.1, before addressing each technology in detail. The range of sensors applied are discussed in section 2.2. Techniques for signal processing, feature extraction and feature selection are covered in section 2.3. Fault detection, diagnosis and prognosis are then discussed in section 2.4.

2.1 A Brief History of Manufacturing Process Monitoring

The ability to collect measured data from equipment and processes has been explored for several decades. Weck *et al.* [15] presented a 'concept of integrated data processing in computer controlled manufacturing systems' in 1980; a method to achieve flexible and automated manufacturing processes is presented and was demonstrated for an aerospace machining application at the University of Aachen. A data-driven system was developed that managed new part orders, automated the transport and storage of components such as pallets, and provided information on the system state. The challenges faced were primarily relating to data distribution and management, real time operating systems and interfacing machines and computers. Due to the revolution in computing technology, these capabilities are now commonly available in machine tools and computers, along with standard communication protocols for ease of programming.

Goldsby *et al.* [16] registered a United States Patent in 1977 for condition monitoring of remotely located machines, such as coin operated vending machines. Switches to convert operating conditions to binary signals are used to transfer data to memory. Such data included clock pulses, load signals from drives and machine address codes. The data is transmitted over telephone line to a control unit. Flags are raised when machine data differs from that previously obtained for that machine, allowing the control unit to present condition monitoring data to a user for a number of machines. The user can then make a decision whether to take further action. Although the technique presented is relatively simple when compared to the monitoring literature today, the comparison of data against

that obtained previously is a common condition monitoring approach in industry applications. Limitations do exist; training data is assumed to be correct, the definition of a significant change is experiential, and the cause of the change in data is not discernible, potentially leaving the user with further analysis to identify a corrective action.

Scott *et al.* [17] presented a paper on 'condition monitoring of gas turbines' in 1978. Oil samples were taken at regular intervals for ferrograph analysis. Two measurements were taken from the samples; area coverage of small particles and area coverage of large particles. Three wear sensitive features, in the form of heuristic linear equations, were derived from this data; total wear, severity of wear and severity of wear index. The features were found to correlate with flying hours for the turbines, therefore the method was proposed as a useful tool for machinery condition monitoring. The paper captures three key steps in condition monitoring from data - measurement, feature extraction and correlation. The measurement and feature extraction is achieved from a physical understanding of the process. The correlation is simplistic, and although the evidence suggests the measurements are useful, the robustness and risk of employing the technique is not examined.

Clearly, the subject of intelligent monitoring systems is broad, but in all fields, systems have moved on dramatically since the examples above. Developments in civil, automotive, aerospace, maintenance and medical applications have transformed the capability of automatic monitoring and control systems. In the manufacturing sector, exploitation is seen in higher volume processes such as automotive, though high value processes are yet to adopt much of the technology. Broadly speaking, this can be attributed to the process complexity, lower part numbers, and higher component costs. Limited statistical data is available to ensure process robustness and process owners are risk averse, given their responsibility to deliver complex, high cost, safety critical components.

A database of the tool condition monitoring literature was published by Teti [18] in 1995 with over 500 references. Extensive research in the area continued for another 15 years and a keynote paper by the same author was published in 2010 [19] that discussed developments in the use of acoustic emission sensing, advanced signal processing, and detection of other response parameters such as surface finish, chip conditions, machine tool state and chatter avoidance. The vast quantity of cited publications in these two reviews alone shows the sustained interest and importance of this research area to the manufacturing sector,

however, it raises questions over the impact and direction of the completed research to date given the limited exploitation seen in industry and the continuation of the same objectives in UK and European research strategy today. Leem and Dorfeld [20] explain that the lack of industrial uptake of these technologies is partly due to the absence of a well-accepted reliable methodology and the ignorance of practical issues in implementation.

The EPSRC *Manufacturing the Future* strategy [21] includes Manufacturing Informatics as a key priority. Aspects of artificial intelligence, control engineering, statistics and probability, sensors and instrumentations fall within this research area, all of which are essential in the development of monitoring and control systems.

The German government established a vision known as *Industry 4.0* [22], a strategy which is built around availability of data and 'the Internet of Things'. The "development of intelligent monitoring and autonomous decision-making processes" is central to the strategy.

Higher Technology Readiness Level (TRL) funding for process monitoring remains a focus from European and UK funding councils. The Technology Strategy Board's (TSB) high value manufacturing strategy includes themes for 'intelligent systems and embedded electronics' and 'flexible and adaptive manufacture'. Process monitoring tools have relevance in many of the challenging areas described in the strategy [23], [24].

The European *Horizon 2020* funding call also cites process monitoring as a key theme, highlighting several areas; "Methods for integrative control and robust optimization of discrete and continuous processes supporting engineers in their aim of detecting, measuring and monitoring the variables, events and situations which affect the performance, energy-use and reliability of manufacturing systems", "Fast and accurate process monitoring systems allowing feedback control of (laser) process parameters in highly dynamic manufacturing processes. Actions should cover, in particular, the development of in-line process monitoring sensors, measurement and non-destructive testing tools including the related high speed data processing and reduction" [25].

The UK government office for science issued the project report *Foresight (2013), The Future of Manufacturing: A new era of opportunity and challenge for the UK* [26]. This also emphasises the importance of these systems stating that "condition monitoring where machines are able to self-diagnose and predict faults before failure" is key. It highlights the

importance of sensors and data networks and that “manufacturers must develop their ability to transform this explosion of data into useful knowledge and value”.

The *UK High Value Manufacturing Future Landscape* report includes themes on ‘intelligent systems and embedded electronics’, ‘plug and play manufacturing’ and ‘flexible and adaptive manufacturing’. These themes all include the requirement to sense, capture and analyse multiple forms of data.

2.1.1 Monitoring System Components

Intelligent process monitoring systems for machining have a focus on several fields of study. The review paper by Teti *et al.* [19] breaks the discussion into sections on sensors, signal processing, application area and decision making. The paper published by Bryne *et al.* [27] followed the same order of discussion, whereas Rehorn *et al.* [28] arrange the discussion of tool condition monitoring systems by each type of cutting process – turning, face milling, drilling and end milling.

According to the review paper by Liang *et al.* [29], the application of machining process monitoring systems has been reported for several recurring application areas; (i) tool condition/wear/breakage, (ii) surface roughness, (iii) workpiece geometry or depth of cut, (iv) workpiece hardness or machinability and (v) surface integrity. The authors also list a number of published measurement signals; acoustic emission (AE), power, torque, force, temperature, vision, vibration, displacement/direct gauges, audio signals and even materials micro-magnetic properties.

The overwhelming majority of publications present methods to identify tool wear state at any given instant in a machining process. Others aim to determine properties of the machined surface such as roughness [30] and surface anomalies [31]. A well-established community of researchers have developed chatter avoidance monitoring systems [32] that are now available for production use [14], though research continues to develop solutions such as active damping [33] and parallel machining [34]. Other publications have investigated opportunities to use monitoring systems for chip management [35], machine condition [36] and coolant performance [37]. These different monitoring scopes and systems are rarely

combined into a single system, with the majority of the papers reviewed in this thesis focusing on a single one of these variables.

Teti *et al.* [19], describe a process monitoring system that consists of five important factors:

1. Process variables
2. Sensorial perception
3. Data processing and feature extraction
4. Cognitive decision making
5. Action

A similar view is shared by other review papers. For example, Abellan-Nebot *et al.* [38] depict a system similar to the flow chart shown in Figure 2-1.

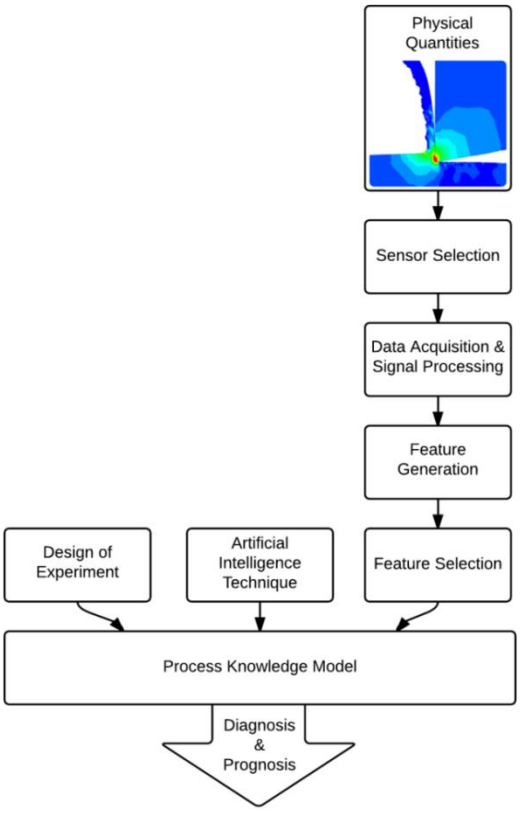

Figure 2-1: Important factors in a process monitoring system [38]

Structural Health Monitoring (SHM) research has covered the use of sensors for detecting damage and classification of damaged structures extensively. Figure 2-2 depicts the data fusion approach to SHM presented by Worden and Manson [39].

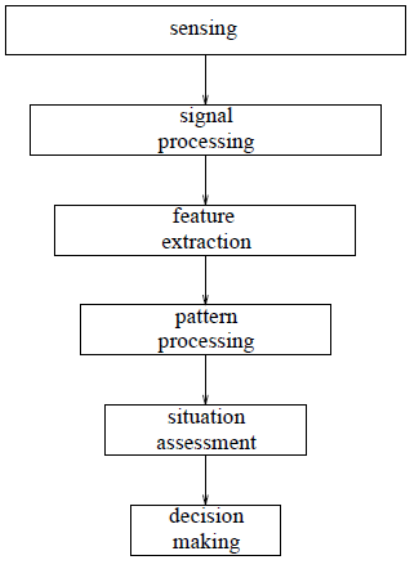

Figure 2-2: Waterfall model for SHM [39]

The field of Machine Learning (ML) covers many computational techniques that allow one to build systems that can learn from data.

The following three sections will discuss sensing, signal processing and decision making aspects of monitoring systems.

2.2 Sensing

A range of sensors are available which convert different physical quantities to electrical signals. In order to highlight the quantity of data available, an ambitious range of sensors was described for a machining scenario in 1995 [27], as depicted in Figure 2-3. The large quantity of measurement data available from such a sensor array requires the application of comprehensive and computationally intensive data acquisition, signal processing and data fusion. Clearly, there is a substantial amount of indirect data available in these applications. However, in applying these technologies one must consider complexity, cost, computation requirements and the value of the data. If a production application is proposed, practical limitations in production must also be considered.

It should also be noted that whilst the quantity of information may be significantly increasing as further sensors are added, the amount of new and useful information may only be a relatively small and diminishing proportion.

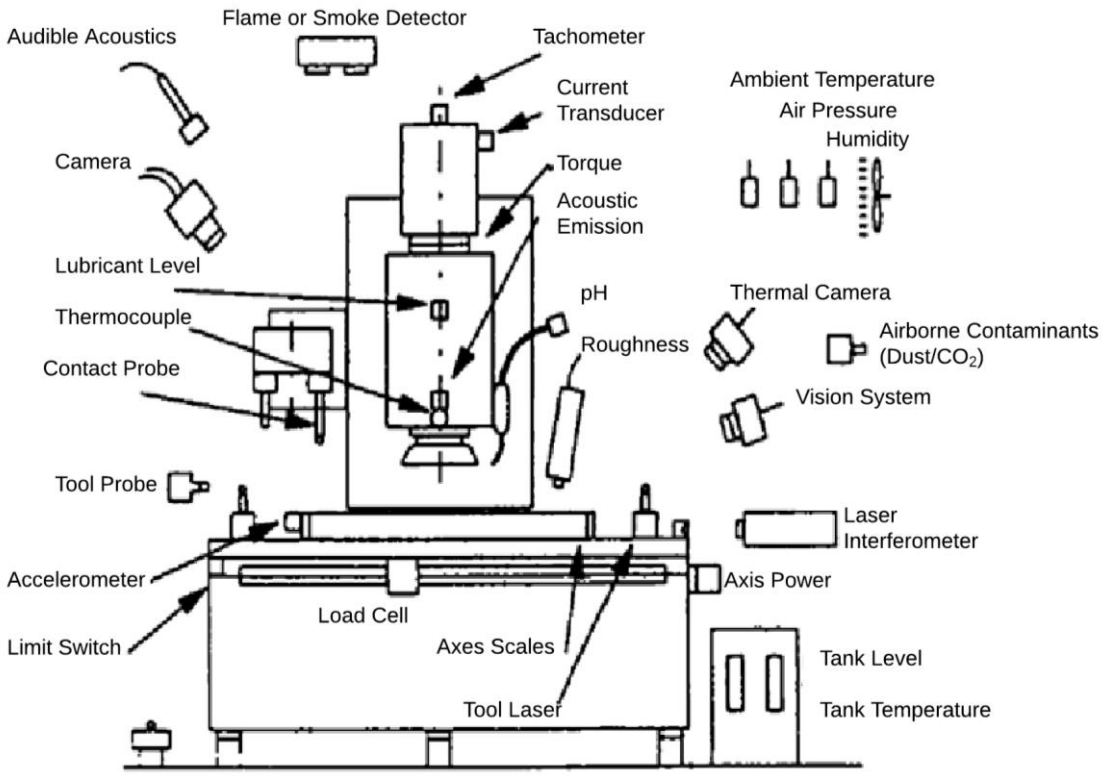

Figure 2-3: Available sensors for machining applications [27]

Although availability of sensors and sensor data remains a challenge in production environments today, the research area has received significant attention since the publication of the highly cited review paper on sensor based tool condition monitoring by Byrne *et al.* in 1995 [27]. In 2004, Liang *et al.* [29] reviewed the application of sensors in machining and provided a short list of relevant and popular sensor types; these were vision, force, AE, power, torque, vibration, audio, temperature, dimensional gauges and a micromagnetic sensor. The issues of sensor placement practicalities, costs and reliability issues were discussed, though not resolved, in the review.

To ensure that industry can exploit a continuous sensing solution, the cost, convenience and performance of sensors must be considered, the data must be informative, and the installation of the equipment must not be intrusive. Cutting force measurement is the most common of all cutting process sensors, yet Dey and Stori [40] explain that *"One important practical hindrance to the industrial deployment of cutting force sensors for process monitoring is the high cost and intrusive nature of multi-axis dynamometers in a production environment".*

In 2010, Abellan-Nebot *et al.* [38] noted that the vast majority of applications used the following sensors; dynamometers, accelerometers, AE and electrical current transducers. Sensors were scored based on the extent of their intrusive nature, cost and signal reliability, as shown in Table 2-1. Temperature measurement was not included in this ranking, given that it had seen little attention in multi-sensor monitoring research.

Table 2-1: Sensor ranking provided by Abellan-Nebot et al. [38]

Sensor	Cost	Intrusive nature	Signal reliability
Dynamometer	★★★	★★★	★★★
Accelerometer	★★	★★	★★
AE	★★	★★	★★
Current/Power sensor	★	★	★

In 2013, Kerrigan and O'Donnell [43] proposed a wireless method for temperature measurement within a rotating cutting tool, Chung [44] presented a self-powered vibration sensor for machining, and Stoney *et al*. [45] presented a dynamic wireless passive strain measurement device. These are a small sample from a surge of research published in recent years which addresses the issue of cost, reliability and intrusive nature of sensors for cutting process monitoring.

The increasing trend in machining process monitoring research presents the need to address sensor cost, reliability and practicality. Wireless systems have become important; wireless data acquisition and wireless power to sensors is under investigation, though broadly these devices are not yet mature enough for production use. Challenges, such as limitations on sampling rates, battery life and the introduction of time delays to signals, are faced.

The main sensor types of interest are described in more detail in the following sections.

2.2.1 Power Transducers

Figure 2-4 shows a typical machine tool spindle. Spindle motor power can be measured using current and voltage data from the motor drive. The majority of industrial spindle motors are three-phase induction motors for which the following calculation must be performed to obtain power from current and voltage measurements on each of the three phases:

$$P = I \times V \times cos\emptyset \times \sqrt{3} \quad (1)$$

Where P is the power for each phase, I is the current, V is the voltage and $cos\emptyset$ is the phase shift between the current and voltage signals. Hall effect sensors are commonly used for current sensing, whilst voltmeters can obtain the potential difference at each phase.

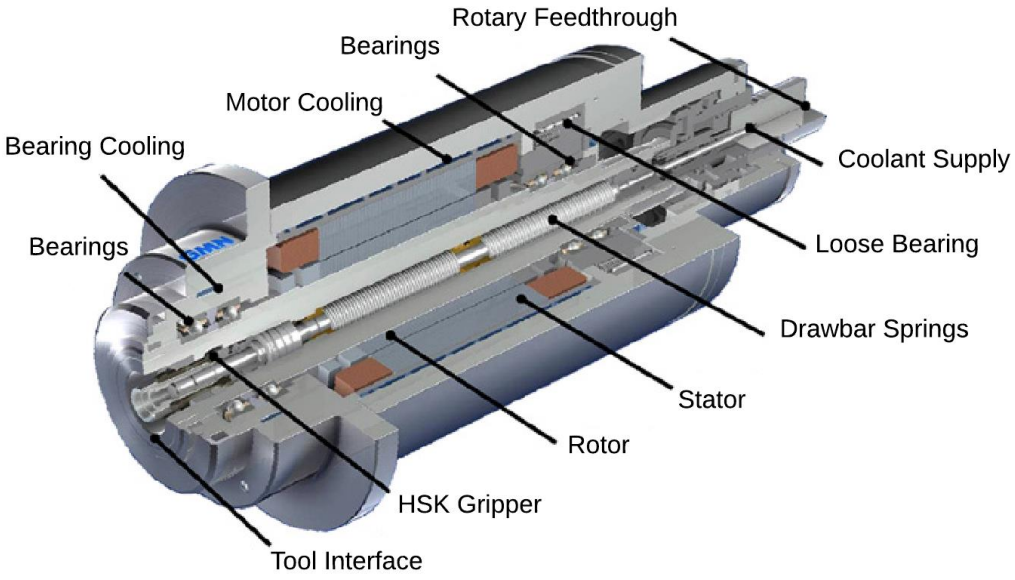

Figure 2-4: Machine tool spindle diagram

Power measurement is an obvious choice for monitoring machines as it is relatively cheap to measure, easy to install, does not interfere with the cutting zone, and gives a signal that is proportional to cutting force. Power of linear and rotary axis drives have also been used for monitoring the machine and process. For these reasons, power monitoring is commonly seen in industry for uses ranging from crash detection, machine axis health monitoring, and cutting tool breakage or wear monitoring.

The measurement of power has a poor dynamic response compared to other sensor types. An established supplier of power transducers for condition monitoring applications (Load Controls Incorporated) provides sensor response times between 15 and 500msec (stated as the amount of time it takes the transducer to respond to a 90% of full-scale change in signal).

It has also been reported that power measurement, as an indirect measure of torque or force, can suffer significant electrical and mechanical noise. The measured power signal from a spindle is a function of several effects from the cutting tool, cutting conditions, bearings and state of other mechanical components of the machine tool. This combination results in the data being less sensitive to small changes in the cutting process. For example, the ability to monitor machining conditions is diminished where power required to overcome inertia and friction in the spindle is large, relative to the power required for machining [54].

Al-Sulaiman *et al.* [46] used spindle power to monitor a drilling process and attempted to reduce the effect of measurement noise, such as that associated with friction within the spindle bearings, by normalising the signal based on the idle spindle power. Several drill diameters, spindle speeds and feed rates were tested and some correlation existed between both measures of spindle power and the cutting tools' flank wear width. There was little evidence to show any improvement when normalising the power signal. The results would be more helpful if the degree of correlation and the robustness of the proposed solution were considered.

Axinte *et al.* [47] evaluated the sensitivity of spindle power measurement for turning, milling and drilling processes. It was found that the ability to detect transient events, such as tool chipping, was particularly challenging in end milling. Continuous tool wear progression could be observed once wear levels were 'distinct' for each of the three cutting processes. The paper did not identify guidance on a suitable threshold level to identify tool wear or chipping, and lacks evidence on whether the power measurement alone was adequate for industrial use, stating 'the signal might not have enough sensitivity to detect small malfunctions such as chipping'. The results could be improved if the sensitivity of power measurement to a known physical quantity, such as force or torque, was tested independently to the cutting process effects.

Kim *et al.* [49] developed a fuzzy logic controller that controls feed rate of a milling process in real time in order to maintain a constant cutting force. The system is first applied with a dynamometer measurement of cutting force. The controller is then applied without the dynamometer, by deriving the cutting force from the spindle power measurement. The results show that although the system performs better with the dynamometer, spikes in cutting forces can be reduced when using spindle power.

Vijayaraghavan and Dornfeld [50] investigated the value of energy consumption data across a manufacturing system in order to consider the environmental impact of the different process planning levels. A framework was proposed where production planning was the highest level of data analysis. Daily usage of a machine could be observed from the data at the production planning level. Below this, feature level energy usage was used to determine the energy consumption associated with different attributes of a components' manufacture. Tool path planning and efficiency such as % time in cut was then evident from the data, and finally, detection of spikes, such as tool failures, could be observed in higher sample rate machine power data. The paper provides an interesting and objective view of how measured energy data can be useful.

2.2.2 Force Sensors

Force measurement is widely used in machining research, given it is a key parameter in machining processes; it has a strong presence in the process monitoring literature covered such as the review papers already listed ([18], [19], [27]-[31]). It has been shown that cutting conditions, tool wear, material variation and many more process variables can be observed indirectly through force measurement; it is also useful for validation of simulation models that provide cutting force estimates.

A stationary, three-component plate dynamometer is commonly used for force measurement in milling, as shown in Figure 2-5. 4-component dynamometers are also available, commonly used in drilling process monitoring, as are 3-component lathe dynamometers. Piezoelectric materials are favoured to strain gauges given the increased dynamic response of the measurement and increased stiffness of the machining setup. These piezoelectric sensing elements generate an electrical charge proportional to the load in the measurement direction. Typically, a separate sensing element is used for each direction.

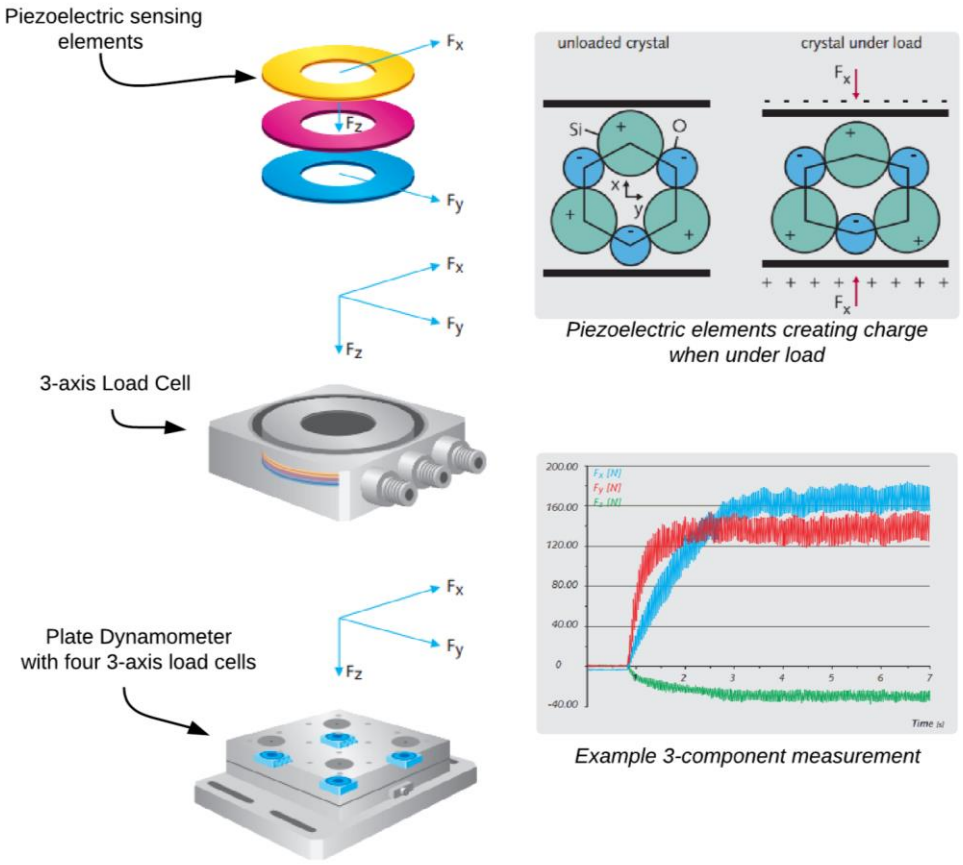

Figure 2-5: Kistler 3-component force dynamometer [5]

There is very little use of direct cutting force measurement in production processes, although there have been good examples of its use for machining experiments in laboratory conditions, such as that presented by Klocke *et al.* in [52]. In fact, no examples of production use of cutting force dynamometers for monitoring machining processes could be found in the public domain. This is not just due to the high cost of accurate measurement equipment, but also the intrusive nature of the equipment in the machining vicinity.

Yaldız *et al.* [53] designed and built a dynamometer for the milling process and demonstrated the high cost and complexity of this approach. The device used strain gauges rather than piezo materials, therefore the stiffness and frequency response of the sensor is likely to be inferior to the more common Kistler device. It can be seen that the instrumentation is significantly invasive to the machining volume, is not practical for large production fixturing, and compromises the stiffness of the workpiece setup. It is not clear how this system is an

improvement on products on the market, therefore a comparison in performance to a more common Kistler system would have been beneficial.

Park *et al.* [51] ambitiously state that '*the most effective method to monitor the states of machining operations and adaptively control the process is through measurements of cutting force signals*'. The authors' attempt to integrate force measurement within a spindle allows the technique to be applied in production, though the accuracy of the sensor system and influence on the spindles' static and dynamic stiffness is unclear. Other less intrusive and less costly force measurement techniques are used in commercial solutions such as strain measurement on axis drives and load cells, or pressure sensors installed in fixturing, though these methods are indirect measurements of the cutting force and are likely to result in an increase in signal noise.

Teti *et al.* [55] attempt to infer the chip condition from cutting force signals in a turning application, concluding that no single feature can reliably indicate the type of chip. More recently, Klocke *et al* [56] developed a method for observing chip evacuation from a drilling process using an optical sensor.

It is a key objective of this study to produce a system that is viable for production use. Due to the practical limitations in using force measurement equipment in production, neither piezoelectric nor strain gauge force measurement have been used for the sensor system in this study.

2.2.3 Microphones

Microphones are intended to convert air pressure oscillations into corresponding voltage oscillations and are typically applied to measure airborne, audible range acoustic emissions. Figure 2-6 shows the basic components of a condenser microphone. Sound waves cause the diaphragm to vibrate and as a result, the capacitance between the diaphragm and the back plate will vary. This varying capacitance in turn generates a voltage change that can be amplified and passed to a data acquisition system.

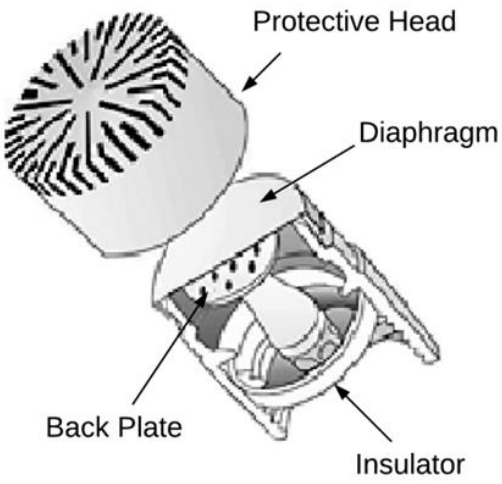

Figure 2-6: Components of a microphone [73]

Microphones can detect vibration frequencies from a system, provided the vibrations cause airborne sound waves that are able to reach the sensor. Microphones have been used extensively for the identification of chatter frequencies in milling and turning. They are less intrusive than accelerometers as they need not be in direct contact with the tool, workpiece or machine; however, they can be prone to signal noise as other airborne sound waves in the measurement vicinity will also be detected by the sensor. To reduce signal noise, unidirectional microphones can be used, where their sensitivity is a function of the direction at which the sound waves approach the sensor. This is referred to as the polar pattern. The specification for a Shure PG81 microphone, that includes the polar pattern and frequency response, is shown in Figure 2-7.

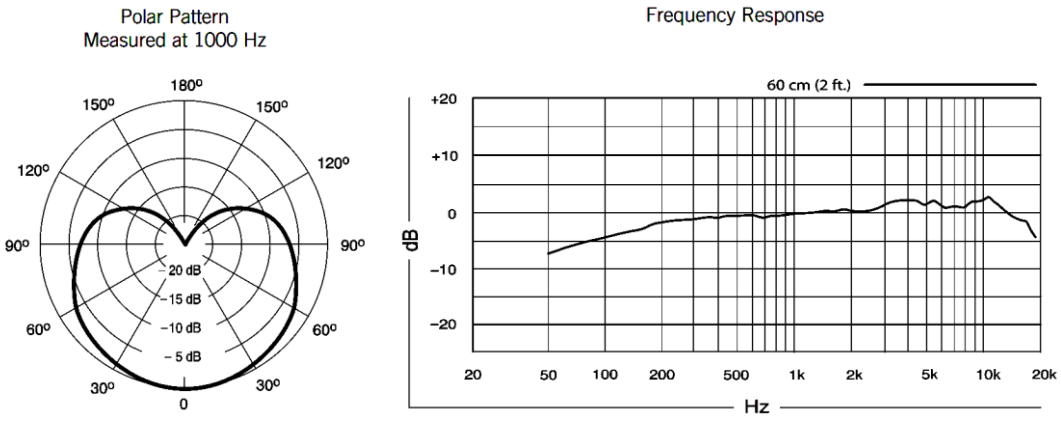

Figure 2-7: Shure PG81 microphone performance data [74]

Many commercial solutions are now available for chatter detection using a microphone, as it has become an applied technique in industry [75], [76]. It has been used to a lesser extent for detection of other key variables as background noise levels from adjacent machines and workshop activity can interfere with the signal.

Delio *et al.* [78] published a comprehensive study on the use of audio signals for chatter detection, demonstrating that a microphone can detect chatter frequencies between 100-13,000Hz. Directional considerations and environmental sensitivity were raised as practical concerns, though the use of a microphone was generally found to be a convenient and reliable method for chatter detection. For low frequency vibrations below 100Hz, typically associated with structural vibrations, accelerometers were recommended.

2.2.4 Accelerometers

Vibration measurement using linear accelerometers is used both in commercially available chatter detection systems and published widely in the machining process monitoring literature. Most commonly, measurements are taken by attaching piezoelectric accelerometers to a fixture, workpiece, tool or spindle.

The cross-section of a single-axis piezoelectric accelerometer is shown in Figure 2-8. The principle of the design is to convert the kinetic energy of a mass into electrical energy. As with the piezoelectric dynamometer, the piezo material creates electrical charge when it is compressed, and an opposite charge when released. The piezo material and mass are pre-loaded so that acceleration of the mass in either direction can be measured. For tri-axial accelerometers, three sensors are assembled with measurement axes perpendicular to each another.

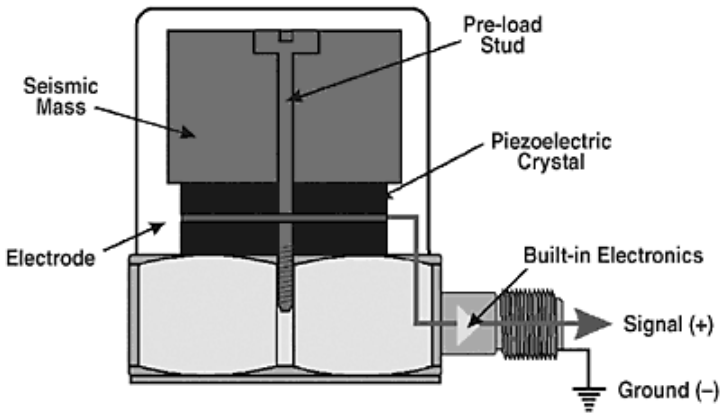

Figure 2-8: Single axis piezoelectric accelerometer [79]

Vibration is an important physical effect in metal cutting processes and is present in the majority of machine and process condition monitoring practices. It has been especially important in extending the understanding of chatter vibrations to that known today, covered in detail by Altintas [58]. The effect of self-excited vibrations in a milling process is illustrated in Figure 2-9.

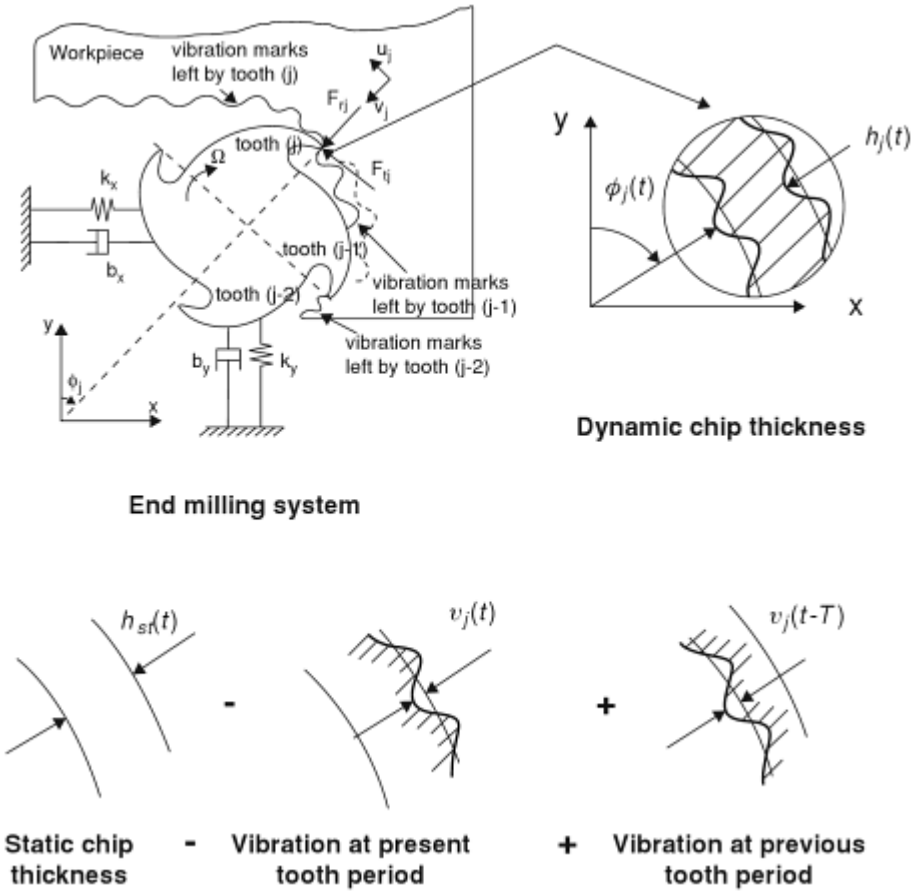

Figure 2-9: Self-excited vibration in milling [58]

A number of methods have been described for the detection of chatter vibrations during machining [32]. Accelerometers have been placed on the spindle, workpiece fixturing to obtain vibration data. A higher dynamic range can be obtained using accelerometers compared to alternative sensing methods such as microphones or dynamometers.

Accelerometers have also been used in intelligent monitoring systems to predict machined surface roughness. Benardos and Vosniakos [59] conduct a review of methods for surface roughness prediction in machining and state that, whilst accelerometers can improve the accuracy of the prediction, other contributions to the roughness formation mechanism are generally overlooked, such as tool wear, static tool deflection and cutting temperatures.

Abouelatta and Madl [60] attempted a surface roughness prediction for turning that used both cutting parameter data and tool vibration. A basic linear model was derived using

regression and the model fit was poor; however, the signal processing and feature extraction detail was minimal. The method was data driven and reliant on extensive testing data.

An accelerometer signal is sensitive to its proximity to the source of vibration and the modal response of the structure; therefore it is good practice to maintain the sensor at a fixed distance from the cutting edge with consistent structural dynamics during use. This constraint presents an issue when applying to industry, particularly for large part manufacture. Specific signal processing and computation methods may need to be considered for applications where this is not possible.

2.2.5 Acoustic Emission

Measurement of Acoustic Emission (AE) from a cutting process has had a lot of interest in literature on monitoring machining processes. The term AE generally refers to measurements in the ultrasonic frequency range, and so further usage of this abbreviation will be with regard to acoustic emissions in the ultrasonic range.

AE can be defined as the class of phenomena where transient elastic waves are generated by the rapid release of energy from a localised source within a material (ANSI/ASTM E 610-77). An AE sensor is designed to convert mechanical energy of an elastic wave into an electrical signal. These sensors are most commonly piezoelectric transducers, such as that shown in Figure 2-10.

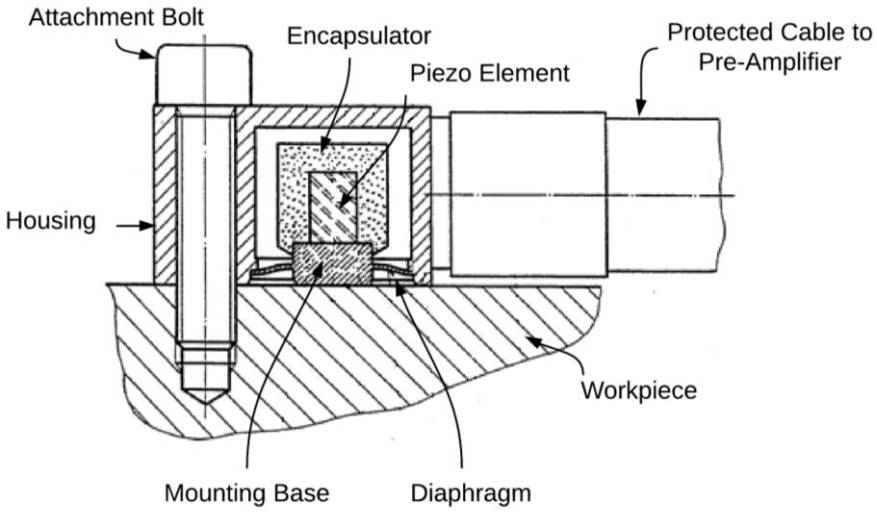

Figure 2-10: Basic components of an AE sensor

To maximize the transmission of acoustic energy to the piezo element, the sensor proximity and any interface between the sensor and the signal source should be considered. Acoustic impedance matching is required to maximize the transmission; sensor suppliers recommend that a flat surface is used for mounting the sensor and high viscosity fluid, such as grease, or epoxy adhesive is applied between the sensor base and the contact surface.

AE sensing for machining is typically considered to be the measurement of ultrasonic frequencies from around 20 kHz to 2MHz.

Konig *et al.* [61] investigated the use of AE measurement for monitoring tool wear when using small drills. 1, 2 and 3mm diameter drills were used for the machining of chromium-molybdenum steel. In all tests shown, drills were run to failure. AE signals showed a rapid increase in RMS magnitude towards the last 10% of a tool's life, consistently resulting in over a 300% increase in RMS magnitude for the penultimate hole machined. The use of spindle power was shown to be insensitive to tool wear given the low forces of the drilling process. This fact demonstrates that, for the process under examination, onset of tool failure can be reliably detected using AE sensing. For the 3mm drill, four repeat experiments showed variation in tool life of over 600%, confirming the requirement for such a system.

Lee *et al.* [62] review the use of AE sensing to monitor precision machining processes. The paper summarises the sources of AE and how, due to the signal-to-noise ratio, the sensor

type favours precision and ultra-precision machining processes. Several claims are made regarding the sources of AE signals, also summarised in Figure 2-11:

- AE is typically generated in the primary, secondary and tertiary shear zone
- Where depth of cut is 0.1mm and above, AE is mainly due to rubbing and friction in the tool/chip interface
- Where depth of cut is below 0.1mm, AE is mainly due to interactions of the tool tip and microstructural properties within the workpiece

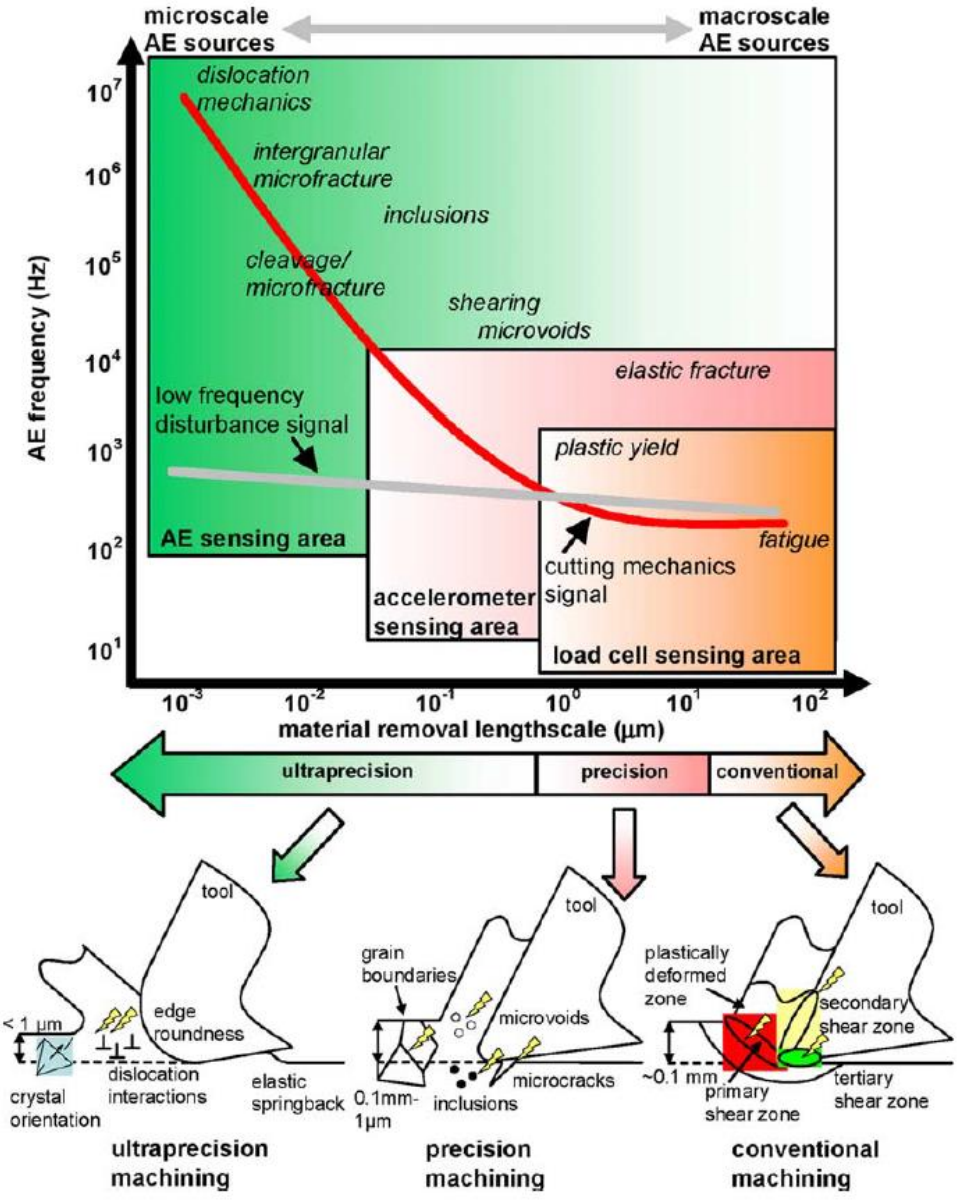

Figure 2-11: Sources of AE signal [62]

Li [63] reviewed acoustic emission methods used in turning. Given that the signal is a product of transient, non-stationary components, a number of particular signal features are proposed, including ring-down count, AE event, rise time, peak amplitude, RMS, short time Fourier transform and wavelet transform.

Marinescu and Axinte [64] explored the use of AE sensing to ensure damage free surfaces during milling. Two measured force components were combined with segmented AE signals to determine tool wear. Some comparisons were made between the sensor signals, the tool life, and the surface finish. There was no explanation, however, of how the multiple sensors added a benefit. Furthermore, the impracticalities of applying force dynamometer measurements in a production environment were not discussed.

Araujo *et al*. [65] tested and analysed AE signals from a turning process to determine the relationships between AE signals and dislocation motions in the chip formation. Tool condition monitoring and chip management scopes were proposed applications, though it was noted that few machining monitoring systems using AE have been reliable enough for production use. It was proposed that the reliability issues are partially resulting from the sensitivity of the signal to the work piece strain, strain rate and temperature. Experimental results supported the hypothesis that AE energy was directly proportional to workpiece strain and strain rate, but inversely proportional to temperature. Similarly, it was claimed that AE mean frequency was directly proportional to strain rate and inversely proportional to temperature.

The literature reviewed presented some merit in the use of AE, such as the insensitivity to low frequency noise and the ability to measure high frequency emission that other sensors cannot. This allows AE sensing to be particularly useful for detecting tool breakage and is popular for monitoring low cutting force operations such as the use of small diameter drills. However, the signal processing steps and degree of success of employing AE sensing does vary in existing literature. Furthermore, the implementation challenges for this sensor type are vast, given the distance and the media between the sensor and the cutting action has a large effect on the sensed signal.

2.2.6 Cutting Temperature

The kinetic energy from a cutting process is predominantly transferred into heat energy during the chip forming process. Heat is one of the most significant limiting factors in the cutting process. Basti *et al.* [66] stated that the detrimental impacts of temperature in the metal cutting process include:

- Acceleration of tool wear and the shortening of tool life.
- Thermal deformation of the workpiece, cutting tool and machine tool which leads to a reduction in machining accuracy.
- Damage to the subsurface layer through phase transformation, residual stress generation and other thermally induced defects.

Given its importance, the monitoring of temperature during the cutting process is desirable for a process monitoring system. The paper from Karaguzel et al. [67] explained that the transient nature of temperature emissions in milling make them particularly challenging to measure accurately. The authors showed that cutting temperature in milling can be estimated more accurately when using a heat conduction model to improve the measurement result. A further example of the use of measured temperature to validate process models was given by Abouridouane *et al.* in [68].

There are several methods for measuring temperature. Byrne [69] divides these into conduction techniques, such as thermocouples and thermal paints, and radiation techniques, such as infrared pyrometers and thermal imaging cameras.

O'Sullivan and Cotterell [70] used two K-type thermocouples embedded in an aluminum workpiece to determine cutting temperatures for a turning process. It was found that the measured temperature increased from approximately 65°C up to 85°C when the new tool, running at 165m/min, was changed to a worn tool of 0.35mm flank wear width. It was also shown that increasing surface speed from 165m/min to 222m/min decreased the new tool measured temperature to approximately 55°C, attributed to more of the thermal energy being dissipated in the chip.

Lin and Liu [71] used an infrared pyrometer to measure the temperature of a silicon nitride cutting tool during the turning of medium carbon steel. An insert was heated in a furnace

and the pyrometer result was compared to a K-type thermocouple. During turning, the temperature was taken at 0.5mm and 1mm from the cutting edge and surface speed was increased from 60 to 600m/min. At 600m/min, the temperature was measured to be approximately 650°C at 1mm from the edge, 800°C at 0.5mm, and extrapolated to 1000°C to estimate the tool-chip interface temperature.

Basti *et al.* [65] designed and manufactured a cutting insert with two embedded thin film thermocouples and tested it in when turning an aluminum alloy. The thermocouples were placed 0.3mm and 0.5mm from the cutting edge and surface speeds from 300m/min to 960m/min were tested. Temperatures between 450°C to just over 600°C were measured. The manufacturing process used for the thermocouples is summarised in Figure 2-12. This method provides a promising means of measuring cutting temperature in a non-intrusive manner that may be viable in production processes.

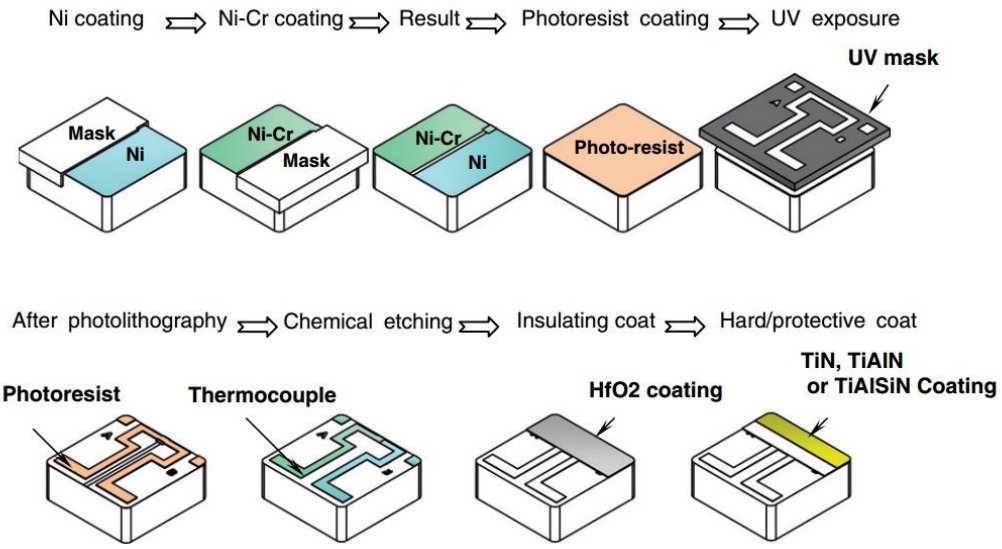

Figure 2-12: Manufacture of insert with embedded thin-film thermocouple [65]

Kerrigan and O'Donnell [43] developed a wireless integrated thermocouple into a milling tool for composite machining applications and compared measurement results to those from finite element models. A K-type thermocouple of 0.2mm in diameter was positioned 0.5mm from the cutting edge of an 8mm diameter tool. An Actarus [72] wireless tool holder system was then used to convert the analog signal to digital and transmit the data wirelessly to a static data acquisition device. Temperatures up to 200°C were measured during milling. A

slow response time of the sensor was observed, though results were shown to correlate well with finite element models.

Despite the value of temperature data in understanding the performance of a cutting process, no method was found that is viable for continuous monitoring in a production environment. Due to the destructive nature of embedding the thermocouples in the workpiece, this method is suited to a lab environment when the aim is to gather experimental data. Line of sight methods, including pyrometers and thermal cameras, are also suited only for lab measurement systems, given that it is not possible to gain continuous line of sight data in most production processes. Embedding thermocouples within tooling offers a possible solution to these issues. Provided wiring and installation of the systems can be non-intrusive to the process, they have potential to be used for continuous process monitoring systems. However, manufacturing processes to embed a sensor are currently bespoke, and data acquisition systems such as wireless tooling can be expensive and limit tooling options.

Specialised indexable tooling for drilling and milling are commercially available where thermocouples are placed below the insert seat [72]. However, given the cost and additional complexity of embedding sensors within solid carbide end mills, as well as the practical limitations of line of sight methods, the measurement of temperature has not been applied in this study. It should be noted, however, that the advantages of an affordable temperature measurement solution would be significant given that the cutting temperature is an important indicator on the cutting conditions. The challenge for this technology is the development of non-intrusive and low cost sensing, whilst the opportunity is the ability to reliably sense the cutting conditions from this single sensor type.

2.3 Digital Signal Processing

This section has considered the processing steps that are applied to a set of sensor signals prior to decision making algorithms being applied. This includes segmentation, feature extraction and feature selection steps.

2.3.1 Segmentation

The purpose of segmentation is to extract the relevant samples of the continuous sensor signal data set for further processing. Data during which there is no activity may be redundant; for example, when a cutting tool is not in contact with the workpiece. This step, described by Ghosh [77] as illustrated in Figure 2-13, will reduce the size of the data set and ensure that further computation is carried out solely on the useful segments of the sensor signals.

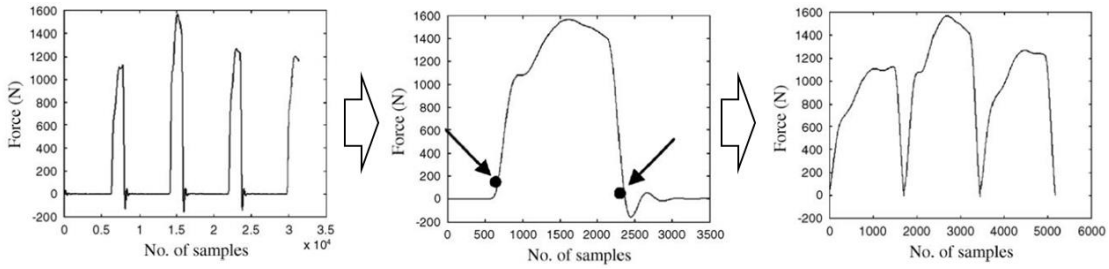

Figure 2-13: Segmentation of sensor signal and data reduction [77]

Segmentation has also been used to differentiate between important regions of the cutting path, such as the engage or retract moves of a cutting tool [80]. This allows different approaches to be taken in the subsequent processing steps for each of these regions. Given that many process failure modes such as tool breakage may occur at any period where the tool is in contact with the material, it is appropriate to monitor all segments of the sensor data.

The segmentation is programmed by the user in commercial monitoring systems, for example using markers in Numerical Controller (NC) code to start and stop recording. Another common approach in these systems is to normalise the sensor data on a short segment of the signal prior to entering cut, thus accounting to some degree for any unwanted sensor signal drift, particularly for spindle power measurement. Researchers have proposed more complex segmentation requirements, such as the ability to differentiate and compare multiple tooth passes in milling [81]. This approach requires a degree of automatic segmentation and sorting to be programmed into the software.

Once segmentation is complete, each segment can undergo time and frequency domain analysis to determine discrete features of interest. This can once again significantly reduce the size of the data set.

2.3.2 Feature Extraction

In its simplest form, the problem of detecting a fault in a sensor signal is that of extracting the fault signal, X(t), in measurement, Y(t), in the presence of noise, N(t), where Y(t)=X(t)+N(t). In many cases signals X(t) are transient in nature, whilst N(t) is stationary.

The previous literature has shown a large number of sensor signal features can be used to extract a fault signal from raw sensor signal data. Each common feature type found in the previous monitoring literature is covered as time domain and frequency domain features in this section. Further methods such as time-frequency and wavelet are briefly covered in section 2.3.3.

Time domain features

Time domain features generally require the least computation as the features can be directly extracted from the sensor waveform data. They are univariate and can be described as 'summary statistics' which provide an overall picture of the time-series under investigation.

For a sensor signal $x(t)$, that has been sampled at a sampling interval Δt, a segment of the signal starting at time t_0 and containing N samples can be described as:

$$x_i = x(t_0 + (i-1)\Delta t); i = 1, \dots, N \quad (2)$$

Popular time domain features are summarised in Table 2-2.

Table 2-2: Time domain features and formula

Name	Formula	Comments
Mean	$\bar{x} = \frac{1}{N}\sum_{i=1}^{N} x_i$	Arithmetic mean of the signal.
Root Mean Squared	$x_{rms} = \sqrt{\frac{1}{N}\sum_{i=1}^{N} {x_i}^2}$	Statistical measure of the signal that is appropriate when data is positive and negative.
Variance	$\sigma_x^2 = \frac{1}{N}\sum_{i=1}^{N}(x_i - \bar{x})^2$	Non-negative value indicating the spread of the signal data. Equal to the standard deviation squared.
Skewness	$\gamma_1 = \frac{1}{N}\frac{\sum_{i=1}^{N}(x_i - \bar{x})^3}{\sigma^3}$	A measure of the asymmetry of the probability distribution of the signal.
Kurtosis	$\gamma_2 = \frac{1}{N}\frac{\sum_{i=1}^{N}(x_i - \bar{x})^4}{\sigma^4}$	A measure of the "peakedness" of the probability distribution of the signal. Higher kurtosis means more of the variance is the result of infrequent extreme deviations, as opposed to frequent modestly sized deviations.
Peak Amplitude	$x_{peak} = \max(x_i)$	The maximum amplitude of any value in the signal.
Peak to Peak Amplitude	$x_{pk-pk} = \max(x_i) - \min(x_i)$	The difference between the maximum amplitude and minimum amplitude of the signal.
Crest Factor	$x_{cf} = \frac{x_{peak}}{x_{rms}}$	The use of the crest factor calculation is to provide a value of the peak amplitude relative to the signal RMS.
Count Rate	$x_{cr} = \frac{C(x_i > Q)}{N}$, where Q is the count threshold	Sometimes called the pulse or burst rate, the number of times the signal exceeds pre-set thresholds per second. This feature is generally specific to vibration and AE signals.

Frequency domain features

The frequency spectrum of a continuous time signal can be obtained using the Fourier transform:

$$X(f) = \int_{-\infty}^{\infty} x(t) e^{-2\pi i f t}\, dt \tag{3}$$

Where f represents the frequency in Hz.

For sampled data, this can be represented as the discrete Fourier transform (DFT):

$$X_n = \sum_{j=1}^{N} x_j e^{-2\pi i n j/N} \tag{4}$$

The fast Fourier transform (FFT) is an algorithm that can compute the DFT. In most cases, it is assumed that the analysed data is stationary.

For frequency domain analysis, the power spectrum has been used, which is the square of the FFT's magnitude. For a power spectrum S(f), with a sample spacing of Δf, a segment of the spectrum from frequency f_0 containing N samples can be described as:

$$s_i = s(f_0 + (i-1)\Delta f); i = 1, \dots, N \tag{5}$$

Table 2-3 lists a number of common frequency domain features.

Table 2-3: Frequency domain features and formula

Name	Formula	Comments
Mean of Total Band Power	$\bar{s} = \frac{1}{N}\sum_{i=1}^{N} s_i$	Arithmetic mean of the frequency power for a selected band of the frequency spectrum.
Sum of Total Band Power	$s_{sum} = \int_{f1}^{f2} s_i df$	The total power in a particular frequency range (f1-f2). The integral of the spectral density over the range of frequencies of interest.
Variance of Band Power	$\sigma_s^2 = \frac{1}{N}\sum_{i=1}^{N} (s_i - \bar{s})^2$	Non-negative value indicating the spread of the frequency magnitude data.
Skewness of Band Power	$\gamma_{s1} = \frac{1}{N}\frac{\sum_{i=1}^{N}(s_i - \bar{s})^3}{\sigma_s^3}$	A measure of the asymmetry of the probability distribution of the spectra.
Kurtosis of Band Power	$\gamma_{s2} = \frac{1}{N}\frac{\sum_{i=1}^{N}(s_i - \bar{s})^4}{\sigma_s^4}$	A measure of the "peakedness" of the probability distribution of the spectra.
Peak Amplitude	$s_{peak} = \max(s_i)$	The maximum amplitude of any frequency in the spectra.
Peak Frequency	$f_{pk} = s_{peak}(f)$	The frequency that corresponds to the peak amplitude.
Spectral Crest Factor	$s_{cf} = \frac{s_{peak}}{\bar{s}}$	Also termed the relative spectral peak.
Harmonic Band Power	$s_{tpf} = \sum_{i=1}^{n+1} s_{ij}$ Where i=1,2,…,n, j is the tooth pass frequency, and n is the number of harmonics.	Sum of the power for the tooth passing frequency and a specified number of its harmonics.

2.3.3 Advanced Signature Analysis

There are a significant number of alternative and more advanced signal processing and feature extraction methods that have been investigated for condition monitoring applications. Some of these techniques, such as the Wavelet transform, have received attention in machining process monitoring literature, but there are also many techniques used in other condition monitoring applications that are yet to be thoroughly tested on machining applications. Given the breadth of the field of signal processing, not all methods are reviewed in this chapter. Several methods reported in the literature have been summarised below.

Windowed Fourier Transform

When the spectral content of a signal changes with time, neither the time nor frequency domain features alone are sufficient to describe the signal properties.

The windowed Fourier transform method effectively divides a signal up into segments before Fourier analysis is applied, then giving information on how the spectral content varies with time. It makes the assumption that the signal is stationary in each segment. For a finite section of data this method is called the Short Time Fourier Transform (STFT). The limitation of this technique is the tradeoff between time resolution and frequency resolution; for smaller windows, the frequency resolution is decreased, whereas for larger windows, the time resolution is decreased. The STFT can be written as:

$$X(\tau, \omega) = \int_{-\infty}^{\infty} x(t) w(t-\tau) e^{-j\omega t}\, dt \tag{6}$$

where $w(t)$ is the window function.

Time-Frequency Analysis

Many time-frequency analysis methods are covered extensively by Cohen [97]. Popular methods for time-frequency analysis for machining applications include the Gabor transform, the Wigner-Ville distribution and the Choi-Williams distribution.

These methods have been particularly popular for acoustic emission sensor signals, such as that presented by Marinescu and Axinte in [91]. The authors developed a monitoring system for the milling process which used time-frequency approaches on an AE sensor signal. The sensor features were shown to indicate missing or damaged cutting edges on an indexable end mill. It was not clear whether these techniques offered any advantage over time or frequency domain data alone.

The Wavelet Transform

The wavelet transform has also been classed as time-scale analysis. Like the Fourier transform, wavelets can be classed as continuous or discrete.

Discrete wavelet transforms have been used for machining process monitoring applications, where the magnitude of wavelet coefficients in a specified frequency band have been used as signal features.

Li *et al*. [92] used the discrete wavelet transform for tool breakage monitoring in the drilling of steel. The system successfully detected drill breakage using AE and spindle power sensor data. The wavelet transform features were not compared to alternative time or frequency domain features, so it could not be concluded whether there was an advantage to applying this technique.

Cyclostationarity

A cyclic function is one where the function itself changes with respect to time. E.g. Fn(x), where n is the cyclic order of the function. A periodic function is one where the function generates a signal which contains oscillations, e.g. $f(t) = f(t + \tau), \forall\tau$, where τ is the period.

The use of cyclostationary signal processing techniques allows signal features to take into account random effects produced periodically with the rotation of the system being monitored. The outputs of the various methods found in the literature allow the angular position and frequency content of periodic transient signals to be determined. Detailed reviews of analysing cyclostationary signals have been published by Antoni [98], [99].

Lamraoui [100] applies time domain, frequency domain and time-frequency domain (in this case, the STFT) analysis to accelerometer measurements from a milling process. The results are then compared to cyclostationary analysis techniques. Four different cyclostationary methods were covered; Wigner-Ville, spectral correlation, cyclic autocorrelation function and instantaneous autocorrelation function. Both chatter vibration and tool wear conditions were tested when full slotting an aluminium work piece with two and three flute solid carbide milling tools. Whilst the signal processing theory was comprehensive, it was not clear that the cyclostationary analysis provided any advantage, either in terms of computational cost or reliability, when compared to more familiar techniques such as time and frequency domain feature extraction.

Time Synchronous Averaging

Time Synchronous Averaging (TSA) is a signal processing technique commonly used when monitoring rotating machinery, such as gearboxes. The method allows periodic waveforms to be extracted from noisy data. The review paper by Bechhoefer and Kingsley [101] describes six methods of TSA and tests them on an accelerometer signal for fault detection in a gearbox. No application of TSA for machining process monitoring could be found.

Spectral Kurtosis

A method for using spectral kurtosis of vibration signals for fault detection in rotating machinery is presented by Antoni and Randall [102]. Both fault detection and fault identification methods were proposed. A faulty condition is shown to be detectable without the need for historical or non-faulty measurement data. The difference of the dB-spectrum from the vibration signal of non-faulty and faulty condition is comparable to the spectral kurtosis of the faulty signal on its own. The technique is reliant on the noise signal being Gaussian, therefore having a spectral kurtosis close to zero.

2.3.4 Feature Selection and Reduction

Feature selection and reduction can be applied to extracted features from raw sensor data in order to reduce the data set in size and dimensionality and to contain only the information of interest. The number of extracted features can be significant, which can add complexity to subsequent data fusion, pattern processing, pattern recognition or decision making algorithms. Feature selection and feature reduction techniques are therefore used to reduce the extracted data set, retain data that contains useful information and remove data that is redundant or has little value. The complexity of subsequent computations is then reduced. Furthermore, the number of sensors required in the system may also be reduced.

Feature Selection

Feature selection is the method of selecting an optimal subset of the given signal features without further transformation of the data. The selection is made in order to optimise a function, such as the classification accuracy of a subsequent decision-making algorithm. Several techniques are available in order to determine which features contain the most information and which have high redundancy. There are normally two methods for feature selection; filter methods and wrapper methods [103]. Filter methods use general characteristics of the features to evaluate whether they are useful without involving any subsequent learning algorithm. Wrapper methods use the performance of a chosen learning algorithm to determine the optimum feature subset. Whilst wrapper methods can lead to an improved output from the learning algorithm, they can be significantly slower to run.

Machining process monitoring literature has used relatively simple filter methods for feature selection, such as the correlation-based feature selection (CFS) used by Cho *et al.* [93], where possible subsets are given a 'Merit' which ranks their overall value. The heuristic scoring method is shown by Equation (7). Features with high correlation to a class (which may be time in cut or tool wear, for example) increase the Merit, whilst mutual correlations between other features in the subset reduce the Merit. The authors also concluded that the CFS method provided an improved feature set compared to an alternative Chi-squared statistics-based feature selection. It is also noted that some full feature sets (such as spindle power) outperform the reduced set for classification accuracy, showing that the Merit ranking is not an optimum selection.

$$\text{Merit} = \frac{k\overline{\mathrm{r}_{cf}}}{\sqrt{k + k(k-1)\overline{\mathrm{r}_{ff}}}} \tag{7}$$

Where *k* is the number of features in the subset, r_{ff} is the mean feature-feature correlation and r_{fc} is the mean feature-class correlation

Jemielniak [96] ranked features suitable for monitoring remaining tool life by first applying a low pass filter to each feature data set, then measuring how well the original feature data approximates the filtered data using the coefficient of determination (R-squared). Many assumptions have been made in selecting this approach. The filtered data has been chosen to represent the true model "to avoid any uncertain suppositions about the mathematical formula of this model". The feature is deemed as useful when the coefficient of determination between the filtered data and the original sensor data is greater than an arbitrary value of 0.4. The author has not explained how the delay caused by using a filter has been dealt with.

Whilst these two methods discussed can rank the features most suitable for tracking a particular variable over time, they may overlook features containing information relating to either transient events or other variables not correlated against. The feature selection method must therefore be considerate of the monitoring system objective(s), whilst still being practical enough that feature subsets can be selected without extensive computation.

Once a function that defines the value of any feature or feature set is derived, a search for the feature subset that optimises this function is required. Given the large number of sensor signal features available in machining monitoring systems, searching for an optimum subset by testing all possible subsets is impractical due to the significant number of subset combinations and therefore the large computational expense. Greedy hill-climbing algorithms, such as that used by Cho *et al.* [93], provide an efficient alternative, though the method does not consider interactions between features.

It is also possible to select a feature set based on theoretical or practical engineering knowledge. A potential difficulty in deriving feature subsets from knowledge of the physical system is that the underlying physical effects for issues such as tool wear and chip formation are complex. Furthermore, the transmission of data from the source to the sensor, particularly for vibration and AE, has an impact on the signal noise. Jemielniak [96] stated

that “it is impossible to predict which sensor signal features will be useful in any particular case”. Though this is rather pessimistic and arguably untrue, it emphasises that there is the impression that the physical mechanisms that lead to sensor signal generation are complex and not well understood. An understanding of the physical system has been important in chatter detection algorithms, such as process damping theory [94], therefore it may be worth pursuing for condition monitoring applications. No research was found to compare practical based feature selection with model based selection in this field.

Feature Reduction

Feature reduction is the method of reducing the dimensionality of a multi-feature (multivariate) data set. It is sometimes referred to as feature transformation. Possibly the most popular of these techniques is principal component analysis (PCA). PCA is used for mapping the variance of multivariate data into a reduced set of principle components, disregarding the dimensions in the original data set that contain the least variance. This also provides a valuable tool for visualising multivariate data sets in 2 or 3-dimensional space. Typically, a subset of features can be chosen using feature selection techniques, followed by reducing dimensionality further with feature reduction.

2.4 Decision Making from Data

Once monitoring data has been sensed and processed, it can be used for decision-making, typically in the form of detection, diagnosis or prognosis. These three functions have been discussed in the hypothesis in section 1.2. Their definitions are covered in more detail in this section including the discussion of the relevant literature.

There are a significant number of approaches to machine learning that can incorporate regression, classification and probabilistic based computation. The following section summarises applications of a number of methods in reviewed literature. Previous text can be referred to which expand on the range of techniques available, such as Worden *et al.* [119].

2.4.1 Fault Detection, Diagnosis and Prognosis

Detection

The detection of a fault is the first important requirement of a monitoring system. A system must identify whether a process is operating outside of a defined specification, regardless of the cause or fault type. Fault detection is essentially a two-state classification problem to determine whether a process state is *normal* or *faulty*.

A suitable set of sensors, signal features and computations for fault detection may not be the same as those for fault diagnosis or prognosis. There may be multiple faults, some of which may not be understood, may be poorly described by existing data or may be unknown. A means of being able to detect any of these fault types, without false alarms, is required from a fault detection system.

Diagnosis

Diagnosis is more specific and insightful than detection. Not only must the fault be reliably detected, but the fault type or cause must also be specified. This is usually achieved by association, either using data-driven models trained to recognise each type of known fault, or by logic derived from theoretical and practical knowledge about the nature of each fault.

According to the Institute of Diagnostic Engineers, it is the science of "determining the existence of a problem in a machine, plant, system or structure and/or appraising the cause(s) of a failure which may have taken place and/or assessing the condition or vulnerability of such machine, plant, system or structure either during use or while under development".

Prognosis

Prognosis most commonly refers to the prediction of how long a process, in its current state, will continue before a fault occurs. ISO13381-1 [104] defines prognosis as "the estimation of time to failure and risk for one or more existing and future failure modes". The only application of prognosis found in the machining process monitoring literature is that of remaining useful life prediction of a cutting tool.

The ability to manage faults using intelligent systems is desirable in a range of industries. Venkatasuubramanian *et al.* [105] explain that in process and chemical engineering, fault detection and diagnosis is central to abnormal event management (AEM). The authors define a *fault* as a departure from an acceptable range of observed variables, and that the *root cause*, *malfunction* or *failure* is the event which led to the process departing from this acceptable range. Several desirable characteristics of a fault management system are listed:

1. Quick detection and diagnosis
2. Ability to distinguish between different failures
3. Robustness to noise and uncertainties
4. Ability to detect whether the cause is a known malfunction or a novelty
5. Classification error estimate / confidence
6. Adaptable to processes changing
7. Explanation on how a fault originated and propagated to the current state
8. Minimal modelling, computation and storage efforts
9. Multiple fault identification

In SHM, the different levels of competence for fault (damage) assessment have been described by Rytter [82]. Cross [83] refined the descriptions to the following:

- Level 1; Detection – automatic detection of damage to the system
- Level 2; Localisation – automatic determination of where damage has occurred in the system
- Level 3; Quantification – automatic assessment of damage type and severity
- Level 4; Prognosis – prediction of the remaining useful life in the structure or component

2.4.2 Monitoring System Framework

The framework by which data is managed, processed and applied to improve a data fusion problem has been studied. A number of data fusion models are presented by Shahbazian [80]. One of which is the Omnibus model, originally proposed by Bedworth and O'Brien [84] and shown in Figure 2-14.

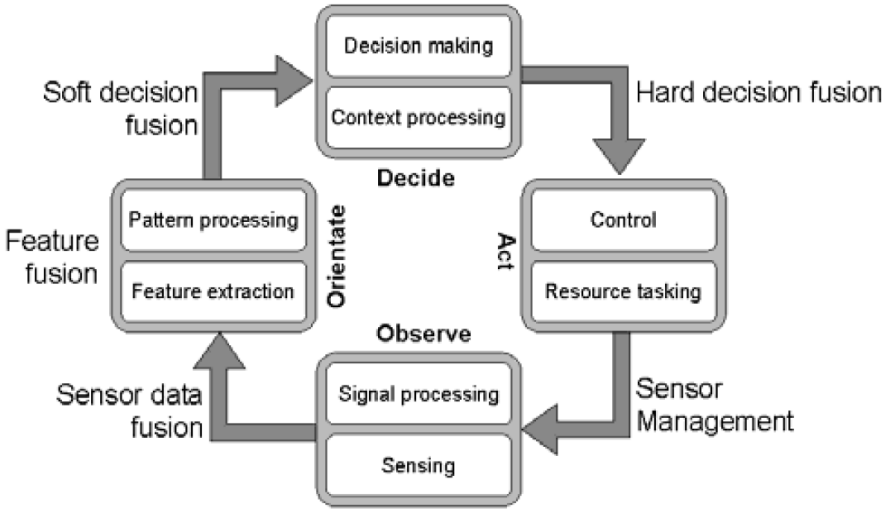

Figure 2-14: Omnibus model proposed by Bedworth and O'Brien [84]

An established data fusion model developed by the Joint Directors of Laboratories, known as the JDL model, has also been widely used, particularly in military applications [85]. The model is still flexible to multiple data fusion applications. The model differentiates itself from others, such as the Omnibus model, by the fact that the various levels of data fusion are not necessarily sequential or hierarchical. Different levels of signal and feature processing can be applied in each of the levels of data processing.

There is little reference to these models in machining process monitoring literature, though data fusion is a common aspect of the systems described. The waterfall model, presented earlier in Figure 2-2, is most appropriate for this thesis, given that the extraction of information from sensor signals, in a manner that provides robustness and flexibility, is essential to deliver the hypothesis.

The point at which data is fused is a consideration when defining a monitoring system. Typically, this will be at the data level, feature level or decision level. The vast majority of machining research applies feature level data fusion. Figure 2-15 presents an arbitrary sensor fusion tree. Whilst sensors 1 and 2 are fused at the signal level, then fused with sensor 3 at a feature level, pattern recognition steps are applied to sensor 4 before fusion takes place.

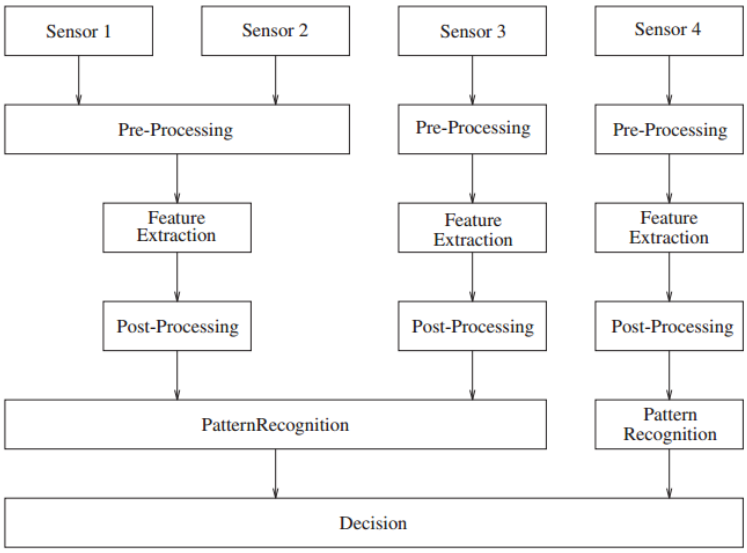

Figure 2-15: Arbitrary Sensor Fusion Tree [119]

Three different forms of learning have been described by Cherkassky and Mulier [88] as:

- Classification - The association of a class, state or condition with a set or vector of measured quantities
- Regression - The construction of a map between a group of continuous input variables and a continuous output variable
- Density estimation/probabilistic - The estimation of probability density functions from samples of measured data

2.4.3 Classification

Classification methods often offer the least computationally expensive approach for health monitoring problems. For example, it is the obvious choice for fault detection where the system must determine if the process is *normal* or *faulty*. Similarly, in SHM, classification is typically used where the objective is to determine whether a structure is *damaged* or *undamaged*. Classification may be for the detection of one of two states (normal, faulty) or there may be multiple classes (normal A, normal B, fault A, fault B, fault C…).

Neural Network and Support Vector Machine Classification

Segreto *et al.* [87] applied a multi sensor fusion system to tool wear assessment in finish turning of Inconel 718 alloy. A tri-axial accelerometer, an AE sensor with RMS signal conditioning and a three-component lathe dynamometer were used for the monitoring setup. Sampling rates were limited with 3kS/sec, 10kS/sec and 10kS/sec sampling rate respectively. Four signal features were selected for each sensor and three neural networks were configured for different sensor combinations; (i) Force and AE, (ii) Acceleration and AE, and (iii) Force, Acceleration and AE. It is concluded that fusing all sensors improves the system performance, however, the issue of dynamometer data not being available in production is not addressed and the performance of single sensor system is not given. The classification success rates are shown in Table 2-4, listed in order of their performance.

Table 2-4: Classification Accuracy reported by Segreto *et al.* [87]

Row Number	Force	Vibration	AE	% Accuracy
1	✓	✓	✓	98.9
2		✓	✓	87.8
3	✓		✓	88.3
4	✓	✓		Not reported
5	✓			Not reported
6		✓		Not reported
7			✓	Not reported

Ghosh *et al*. [77] used a neural network approach to fuse features from multiple sensors for tool condition monitoring in a milling process. The authors gave a poor explanation of feature selection and fusion methods, and the performance of the final system was not quantifiable.

Cho *et al.* [93] designed a multi-sensor based monitoring system for a milling process that investigated both feature-level and decision-level fusion. A combination of correlation-based feature selection and machine learning algorithms were used to classify tool wear state as shown in Figure 2-16. The system was trained using flank wear width measurements. The multi-sensor system was comprised of 8 sensor signals; a three-component dynamometer, a three-axis accelerometer, an AE sensor and a spindle power sensor. A total of 68 possible

features were extracted in the time domain and a further 67 in the frequency domain. The spindle power sensor did not include any frequency domain features. Two feature selection methods were employed to reduce the large feature list to below 25 features. Both feature-level and decision-level fusions were used. A majority vote role was used for decision-level fusion; however, the results showed there was no advantage from combining multiple sensor classifications at a decision level, with single sensor force data providing the most reliable classification result of approximately 90% accuracy. The majority rule is a relatively basic classification technique and better results may be possible with probability-based decision fusion such as the evidential reasoning approach presented by Yaxin *et al.* [95].

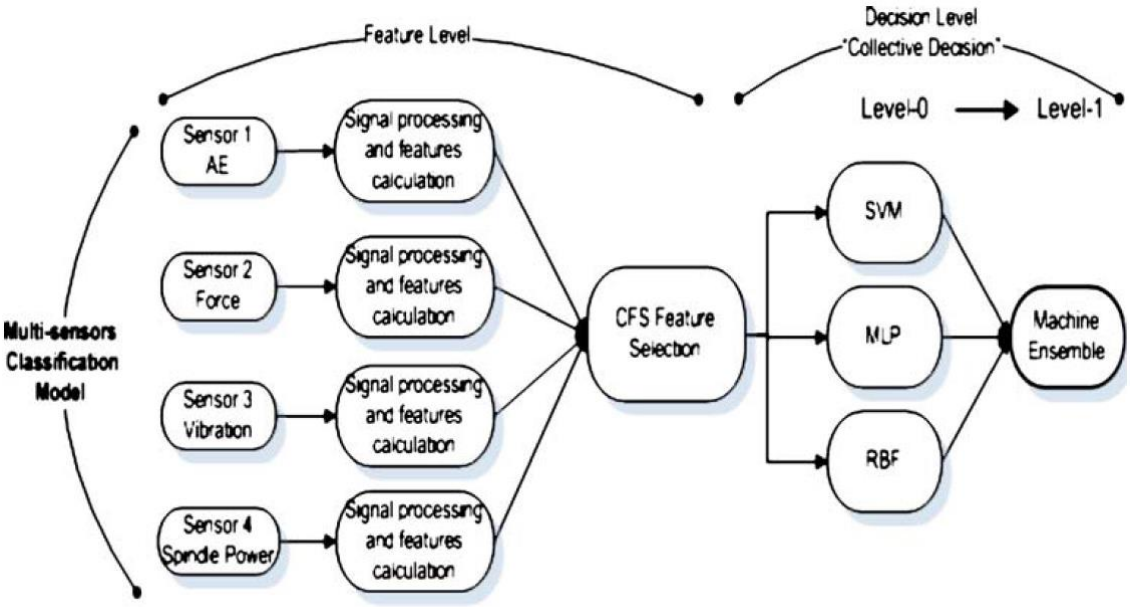

Figure 2-16: Feature level and decision level fusion for tool condition monitoring [93]

It is also uncertain whether there was any advantage of a multi-sensor system, used by Cho *et al.,* when using feature-level fusion. The results of the correlation-based feature selection method using a machine learning ensemble for classification, which were found to be the most accurate methods, are summarised in Table 2-5, listed in order of their performance. Clearly the force sensor is critical to the accuracy achieved, with the vibration sensor the second most influential. It is interesting to see that force, AE and spindle power sensors combined, provide the greatest accuracy (row 1), whereas the AE and spindle power sensors combined provide the least accuracy (row 12). The degree of accuracy improvement should

also be quantified; without the force sensor, rows 7, 9 and 10 have just 2% difference in performance which is less than the classification % errors.

The performance of vibration, AE and spindle power single sensor classification is not reported, otherwise, the paper is a thorough investigation into common sensor combinations. The results could have been improved if the sensor signal feature types were also evaluated and ranked. It is not clear whether the choice of sensor signal features has significant effect on the system, and furthermore, whether there is a need for numerous features to be extracted.

Table 2-5: Classification Accuracy reported by Cho *et al.* [93]

Row Number	Force	Vibration	AE	Spindle Power	% Accuracy	% Error
1	✓		✓	✓	97.67	1.39
2	✓	✓	✓	✓	97.28	1.7
3	✓	✓			96.22	2.23
4	✓	✓		✓	95.82	1.91
5	✓		✓	✓	94.27	2.19
6	✓		✓		92.81	2.7
7		✓	✓	✓	91.58	2.53
8	✓				90	Not reported
9		✓		✓	89.63	2.27
10		✓	✓		89.57	2.43
11	✓			✓	88.85	2.7
12			✓	✓	71.08	2.34
13		✓			Not reported	
14			✓		Not reported	
15				✓	Not reported	

Liu *et al.* [123] split tool wear into five classes depending on the wear stage, as shown in Figure 2-17, although this assumed that the primary wear mechanism was uniform abrasive wear measured by the flank wear width. A neural network was trained to recognise each class based on experimental training data and achieved mean classification error of 8%.

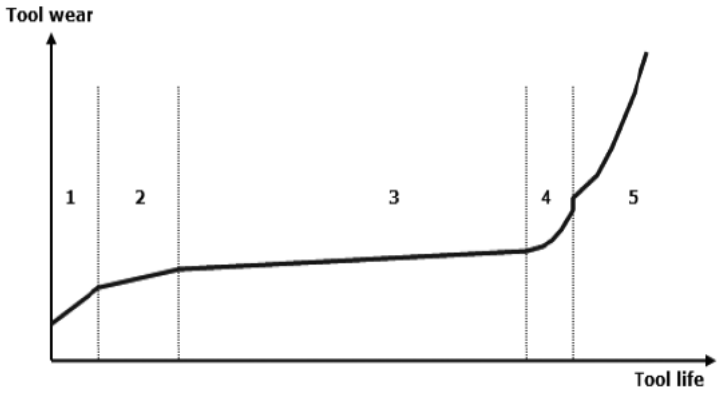

Figure 2-17: Wear classes; 1. initial 2. slight 3. moderate 4. severe 5. worn [123]

Abu-Mahfouz [124], divides each wear mechanism of a drill by five classes; 1. chisel, 2. crater, 3. flank, 4. edge and 5. corner wear. A neural network was trained from drilling data in each of the 5 classes to recognise the wear class. However, there was no discussion of any physical meaning of the sensor signal features in the paper. Given the limited number of tests (4 different tests for training and 2 for validation), it is uncertain if the system would perform in a different machining setup or with different process parameters. Physical interpretation of the sensor data and its relationship to the wear mechanism would provide more confidence in the data-driven model.

Dimla *et al.* [125] select six classes of wear for a milling tool; 1. nominally sharp (low flank, low nose), 2. high flank wear, 3. high nose wear, 4. chipped/fractured nose, 5. high flank and high nose, 6. high flank, high nose and fractured or chipped. Training data was used to populate a neural network for a specific operating condition, though the capability of the network to operate on unfamiliar cutting processes was not discussed. In particular, it was noted that the prediction was still accurate for a different grade of cutting insert, although this was only the case for predicting severe wear. It is generally accepted that the detection of severe wear is easily measurable in such a process and is used frequently in industry. It was also noted that the system deteriorated significantly when changes were made to depth of cut and feed rates.

Fuzzy Classification

A Takagi-Sugeno fuzzy model used for decision level sensor fusion was presented by Aliustaoglu *et al*. [42]. In this example three sensors are used - force, a microphone and an accelerometer. A first stage fuzzy model obtains a membership function for each sensor individually by assessing 4 sensor signal features (mean, standard deviation, RMS and maximum). This is a feature level data fusion step. The decision level data fusion then follows - the outputs of the first model are entered into a second fuzzy system combining the three sensors predictions from the first model. This model then classifies the tool wear state as sharp, workable or dull. Some issues are observed in this method, including the apparent normalisation of the sensor signal data to between 0 and 1; a step that will require additional training data and one which will be fundamental to the performance of the system. Uncommon classifications terms were stated as sharp, workable and dull. However, there is no discussion of the wear magnitude or wear mechanism. The evidence for requiring application of such sensor fusion techniques to machining is not clear as no comparison is made to alternative techniques, such as linear regression or simply setting scalar thresholds on feature magnitudes.

Morgan *et al.* [41] implemented a fuzzy classification system in order to troubleshoot faults occurring in a milling process. The system allowed common issues such as chatter, material condition, tool run-out and machinability variation to be managed effectively with a machine operator's guidance and, in some cases, autonomously.

Other Classification Examples

A potential issue with the multi-class approach is that each tool, process or material type may result in different class definitions, resulting in extensive training data requirements when trying to apply a common method to a range of machining processes.

In order to improve the performance and flexibility of tool wear classification, different tool wear mechanisms and wear patterns and their relationship to sensor signals must be better understood. Consistent, well-defined classes of a tool's wear state across the research community would be a great benefit, allowing comparison to be made between different published results.

A good example where attempts have been made to link specific cutting process faults to sensor signal effects is given by Marinescu and Axinte 2009 [91], where the authors attempt to detect the condition of individual flutes on an indexable end mill. The entry and exit of individual teeth can be identified from the AE sensor signals for a single tooth engaged at a time. There was some evidence that this could also be achieved for up to 3 flutes engaged at one time. However, the research did not manage to isolate single tooth failures from the sensor signals and focussed mainly on a specific small number of AE sensor signal features in the frequency domain. The same author then applied a real-time controller to the issue of a single damaged flute to allow the feed rate to be reduced during a single flute pass then returned to normal for the non-worn teeth [31]. An automated solution was presented for a two-flute indexable tool. However, a particularly slow tooth passing frequency (TPF) was used of almost 0.1 seconds between tooth passes, meaning the controller only requires good performance at low frequencies. The example does not describe the systems' dynamic response; therefore this frequency limitation of the control system cannot be identified.

Shao *et al.* [48] investigated the possibility of classifying a 4-flute indexable milling tool as new, one tooth broken and two teeth broken, using frequency domain content of the spindle power signal. The results presented were inconclusive. Some evidence showed that the difference between the two failures could be detected from the signal processing technique applied. However, it was concluded that this was only tested for severe tool damage and it is therefore arguably far from the sensitivity requirement to detect tool condition prior to sever failure. Furthermore, the experiment applied a particularly low TPF of less than 5Hz. TPFs of above 50Hz are more common, and have been found to be outside of the band width of power measurement.

Siddhpura [126] discusses methods of flank wear width prediction in turning and presents all previous work as classification problems without mention of regression or probabilistic methods. The author lists the available classification methods as neural networks, fuzzy logic, neuro-fuzzy, hidden Markov models and support vector machines. No direct probabilistic methods are discussed.

Most of the classification approaches discussed attempt to classify a tool wear state, assuming that the tool wear states can be defined. Due to the complex nature of tool wear, however, these states cannot be defined easily, and in production environments it is not

practical to obtain tool wear status. If class definitions are not known or training data is unavailable for a monitoring system, these supervised learning algorithms would be unsuitable. All classification methods reviewed required training data to define classes.

2.4.4 Regression

Regression is concerned with the prediction of continuous quantities. It is a field that has been applied extensively in condition monitoring and predictive maintenance; however, only a few publications have been found where regression is used in metal cutting monitoring systems.

Jemielniak *et al.* [96] developed a tool condition monitoring system for turning that estimates the proportion of a tool's life that has been consumed. Force, accelerometer and acoustic emission sensors were used and 582 features were obtained initially from 6 sensors. The features were down-selected based on their correlation to tools' time in cut, resulting in a selection of 62 features. The model estimate of a tools consumed life was also ranked using correlation (root-mean-square estimate, RMSE) to the true remaining useful life. The result of different sensor combinations is presented in Table 2-6, listed in order of their performance. Clearly, the force data provides the most useful information; the performance is diminished when combining with the other sensors. The combination of vibration and AE data (row 3) improves the RMSE value by only a small amount when compared to these sensors individually (rows 4 and 5). Should the computation time of the RMSE be a constraint, a faster alternative, such as median absolute deviation, could be considered.

Table 2-6: Classification Accuracy reported by Jemielniak *et al.* [96]

Row No.	Force	Vibration	AE	RSME
1	✓			8.7
2	✓	✓	✓	10.3
3		✓	✓	12.5
4		✓		13.4
5			✓	14.4
6	✓	✓		Not reported
7	✓		✓	Not reported

Remaining Useful Life

A common function of condition monitoring systems is the ability to estimate both the current state of a system and its future degradation. A useful parameter in prognostics is the remaining useful life (RUL) of a system. This is the estimated time for the system to go from its current state to its end of useful life. It is important to assess RUL for asset management across the engineering disciplines as this impacts the planning of maintenance, replacement part delivery, operational performance and use of an asset's full useful life before replacement or repair takes place.

The remaining useful life of a product is a variable which depends upon the current age, the operating environment, the observations over its current use and the quality and integrity of the product at the start of its life.

Si *et al*. [107] review probabilistic data-driven approaches to RUL estimation. Two methods are defined; those which use recorded failure data, and those which use Condition Monitoring (CM) data. The latter is typically where assets cannot be run to failure or where this data is sparse. Where CM data is concerned, the author identifies that the choice of RUL model and failure threshold will be dependent on whether this data is direct or indirect monitoring data. It is also noted that very few studies have been carried out into combining physics-based models with data-driven models. The paper focuses on probabilistic methods, as it states that probability density functions (PDF) of the RUL of a product are essential for risk analysis and decision making.

Zaidan *et al*. [108] developed a degradation model for civil aircraft gas turbine engines. The 'normalized turbine gas temperature margin' was used as the single measure of the aircraft engine health over time. Previous data were combined with live data from the aircraft to estimate the degradation model, from which the failure time distribution and remaining useful life of the engine was estimated. The end of life was defined by the point at which the normalized turbine gas temperature margin reached a threshold value. A Bayesian framework was used, shown in Figure 2-18. This approach provides a rigorous framework to predicting remaining life of a system, however there are some limitations that would need to be addressed to apply this approach to the monitoring problem presented in this thesis. Firstly, the degradation model is linear which is not representative of many systems in

machining such as tool wear. Secondly, the input is a single pre-defined variable that is not derived within the paper. The derivation of this scalar input and the failure threshold value are critical constraints to the overall system performance. Multiple sensor signal features may be available to improve the performance of the system and the derivation of the failure point would ideally be derived from physical process knowledge or models.

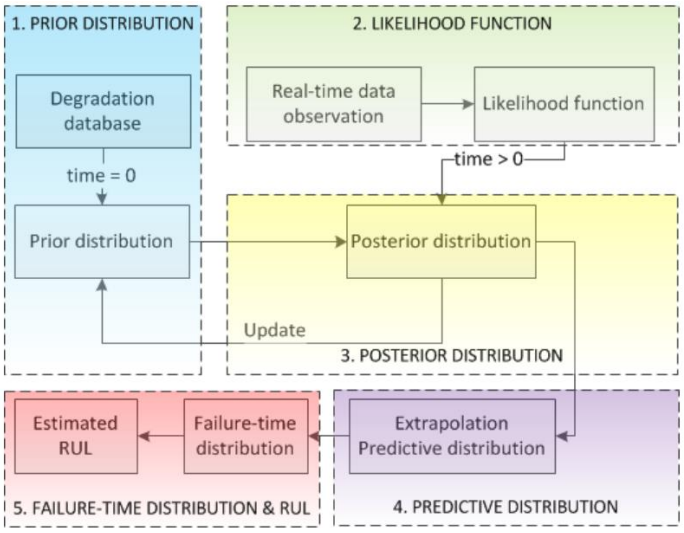

Figure 2-18: Bayesian framework proposed by Zaidan *et al.* [108]

Tobon-Mekjia *et al*. [106] presented a diagnostic and prognostic system using dynamic Bayesian networks. A database of previous laboratory data on tool life is used in conjunction with live data to determine both the current condition of the tool and its remaining useful life. Both estimations are provided with confidence values. Extensive previous tool sensor and tool wear measurement data were required to train the data-driven system. The author explains that analytical models and experience data was not used due to the complexity of degradation phenomena.

2.4.5 Unsupervised Learning

Farrar and Worden [89] explain that if “training data comes from multiple classes and the labels for the data are known, the problem is one of supervised learning. If the training data do not have class labels, one can only attempt to learn intrinsic relationships within the data and this is called unsupervised learning”.

In the absence of class labels, a 2-class classifier can still be formed which can separate normal data with faulty data. This technique is novelty detection (it has also been referred to as anomaly or outlier detection). It is surprising to see such little discussion of unsupervised learning in machining process monitoring literature. In fact, there is only a very brief mention of it in the highly-sited review paper by Teti *et al.* [19] referencing a computer science text book from 1989 [110]. The review paper by Liang *et al.* [29] has no discussion of unsupervised learning at all, nor have the review papers by O'Donnell *et al.* [54] or Bryne *et al.* [27]. Each of these review papers, however, do highlight the issue that training data is expensive and presents a challenge to production application, therefore it is surely appropriate to investigate learning algorithms that overcome the need for much or all of this training data.

Sick [109] provides a more rigorous review of both supervised and unsupervised neural networks for tool wear monitoring in turning. The author explains that unsupervised network paradigms are used for classification tasks only, as opposed the estimation of a continuous quantity. Tool wear measurements and cutting experiments are said to be costly and make unsupervised training an interesting approach. It is proposed that an unsupervised approach will only work if classes are easy to separate, yet with no explanation the author states that "it is hard to believe that unsupervised paradigms can be successfully used in a monitoring system which is designed for practical applicability".

Silva *et al.* [111] apply a self-organizing map (SOM) to sensor data in order to predict flank wear width. The results show a good correlation between the SOM prediction and the true FWW; however, it is unclear how this prediction can be made without some training from measured tool wear data. The paper concludes that for a TCM application in turning, unsupervised algorithms may perform significantly better than supervised ones. This is inconsistent with the view from pattern recognition experts such as Bishop [90], who states that "methods based on unsupervised techniques take no account of the target data, and can therefore give results which are substantially less than optimal". It should be noted that Bishop also states that "in practice dimensionality reduction by unsupervised techniques can prove useful in many applications".

Burke [112] uses both supervised and unsupervised neural networks to monitoring the wear on a cutting tool. Tool wear data is required in order to select appropriate features from an

optimisation function. This required 15 new tool measurements and 15 worn tool measurements, therefore the system, as a whole, already demands what are considered expensive measurements for training, regardless of the subsequent neural network chosen. Furthermore, the author requires tool wear class labels in order to evaluate the results.

Jammu *et al.* [113] use an unsupervised neural network as a 2-class classifier for tool breakage detection in turning. Only normal cutting condition data was required to train the network and no response data was needed, such as tool wear measurements. All tool breakage cases were noted to be very severe, where more than a third of the insert was lost. Whilst the unsupervised learning approach was interesting, tool breakage detection systems are commercially available and adequately detect relatively minor tool breakage events with basic limit setting methods. The neural network method presented is therefore not suitable for the experiment chosen.

A relatively small number of unsupervised learning techniques have been applied to machining. A handful of further publications including Dimla *et al.* [114], Ko *et al.* [115], Li *et al.* [116] and Niu *et al.* [117], provide similar findings to those discussed above.

2.5 Literature Review Summary

The literature review has covered many aspects of machining process monitoring systems. A brief summary of the key outcomes from the literature review are listed below.

The review has shown that an extensive body of previous literature has been published in the area of sensor based monitoring of machining processes. Several previous authors have identified the implementation challenges of the systems studied and highlight that the integration of sensing into a production machine is a challenge. Authors have also highlighted that there is no common approach to the design choices of a sensing system, such as the sensor types and specifications, the signal processing steps and the machine learning algorithms.

Sensor types have been summarised and the common selection of vibration, spindle power and acoustic emission sensors are practical for production implementation, whilst force and temperature sensors are not currently feasible in most production systems.

Feature extraction, selection and reduction algorithms are not in themselves novel in the machining literature, and many common machine learning algorithms have also been employed. However, the limited applied research using unsupervised learning algorithms is noted.

For further reading on the application of machine learning techniques, particularly to SHM applications, see the texts by Farrar and Worden [89] and Bishop [90].

3 MONITORING SYSTEM DESIGN CONSIDERATIONS

The previous chapter identified that there are implementation challenges preventing exploitation of monitoring systems research. It was highlighted that there is no common approach to solving monitoring system problems for machining applications. Issues such as training time or false alarms from current systems make the cost of implementing production solutions prohibitive. The production challenges and opportunities should therefore be reviewed.

This chapter explores a number of design considerations when defining a monitoring system for application to a machining process. A Process Failure Mode Effect Analysis (PFMEA) was carried out to identify the functional requirements of the system. Some of the design hierarchies were then considered, followed by a look at a key software design choice in the selection of supervised or unsupervised learning algorithms. A more specific look at the practical requirements and limitations for tool condition monitoring is discussed at the end of this chapter.

3.1 Process Failure Mode and Effect Analysis

The first step in understanding the need for a monitoring system for a machining process is to consider what is missing from current processes. For this study, existing machining processes have been interrogated to determine the failures that have occurred, the causes of these failures, the effects from the occurrence and the detection methods currently in use. Established PFMEA methods have been used to obtain this data.

A significant amount of recent process monitoring literature aims to identify root causes of process variations to allow the manufacturing process to be adaptable and autonomous and to allow failure events to be predictable ahead of time. An investigation into the relationships between key process variables, observable events and failures is therefore appropriate.

Dey and Stori [40] state that the most notable root causes of machining process variations are workpiece hardness, stock size and tool wear variations, though there is no specific root cause analysis. The system developed in the paper measures acoustic emission and spindle

power sensor signals collected from sequential machining operations that include drilling and face milling. A Bayesian network approach attempts to differentiate between tool wear, workpiece stock or workpiece hardness variation. The applicability of this approach is limited; it does not consider the wide range of process variables and their interactions and therefore it may not be robust when operating under different conditions.

A more thorough root cause analysis was completed by Alaeddini and Dogan [120], where a Bayesian network is used for fault diagnosis from statistical control chart data. The network attempts to relate 22 statistics from the process and 5 control chart patterns to one of 7 assignable causes.

Lewis and Ransing [121] introduced a defect / meta-cause / root cause relationship diagram, which formed the backbone of the Bayesian network. This directed network was constructed to determine the probable root causes and meta-causes from a given defect. The same authors applied this approach to a casting process in [122], where some 30 defects, 38 meta-causes and 112 root causes were included in the network.

The flexibility and accuracy of a diagnostic network such as those described will fundamentally depend upon the quality of data that can be measured from the process. If the data does not contain any information that allows one to distinguish between faults, the fault identification system is redundant. The task of generating the causal relationships is still an important prerequisite to ensure the complexity of the process is understood.

3.1.1 PFMEA Results and Analysis

A PFMEA was carried out as part of the problem formulation, engaging industry experts to identify common machining process issues.

Machining processes are continuously being developed and improved in industry, though in all cases, uncertainty in the input variables can result in the occurrence of process failures. In a production environment, such occurrences lead to conservative operating conditions being selected, additional manual intervention times and in many cases the need for re-work or scrap.

The full PFMEA data is included in Appendix A. The first aspect of the PFMEA is to form the process steps. These are listed in Table 3-1. The single step of 'Run Milling Process' is investigated further. All other steps are available in the Appendix.

Table 3-1: PFMEA Process Steps

Number	Description
10	Assemble tool
20	Load tool
30	Assemble fixture
40	Load Fixture
50	Align fixture
60	Load part
70	Clamp part
80	Load program
90	Run turning program
100	Run drilling program
110	Run milling program

From the 'Run milling program' step, 18 different failure modes and 25 different causes were identified, which resulted in 87 different failure mode and effect combinations.

As an example of the data gathered, the potential causes of tool breakage are listed in Table 3-2, along with current process controls and associated scores for severity of occurrence (SEV), frequency of occurrence (OCC), effectiveness of detection method (DET) and finally the risk priority number (RPN = SEV*OCC*DET).

Table 3-2: PFMEA for tool breakage

Process Step	Potential Failure Mode	Potential Effect(s) of Failure	SEV	Potential Cause(s) of Failure	OCC	Current Process Controls		DET	RPN
						Prevention of Failure Mode Escape	Detection of Failure Cause		
Run Milling Program	Tool breakage	Geometric part error, tool damage, delay,	8	Part condition has changed	6	None	Operator observation/CoC	6	288
				Material condition changed	5	None	CoC	8	320
				Cutting parameters too aggressive	6	None	Double sign off	5	240
				Spindle speed excites part vibration mode	5	None	Tap test / harmoniser	8	320
				Wrong tool used	4	Tooling control & spec.	Double sign off	5	160
				Wrong cutting parameters used	6	None	Double sign off	5	240
				Tool is worn or damaged	5	Tooling control & spec.	Double sign off	5	200
				Part position error changes depth of cut	4	None	Double sign off	7	224
				Tool length error changes depth of cut	4	None	Double sign off	7	224
				Tool not clamped correctly	4	None	Double sign off	6	192
				Excessive cutting force	5	None	Operator observation	6	240
				chatter due to tool stiffness	6	None	Operator observation	6	288
				chatter due to part stiffness	5	None	Operator observation	6	240
				Collision	4	None	Operator observation	6	192
				Insufficient coolant flow	6	None	Operator observation	6	288
				Incorrect coolant mix	4	None	operator observation	6	192

Once the data is gathered on the process, the application of it in pursuit of a robust monitoring and control system requires further interrogation. In order to effectively apply PFMEA to the machining problem presented in this thesis, the definition of failure mode and failure cause are examined. Standard definitions generally specify the following:

Failure Mode: Specific way in which the process can fail

Failure Cause: The root cause of the failure mode

Effect of Failure: The way in which the failure mode affects the process downstream

The definition of root cause can be subjective. Judgement is required to identify where the initiation of a fault should be defined for the PFMEA to be useful. The term 'meta-cause' has therefore been applied in this study in order to capture events that follow the root cause and precede the failure. An example is shown in Figure 3-1. This also demonstrates the multiple failure modes that can have a common cause, and multiple causes can reach the same failure mode. The failure mode has been highlighted in the figure as a worn tool condition. The root cause has not been selected.

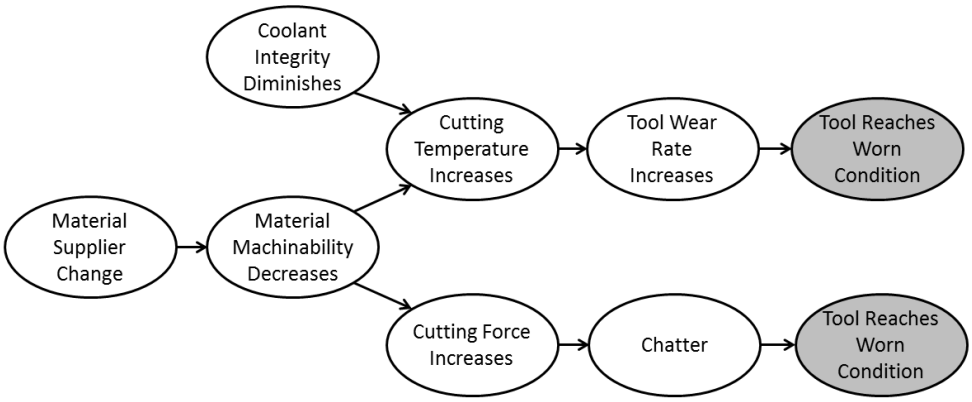

Figure 3-1: Failure cause and failure mode example

For the purpose of this research, the following criteria will be applied to the standard definitions:

- A failure mode must be the first measurable event that confirms the process is no longer achieving requirements.
- An effect of the failure is any observable event that follows as a result of the failure mode.

- A root cause is the first observable physical change to any key process variables that leads to the failure.
- A meta-cause is any intermediate effect between the root cause and the failure.

In the case of tool breakage, this is an effect that follows a measurable worn tool condition, but it is a failure mode where a tool has sudden failure without the usual tool wear progression. There are many root causes that could lead to tool wear or breakage. The number of meta-causes is vast, growing in number as the desired resolution to technical details increases.

The usual PFMEA approach in table form cannot present these complex relationships; therefore, a directed acyclic graph (DAG) has been constructed from the PFMEA data with consideration to the definitions above. Some of the items in the PFMEA that gave a low risk priority number (RPN) have been removed to rationalise the graph to those of most importance. The result of the study is shown in Figure 3-2.

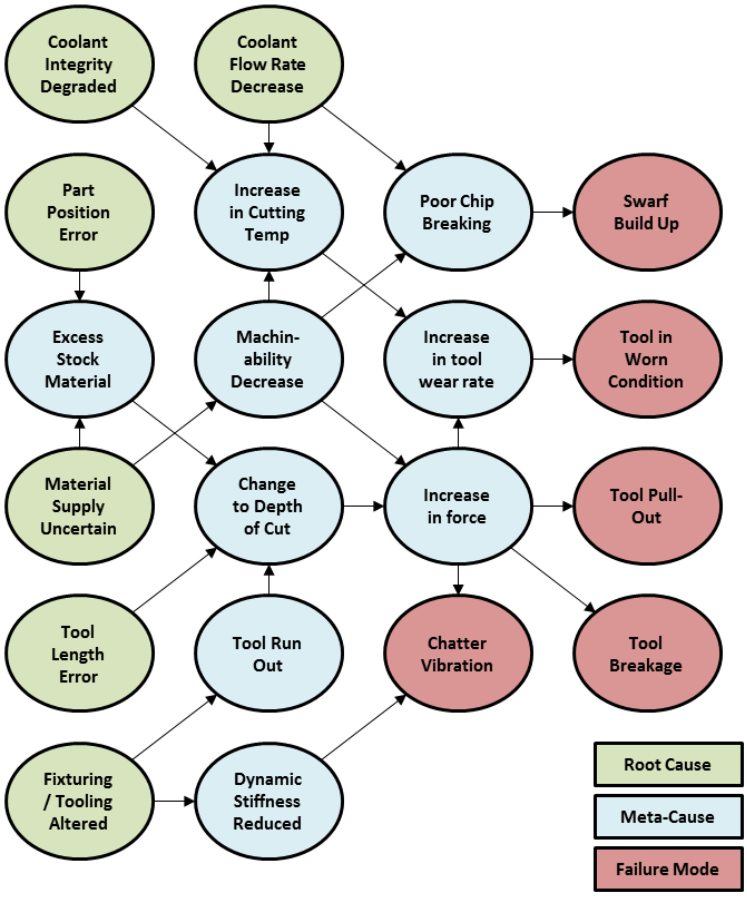

Figure 3-2: DAG relating root causes, meta-causes and failure modes

Each failure mode shown in Figure 3-2 can lead to common effects, including surface finish and surface integrity damage, increase in tooling costs, manual intervention and machine down time. Clearly the ideal scenario is to be able to detect the root causes and take corrective action early on, though there are practical limitations to this. In some cases, these variables are not easily measurable, such as the machinability of a material supply. It is particularly challenging to predict the impact of variation to these input variables, such as tool length accuracy, part positioning accuracy and coolant or filter replacement frequency.

3.2 A Common Design Framework

The complexity of machining processes leads to most publications addressing just one or two of the cutting process methods, key process variables, available sensors and computational techniques. It is impractical to test the systems on a full range of scenarios and processes due to the sheer number of combinations; however, the expert community has not established a common methodology for manufacturers to follow to apply process monitoring and control in production.

Papers referenced in this thesis that present a new method in process monitoring can be summarised through the 8 considerations listed in Table 3-3. It has been observed that most papers omit at least one of the considerations and very few combine all aspects into a single system or test. Whilst it may be pragmatic to look at one key area in the system during early stage research, the absence of a holistic view of the system may be an indication to why there has been limited uptake by industry.

Table 3-3: Considerations for an intelligent monitoring system study

1. What is the target machining process? Drilling, Milling, Turning, Grinding, Broaching, Water Jet.
2. Which process variables motivate the system? Tool Condition, Surface Finish, Machinability, Workpiece Geometry, Dynamic Stiffness, Static Stiffness, Coolant Application, Cutting Tool Design or Selection, Machine Tool or Fixture, Chip Management/Geometry, Non-specific / Root Cause Analysis.
3. What measurements will be taken? Force, Power, Torque, Vibration (≈0-20kHz), Vibration (≈20k-100kHz), Audible Acoustics (≈0-20kHz), Acoustic Emission (≈20k-1MHz), Cutting Temperature, Ambient/Workpiece/Machine Temperature, Vision Systems, Statistical Process Data.
4. How will the signals be processed? Time Domain and Statistical, Frequency Domain, Time-Frequency Approach.
5. How will the useful signal features be determined? Correlation, Entropy/Energy Functions, Segmentation (though process understanding), Follow Previous Publication.
6. What computational methods will be used? Classification, Regression, Neural Network, Bayesian, Fuzzy logic, Hidden Markov Model, Support Vector Machine, Other.
7. What will be computed? Tool Wear, Remaining Tool Life, Tool Breakage / Tool Failure, Depth of Cut, Machinability/Hardness, Workpiece Geometry, other Specific Process Characteristic
8. How will the cutting process be controlled or rectified? Real Time Feed Rate Control, Scheduled Feed Rate Control, Real Time Spindle Speed Control, Scheduled Spindle Speed Control, Tool Change, Manual Intervention.

It is useful to compare the SHM based framework described by Cross [83] to machine tool applications:

- Level 1 (Detection) – automatic detection of fault occurrence
- Level 2 (Classification) – automatic determination of which fault has occurred
- Level 3 (Quantification) – automatic assessment of faults impact on the process

- Level 4 (Prognosis) – prediction of the remaining time until a fault will occur

Given the significant quantity of academic research in manufacturing process monitoring, yet the limited exploitation, it is proposed that an important advancement that must be made in future is a commonly accepted methodology to monitoring system design and test. A design hierarchy for machining process monitoring and control systems is proposed in Figure 3-3.

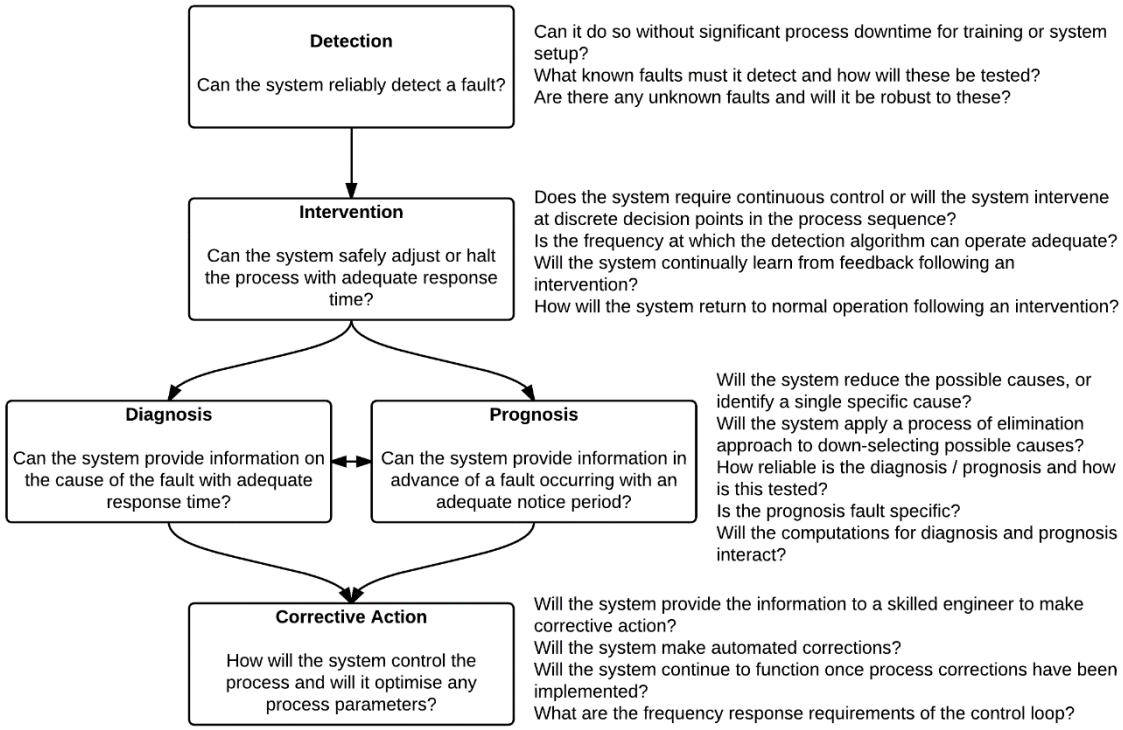

Figure 3-3: Monitoring and control system design hierarchy with context

Fault detection is always the first step in a monitoring system and it may be appropriate to immediately intervene or stop the process to avoid any further costs or damage to occur. Should adequate information be available, fault diagnosis or prognosis may be possible. These steps are the principle of 'intelligent' monitoring, whereby the process does not simply stop at the occurrence of a fault, but provides further information to the operator or machine. In some cases, a corrective action may be identified automatically without manual intervention or process down time.

The computational technique for detection, diagnosis and prognosis often differ. In fact, the computations may be specific for different faults. For example, where a vibration magnitude

threshold is exceeded and frequency domain analysis examines evidence of chatter vibration:

- A faulty condition is identified due to an unacceptable vibration magnitude (detection)
- The feed rate is held immediately to avoid part damage (intervention)
- A chatter diagnosis module compares the X-axis vibration peak frequency magnitude to a threshold value in order to determine the presence of chatter (diagnosis)
- A new spindle speed is selected for the process to continue (corrective action)

Figure 3-4 presents a simplified flow for this fault and also a worn tool fault example.

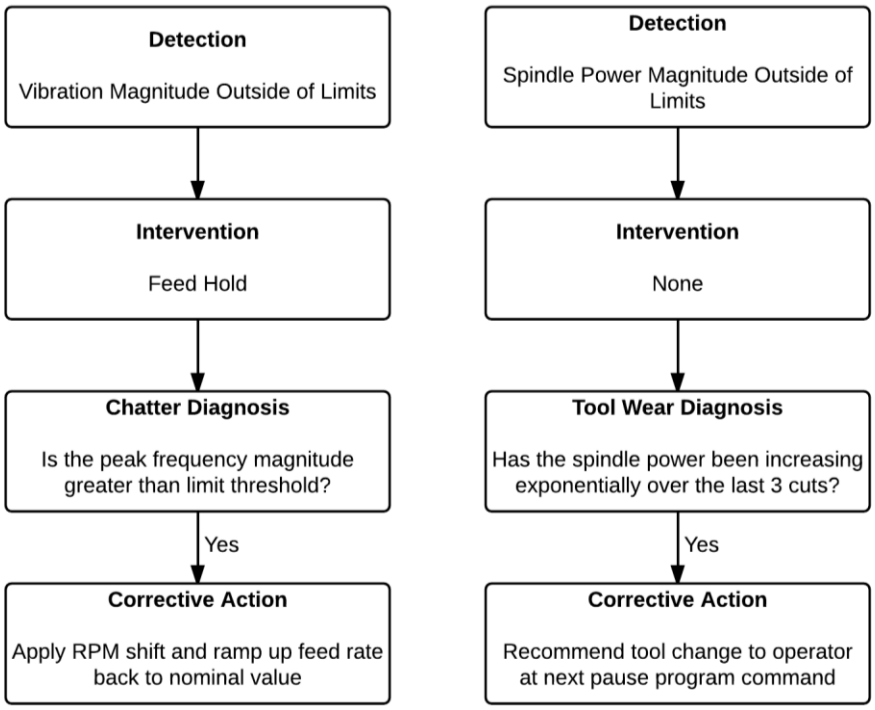

Figure 3-4: Example fault detection and diagnosis scenarios

The example demonstrates that faults can have specific methods for detection, diagnosis and corrective action. Often, these methods will be relatively simple and derived from practical experience. Given this, an understanding of the individual fault types and the solutions to rectify the process is essential when designing a monitoring and control system.

3.3 Supervised or Unsupervised Learning?

With the majority of previous literature applying supervised learning methods, class labels must be measured during the training of the machine learning algorithm. Class labels for machining processes may include tool wear, surface roughness, part geometry and multiple process fault types.

The extensive range of challenges raise questions over how viable the measurement of labels and subsequent training of supervised learning models may be in a production environment. Silva *et al.* [111] state that unsupervised techniques would be an advantage in TCM due to the expense of collecting training data; however, supervised learning techniques dominate machining process monitoring literature. Table 3-4 lists a short selection of research papers that apply supervised learning. The class labels and the measurement method for these labels are also listed.

Table 3-4: Supervised Learning Methods Found in Literature

Reference (first author and title)	Learning Method	Class Labels
[42] Aliustaoglu "Tool wear condition monitoring using a sensor fusion model based on fuzzy inference system"	Supervised: Sugeno Fuzzy Model	Sharp, Workable, Dull (Manual inspection of the cutting tool)
[60] Abouelatta "Surface roughness prediction based on cutting parameters and tool vibrations in turning operations"	Supervised: Regression Model	Surface roughness (Manual inspection of the machined surface)
[77] Ghosh "Estimation of tool wear during CNC milling using neural network-based sensor fusion"	Supervised: Neural Network	Flank wear width (Manual inspection of the cutting tool)
[87] Segreto "Multiple Sensor Monitoring in Nickel Alloy Turning for Tool Wear Assessment via Sensor Fusion"	Supervised: Neural Network	Flank wear width (Manual inspection of the cutting tool)
[118] Özel "Predictive modeling of surface roughness and tool wear in hard turning using regression and neural networks"	Supervised: Neural Network	Flank wear width and surface roughness (Manual inspection of the cutting tool and machined surface)
[123] Liu "Intelligent classification and measurement of drill wear."	Supervised: Neural Network	Flank wear width (Manual inspection of the cutting tool)

There are a number of challenges in collecting class labels from machining processes, for example:

- The labels may be time consuming or costly to define and measure. For example, microscopes, surface measurement equipment and skilled users are typically required for tool or surface measurement.
- The labels may require the machining process to stop for long periods that are not feasible alongside production flow.
- The labels may only be possible to collect accurately under specific machining conditions, for example tool wear such as built up edge obscures flank wear width measurement and surface roughness may be difficult to measure on difficult to access features.
- The labels may be redundant when any change is made to the machining process and therefore new training data would be required on a regular basis.
- Where the label is the occurrence of a fault, the fault must have occurred at least once during the training phase. It is not desirable to run a process to failure due to the potential costs; therefore this data is rarely available.

Previous application of unsupervised learning for machining process monitoring has been reviewed in Chapter 2, though there are still many areas to explore. Given the challenges associated with collecting class labels, as listed above, this thesis will focus on unsupervised learning methods.

3.4 Practical Requirements for Tool Condition Monitoring

The majority of machining process monitoring research is focused on the requirement to monitor tool condition during machining; therefore, this section will investigate this further.

Firstly, the meaning of tool condition monitoring and its purpose should be discussed.

A tool condition monitoring system should be able to provide one or both of the following functions:

(i) The ability to detect when a tool has surpassed its useful life, with a minimum time delay between the point at which the tool's useful life expired and its removal from the process. (Detection)

(ii) The ability to predict when a tool is going to surpass its useful life with sufficient notice to allow a tool change to be carried out prior to end of life. (Prognosis)

The business need for a tool condition monitoring system for a production process can be captured by quantifiable measures on how the system will;

(a) Reduce instances of tools being used beyond their useful life.

(b) Consume more of the useful life of a tool before a tool change, without adversely affecting part quality or process time.

A tool condition monitoring and control system may have additional functionality, such as:

(1) The ability to determine tool wear mechanisms (Diagnosis), leading to;

(2) The ability to select process parameters which extend the useful life of the tool. (Control)

Given that research in this area is extensive, spanning over three decades, it is somewhat surprising that no common method has been followed for a tool condition monitoring system and research approaches have been vastly different. A standard and accepted method by which any tool condition monitoring system can be assessed against measurable performance metrics would be a great help for future research in the area.

Tool change times are generally programmed into machining processes, allowing the tool change to be at a suitable frequency, based on a given tool life criteria, and at a safe point in the machining tool path. Tool change times are generally conservative, especially for high value manufacturing where there is a high impact if a tool fails during its use. A means of measuring the lost opportunity in a current production process is important for comparison purposes. Figure 3-5 shows a hypothetical normal distribution representing the possible tool life for a process. Note that the tool change points are necessary for the majority of production processes, for example, in drilling it may be a practical requirement to drill a complete hole and not change during this task. In this case, the opportunity to increase tool life will be reduced by this resolution.

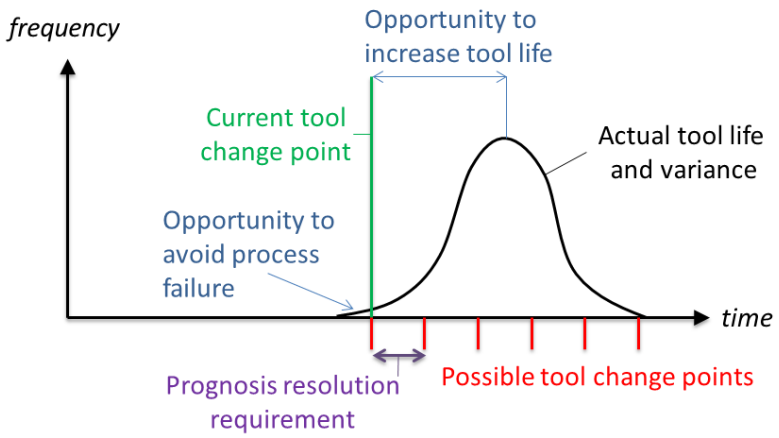

Figure 3-5: Tool condition monitoring opportunity

A popular method in industry is to consider the 'spiral cut length' (SCL) for finish turning tools, whereby the tool may pass over a particular distance before it is likely to be worn. Tool life that was previously expressed in minutes, hours or number of features, can be expressed independently of surface speed and feed rate using the SCL criteria. This may be a good indication of tool life, but given surface speed and feed rate influence wear mechanism and rates, it is unlikely the SCL estimate is precise for a wide range of cutting parameters.

There are many criteria that can be used to define a tool's end of life, such as flank wear width, notch wear, crater wear, volumetric difference, temperature, force, surface finish and surface integrity; therefore, if defining wear state classes, their transferability to other processes is important. For example, it may be that in a machining process for a single component, several tools are defined as worn from different criteria. A roughing tool may be considered worn when it has reached large levels of force that cause chatter, a finishing tool may be worn when the surface integrity is no longer within specification, and other tooling (such as "ripper" geometry end mills) may be considered worn based on a re-grind specification.

3.5 Design Considerations Summary

This chapter has explored several design considerations for a monitoring system for machining applications. From a PFMEA and further consideration of implementation challenges, a number of choices can be made that allow an experimental method to be defined. The key outcomes of this are listed as follows:

- The key failure modes and causes that this research should consider are summarised from the PFMEA in section 3.1
- A list of 8 key design questions presented in section 3.2 will allow the monitoring methods to be chosen
- Unsupervised learning methods will be used given the benefits of not defining or collecting class labels, as described in section 3.3
- The business case for a tool condition monitoring system must be met as described in section 3.4

4 EXPERIMENTAL METHOD

In light of the conclusions presented in sections 2.5 and 3.5, an experimental method was designed to monitor sensor signals from a machining process in order to detect faulty conditions and diagnose fault types. The hardware design, presented later in this chapter, was selected to ensure good coverage of signals emitted from the machining process whilst remaining minimally intrusive in a production scenario. The software was developed in both LabView, for the data acquisition and feature extraction, and Matlab, for all subsequent analysis steps. Further information on the software can be found in Appendix D.

4.1 Selection of Fault Types for Testing

The PFMEA in section 3.1.1 listed the potential failures and causes that a process should be resilient to. The investigation in this earlier section showed that there can be many failure modes and many interactions between causes and meta-causes. All items shown in the DAG in Figure 3-2 have been grouped into six types of fault class; wear, load, machining offsets, tool malfunction, chip formation and dynamics. These have been listed in Table 4-1.

Direct measurement systems are appropriate for the detection of many sources of variation listed. This includes tool run-out, tool pull out, tool breakage, tool length error, part positioning error, workpiece stock, coolant flow rate and coolant integrity. These variables are typically measured using on-machine cutting tool and part probing systems or coolant management and filtration systems that can be found in production today. Fault detection can then be achieved using traditional statistical process control methods.

There has been extensive research and industrial applications of dynamic stiffness testing and chatter detection. Milling chatter avoidance systems are now common in industry and so these sources of variation will be omitted from the experiment.

The automatic measurement of cutting temperature, chip evacuation and chip geometry is not yet viable in production due to issues with sensing, such as line of sight requirements. Whilst the effects of these sources of variation may be inferred from other indirect sensors, these sources of variation can be difficult to control and will be omitted from the experiment.

Section 4.2 will present the design and build of an indirect sensing system that is sensitive to changes in the remaining sources of variation, highlighted in bold in the table; tool wear rate, tool in worn condition, material supply, material machinability, depth of cut, excess stock and cutting force.

Table 4-1: Sources of Process Variation

Fault Class	Source of Variation	Description
1. Wear	**Tool Wear Rate**	This meta-cause is influenced by most changes that can be made to cutting conditions
	Tool in Worn Condition	This failure occurs the first instant a tool that is classed as worn is used
2. Load	**Material Supply**	This is a root cause that includes machinability and geometry variation
	Material Machinability	This meta-cause, a product of the material supply, is influenced by hardness, grains size and Young's modulus
	Depth of Cut	This meta-cause can be a product of multiple causes, including tool length, stock material and part positioning
	Excess Stock Material	This meta-cause is a result of workpiece geometry variation in the form of depth and uniformity of cut
	Cutting Force	This meta-cause can be simulated and measured in the lab, but is difficult to measure directly in production
3. Machining Offsets	Tool Length Error	This root cause may be due to inaccuracy on a tool measurement device, or incorrect tool offset call
	Part Positioning Error	This root cause may be due to part loading, machine tool positioning or coordinate system setting
4. Tool Malfunction	Tool Run Out	The tool run out can impact on surface finish and tool wear in certain finishing operations
	Tool Breakage	A failure has occurred when the tool receives damage that is not a product of wear
	Tool Pull-Out	A failure mode has occurred when the tool holder cannot maintain grip on the tool
5. Chip Formation	Cutting Temperature	This meta-cause is central to machining, but is not possible to measure directly in production
	Coolant Integrity	This root cause may include changes to concentration, chemistry and filtration
	Coolant Flow Rate	This root cause has a direct impact on cooling and may include coolant jet obstruction
	Swarf Collected	This failure has occurred when the swarf has collected to the degree that it is obstructing the cutting edge
	Chip Evacuation	This meta-cause leads to collection of swarf and is usually feature specific
6. Dynamics	Chatter	This failure has occurred once chatter has an impact on the machined surface
	Stiffness of Setup	This root cause exists where components, such as tool or fixture, are insufficiently stiff for the operation

4.2 Design and Build of a Sensing System

The selection of a measurement system is required in order to capture process data that indicate a fault. In order to avoid disruption and intervention, and to be consistent with the reviewed literature, an indirect sensing system will be used in this research. Vibration, acoustic emission, spindle power and microphone sensors have shown to be suitable for monitoring the condition of a machining process without being intrusive.

The design and build of a robust sensing set up that would be feasible in a range of industry settings was important to ensure methods developed were transferable. Sensors could not be installed within the spindle due to access limitations in the machine tool; therefore, the design was to embed vibration and acoustic emission sensors in the work holding. In addition to this enclosure, two microphones were placed in the machine volume and a power transducer was used for spindle power measurement. The result was a portable multi-sensor platform that was minimally intrusive to a machining process, but still able to capture a range of signals from the cutting process.

The sensor enclosure is shown in Figure 4-1 and the fully dimensioned drawing is shown in Figure 4-2. The enclosure was milled on a 3-axis milling machine from a rigid stainless steel plate of 450x450x46mm external dimensions once machined. The plate has 4 M12 clearance holes to attach to the machine bed and 18 M12 attachment holes to allow workpieces to be held in place. All electronics are located inside the cavity with 3 sensors making direct contact with the workpiece; the AE sensor, a current transducer for measuring the proximity/presence of the located component and a spring loaded thermocouple to take an approximate reading of the workpiece temperature. A tri-axial accelerometer and a single axis high frequency accelerometer are contained in the cavity.

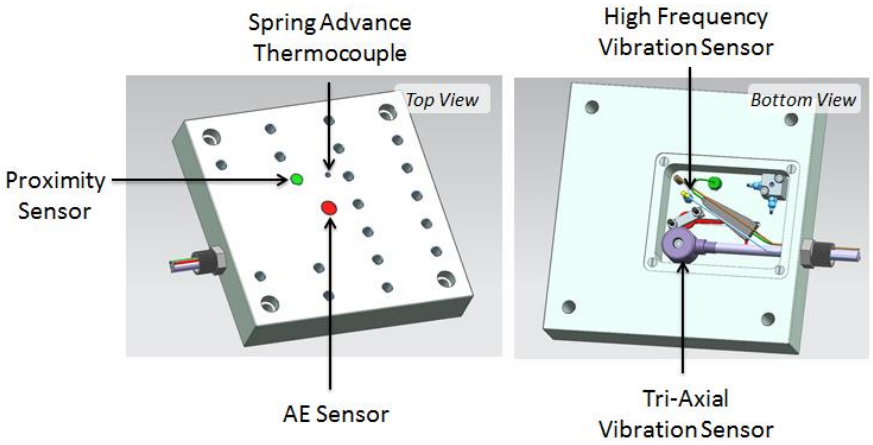

Figure 4-1: Sensor Enclosure

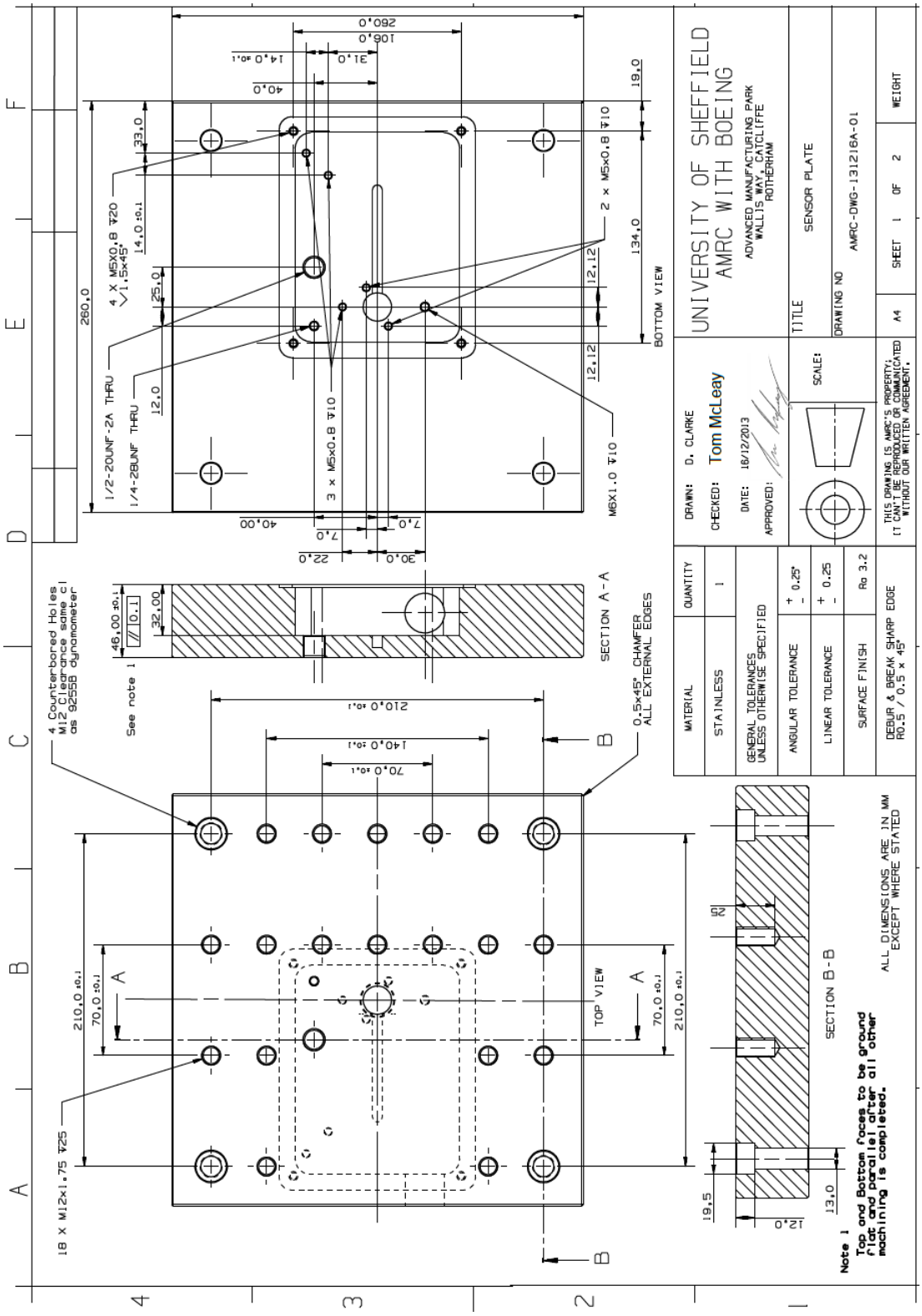

Figure 4-2: Sensor Enclosure Dimensioned Drawing

A microphone unit is also placed in the machine volume using a magnetic base. This enclosure contains two microphones of different frequency response characteristics and is shown in Figure 4-3. The microphones are directed towards the workpiece at approximately 2 metres' distance.

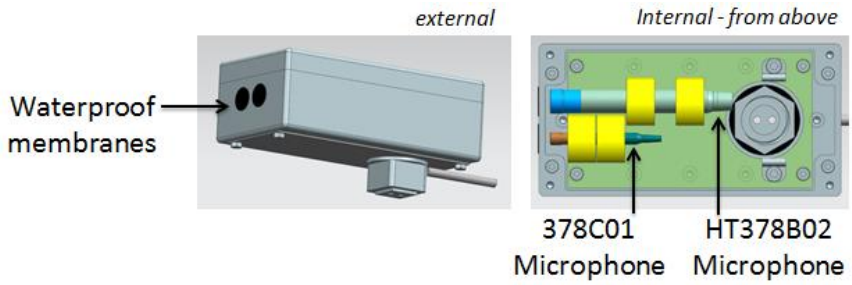

Figure 4-3: Microphone unit

All sensor cables are connected to the data acquisition unit shown in Figure 4-4, where a National Instruments compact data acquisition module (DAq) converts the signals to digital form. The acoustic emission sensor requires a pre-amplifier prior to connection to the DAq.

The machining setup with a titanium work piece loaded can be seen in Figure 4-5. A summary of the sensor properties is shown in Table 4-2.

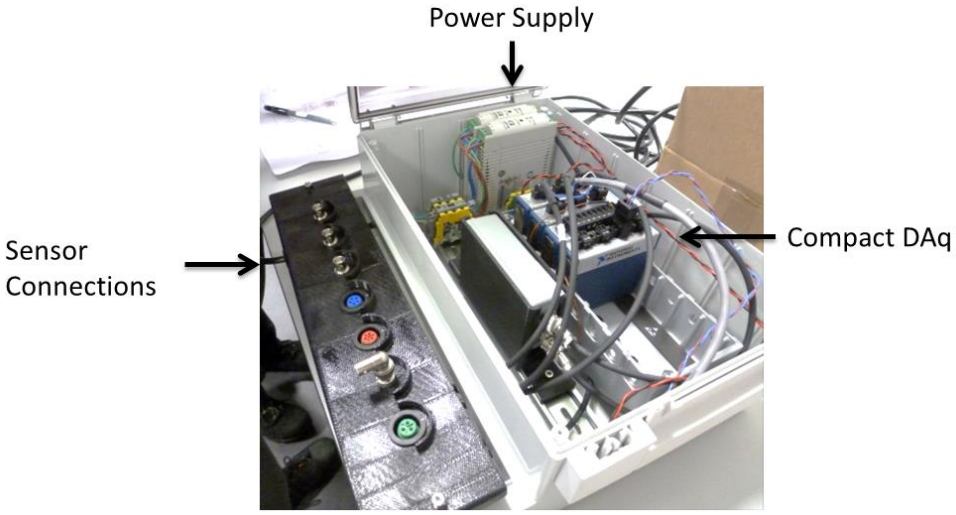

Figure 4-4: Data acquisition unit

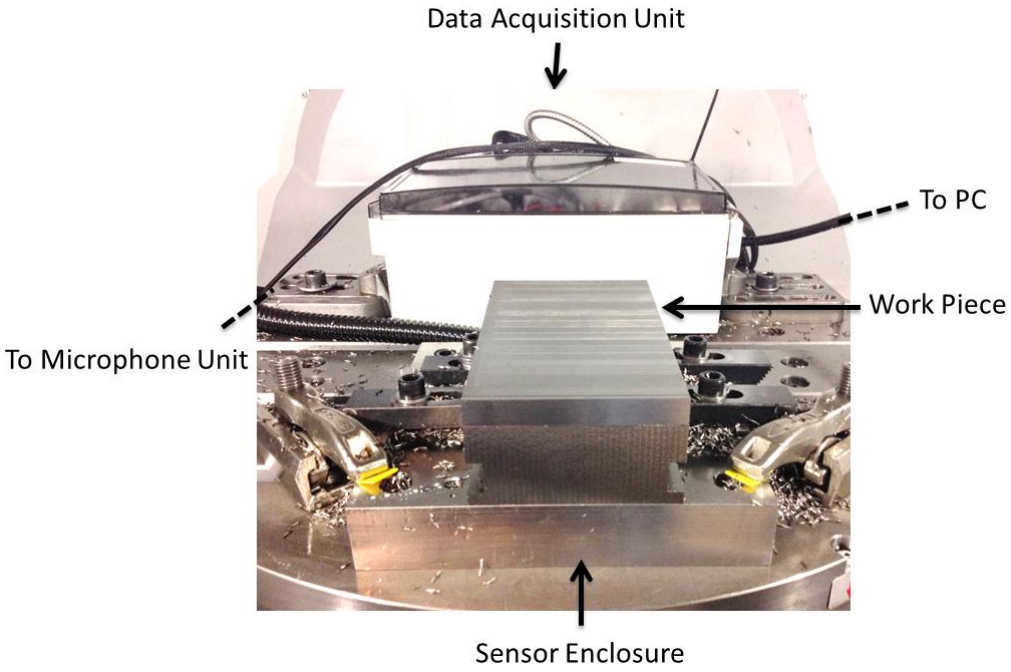

Figure 4-5: Machining setup

Table 4-2: Sensor Summary

Sensor Description and Manufacturer	Short Name	Location	Bandwidth	Sensitivity
Tri-Axial Accelerometer (PCB, 604B31)	*XV, YV, ZV*	Fixture (X, Y and Z)	0.5-5000Hz	100mV/g (+/- 50g scale)
High Freq. Accelerometer (PCB, 352A60)	*HF*	Fixture (Z only)	5-60kHz	10mV/g (+/- 500g scale)
Acoustic Emission (Physical Acoustics, R15/S)	*AE*	Fixture (mating workpiece)	50k-400kHz	Peak, Ref V/(m/s), 69dB
Microphone 1 (PCB, 377B02)	*M1*	Machine Volume (free-field)	5-10kHz (1dB) 3.15-20kHz (2dB)	50mV/Pa
Microphone 2 (PCB, 377C01)	*M2*	Machine Volume (free-field)	6-12.5kHz (1dB) 4-80kHz(2dB)	2mV/Pa
Thermocouple (Nanmac, B9-1-K)	*T*	Fixture (mating workpiece)	N/A	41µV/°C (max 230°C)
Proximity Sensor (LORD, NC-DVRT-2.5)	*D*	Fixture (mating workpiece)	Max 800Hz	0.25mm/V
3-Phase Power Transducer (Load Controls, PPC-3)	*SP*	Electrical Cabinet (spindle motor)	0-50Hz	0.3kW/V (Max 3kW)

(Although the high frequency accelerometer is measuring in the z-direction, to avoid ambiguity, the accelerometer signals will be referred to as 'x-accelerometer' (604B31), 'y-accelerometer' (604B31), 'z-accelerometer' (604B31) and 'high frequency accelerometer' (352A60)).

The literature review identified that cutting processes exhibit signals from lower frequencies, such as structural vibrations, through to ultrasonic frequencies relating to the chip mechanics. Sensors have been selected to cover as wide a range of frequencies as possible. Figure 4-6 shows the sensor bandwidths on a logarithmic scale, where all frequencies between 0.5 and 400 kHz are covered by at least one sensor.

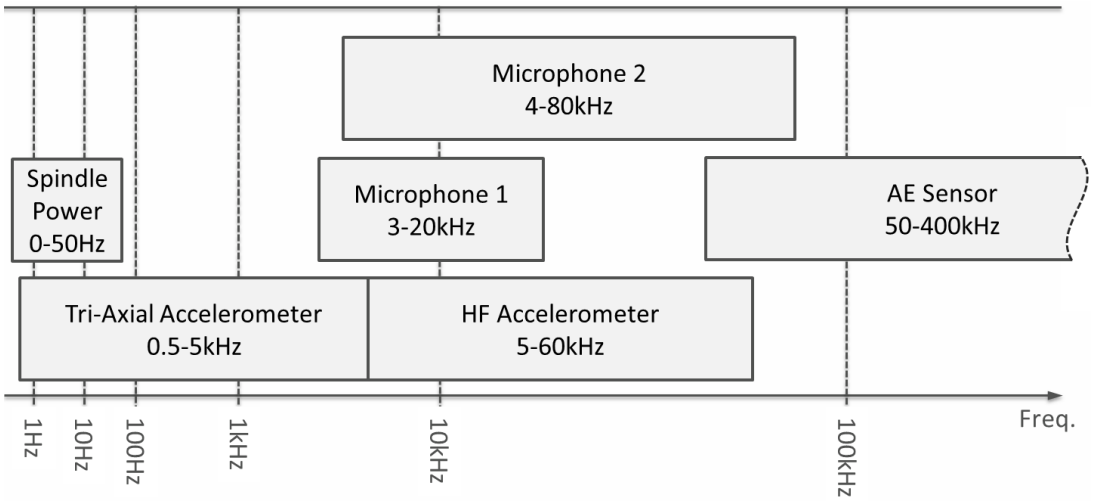

Figure 4-6: Bandwidth of Selected Sensors

4.3 Experimental Setup

The proposed experiment enables multi-sensor data to be captured in a milling process, where the sensing is minimally intrusive. A 3-axis finish profile milling process for titanium 6Al-4V was selected as this is a common application in high value manufacturing. The experiment included two tests; one for each of the two fault classes of wear and load.

A final case study experiment has been obtained from previous literature. This experiment allows the methods proposed and tested on experiment 1 and 2 data to be validated on an additional data set with different machining conditions. Each experiment is described in more detail below.

4.3.1 Experiment 1: Tool Wear Test

Tool wear is an important indicator in cutting processes and has previously been measured in laboratories by examining wear mechanisms and wear rates under a microscope. An unsupervised monitoring system will be demonstrated in this research; therefore, the experiment will run all cutting tests with minimal stopping of the process for the direct inspection of tool or workpiece.

This experiment will carry out repeat profile mill cuts stepping across into the workpiece (perpendicular to the feed direction) after each cut. The test will begin with a new tool and continue until the tool is considered severely worn by the machine operator's judgement. The experimental parameters are listed in Table 4-3.

Table 4-3: Experimental Constants – Tool Wear Test

Parameter	**Value**
Machine Tool	Mori Seiki NMV8000 5-axis Mill Turn
Work Piece Material	Titanium 6AL-4V
Tool Holder	Hydraulic grip BT50 (392.369HMD-50 32 110)
Cutting Tool	3 flute, 16mm diameter carbide end mill (1P330-1600-XA 1620)
Tool Stick Out	55mm (tool length to gauge point 165mm)
Tool Path	Straight cut profile milling
Axial Depth of Cut	8mm
Radial Depth of Cut	0.5mm
Surface Speed	80m/min
Rotations per Minute	1592 RPM
Feed per Tooth	0.18mm/tooth
Feed per Minute	859mm/min
Tooth Passing Frequency	79.6Hz
Coolant	Coolant off

Coolant will not be used in this trial given that it substantially increases the life of the cutting tool, and therefore the cost of the experiment. Practical limitations mean that it is necessary to preserve material and ensure all preparation and cutting tests can be completed in the short time available on the machine tool. A number of microscope images will be taken during the experiment to confirm the wear mechanism; however more extensive tool wear measurements will not be available.

A cross section of the chip (normal to the tool axis) produced from the listed cutting parameters is shown in Figure 4-7. Note that the time for the tooth to pass over the 2.9mm distance is approximately 2.2 milliseconds. When considering helix of 45 degrees and 8 mm axial depth of cut, a single flute pass continues for another quarter of a revolution of the tool. The total time for each flute pass can therefore be calculated to be just below 12 milliseconds.

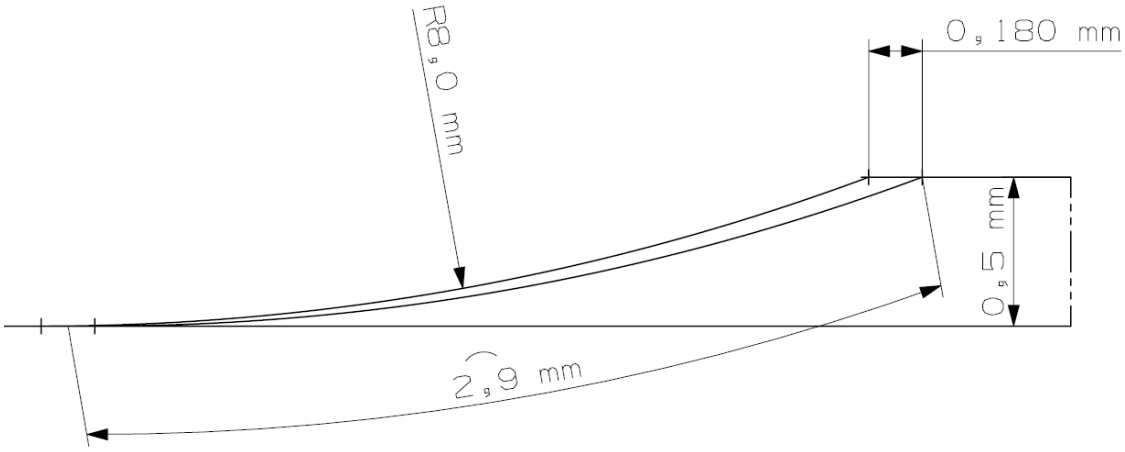

Figure 4-7: 2D cross section of chip thickness

The tool and work piece in mid cut are shown in Figure 4-8

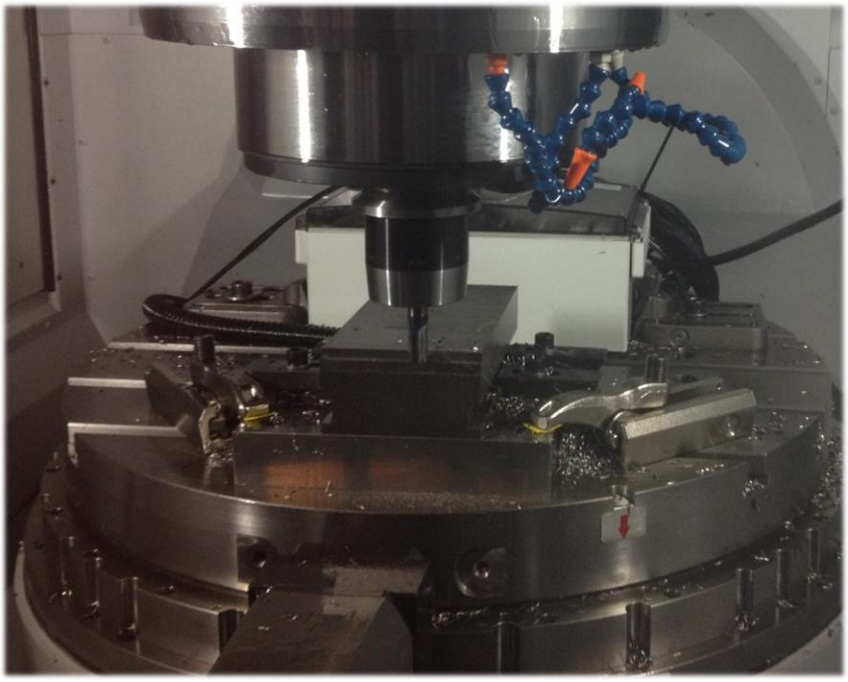

Figure 4-8: Tool and workpiece during cutting trial

4.3.2 Experiment 2: Depth of Cut Test

A number of parameters are linked to cutting tool loads, including depth of cut and machinability. This test will introduce variation in the radial depth of cut for a new cutting tool. The data from this cutting condition will be used as an example fault condition.

Changes to the tool load that are not a product of tool wear may lead to issues such as increased wear rate, chatter and poor surface finish. Whilst tool load can be detected using spindle power, small changes to tool load, that are not simply a result of the current tool wear state, may be more challenging to identify.

This experiment will use the same conditions as the first, however radial depth of cut will be altered and an unworn tool will be used for all tests. Four cuts will be taken using a radial depth of cut of 0.25, 0.75, 1.0 and 1.25mm. Each of these examples will be used as fault conditions in the analysis section.

4.3.3 Experiment 3: Published Case Study Data

The Prognostics Health Monitoring (PHM) Society made a set of milling tool wear sensor data available for the PHM challenge 2010. These data have been used as a case study in this thesis in order to demonstrate that the methods derived in the analysis are easily transferable to other experimental conditions. Further information is available at https://www.phmsociety.org/competition/phm/10S.

The data set comprises of 6 tool life experiments where a three-flute ball nose end mill profile milled an angled face of a HRC52 stainless steel plate. Cutting parameters of 10400RPM, 1555mm/min, 0.125mm radial depth and 0.2mm axial depth were used and a total of 315 cuts each 108mm in length were taken with each tool. The cutters flank wear width was provided after each cut for 3 of the 6 tools used. During machining, a three-channel dynamometer (Fx, Fy, Fz), a three-channel accelerometer (Vx, Vy, Vz) and an RMS filtered signal from an AE sensor were measured at 50kS/sec. Full details on the experimental setup are provided at the PHM Society website and in an associated conference paper by Li *et al.* [129].

4.3.4 Experiments Summary

Table 4-4 provides a brief summary of the proposed experiments and their purpose in the context of the aims of this research.

Table 4-4: Summary of three experiments

	Experiment 1	**Experiment 2**	**Experiment 3**
Title	Tool Wear Test	Depth of Cut Test	Tool Wear Test (Repeats)
Process Type	Finish Profile Milling	Finish Profile Milling	Finish Ball Nose Milling
Summary	Capture sensor signals over the course of a cutting tools life	Capture sensor signals under variable depth of cut conditions	Use published data to validate the results of the first 2 experiments
Aim of Experiment	To examine the sensor signals, define the signal segmentation and feature extraction steps, carry out feature subset selection and develop a novelty/fault detection method	To use the optimum feature subsets that have been selected through experiment 1, demonstrate the novelty detection method works under varying depth of cut conditions. Develop a fault diagnosis method to distinguish between wear and depth of cut faults	To use repeat data on the feature selection, novelty detection and fault diagnosis methods developed in experiments 1 and 2. Evaluate how this performs for repeat test data for different machining conditions

5 FEATURE SELECTION AND ASSESSMENT

This chapter presents the analysis of data collected from experiment 1, as described in Chapter 4. Section 5.1 examines the results and sensor signals from the experiment, evaluating the content of the data in the time and frequency domain for each sensor type. Section 5.2 investigates segmentation and feature types from each signal in order to provide a reduced data set of extracted features to go on to feature selection steps. Section 5.3 evaluates methods of feature selection and chooses several options of reduced feature subsets. The following chapter then applies the feature subsets for fault detection using a novelty detection method.

Figure 5-1 summarises the content of this chapter. Three main themes for driving the feature selection method are listed; a continuous fault signal, a transient fault signal and the ability to separate data into multiple classes or fault types.

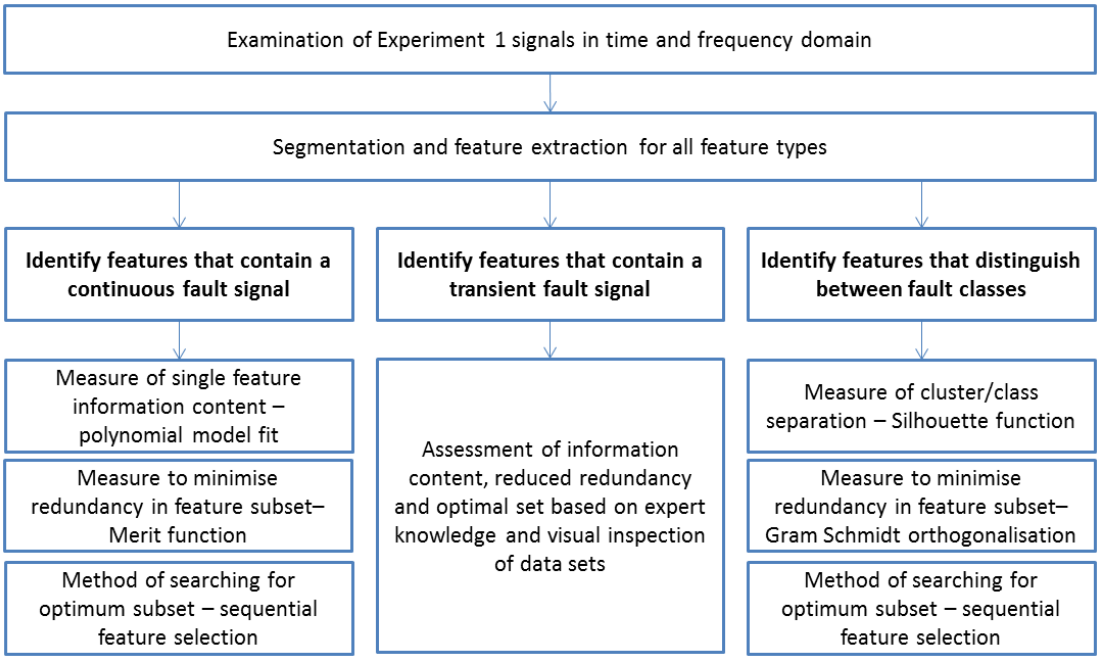

Figure 5-1: Summary of feature selection and assessment topics

5.1 Examination of Sensor Signals

In this section, the results of the two experiments are explained and the first cut taken in Experiment 1 is examined.

Both Experiment 1 and Experiment 2 began with a new tool. The shank of the tool was measured using a dial test indicator (step size 0.002mm) to have a run out of approximately 0.005mm in both cases. The workpiece surface was previously machined using another new tool of the same type with the same cutting parameters that was replaced after every 100 cuts. The length of each cut for both experiments was 131mm, equating to 9.2 seconds in cut at the given cutting feed and surface speed.

The cutting tool was intermittently inspected using an ISM-PM200SB USB microscope, suitable for rapid measurement on or beside the machine tool. Preliminary trials demonstrated that the presence of built up edge made non-intrusive and accurate notch and flank wear measurement impossible, therefore the lower cost microscope that would allow on-machine tool measurement was deemed adequate for these experiments.

The tool could immediately see small signs of wear after the first cut in experiment 1, with marks on the flank face of the tool and built up edge chips attached to the rake face. The tool image for the 2nd flute after one cut is shown in Figure 5-2.

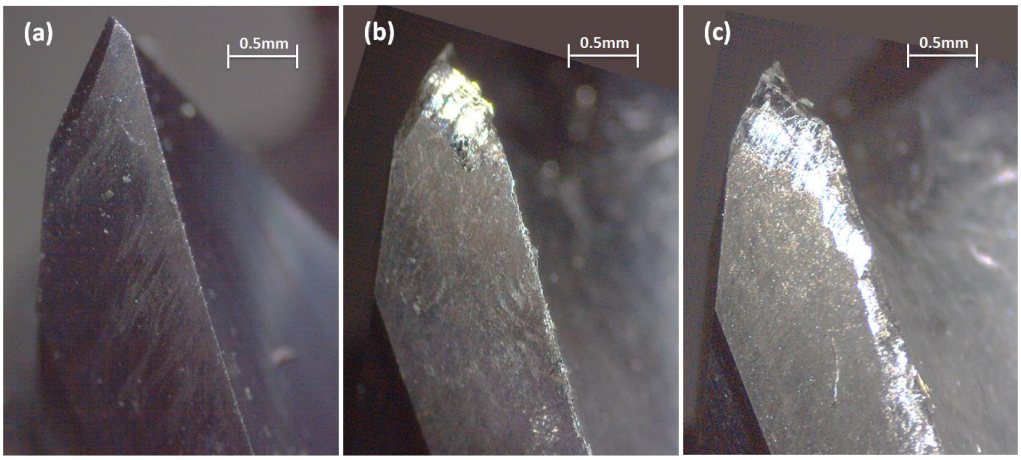

Figure 5-2: A single cutting flute from experiment 1 showing wear effect after cuts (a) 3, (b) 110 and (c) 240.

The time domain data for each sensor is presented in Figure 5-3 through to Figure 5-8. The raw signals are shown in the blue plots, the RMS of the signals (RMS calculated from raw signal at 100 samples per second) are shown in the green plots and the raw signal zoomed in to show one tool revolution is shown in the separate orange plots (also labelled in the figures).

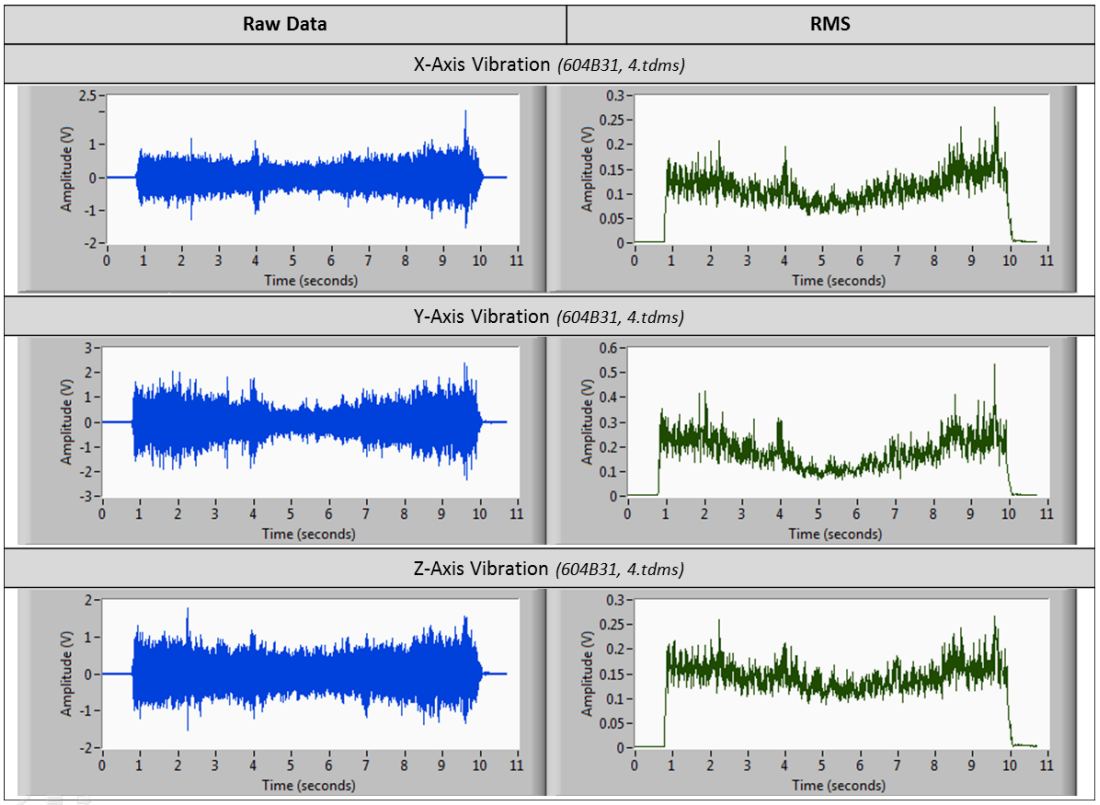

Figure 5-3: Signal for first cut (Tri-Axial Accelerometer)

The signal from the Tri-axial accelerometer, shown in Figure 5-3, provides a significant change on entering and exiting cut, making it suitable for identifying where to segment signals. The y-axis direction shows the highest magnitude and the RMS plot emphasis the drop-in signal magnitude to the centre of the cut in each of the three directions. When zooming into a plot of a single revolution of the tools, shown in Figure 5-4, each flute pass is clear and it is apparent that the magnitude at each flute pass is not constant.

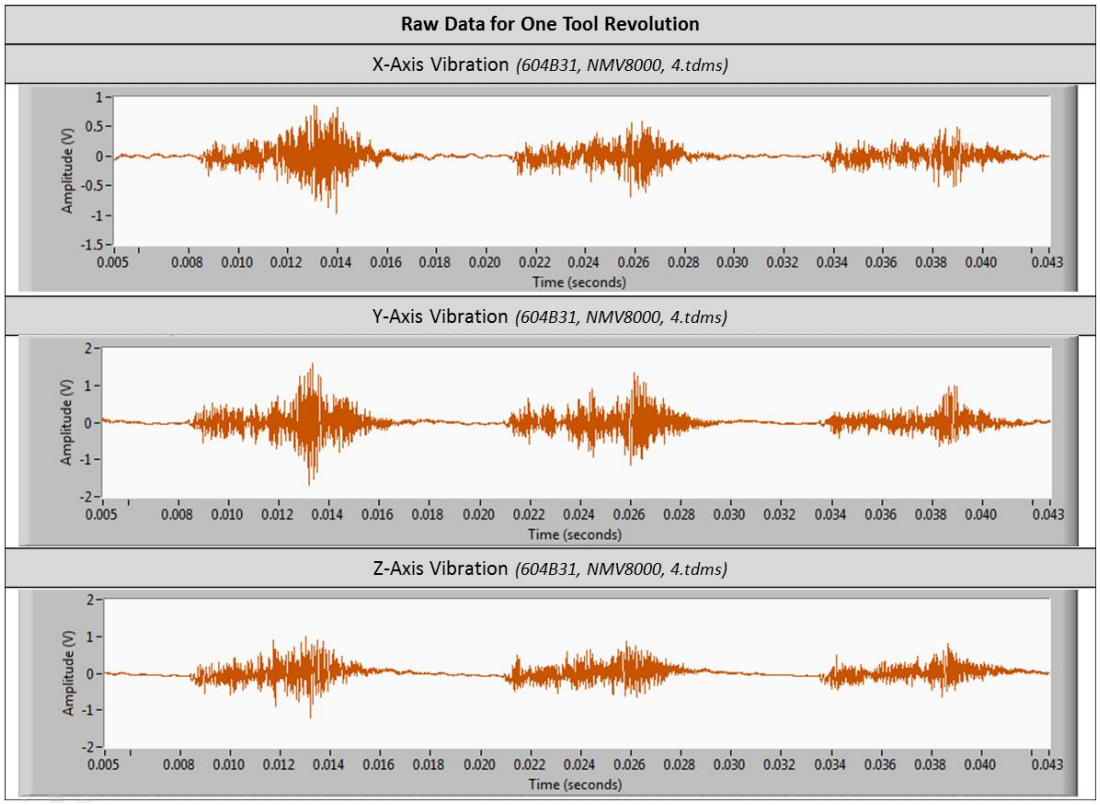

Figure 5-4: Signals for one revolution (Tri-Axial Accelerometer)

Figure 5-5 shows the high frequency vibration sensor data, which is aligned to the z-direction, as well as the two microphone signals. It is clear that the crisp signal from the vibration sensors, that shows when the tool enters and exits the cut, is not the same in the microphone signal. The lower resolution of the microphone signal is again seen in Figure 5-6, where the entry and exit of each flute is unclear, though the tooth passing frequency is present in the form of a sine wave. This wave appears slightly out of phase with the vibration data. The high frequency vibration signal increases quickly in magnitude towards the end of the cut.

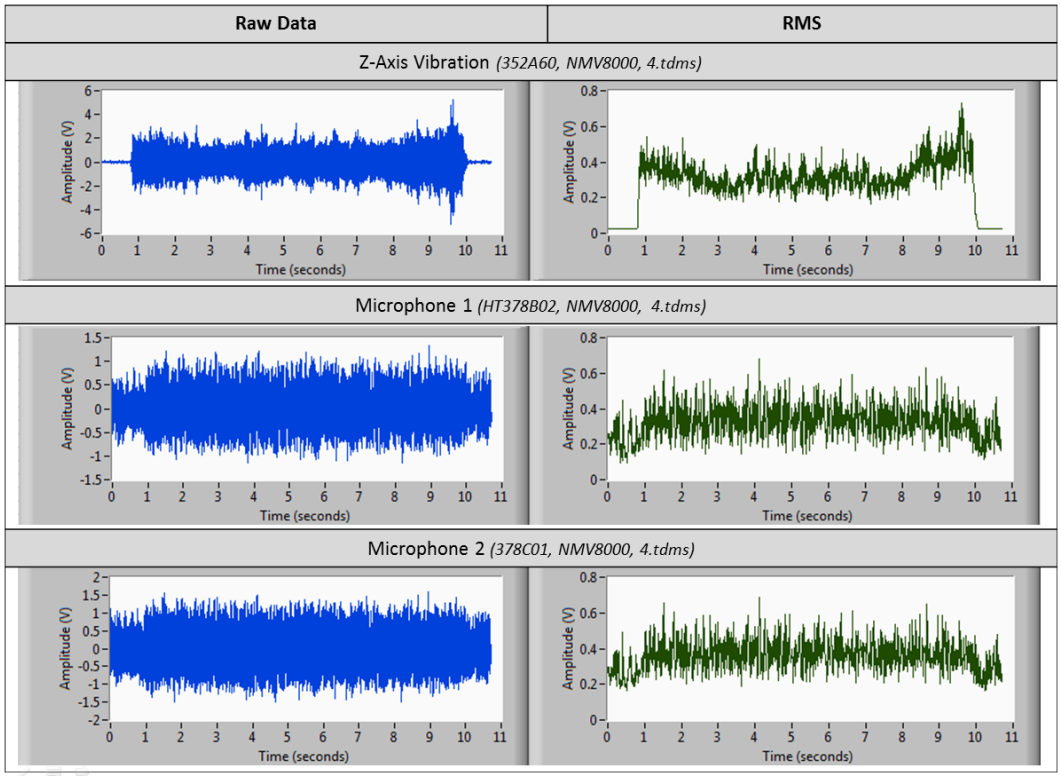

Figure 5-5: Signals for first cut (Microphones and High Freq. Accel.)

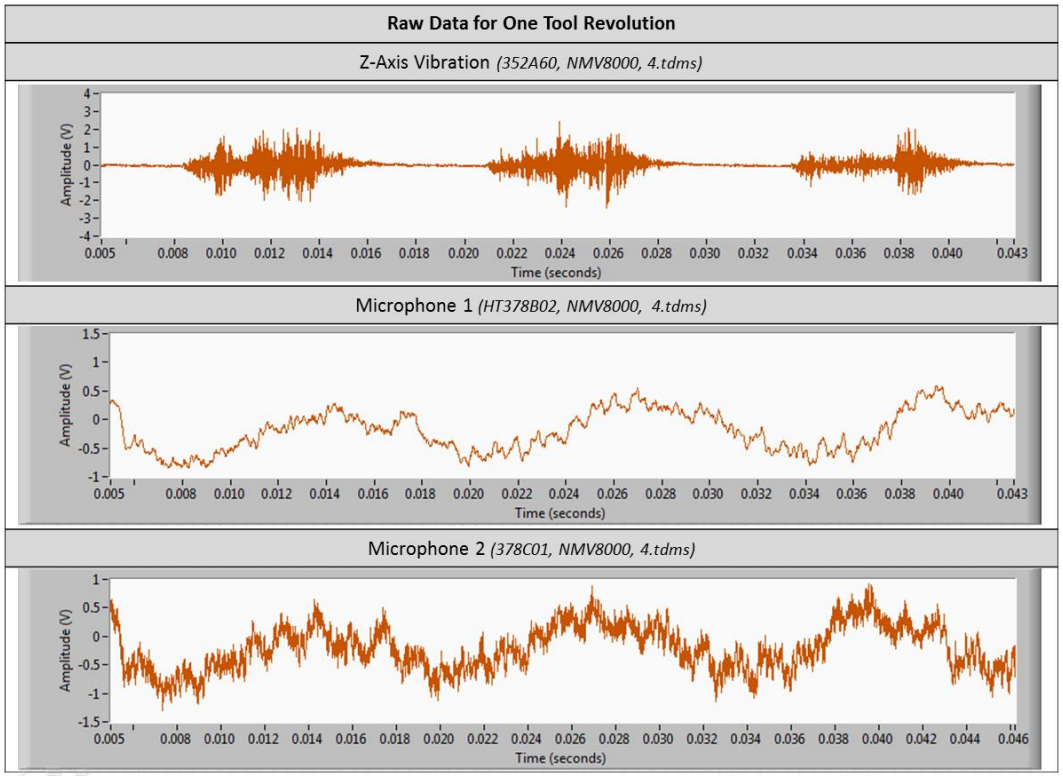

Figure 5-6: Signals for one revolution (Microphones and High Freq. Accel.)

Figure 5-7 shows the AE and spindle power signals. The AE has a similar definition to the vibration signals, showing clearly when the tool enters and exits cut. There is a rise in AE magnitude near to the exit of the cut. The spindle power data shows a large amount of signal noise; however, this is largely eliminated in the RMS signal, suggesting this is a higher frequency noise that the RMS calculation of 100HZ. A lag is seen in the entry to cut in the spindle power signal, possibly a result of the lag in the electric circuit and the Hall Effect sensor used. Looking at the zoomed data for one revolution in Figure 5-8, the AE flute passes are clearly seen, whereas there is no evidence of tooth passing frequency data in the power signal.

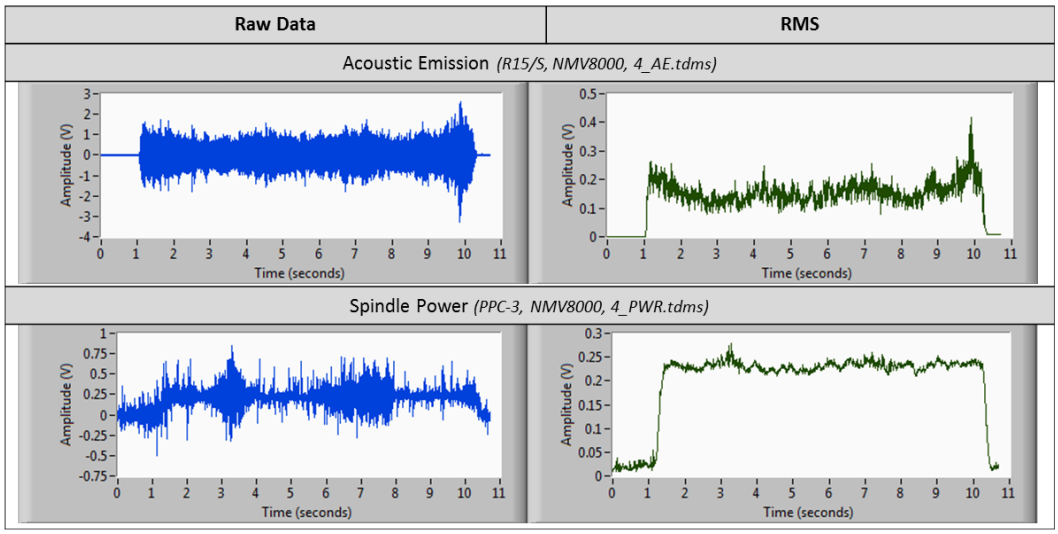

Figure 5-7: Signals for first cut (AE and Spindle Power)

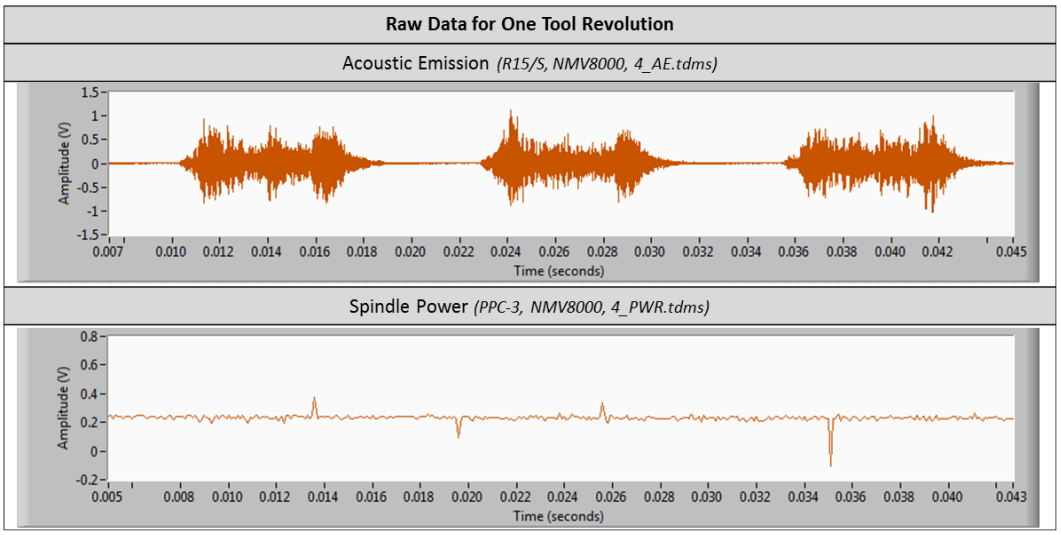

Figure 5-8: Signals for one revolution (AE and Spindle Power)

Several initial observations can be summarised from the sensor signal data in the time domain:

- The sensor data for X, Y and Z vibration using the standard three axis accelerometer appears to give similar data. Each signal drops in magnitude during cutting, increasing at the entry and exit regions of the cut. These sensors all clearly show the tooth passes with the signal settling to almost zero between each flute pass.
- The high frequency accelerometer, obtaining data in the z direction, provides similar results to the other accelerometers. The signal again settles to almost zero between each flute pass.
- The microphone data shows significantly more signal noise when not in cut, making it less clear precisely when the tool enters cut. The data shows the tooth passing frequency, but does not return to zero between flute passes and is out of phase with the accelerometer data. The entry and exit of each flute cannot be seen.
- The acoustic emission data shows some reduction in magnitude during the centre of the cut with a rise on exit. The magnified data for one revolution clearly shows each flute pass and returns to zero between each.
- The spindle power data shows significant signal noise both in and out of cut, though this is removed when converting to RMS. There is no evidence of tooth passing data in this signal.

In order to assess the content of the signals in the frequency domain, a linear spectral density graph was calculated for each signal for the in-cut region (from approximately 1 second to 10 seconds as seen on the previous graphs).

All sensors showed the clear presence of the TPF at 79.6Hz other than the spindle power spectrum where no distinguishing features were present in the spectral data. The following frequency domain plots have chosen to use the linear magnitude, rather than the log magnitude, in order to show the dominance of the peak frequencies in the signals. The power spectrum for the Z-axis accelerometer is shown in Figure 5-9. The data in the bottom graph has then been filtered of the TPF and its harmonics, leaving only very low magnitude data. The next highest frequency is 500 times lower than the TPF magnitude. This is similar with X and Y axis accelerometer data and both microphones.

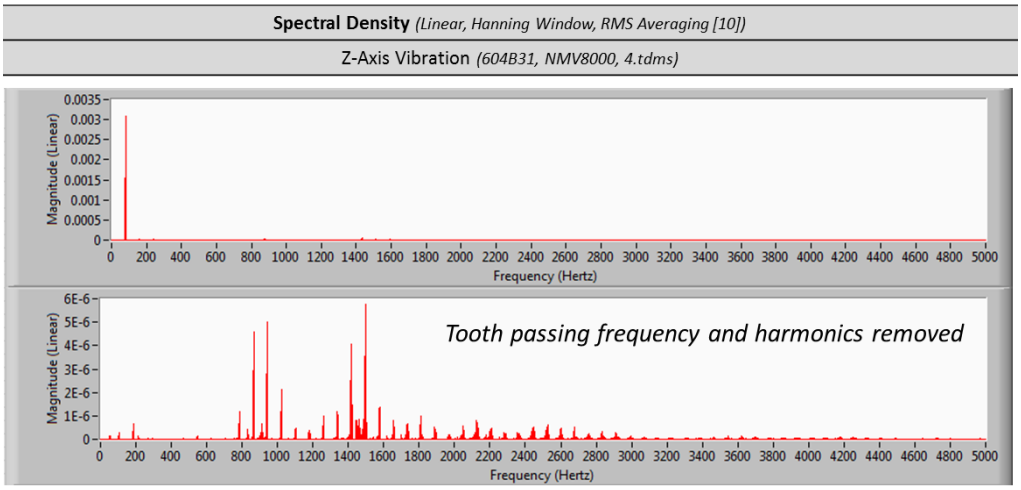

Figure 5-9: Power spectrum for Z-axis vibration with (top) & without (bottom) TPF filter

The high frequency accelerometer was sensitive to frequencies up to 60kHz; however, the data acquisition system allowed sampling frequencies up to only 102400 samples per second for this sensor. The power spectrum, shown in Figure 5-10, presents the frequency content of this sensor up to 50kHz. It can be seen that the data contains frequency content between 17kHz and 45kHz, with a dominant frequency of 27,013Hz. From the reviewed literature (refer to section 2.2.5), this frequency range is likely to be a result of dislocation mechanics and micro-fractures in the tool and workpiece materials when in contact. They may also relate to chip segmentation frequencies.

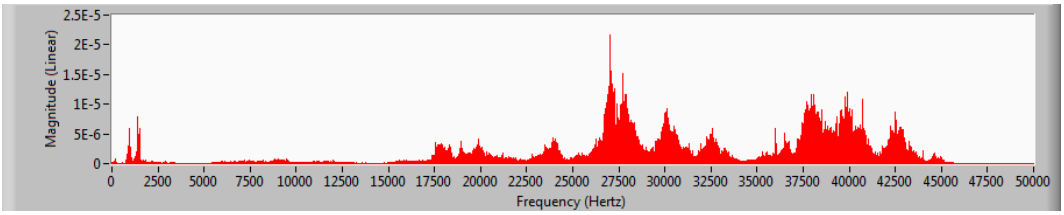

Figure 5-10: Power spectrum for high frequency Z-axis accelerometer with TPF filter

The acoustic emission sensor could be sampled at 1 million samples per second. This allowed frequency content up to 500kHz to be observed. However, there was little frequency content above 170kHz or below 20kHz within the signal for this cut. Figure 5-11 shows the power spectrum for the sensor signal in this range, with the majority of the content around the 40-50kHz range and a dominant frequency of 45,158Hz. These frequencies may again relate to the potential causes noted above.

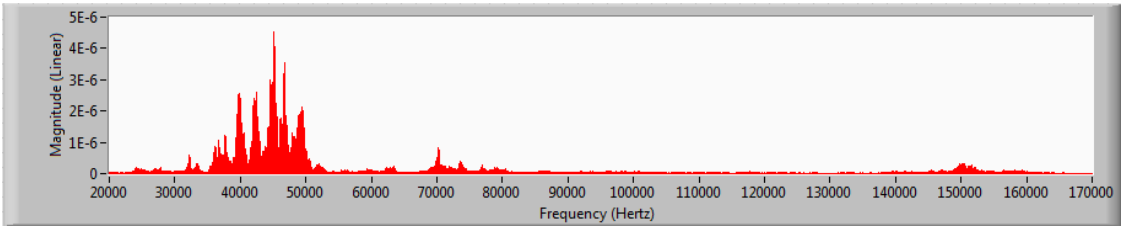

Figure 5-11: Power spectrum for AE sensor from 20k – 170kHz

5.2 Segmentation and Feature Extraction

It is most common to extract features once for each cut taken in a machining process. In this study, the segmentation of data will be once per cut as shown by the segment in Figure 5-12.

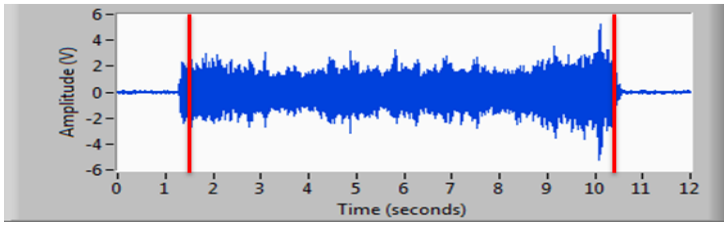

Figure 5-12: Example segmented sections of sensor signal

The most common signal features found in the literature review are listed in Table 5-1. The frequency domain features have been applied to three spectra; (i) the complete spectrum as extracted from the raw data, (ii) the filtered spectrum with all TPF harmonics removed, and (iii) a clipped frequency band of the spectrum after TPF harmonics have been removed. The TPF harmonics are removed between 0 and 5kHz, above which there was found to be further harmonics. The frequency band chosen is specific to each sensor and has been chosen based on the sensor's specification and the presence of activity observed in the spectra; Vibration

and microphone, 10-5000Hz; high frequency vibration, 17k-45kHz; spindle power, 10-100Hz; AE, 30k-80kHz.

The peak frequency from each power spectrum is also calculated. This data may be useful to detect changes in the state of the cutting process, such as a change to RPM or the onset of chatter vibration. However, it does not provide a meaningful correlation with time in cut so is not included in the R-squared calculations.

Table 5-1: Sensor signal feature table (and short names for reference)

		Time Domain Signal	Original Power Spectrum	Filtered Power Spectrum[1]	Band of Power Spectrum[2]
		TD	*FD*	*FDf*	*FDb*
Mean	*M*	B	A, B , C	A, B	A, B , C
RMS	*RMS*	A, B , C	-	-	-
Variance	*V*	A, B , C	A, B , C	A, B	A, B , C
Kurtosis	*K*	A, B , C	A, B , C	A, B	A, B , C
Skew	*S*	A, B , C	A, B , C	A, B	A, B , C
Peak to Peak (Range)	*Rng*	A, B , C	-	-	-
Crest Factor	*CF*	A, B , C	-	-	-
Peak (absolute)	*P*	A, B, C	-	-	-
TPF Magnitude	*TPF*	-	A	-	-
Peak Frequency	PF	A, B, C	A, B, C	A, B	A, B, C
A = all accelerometer and microphone signals, B = spindle power signal, C = AE signal					

[1] TPF Harmonics Filtered between 0-5000Hz

[2] TPF Harmonics Filtered between 0-5000Hz (other than AE) and clipped to select frequency band. Vibration and microphone; 10-5000Hz, high frequency vibration; 17k-45kHz, spindle power; 10-100Hz and AE; 30k-80kHz.

5.3 Feature Selection

In order to select a feature subset, a method is required to determine the amount of information contained within each feature that supports the monitoring system objective. Once a function is derived that defines the value of any given feature subset, a search for the feature subset that optimises this function is required.

Previous studies have measured information content of sensor features, as well as redundant information in multi-feature subsets, which have been detailed in the literature review. This section of the analysis will apply several different filter based feature selection methods using the data set from Experiment 1.

Features that indicate changes in the process over a tool's life are selected using a polynomial curve fitting method in section 5.3.1, building on previous work by authors that include Cho *et al.* [93] and Jemielniak [96]. The proposed method will use the correlation against time in cut, rather than a measured tool wear value, in keeping with the practical requirement to use no training data as stipulated in the hypothesis.

In section 5.3.2, features are selected based on practical knowledge, in order to ensure transient events are reflected in the feature subset, as well as content that may relate to unknown faults. Again, no training data is required for this approach; however, an expert judgement on the signal content is required.

Section 5.3.3 uses a classification algorithm to score feature subsets based on their ability to separate multivariate data from different classes. Expert opinion is required in order to define classes; however, again no supervised training data is necessary.

5.3.1 Feature Selection for a Continuous Fault Signal

The correlation between a sensor signal feature and the time in cut will be used as a measure of continuous signal content that provides information about the cutting conditions. All features are plotted against number of cuts and polynomial models are fit to each feature vector. The coefficient of determination (R-squared) of the resulting polynomial models will indicate whether these features are well described by the model. The onset of tool wear is generally not linear and may pass through several tool wear states before tool failure;

therefore, the polynomial model order has been tested from 1st to 5th order models. Whilst higher orders were considered initially, the analysis of models only up to a 5th order was chosen as the trends observed in signals were generally low frequency and could be approximated by basic models. Higher order and more complex models would have led to further analysis time. The time domain RMS signal for the Z-axis accelerometer will be used by way of example.

In Figure 5-13 and Figure 5-14, the Z-axis vibration time domain RMS is shown to increase with time. Two polynomial models have been used to fit the data, a 1st-order and a 5th-order polynomial in the two figures respectively. The strong correlation between this sensor signal feature and the number of cuts indicates that the feature is sensitive to the changing cutting conditions with low signal noise.

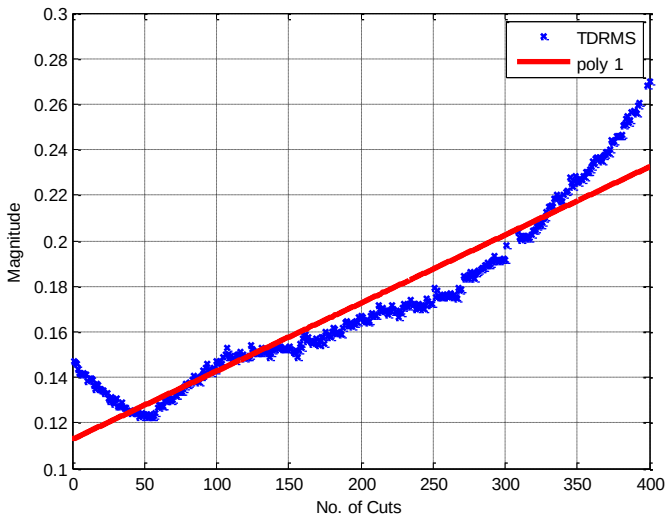

Figure 5-13: Z-axis RMS of vibration signal against number of cuts with 1st order polynomial model

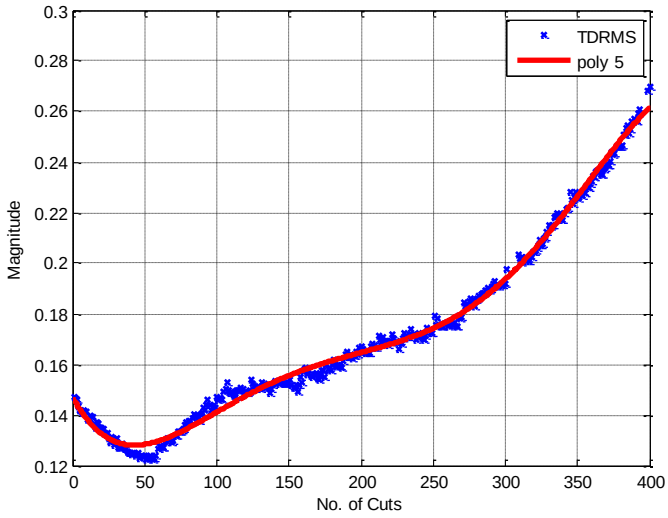

Figure 5-14: Z-axis RMS of vibration signal against number of cuts with 5th order polynomial model

Example Using Z-Axis Vibration Time Domain Features

Figure 5-15 shows plots of all eight time domain features for the Z-axis accelerometer. The mean is not applicable for vibration data, given that the sensor is fixed and so its average displacement is zero. This is apparent in the plot as there is no correlation to number of cuts. The variance, however, shows a strong correlation, particularly for 3rd, 4th and 5th-order polynomial models. The R-squared results for each feature for this sensor are listed in Table 5-2.

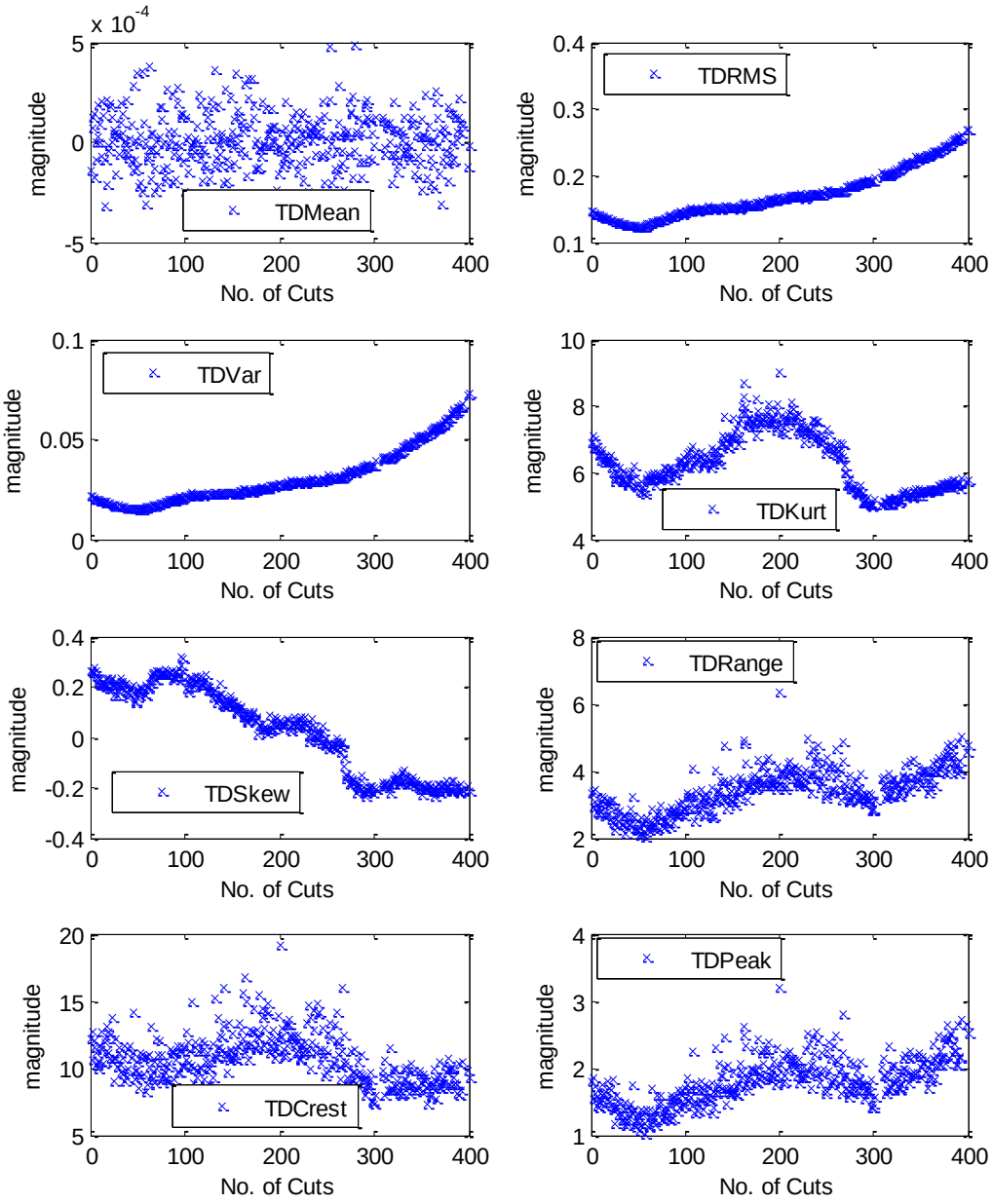

Figure 5-15: All time domain features for Z-axis vibration

Table 5-2: R-squared values for all time domain features

Time Domain					
	1st Order	**2nd Order**	**3rd Order**	**4th Order**	**5th Order**
Mean	0.0001	0.0003	0.0018	0.0037	0.0044
RMS	0.9013	0.9755	0.9804	0.9874	0.9942
Variance	0.8494	0.9712	0.9856	0.9929	0.9960
Kurtosis	0.0841	0.4377	0.4412	0.8463	0.8551
Skew	0.8957	0.9069	0.9460	0.9483	0.9491
Peak-to-Peak	0.4694	0.4917	0.4931	0.6956	0.7023
Crest Factor	0.1200	0.3008	0.3009	0.4786	0.4788
Peak	0.4224	0.4380	0.4404	0.6328	0.6374

The kurtosis has a strong model fit only for 4th and 5th order models, with a clear rise in magnitude during cuts 100-300. Despite having low correlation for low order models, this may give meaningful insight into the cutting process. For example, there may be an intermediate tool wear state during this period.

Example Using Z-Axis Vibration Frequency Domain Features

The features taken from the original power spectrum are shown in Figure 5-16. Spectral variance and TPF magnitude features are of particular interest, given they show a sharp rise initiated on cut number 267. This may indicate a sudden wear state transition such as a notch or chipping, therefore this event will be investigated further in section 5.3.2. Figure 5-17 and Figure 5-18 show the features taken from the filtered power spectrum and the band of power spectrum respectively.

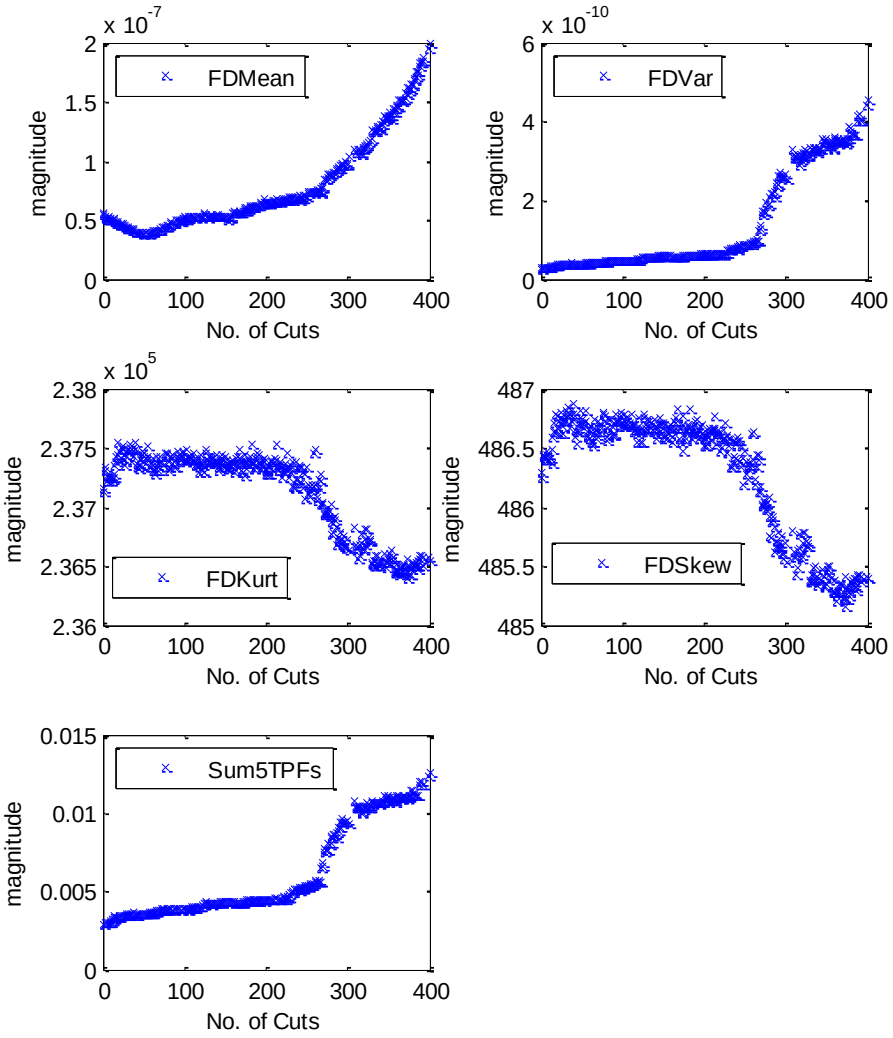

Figure 5-16: Original power spectrum features for Z-axis vibration

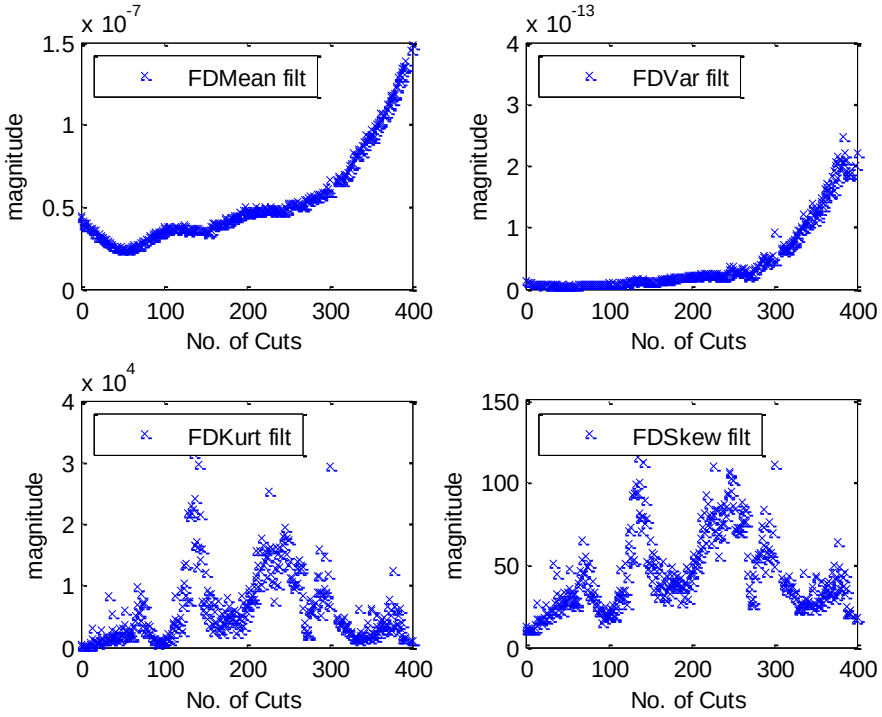

Figure 5-17: Filtered power spectrum features for Z-axis vibration

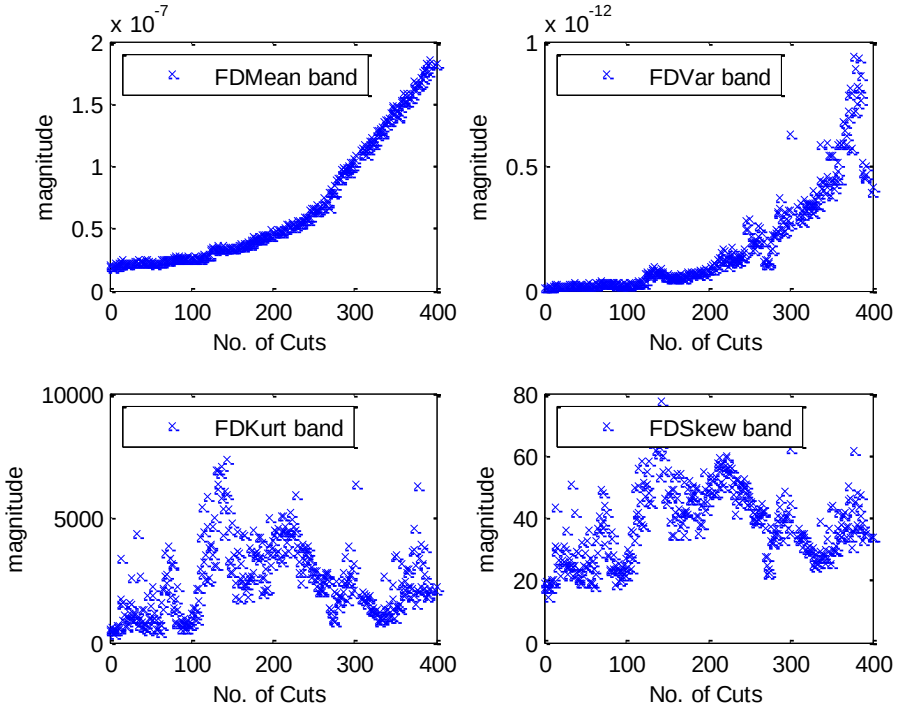

Figure 5-18: Band of power spectrum features for Z-axis vibration

A total of 151 features have been extracted from the 8 sensor signals. The following analysis will summarise the model fit data and pick out key observations. Additional data is included in Appendix B.

Figure 5-19 shows the number of features by their R-squared value for each order of polynomial model. Only 1 feature has an R-squared value greater than 0.9 when using a 1st order model. This increases to 31 and 51 features for 2nd and 5th order models respectively.

None of the 16 power sensor feature models exceeded an R-squared of 0.9 for any model order tested.

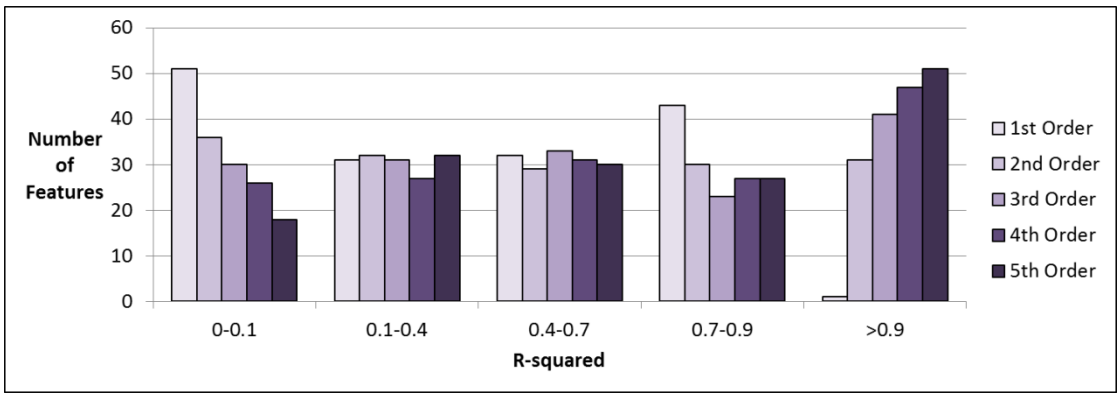

Figure 5-19: Number of features for all sensors by R-squared value

The highest R-squared achieved for 2nd order and all higher order models was the mean of the 10-5000Hz band of the filtered power spectrum for the Z-axis vibration data. This feature gave an R-squared value of 0.853, 0.992, 0.994, 0.996 and 0.997 for the 1st to 5th order models respectively. This feature and its 2nd order polynomial model are shown in Figure 5-20.

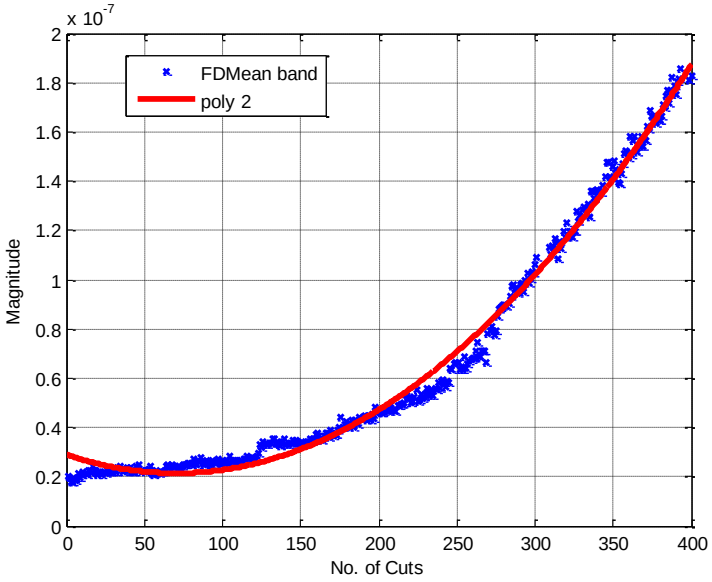

Figure 5-20: Mean of band of power spectrum for the Z-axis vibration data

Some sensor signal features showed poor correlation with low order models, but gave a significant increase in R-squared value for higher order. Figure 5-21 shows the Z-axis kurtosis as an example of this.

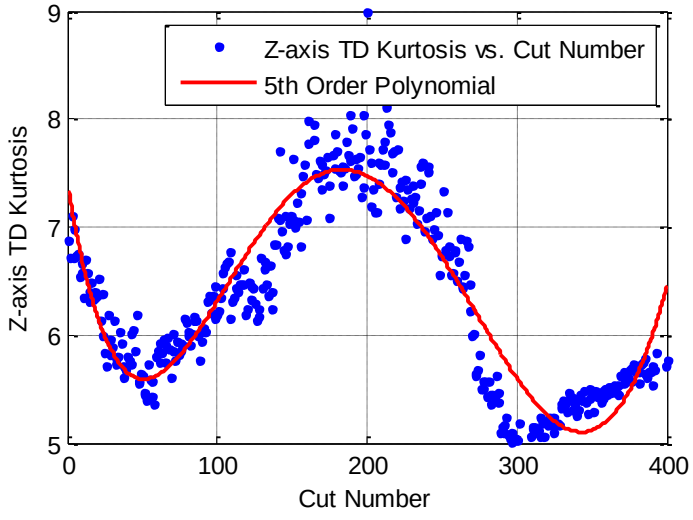

Figure 5-21: Z-axis vibration kurtosis with 5th order polynomial fit

Avoiding Over Fitting of the Polynomial Model

Increasing the order of the polynomial model will generally increase the goodness of fit; however, it can also lead to over fitting. The appropriate order of the polynomial model should be selected with consideration to over fitting to the data.

In order to account for over fitting, the data has been separated into training data and validation data in a conventional approach to mitigate overfitting. One hundred of the cuts have been randomly selected to create the testing data set, whilst all other cuts have been used to generate the model. The optimum model is then determined by the fit of the testing data set, measured using either the R-squared coefficient of determination or the root-mean-squared-error (RMSE) value.

The model with the best fit (or lowest RMSE) over the polynomial order from 1 to 5, is selected as the optimum model.

It was found that the result gave small differences in optimum model order selection depending on the selection of the training and testing data sets, although 5^{th} order models were most common. The box plot in Figure 5-22 presents the result of 60 runs using a different split of testing and training data. One hundred testing cuts are still used in each case. Whilst there is some variance in the selected model orders, the majority of the 151 features favour 5^{th} order models.

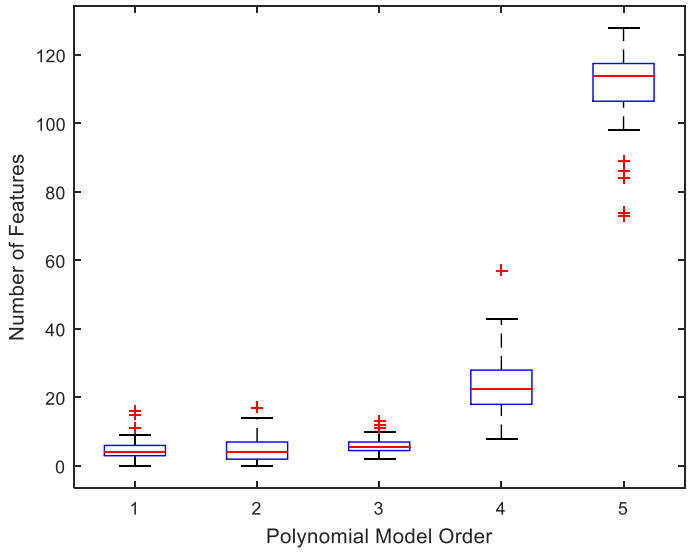

Figure 5-22: Box plot of optimum polynomial order

The optimum polynomial model order has been selected by taking the most common order (mode) chosen over the 60 runs. These results comprise of 131 x 5thorder, 10 x 4th order, 2 x 3rd order, 2 x 2nd order and 6 x 1st order features. They are listed in full in Appendix B.

Continuous Fault Signal Subset Selection

The model fit provides an individual ranking of each feature; however, the optimum feature subset should retain minimal redundancy within the subset. A method of finding a suitable feature subset was discussed in the literature review, where Cho *et al.* [93] ranked subsets by 'Merit' formula. The formula was not fully described in the paper; however, its application gave good results. A detailed explanation of an extended formula is described below.

The formula for the Merit of any feature subset is shown in equation (8).

$$\text{Merit} = \frac{k\overline{\text{r}_{cf}}}{\sqrt{k + k(k-1)\overline{\text{r}_{ff}}}} \tag{8}$$

Where k is the number of features in the subset, $\overline{\text{r}_{cf}}$ is the mean correlation between each feature and class, and $\overline{\text{r}_{ff}}$ is the mean correlation between any two features, averaged over each possible pair of features within the subset.

This formula has been extended further in this thesis to use the Pearson's correlation coefficient as the measure of correlation between a feature and its chosen polynomial model; leading to the formula for $\overline{\mathrm{r}_{cf}}$ shown in equation (9), where x is the feature data and y is the polynomial estimate. The mean correlation is calculated for features from 1 to k. Each features' data runs from 1 to n, where n is the number of cuts taken.

$$\overline{\mathrm{r}_{cf}} = \frac{1}{k}\sum_{j=1}^{k} \frac{\sum_{i=1}^{n}(x_{ij} - \bar{x}_j)(y_{ij} - \bar{y}_j)}{\sqrt{\sum_{i=1}^{n}(x_{ij} - \bar{x}_j)^2}\sqrt{\sum_{i=1}^{n}(y_{ij} - \bar{y}_j)^2}} \tag{9}$$

The Pearson's correlation coefficient has also been used to calculate $\overline{\mathrm{r}_{ff}}$ using equation (10).

$$\overline{\mathrm{r}_{ff}} = \frac{1}{C(k,2)}\sum_{a,b} abs\left(\frac{\sum_{i=1}^{n}(x_{ia} - \bar{x}_a)(x_{ib} - \bar{x}_b)}{\sqrt{\sum_{i=1}^{n}(x_{ia} - \bar{x}_a)^2}\sqrt{\sum_{i=1}^{n}(x_{ib} - \bar{x}_b)^2}}\right) \tag{10}$$

Where $C(k,2)$ is the number of combinations of 2 features within subset size k. Each combination of feature pairs is described by a and b, where $0 > a > b$. I.e. The coefficient for each possible feature pair combination is without repetition and is not inclusive of the correlation of each feature with itself (which would bias the data towards a correlation of +1).

If a feature is negatively correlating with another, this can be considered an indication of mutual information to the same degree as a positive correlation; therefore the absolute value of the correlation has been taken.

It is not always possible to test each possible subset due to the significant computational expense. There are (2^151 -1) possible subsets from 151 features. A greedy algorithm has been chosen in order to search for the optimum subset while reducing the number of tests, also termed sequential feature selection. Initially, the algorithm has been used by increasing subset size from a set of 1 through to a full subset of 151 features.

The greedy algorithm adds one additional feature to the subset at a time and retains the feature which results in the maximum Merit. The process is repeated until no further increase in the Merit score can be achieved. In case of local optima the process is continued with the highest Merit available until a full set of 151 features is reached. The algorithm has

been used both in forward (increasing subset size from 1 to 151) and in reverse (decreasing subset size from 151 to 1).

There are some limitations of sequential feature selection as the algorithm ranks the value of each single feature and does not look at interactions between multiple features.

Figure 5-23 shows the Merit result plotted against subset size for both forward and reverse sequential feature selection. The first order polynomial models have been used in this instance. The optimum feature subset was found using forward sequential feature selection. This gave a subset of 18 features and a Merit of 0.997. It is also apparent that forward and reverse sequential feature selection methods give different subsets; Figure 5-24 shows the percentage of common features in these two results.

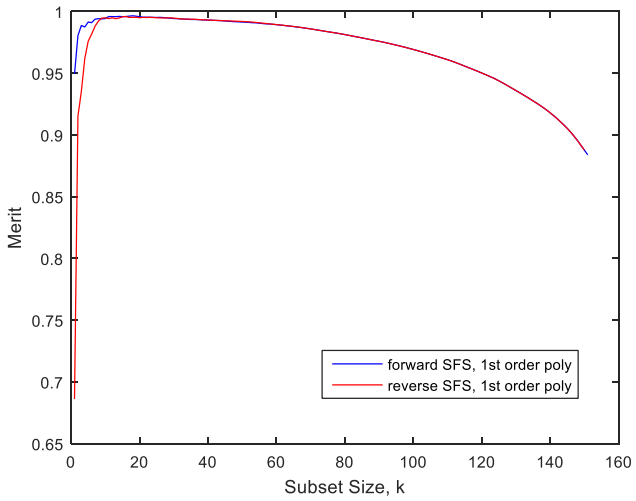

Figure 5-23: Sequential Feature Selection; Subset Merit for 1st Order Models

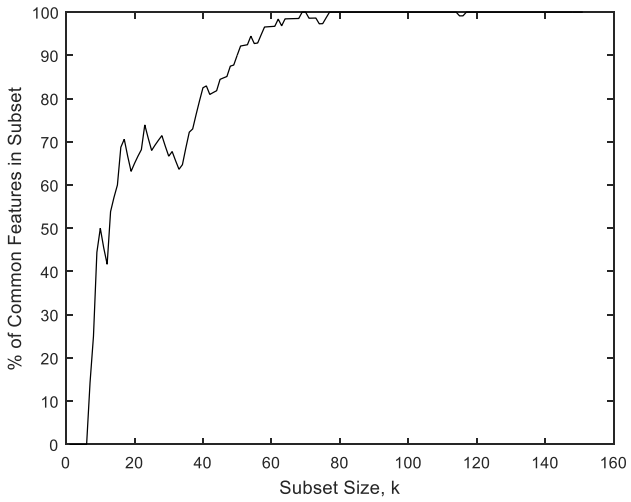

Figure 5-24: % of common features for 1st order model forward and reverse sequential feature selection

The features selected in the optimum subset from the 1st order model data are shown in Figure 5-25, grouped into subplots of similar features. For ease of comparison, each feature has been normalised to have zero mean and unit variance.

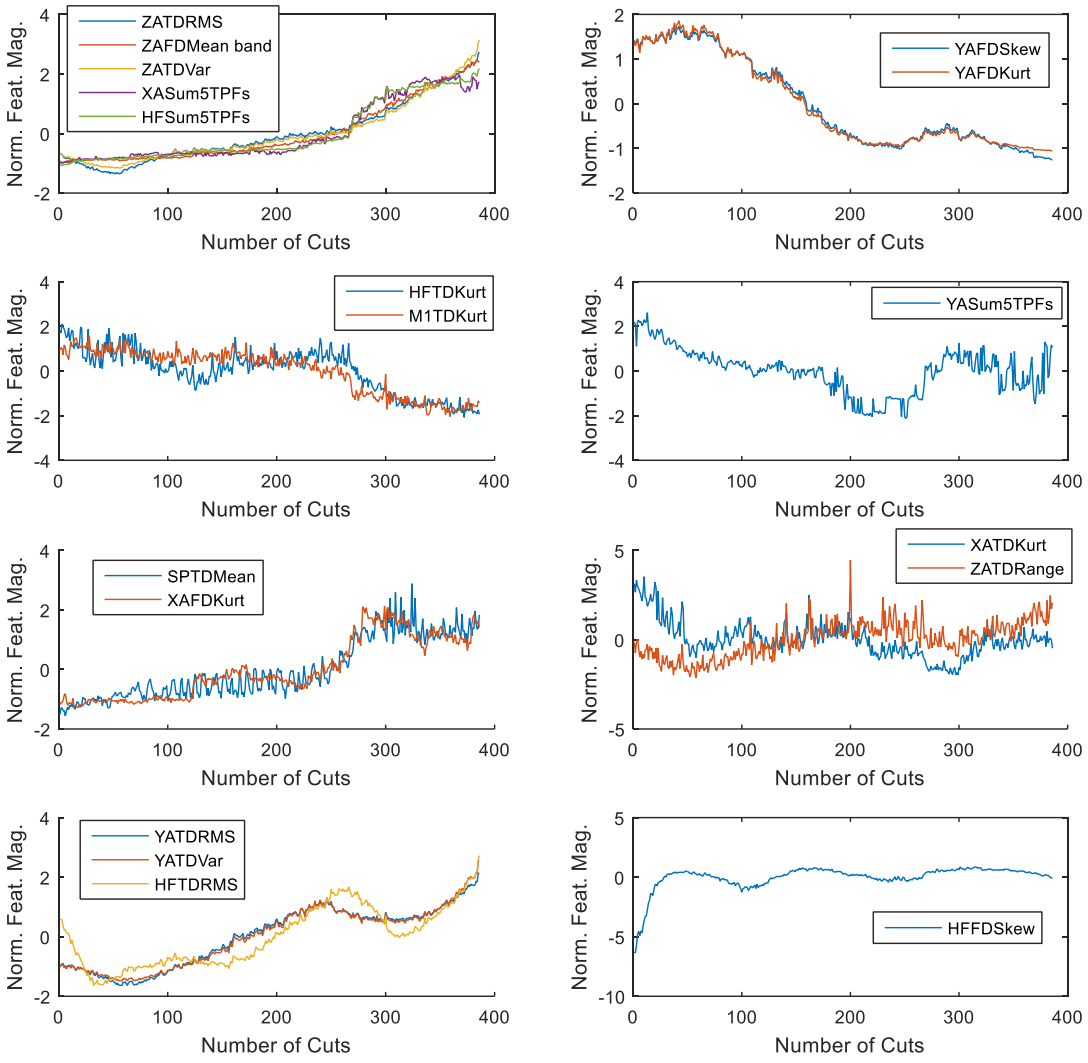

Figure 5-25: Features contained within the optimal subset for 1st order models

Figure 5-26 presents the same data for the optimum model order, selected by using training and testing data sets as described earlier. In this case, the optimum feature subset was found using reverse sequential feature selection. This gave a subset of 14 features and a Merit of 1.482. The features differed considerably between the forward and reverse feature selection, as shown in Figure 5-27.

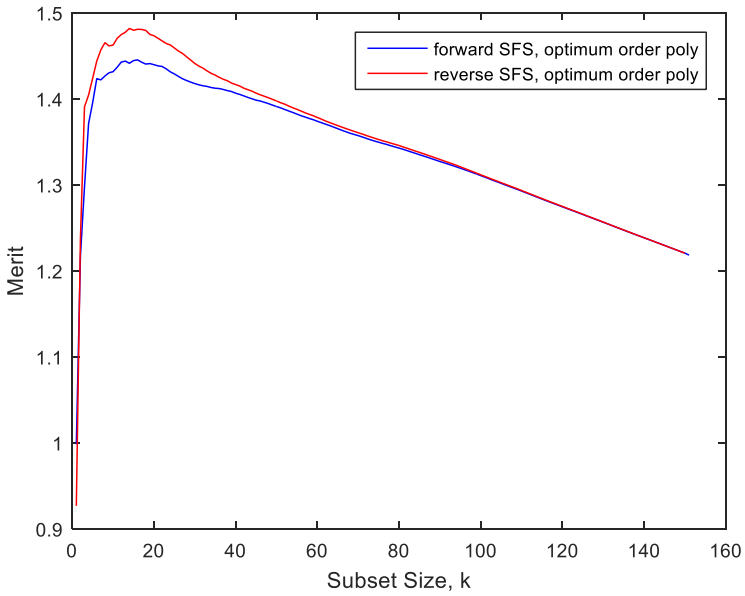

Figure 5-26: Sequential feature selection; subset merit for favoured model order

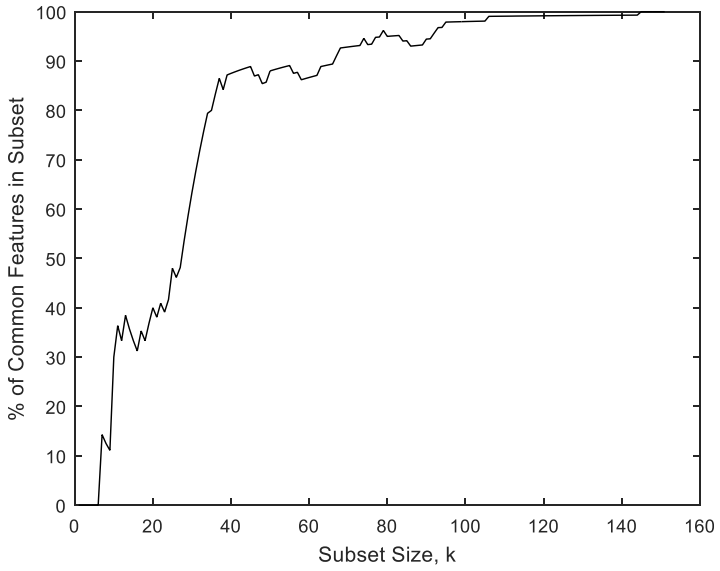

Figure 5-27 - % of common features for favoured model order
forward and reverse sequential feature selection

The features selected in the optimum subset from the favoured model order data are shown in Figure 5-28, grouped into subplots of similar features. The favoured model for all of these features was 5th order.

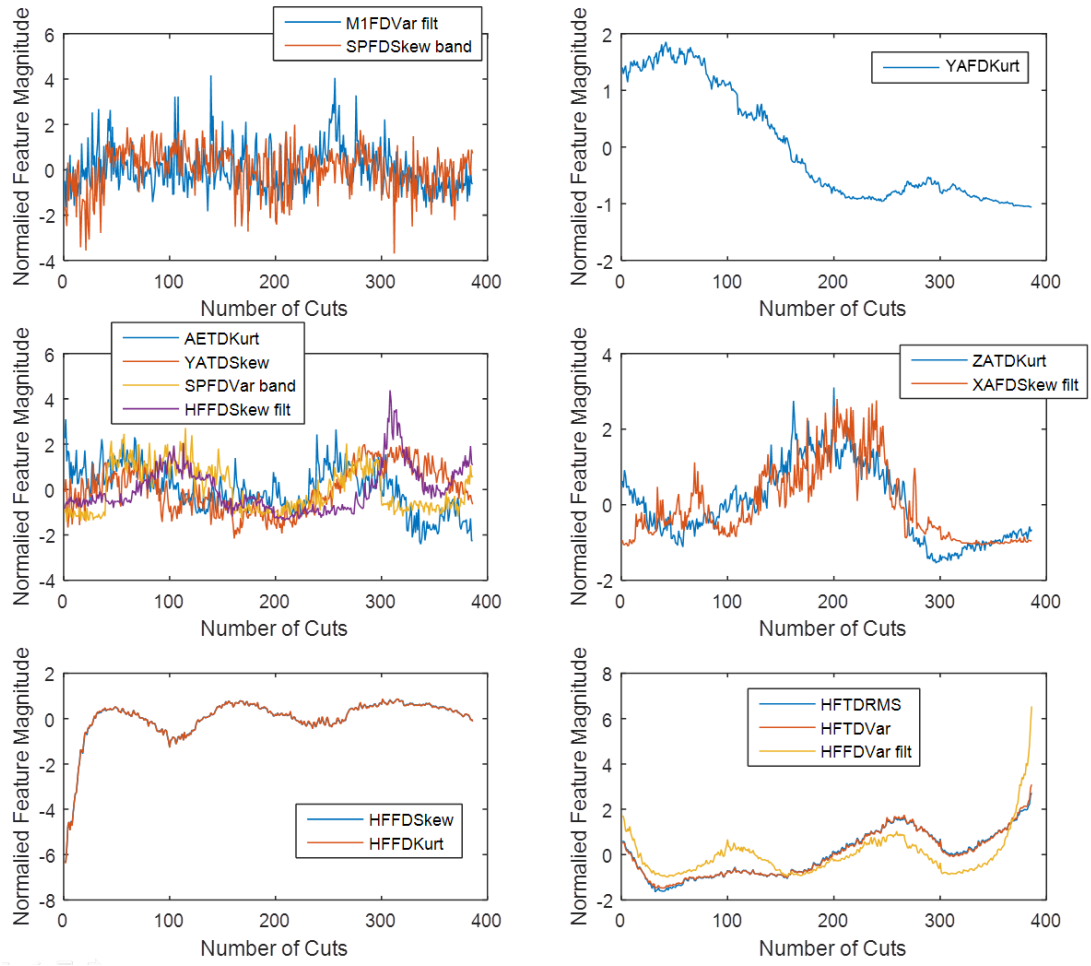

Figure 5-28: Features contained within the optimal subset for favoured model order

The features that make up the optimum subsets for the previous two examples are listed in Table 5-3. There are just three common features in each subset which are highlighted in bold.

Table 5-3: Feature subsets selected for alternative order polynomial models using the Merit function

	1st Order Models	Favoured Order Models
1	Z Vibration Time Domain RMS	**HF Vibration Time Domain RMS**
2	Y Vibration Frequency Domain Skew	Z Vibration Time Domain Kurtosis
3	Spindle Power Time Domain Mean	**HF Vibration Frequency Domain Skew**
4	**Y Vibration Frequency Domain Kurtosis**	AE Time Domain Kurtosis
5	Z Vibration Frequency Domain Mean Band	X Vibration Frequency Domain Skew Filtered
6	X Vibration Time Domain Kurtosis	HF Vibration Time Domain Variance
7	Z Vibration Time Domain Variance	Spindle Power Frequency Domain Variance Band
8	Y Vibration Time Domain RMS	HF Vibration Frequency Domain Kurtosis
9	X Vibration Sum TPF	Spindle Power Frequency Domain Skew Band
10	Y Vibration Sum TPF	Y Vibration Time Domain Skew
11	HF Vibration Sum TPF	HF Vibration Frequency Domain Variance Filtered
12	X Vibration Frequency Domain Kurtosis	Mic1. Frequency Domain Variance Filtered
13	Z Vibration Time Domain Range	HF Vibration Frequency Domain Skew Filtered
14	HF Vibration Time Domain Kurtosis	**Y Vibration Frequency Domain Kurtosis**
15	Y Vibration Time Domain Variance	
16	**HF Vibration Frequency Domain Skew**	
17	**HF Vibration Time Domain RMS**	
18	Mic.1 Time Domain Kurtosis	

5.3.2 Feature Selection for a Transient Fault Signal

The previous section evaluated features suitable for tracking changes in the sensor signals over the life of the tool. A number of sensor signal features have a good fit with low order polynomial models. The assumption for this approach is that the extracted fault signal is continuous, resulting in a permanent change in the sensor signals. Figure 5-29 illustrates the difference between transient and continuous fault signals.

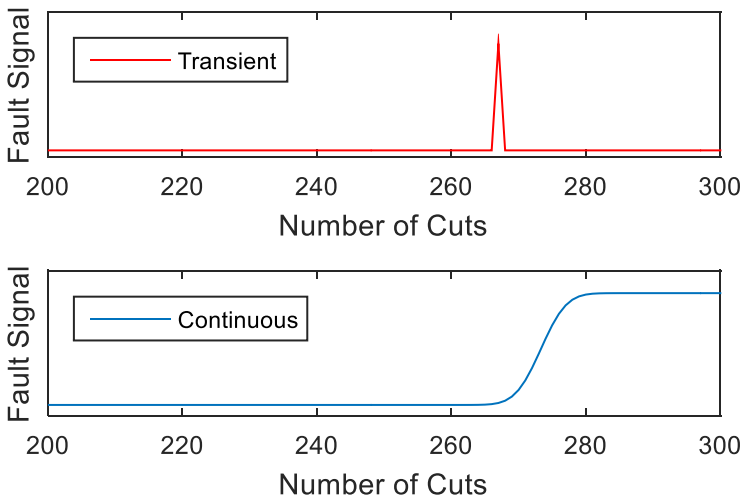

Figure 5-29: Example of Transient and Continuous Fault Signal

Suppose that the chipping of a tool occurs; the features obtained from section 5.3.1 may be suitable for observing a change in the signal before and after the event. This is assuming there is a continuous fault signal introduced as a result of the chipping. The same feature or feature subset may not be sensitive to the event itself as the associated signal may be of a different form and it will be transient in nature.

Several features have been investigated in this section to identify which can be used to detect transient events.

Transient events such as tool chipping are important indicators of the process condition, especially where a process may rapidly fail following such an event without providing other evidence of failure in the signals. Many unknown faults may also manifest themselves as transient events. The feature extraction method, described earlier in section 5.2, extracts each feature data point from 9.2 seconds in cut, yet a single flute pass occurs in less than 10

milliseconds. Many features will average the signal leaving little information on transient events that have only affected a small part of the signal. In fact, these features in particular have given the best fit to polynomial models, such as time domain RMS. Features that do not average the signal, such as time domain maximum, have a relatively poor fit to polynomial models in the previous section.

Referring back to Figure 5-16, sharp increases in two features from the Z-axis vibration power spectrum were observed; the variance and the sum of TPF. This initiated after cut number 267. Whilst most time domain features show a gradual increase over the tools life, the sudden change after this cut is only prominent in these two frequency domain features.

Figure 5-30 shows the RMS value of the Z-axis vibration for all cuts, with cuts 250-275 magnified on the second plot. There is little evidence here of any sudden change at cut 267. A similar result is observed for two frequency domain features; the variance and the sum of the tooth passing frequencies. The latter is shown in Figure 5-31 and it can be seen that the magnitude increases following cut 267.

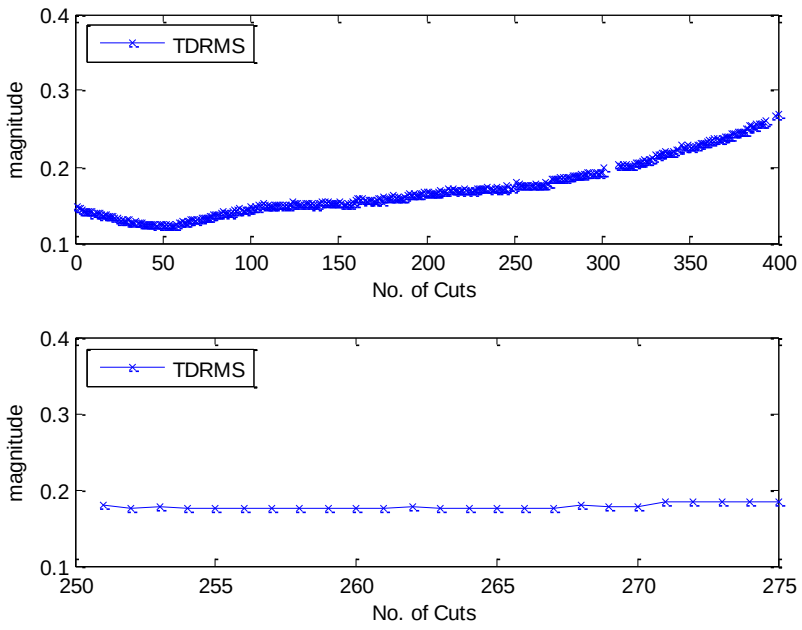

Figure 5-30: Z-axis vibration RMS for all cuts with cut 250-275 magnified

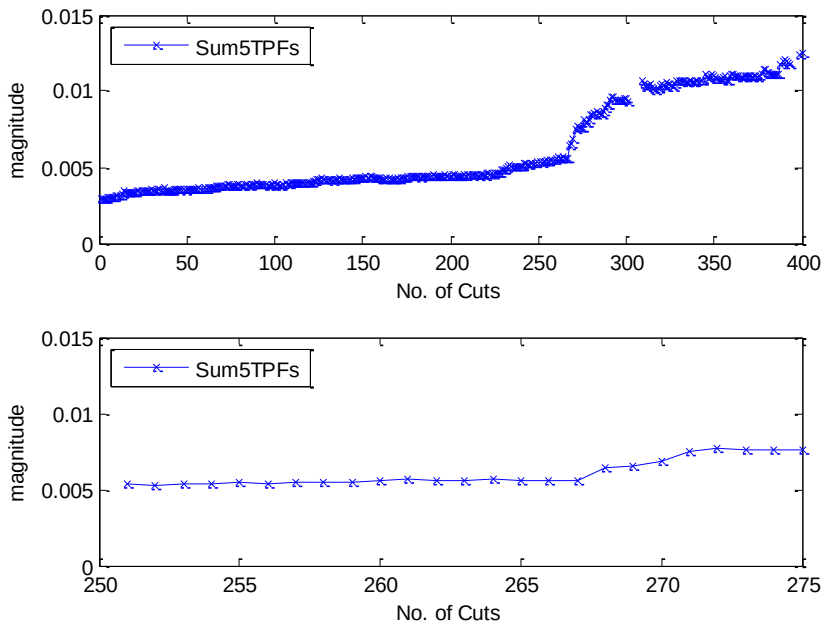

Figure 5-31: Z-axis vibration sum of tooth passing frequencies for all cuts with cut 250-275 magnified

Figure 5-32 shows three z-axis vibration time domain features which show a spike at cut 267; the peak, peak-to-peak (range) and crest factor features. Note that these three features all have relatively poor fit to the polynomial models in the previous section. The three features where the event cannot be detected (RMS, Skew and Variance) scored well when correlated against time in cut. (Kurtosis gave poor results in both cases).

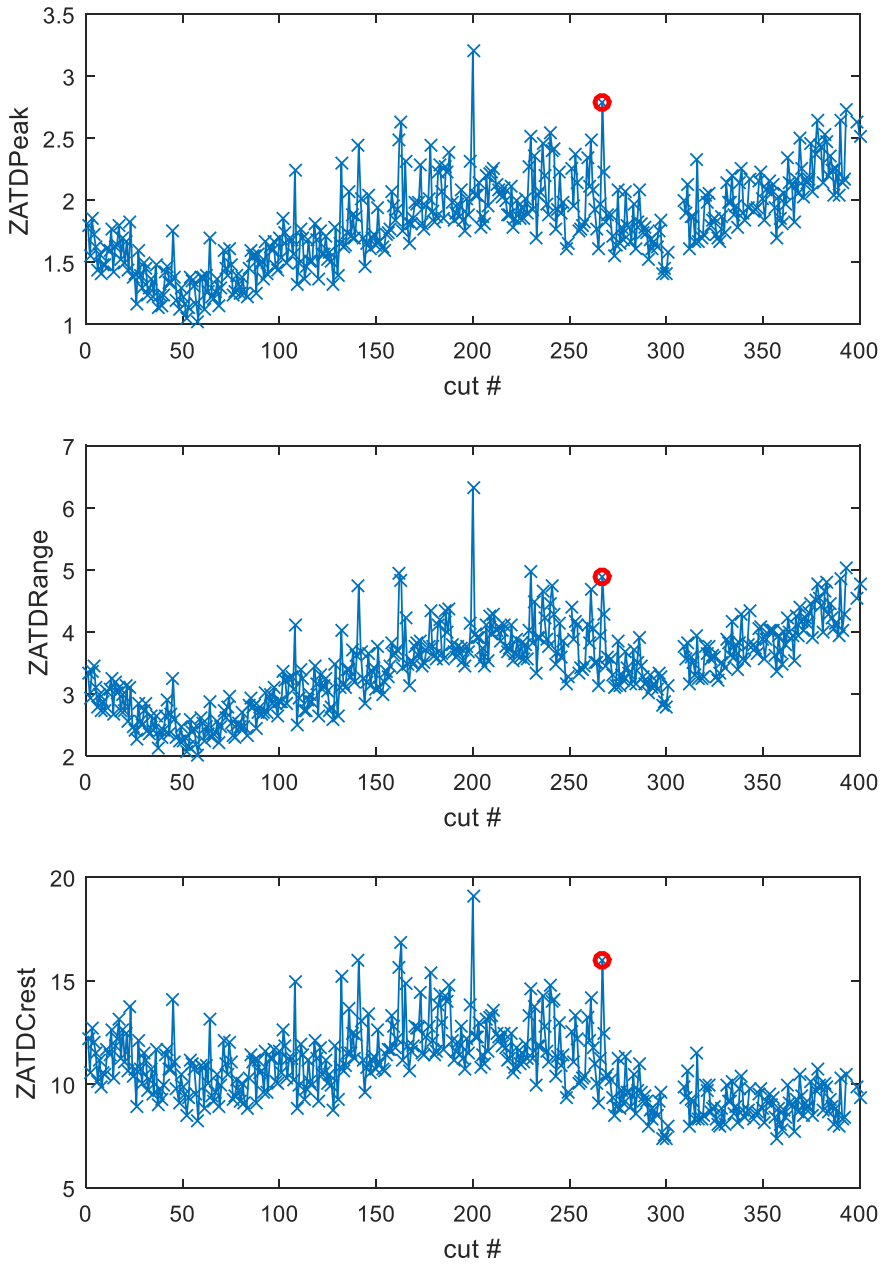

Figure 5-32: Z-axis vibration TD peak, range and crest factor for all cuts with cut 267 data points circled

It can be seen in Figure 5-32 that a number of cuts prior to cut 267 also have high magnitude. Cut 200, for example, has the highest magnitude for each of the features shown. The same feature data for other accelerometers can be seen in Appendix B and comparisons can be made as follows:

- The same three features from the x-axis vibration showed no spikes for cut 267 or 200.
- The y-axis vibration did not spike at cut 267 but had the highest magnitude point at cut 200.
- The high frequency accelerometer (z-axis) had the highest magnitude point at cut 267 but showed no spike at cut 200, see Figure 5-33.

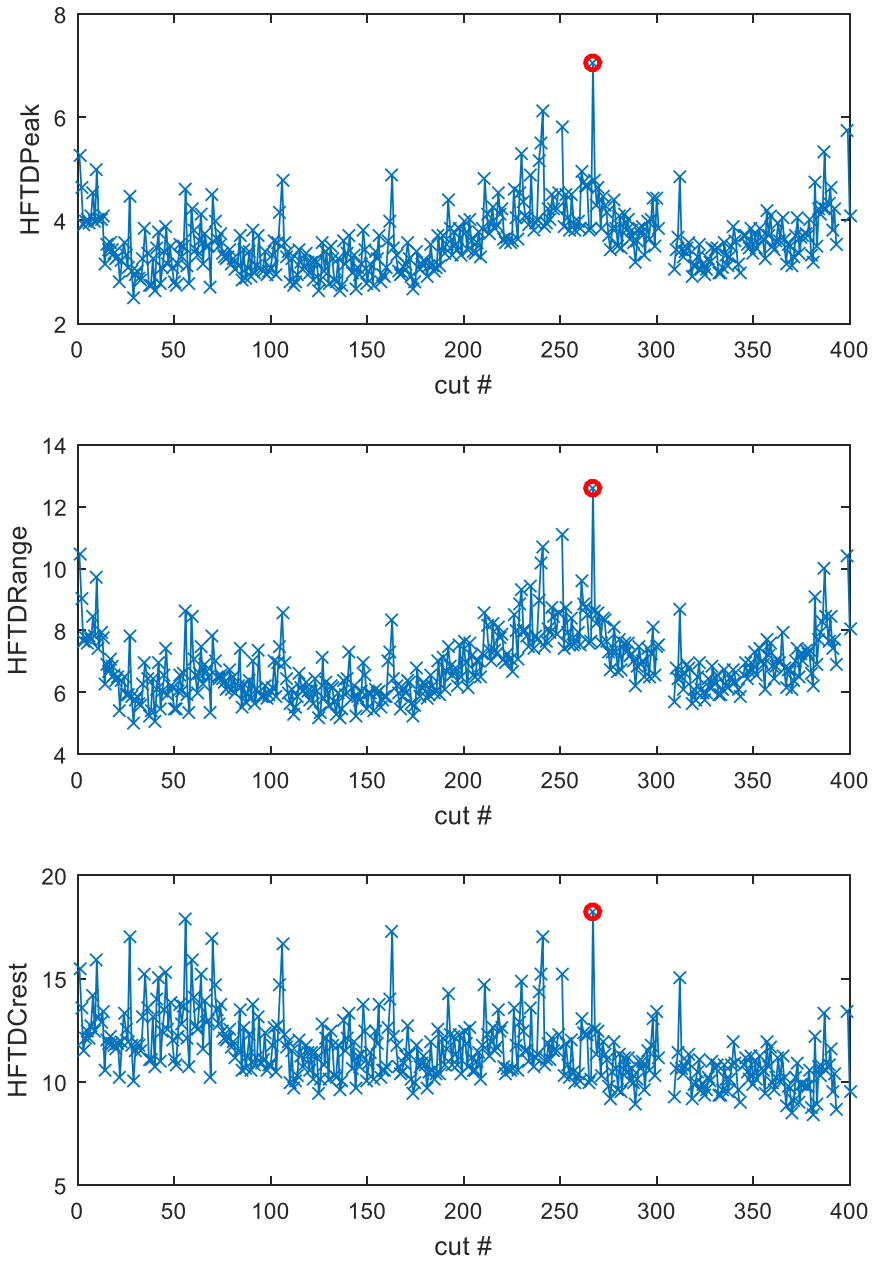

Figure 5-33: HF vibration (z-axis) TD peak, range and crest factor for all cuts with cut 267 data points circled

Looking closer at this event, the z-axis vibration time domain RMS and peak for each revolution of the tool during cut 267 has been plotted in Figure 5-34 and Figure 5-35 respectively. Cut 265 has also been shown for comparison. Note that the same data for HF vibration and for cut 200 is shown Appendix B.

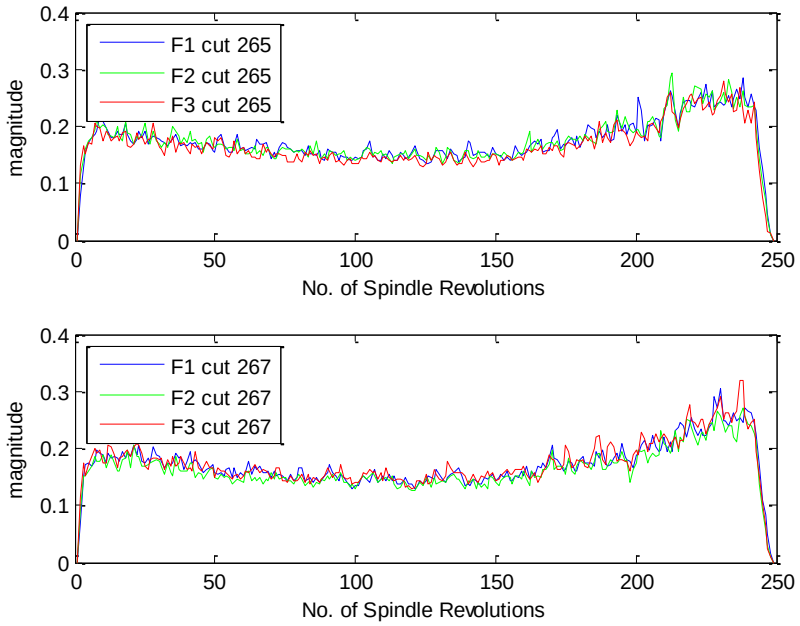

Figure 5-34: Z-axis vibration RMS for cut 265 and 267 vs spindle revolution

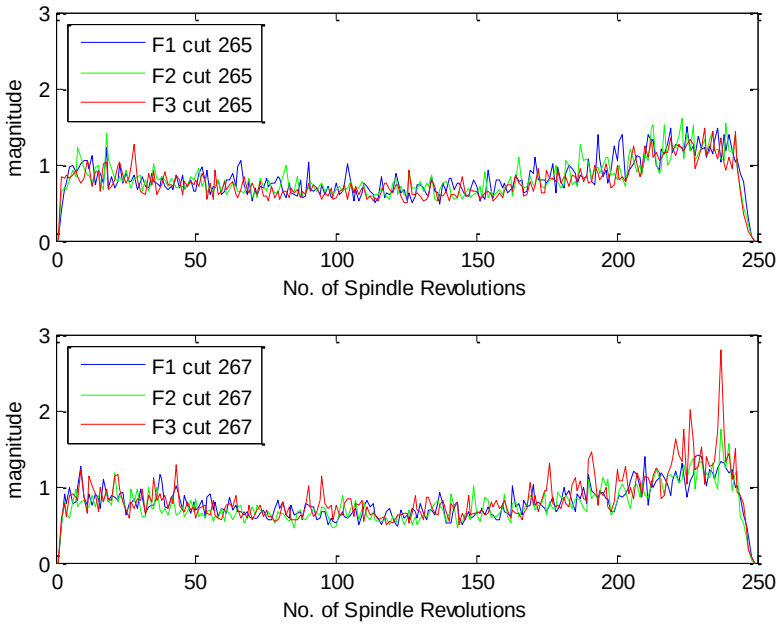

Figure 5-35: Z-axis vibration TD peak for cut 265 and 267 vs spindle revolution

The event resulting in the spike in peak magnitude can be seen late in the cut. The change in the signal can be observed in the X-axis, Z-axis, high frequency vibration and AE sensor signals. Figure 5-36 and Figure 5-37 show just 10msec of the signals from each of these sensors, comparing the equivalent flute pass in cut 265 to that in cut 267.

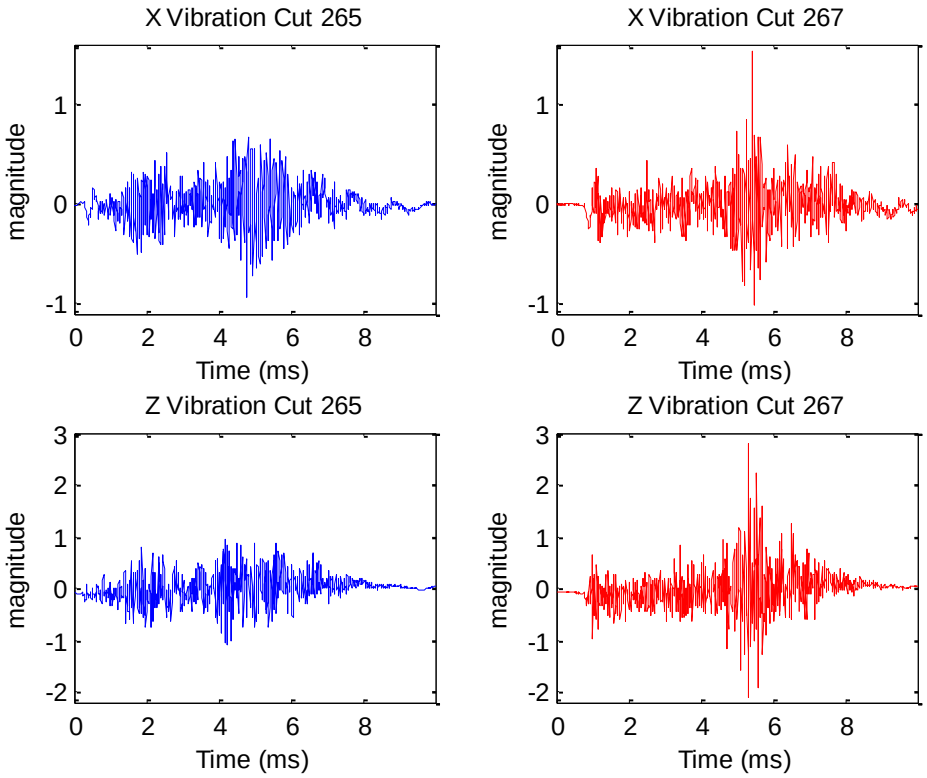

Figure 5-36: Flute pass from cut 265 (left) compared to notable flute pass in cut 267 (right) for X and Z-axis accelerometers

Figure 5-38 shows the high frequency vibration and acoustic emission signals over 0.25msec where the spike in the signals occurs. The event is not noticeable in the Y-axis vibration, microphones or the spindle power data.

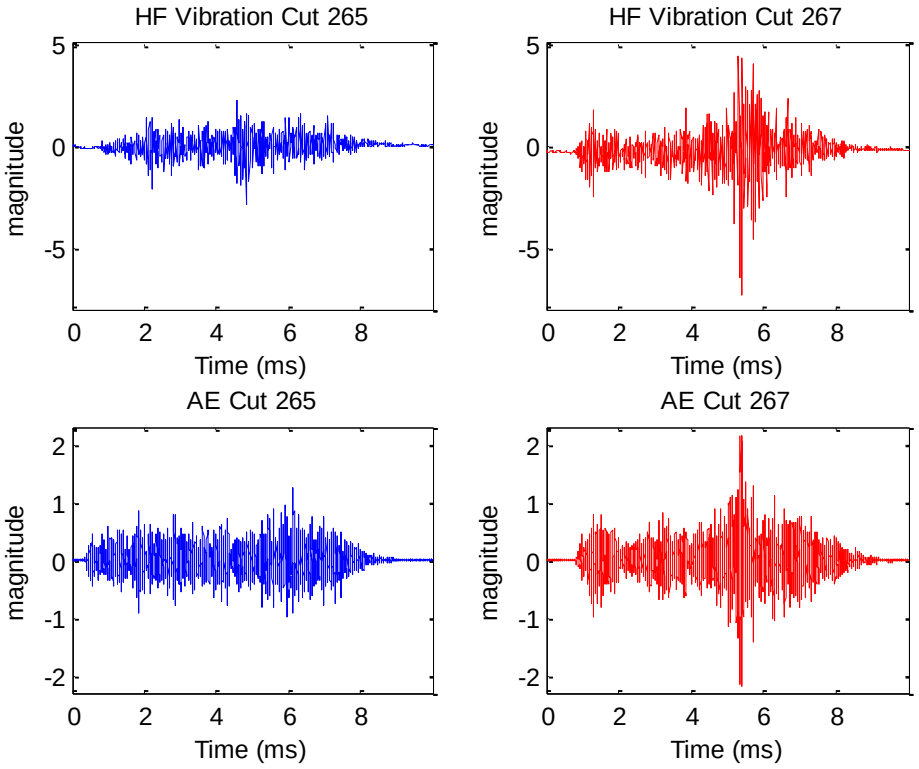

Figure 5-37: Flute pass from cut 265 (left) compared to notable flute pass in cut 267 (right) for high frequency vibration and AE sensors

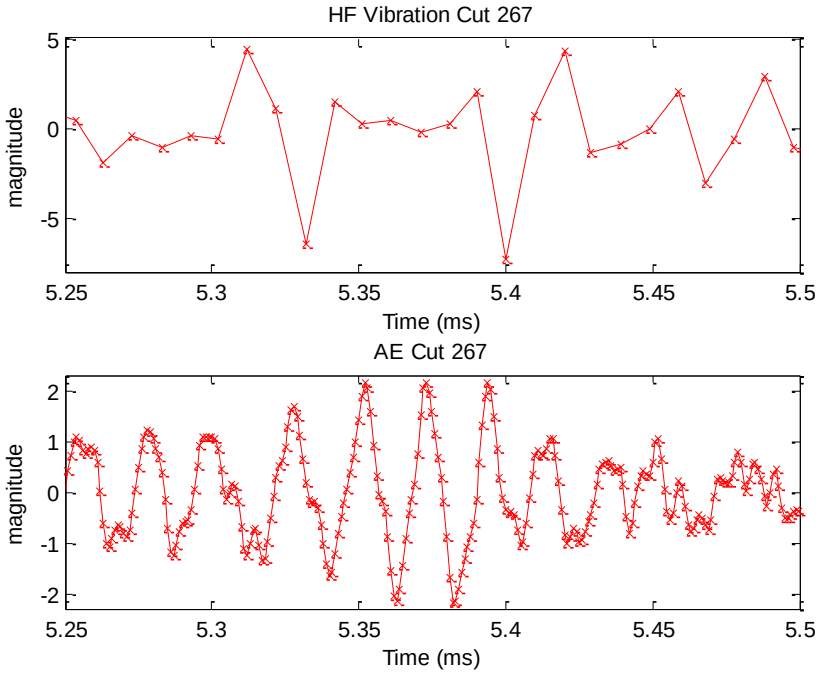

Figure 5-38: 0.25msec zoom of event in cut 267 for HF vibration (top) and AE (bottom)

With a sampling interval of 10µsec for the accelerometer and 1µsec for the AE sensor, only a small number of samples capture the occurrence. With such a limited number of samples to describe the transient event, advanced signal processing steps such as time-frequency domain analysis are unlikely to be useful.

Transient Fault Signal Subset Selection

Features have been selected in this section based on the evidence that they respond to meaningful transient events from the cutting process, such as tool chipping. A number of features chosen for the purpose of detecting such events are listed in Table 5-4.

Table 5-4: List of features selected to detect transient fault signals

1	HF Vibration Time Domain Peak
2	HF Vibration Time Domain Range
3	HF Vibration Time Domain Crest
4	Z Vibration Time Domain Peak
5	Z Vibration Time Domain Range
6	Z Vibration Time Domain Crest
7	X Vibration Time Domain Peak
8	X Vibration Time Domain Range
9	X Vibration Time Domain Crest

5.3.3 Feature Selection to Distinguish Between Fault Types

In order to classify the state of a process, it is necessary to differentiate between the sensor data associated with each class or fault type. Classification and data clustering methods, such as k-means, decision trees and support vector machines, allow multivariate data to be separated into and associated with multiple labelled clusters.

The principle of developing an unsupervised learning method is based on the wish to eliminate the measurement of response data, such as tool wear, whilst continuing to learn

intrinsic relationships in the signals measured. The proposed clustering techniques require class labels in the data set; therefore, approximate class labels that do not need additional experimental measurements have been used in this section. Two or more wear state classes can be defined by expert judgment, for example, based on the number of cuts the tool is expected to complete or on trends observed in the sensor signals. There is a requirement for a feature subset that improves separation of these defined clusters.

Greater separation between clusters is desirable in order to reliably identify which cluster a new data point should belong to. Clustering methods can therefore be measured on their ability to separate each cluster from another. A common method for optimising the performance of a clustering algorithm is to maximise the mean inter-cluster distance (distance between the centroids of each cluster) and minimise the mean intra-cluster distance (distance between points within each cluster). The Silhouette function [127] is a commonly accepted method for measuring the degree of separation of a point to one or more clusters. This has been used here to determine the optimum cluster set.

It is also necessary to minimise redundancy in feature sub-sets, as has been described earlier using the Merit function. In this section, Gram-Schmidt orthogonalisation has been used to reduce redundancy in the feature subset, thus avoiding the optimum subset being a set of features that contain the same information. Gram-Schmidt is a widely used for transforming data sets to remove redundancy. This process has been described in detail in [128]. The Gram-Schmidt method generates an orthogonal set of vectors from a linearly independent set where the orthogonal set occupies the same vector space as the original set. When applied to feature selection problems, the method allows mutual information between a new feature and a feature subset to be removed by only retaining the orthogonal component of the new feature. For example, see Figure 5-39; to remove redundancy from a set of two features, f_1 and f_2, the projection of f_2 normal to f_1, proj(f_2), should replace the f_2 in the feature set. The normal component of f_2 to f_1 is then removed from the feature set.

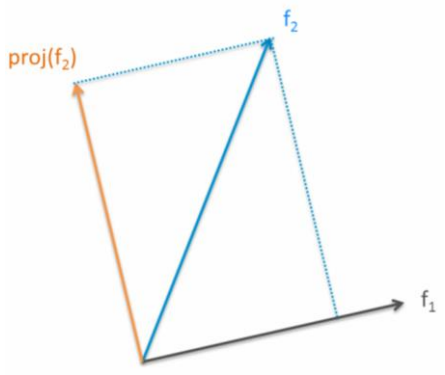

Figure 5-39: Removing redundancy using Gram-Schmidt

A feature selection method that applies the Gram-Schmidt and Silhouette functions will now be derived.

Consider a feature vector of m data points that has been normalised to have zero mean and unit variance:

$$f = (x_1, x_2, x_3, \dots x_m), \tag{11}$$

Each data point is assigned to one of c classes, where $1 < c \leq m$.

A full set of N feature vectors is obtained:

$$F = (f_1, f_2, f_3, \dots f_N). \tag{12}$$

A subset of n feature vectors is selected to be:

$$\hat{F} = (\hat{f_1}, \hat{f_2}, \hat{f_3}, \dots \hat{f_n}), \tag{13}$$

Where, for example, $\hat{f_1}$ denotes the first selected feature in the subset. (Note it is not necessarily equal to f_1).

Redundancy in the subset can be removed using the Gram-Schmidt process, resulting in the subset:

$$\hat{F^*} = (\hat{f_1}, \hat{f_2^*}, \hat{f_3^*}, \dots f_k^*) \tag{14}$$

Where $\hat{f_2^*}$ is the component of $\hat{f_2}$, that is orthonormal to $\hat{f_1}$,

$\hat{f_3^*}$ is the component of $\hat{f_3}$, that is orthonormal to $\hat{f_1}$ and $\hat{f_2}$, and

f_k^* is the component of $\hat{f}_k$ that is orthonormal to all features from 1 to $k-1$.

The inner product between any two feature vectors f_u and f_v can be calculated by:

$$\langle f_u, f_v \rangle = \sum_{i=1}^{m} f_u^i f_v^i \tag{15}$$

Where f^i is the i^{th} point in the feature vector.

$\hat{f}_2^*$ is calculated using the Gram-Schmidt process by the following equation:

$$\hat{f}_2^* = \hat{f}_2 - \frac{\langle \hat{f}_1, \hat{f}_2 \rangle}{\langle \hat{f}_1, \hat{f}_1 \rangle} \hat{f}_1 \tag{16}$$

$\hat{f}_k^*$ is the component of $\hat{f}_k$ that is orthonormal to all other features included the subset $\hat{F}$

$$\hat{f}_k^* = \hat{f}_k - \frac{\langle \hat{f}_1, \hat{f}_k \rangle}{\langle \hat{f}_1, \hat{f}_1 \rangle} \hat{f}_1 - \frac{\langle \hat{f}_2, \hat{f}_k \rangle}{\langle \hat{f}_2, \hat{f}_2 \rangle} \hat{f}_2 \dots - \frac{\langle \hat{f}_{k-1}, \hat{f}_k \rangle}{\langle \hat{f}_{k-1}, \hat{f}_{k-1} \rangle} \hat{f}_{k-1} \tag{17}$$

The amount of information in any feature subset will be measured by the degree of separation between classes. The mean Silhouette over points 1 to i in any feature subset is derived by:

$$S(\hat{F}^*) = \frac{1}{m} \sum_{i=1}^{m} \frac{(b_i - a_i)}{\max(a_i, b_i)} \tag{18}$$

Where a_i is the average distance from the *i*th point to all other points in the same class as i, and b_i is the minimum average distance from the *i*th point to all points in a different class, minimised over the classes.

A forward sequential feature selection method will be used to find the optimum subset. The first feature selected does not require the Gram-Schmidt process as it will be the feature that obtains the maximum Silhouette value for a subset size of 1.

This technique has been applied as an alternative to the Merit ranking method applied in section 5.3.1. The Merit function was used to retain features that have a good fit to approximated polynomial models, whilst minimising the redundancy by including feature-

feature correlations in the function. In this section, the Silhouette method has been used to retain features that show a larger separation in the data, when associated to two or more classes. The addition of the Gram-Schmidt transformation allows redundancy to be avoided in the final feature subset. The use of the Silhouette method for ranking feature subsets is favourable when the objective is to detect outliers from clusters. The advantage in the Merit function is that it can be used where points cannot be reliably associated with a class.

Two Class Separation (without Gram-Schmidt)

Fault detection in its most basic form is a 2-class classification problem where a process is either normal or faulty. The data has been divided into normal and faulty classes based on observation of the process. The first class, considered to be normal operating conditions, is all cuts taken up to and including cut 266. The second class, considered to be faulty operating conditions, is all cuts beyond cut 266. Subjectivity in this class separation will be considered later in this chapter.

In order to ensure the feature selection is not biased towards features greater in magnitude or variance, all features have been scaled to have zero mean and unit variance by deducting the mean from each data point and dividing by the standard deviation.

The results of forward and reverse sequential feature selection based on maximising the mean silhouette value are shown in Figure 5-40. Both forward and reverse methods provided identical results. It can be seen that the maximum silhouette is achieved using a single feature.

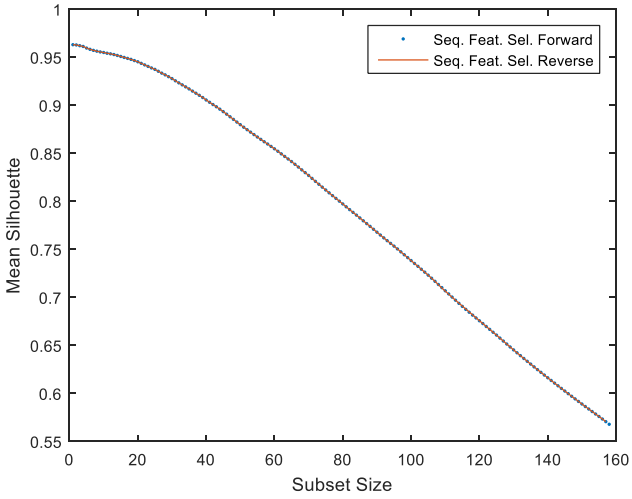

Figure 5-40: Sequential feature selection using 2-class cluster separation

The optimum cluster separation is achieved using Microphone-1 Frequency Domain Variance and is shown in Figure 5-41 and Figure 5-42. It can be seen that there is a clear separation between the two classes using only this single feature.

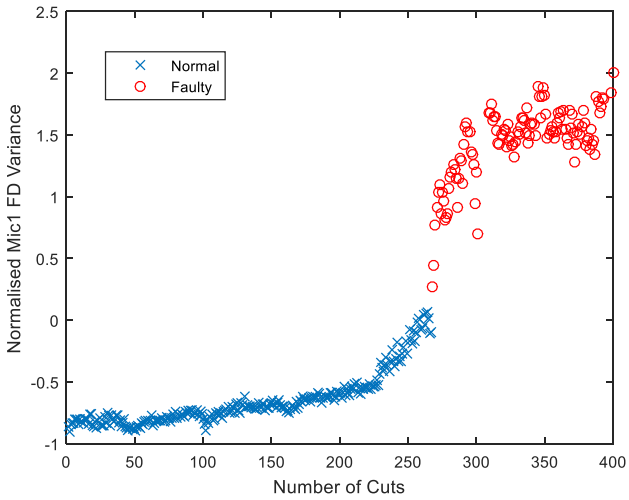

Figure 5-41: Normalised Microphone-1 Frequency Domain Variance

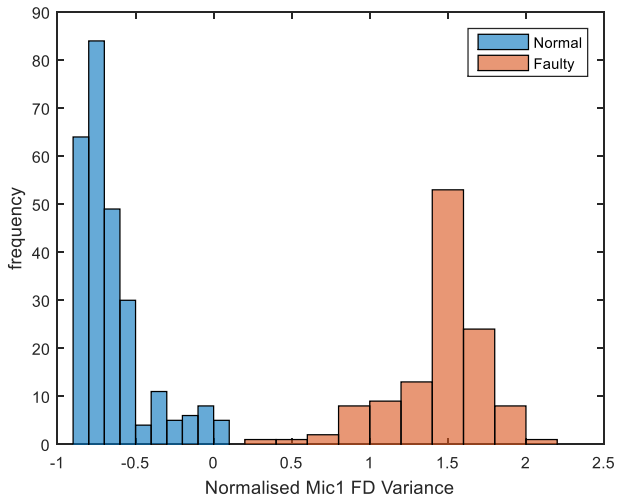

Figure 5-42: Microphone-1 Frequency Domain Variance Shown as a Histogram for 2 Classes

The highest scoring features are different to those found in section 5.3.1, which are now predominantly made up of microphone sensor features. This method of feature selection does not use a measure of redundancy as was the case in the Merit ranking method used in section 5.3.1. As a result, it is apparent from Figure 5-43 that the highest scoring features contain similar information.

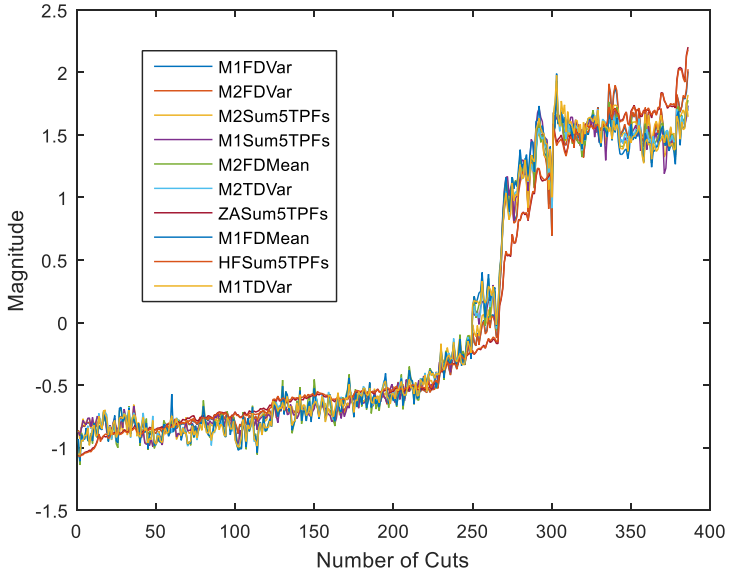

Figure 5-43: High redundancy in features selected using 2-class cluster separation without Gram-Schmidt

Two Class Separation (with Gram-Schmidt)

It is apparent from the previous plot that without accounting for redundancy in the feature set, features which behave the same are selected. The Gram-Schmidt method described earlier is now included so that each additional feature contains only the orthogonal component to the existing feature set.

It can be seen from Figure 5-44 that the subset size of 1 provides the highest mean silhouette, diminishing more rapidly than without Gram-Schmidt as the subset size increases. This rapid decline can be expected, given that the mutual information has been removed.

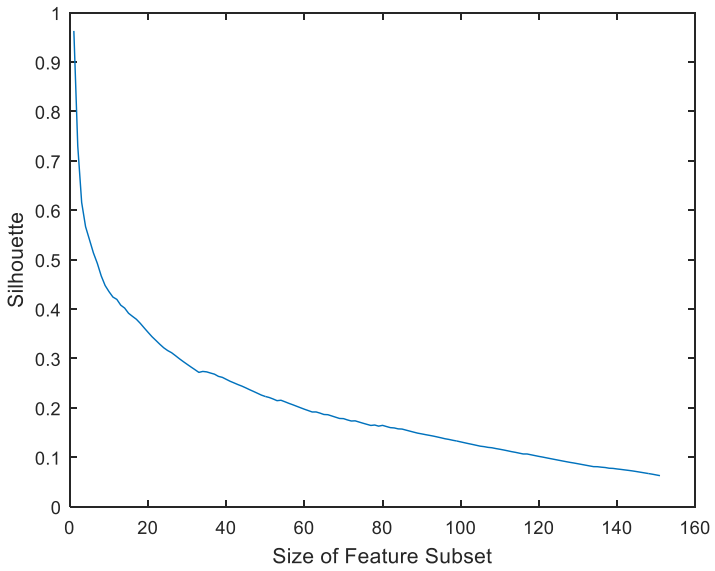

Figure 5-44: Mean silhouette against subset size for 2-class case with Gram-Schmidt

The first 5 features selected are shown in Figure 5-45. The orthonormal components of these features are also shown in Figure 5-46. Note that the first selected feature, M1 FD Variance, is the most influential feature, having the form of features. See Figure 5-43. This feature has no component removed in the second plot but has been normalised.

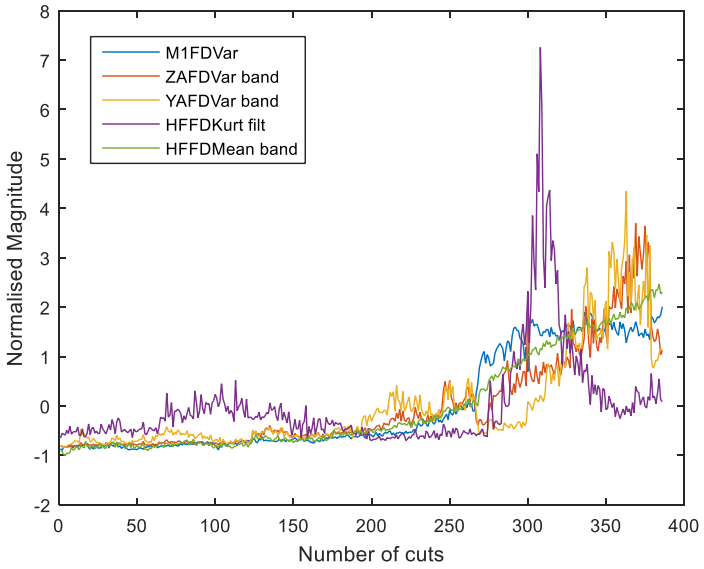

Figure 5-45: First 5 features selected for 2-class case

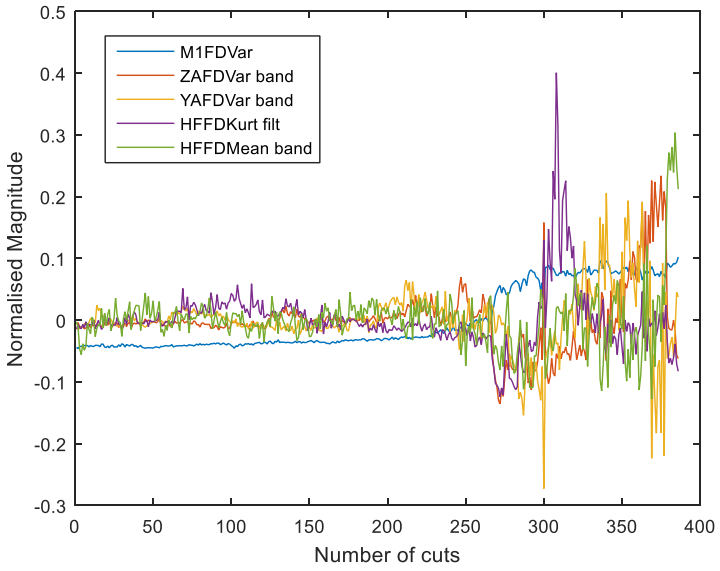

Figure 5-46: First 5 orthonormal features selected for 2-class case

Four Class Separation (without Gram-Schmidt)

The cluster separation approach has also been applied to a multi-class problem. The data set is divided into 4 arbitrary wear classes from cuts 1-100, 101-200, 201-300 and 301-400.

Forward sequential feature selection provides the results shown in Figure 5-47, initially without using the Gram-Schmidt method.

Note that the function optimises the mean silhouette for all classes, so the figure shows the contribution of the mean silhouette for each class. It can be seen that cuts 201-300 have the least separation from other data sets, while cuts 0-100 and 301-400 have high separation.

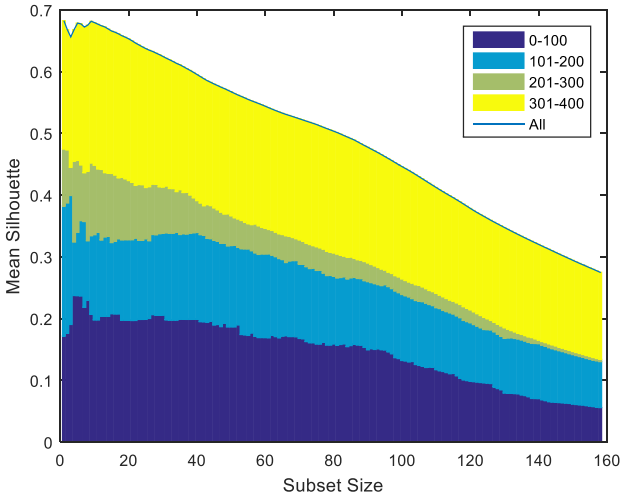

Figure 5-47: Sequential feature selection using 4-class cluster separation

The highest silhouette value achieved was reduced from the 2-class system from 0.96 to 0.68, highlighting as one would expect that the 4-class problem is more difficult to classify correctly. This is also evident from the overlap between classes shown in Figure 5-48.

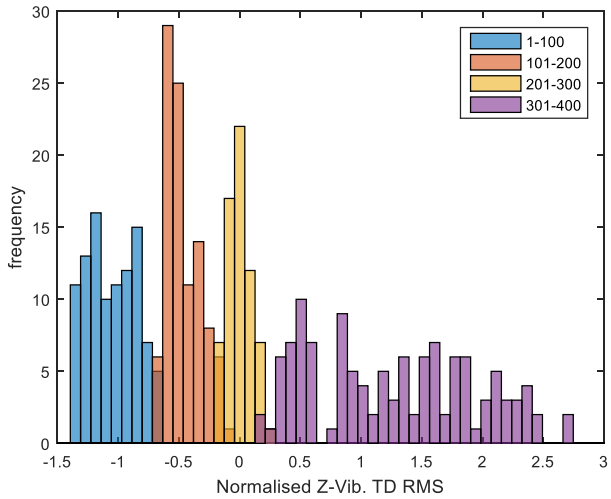

Figure 5-48: Z-Vibration Time Domain RMS Shown as a Histogram for 4 Classes

The top 10 features for classification of the 4-class tool state are found to be:

1. Z-Vibration Time Domain RMS
2. Z-Vibration Time Domain Variance
3. Z-Vibration Frequency Domain Mean Band
4. Y-Vibration Frequency Domain Kurtosis
5. Y-Vibration Frequency Domain Mean Band
6. HF-Vibration Frequency Domain Mean Band
7. AE Sensor Frequency Domain Mean
8. Y-Vibration Frequency Domain Skew
9. HF-Vibration Time Domain RMS
10. AE Sensor Frequency Domain Mean Band

Less redundancy can be seen in the data, although some features containing similar information remain. Figure 5-49 shows similarities between the selected features.

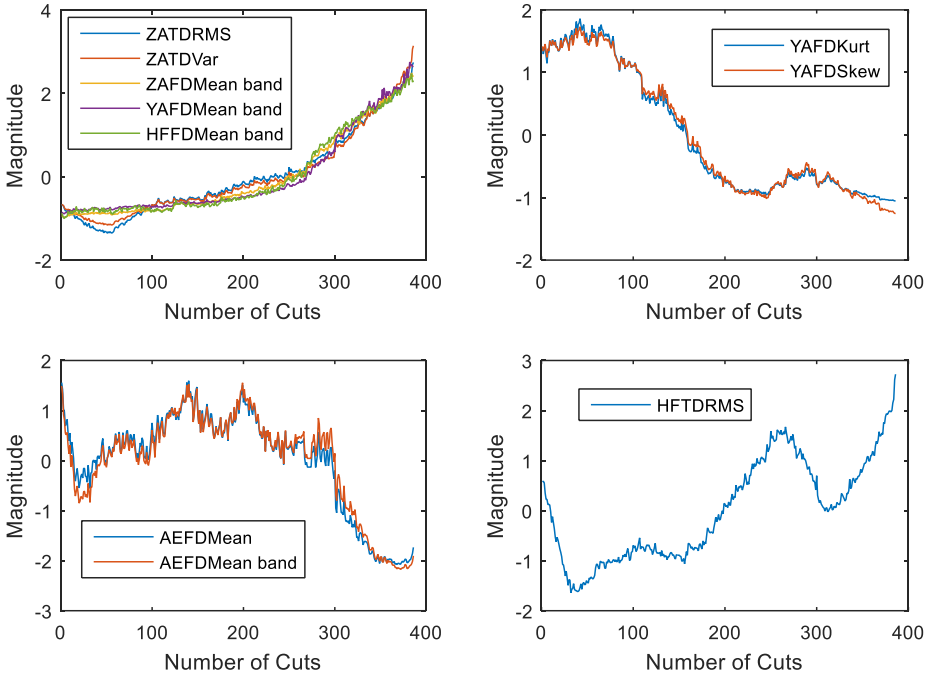

Figure 5-49: First 10 normalised features selected using 4-class cluster separation

Four Class Separation (with Gram-Schmidt)

The Gram-Schmidt is now used for the 4-class case where each additional feature added contains only the orthogonal component to the existing feature set. The optimum subset size is 1 as shown in Figure 5-50.

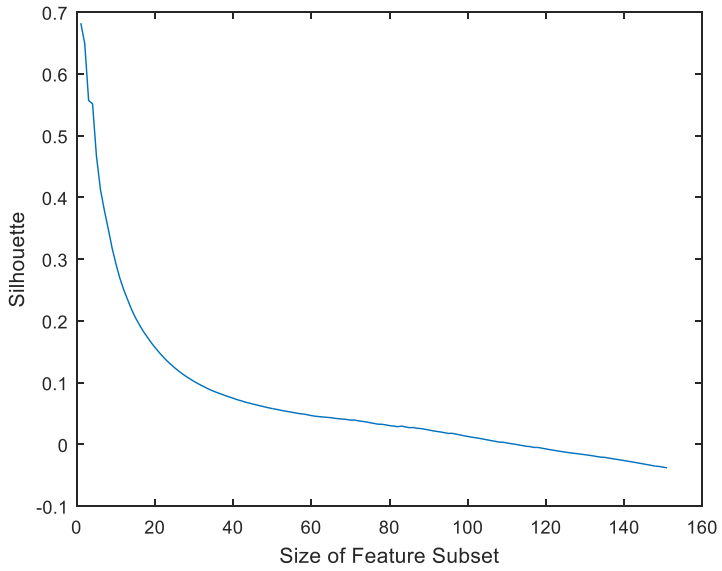

Figure 5-50: Mean silhouette against subset size for 4-class case with Gram-Schmidt

The first 5 features selected are shown in Figure 5-51. The orthonormal components of these features are also shown in Figure 5-52.

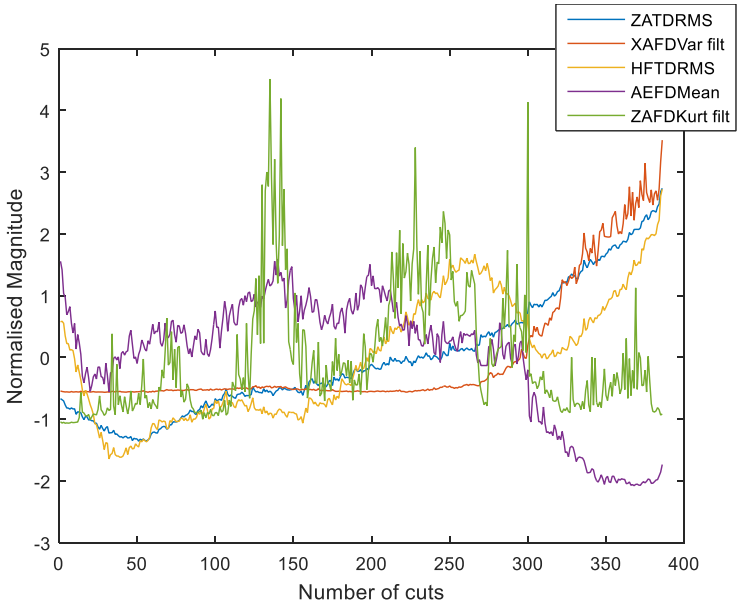

Figure 5-51: First 5 features selected for 4-class case

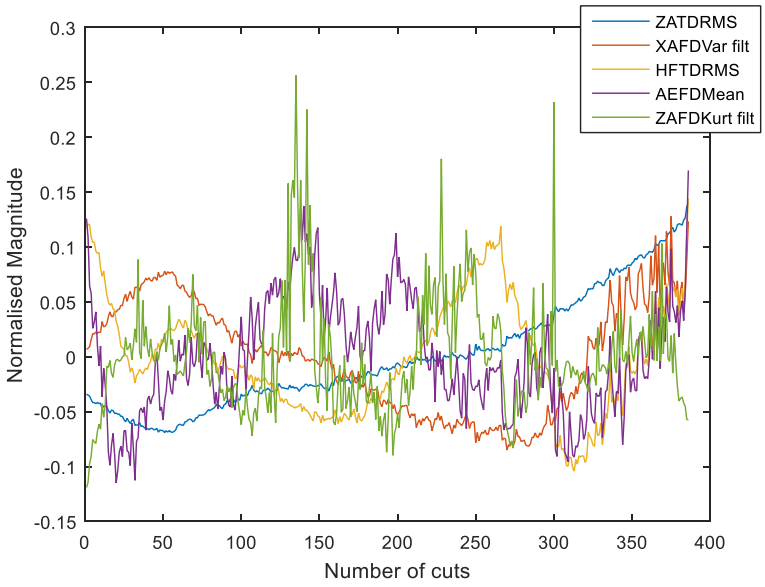

Figure 5-52: First 5 orthonormal features selected for 4-class case

This section evaluated the degree of separation between data in the feature subsets for a 2 and 4-class example. If the results shown are an accurate representation of the process, these conclude that the single feature contains the majority of information.

5.3.4 Feature Selection Summary

Section 5.2 presented the data from Experiment 1, where a milling tool is used from a new condition through to a severely worn condition. The analysis of the sensor data has led to the selection of sensor signal features that are sensitive to the changes in the cutting process over the tool's life.

It has been shown that a number of features correlate well to the time in cut. A polynomial model fit method has been proposed to down select such features. A sequential feature selection technique has been used to determine the optimum feature subset based on a Merit measure of information which considers both the correlation to the model and correlation with each other. The Pearson product-moment correlation coefficient has been used here. However, it may be worth considering a rank correlation, such as Spearmen's rank correlation coefficient, in future work as this can detect monotonic relationships, and does not assume a linear relationship as with the Pearson method.

The features selected based on their fit to polynomial models transpire to be those which are insensitive to transient events during cutting. Such events may have useful meaning when determining the condition of a cutting process, such as those observed in the vibration data during cuts 200 and 267 that may be related to chipping of the tool. The detection of these events is important in order to allow a tool to be removed from the process prior to damage being caused to the surface. In the case presented, it is proposed that the point in time where tool chipping occurs can be observed using several features, one of which is found to be the peak magnitude of the Z-direction vibration signal. The time domain range and time domain crest factor also provide good results, as do the high frequency and X-direction accelerometers.

Classification methods are often used to identify the condition of a process and will be applied further in the next chapter. The degree of separation between data for different process states has been evaluated during the feature selection process. A 2-class and a 4-class example have been used. The microphone data has shown a strong separation between data for the define normal (cuts 1-266) and fault (cuts267-400) states, whereas vibration data provides more reliable results for the 4-class problem. This feature selection method

has removed redundancy in the data by applying the Gram-Schmidt method, however the Silhouette method for determining class separation gives an optimum subset size of 1.

This analysis has assumed that signals that are sensitive to changes in cutting conditions over the life of a tool provide good indications of the machining conditions. On this basis, it is assumed that the features selected will be suitable for the forthcoming sections of this thesis when covering fault detection and diagnosis. The final selection of an optimum feature subset is not settled by this section. The analysis does, however, provide a suitable set of features from each of the three sub-sections; (5.3.1) feature selection from continuous fault signals over the tools life, (5.3.2) feature selection from transient fault signals observed in the sensor signal, and (5.3.3) feature selection based on class separation.

Table 5-5 summarises the selected features (using the short names defined earlier in Table 4-2 and Table 5-1). Although the class separation method selected a feature subset size of 1, the first 10 features have been listed and are used for the feature subset in the analysis in later sections. Each feature subset (FS) has been given a number for reference in future sections of this thesis.

Table 5-5: Summary of feature subsets

FS1	FS2	FS3	FS4	FS5	FS6
Polynomial Model/Merit	**Transient Fault Signal**	**2-Class Separation**	**2-Class Separation (G-S)**	**4-Class Separation**	**4-Class Separation (G-S)**
HF.TD.RMS	HF.TD.P	M1.FD.V	M1.FD.V	ZV.TD.RMS	ZV.TD.RMS
ZV.TD.K	HF.TD.Rng	M2.FD.V	ZV.FDb.V	ZV.TD.V	XV.FDf.V
HF.FD.S	HF.TD.CF	M2.TPF	YV.FDb.V	Z.FDb.M	HF.TD.RMS
AE.TD.K	ZV.TD.P	M1.TPF	HF.FDf.K	YV.FD.K	AE.FD.M
XV.FDf.S	ZV.TD.Rng	M2.FD.M	HF.FDb.M	YV.FDb.M	ZV.FDf.K
HF.TD.V	ZV.TD.CF	M2.TD.V	M2.FD.V	HF.FDb.M	YV.TD.K
SP.FDb.V	XV.TD.P	ZV.TPF	XV.TPF	AE.FD.M	XV.TD.RMS
HF.FD.K	XV.TD.Rng	M1.FD.M	M1.TPF	YV.FD.S	SP.FDb.V
SP.FDb.S	XV.TD.CF	HF.TPF	ZV.FD.V	HF.TD.RMS	M1.TPF
YV.TD.S	*(optimum set)*	M1.TD.V	HF.FD.V	AE.FDb.M	YV.FD.K
HF.FDf.V		-	-	-	-
M1.FDf.V					
HF.FDf.S					
YV.FD.K					
(optimum set)					

Given the large redundancy that was found in FS3 and FS5, these subsets will not be taken further. Furthermore, the features chosen for FS2 may be appropriate for fault detection problems where the fault is transient. These will not be included in further analysis, however, they are recommended as additional features to add to a subset where transient faults are being overlooked by a fault detection algorithm.

6 Novelty Detection and Fault Diagnosis

This chapter takes the feature subsets from the previous chapter and evaluates several methods for novelty detection and fault diagnosis. Figure 6-1 summarises the reasearch areas of this chapter, separating sections into fault detection and fault diagnosis.

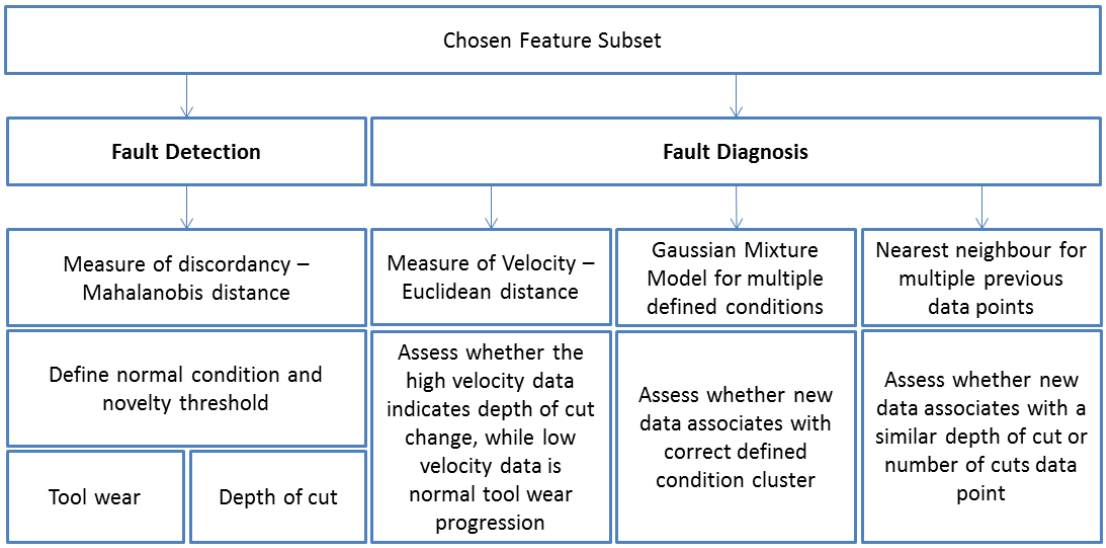

Figure 6-1: Summary of fault detection and diagnosis topics

Section 6.1 applies a novelty detection method to the data by using the Mahalanobis distance as a measure of discordancy and defining a principled novelty threshold. The ability to detect changes to depth of cut is presented, now including the fault data obtained through Experiment 2.

Section 6.2 covers fault diagnosis, extending the method used for fault detection by using clustering to differentiate between different fault types.

Finally, section 6.3 summarises the preferred monitoring methods and applies them to Experiment 3 - an existing data set for a repeat ball nose milling operations.

6.1 Fault Detection

A fault detection system is dependent on sensor data containing adequate information to show the difference between a normal and a faulty process. False alarms must be avoided. Therefore the fault signal must be distinguishable from confounding influences, including signal noise and benign operational and environmental changes. The previous section has aimed to select the appropriate sensor feature sets that achieve this. Feature sets FS1, FS4 and FS6 are used to demonstrate fault detection in this section.

As has been discussed in the literature review, an unsupervised learning approach is appropriate to avoid the significant experimental costs associated with training a supervised learning algorithm. A novelty detection method will be investigated in this section. The recreation of many fault types may not be achievable in a production environment; therefore the system will define the normal condition and classify outliers from this definition as faults.

Section 6.1.1 will investigate the use of the Mahalanobis distance to obtain a measure of discordancy from the normal condition data set. The data from Experiment 1 will be used here. Section 6.1.2 will then go on to define a principled novelty threshold that is used to determine when a novelty or fault has occurred. The influence of the size of the data set that defines the normal condition will be considered. Section 6.1.3 will test the novelty detection method using the data from Experiment 2, where multiple depths of cut are used as proxies for faults.

6.1.1 Novelty Detection Using the Mahalanobis Distance

Novelty detection requires a measure of how dissimilar a sample of feature data is, compared to other samples. This measure is often referred to as discordancy. A novelty is a sample which has a large discordancy in comparison to other samples in a data set. The magnitude of the discordancy over which a data point is considered a novelty is determined by a threshold value.

When a process begins with no prior sensor data, a definition of the normal operating condition must be generated with the data as it is collected. A discordancy measure must then be calculated for subsequent data points to determine if they are an outlier.

The definition of normal operating conditions can be obtained by stating that cuts 1-*n* are normal. The value *n* may be gained from prior information about the process or operator feedback, for example. Cuts >*n* are of unknown condition; therefore the condition must be estimated by comparison to the defined normal state.

To demonstrate the proposed method of fault detection, an estimate of the end of the tool's life is used to define the normal condition data set in Experiment 1; all cuts through to cut 266 (as discussed in the previous section) will define the normal condition, and all subsequent cuts will be considered a faulty condition.

The Mahalanobis distance will be used as it is an established method to determine the degree of discordancy of a data point from the normal condition data set. The Mahalanobis distance is a measure of the distance between a point and a Gaussian distribution, calculated from the following equation:

$$D(x,y) = \sqrt{(x-\mu)^T S^{-1}(x-\mu)} \tag{19}$$

Where,

- $D(x,y)$ is the Mahalanobis distance between set of observations x from the normal condition defined by y
- x is a set of observations or sensor signal features
- μ is the set of mean values for normal condition y for each signal feature
- S is the covariance matrix for normal condition y

A fault detection solution will be assessed using feature subsets FS1, FS4 and FS6 from Table 5-5. There are 14 features in FS1, therefore the first two principal components, obtained using PCA, have been used to plot the data. For FS4 and FS6, the first two components have been used to plot the data, given the Gram-Schmidt method has already transformed the data to be orthonormal, which is adequate for visualisation.

Figure 6-2 presents a scatter plot of FS1 using the first two principal components from PCA for the x and y axis. The colour bar shows the log of the Mahalanobis distance from the normal condition data (calculated without PCA transformation, though this would not change the result given that PCA is only a rotation of the data). There is a clear divide between the normal and faulty data sets.

There is also evidence of an additional incipient fault cluster consisting of the points in the bottom left of the normal condition cluster. If the data is in fact two separate clusters, the normal condition Gaussian may be poorly defined. This possibility will be discussed again in section 6.2.1.

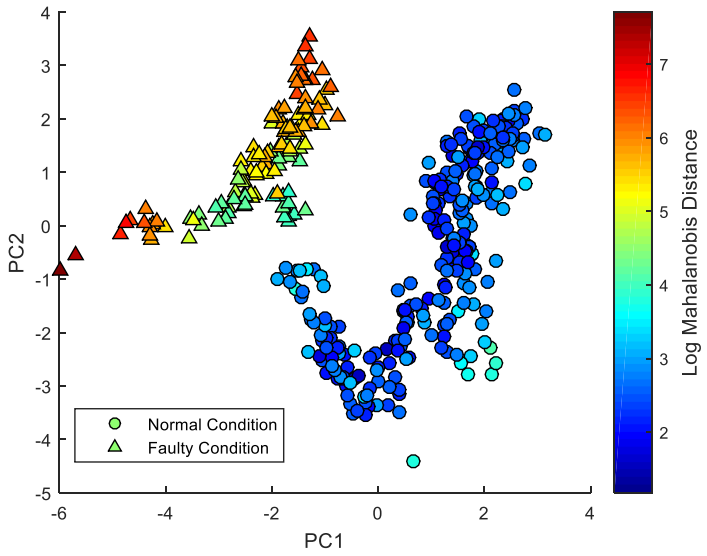

Figure 6-2: Scatter plot of Log of Mahalanobis distance for colour bar FS1

Figure 6-3 shows the Mahalanobis distance against the number of cuts. An increase in magnitude is observed around cut 266. A novelty threshold will be defined in section 6.1.2.

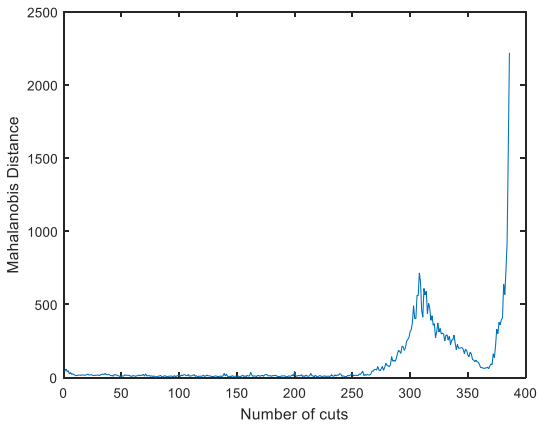

Figure 6-3: Mahalanobis distance vs number of cuts for FS1 (novelty threshold not yet defined)

Figure 6-4 presents a scatter plot for FS4, using the first two features for plotting on the x and y axis. The Mahalanobis distance is computed from the full set. Again, there is a clear divide between the normal and fault data sets. There is further evidence of an incipient fault cluster to the top right of the normal condition cluster.

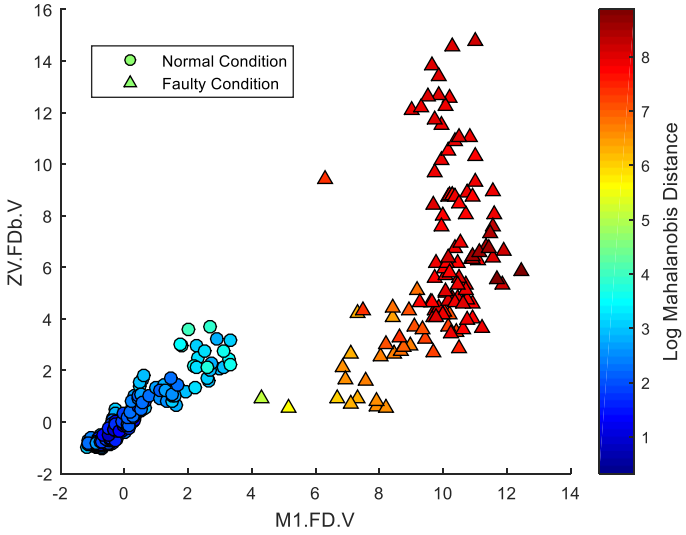

Figure 6-4: Scatter plot of Mahalanobis distance using FS4

Figure 6-5 shows the Mahalanobis distance against the number of cuts. There is a significant rise in the distance, initiated at cut 266 and continuing to rise to around cut 310.

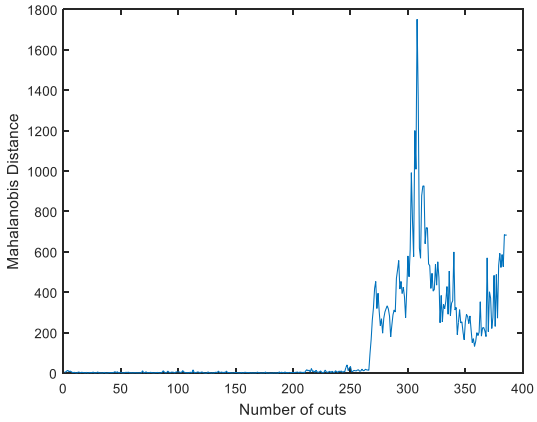

Figure 6-5: Mahalanobis distance vs number of cuts for FS4 (novelty threshold not yet defined)

Figure 6-6 and Figure 6-7 present the same information for FS6. For this feature set, the distance increases more gradually, continuing to increase exponentially through to the end

of the data set. Note that novelty thresholds have not yet been plotted. These will be defined later in section 6.1.2.

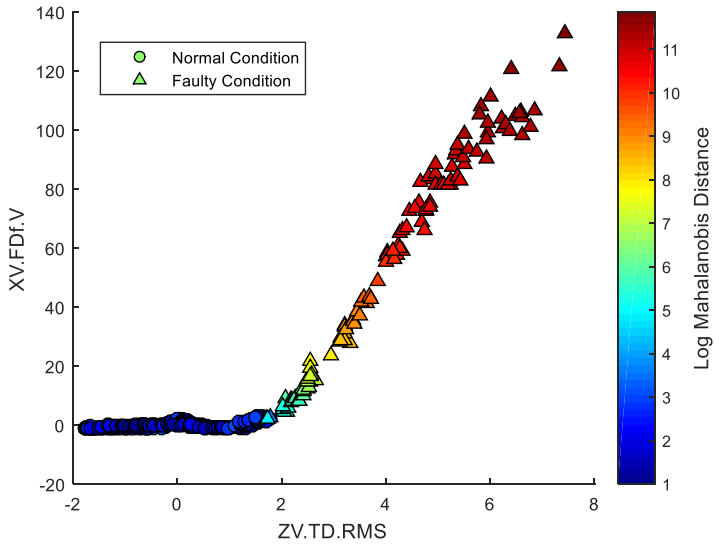

Figure 6-6: Scatter plot of Mahalanobis distance for FS6

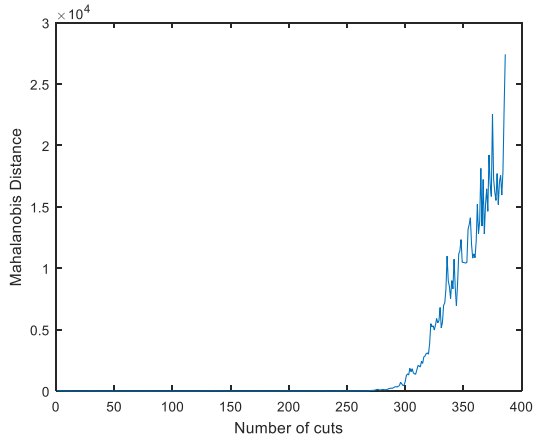

Figure 6-7: Mahalanobis distance vs number of cuts for FS6 (novelty threshold not yet defined)

Note that the Mahalanobis distance is not affected by Gram-Schmidt orthogonalisation, therefore the orthonormal data has only been used for feature selection and the original feature data is used here.

It can be seen that for each of the three feature subsets chosen, all give increasing Mahalanobis distance towards the end of the tool's life.

6.1.2 Selecting a Principled Novelty Threshold

A principled method of selecting the novelty threshold can be achieved by using the Monte Carlo method presented in [83] and [89]. A matrix of the same size as the data set that defines the normal condition is populated with elements randomly drawn from a normal distribution of zero mean and unit variance. (Note that each feature within the normal condition feature set has also been normalised to have zero mean and unit variance at this point). The Mahalanobis distance is calculated for each feature set in this matrix and the largest distance is recorded. The process is repeated a 10,000 times, until a distribution of the Mahalanobis distance is obtained. An appropriate percentile of this distribution (e.g. the 90th and 99th percentile in the later example) can then be selected to define the novelty threshold.

Figure 6-8 presents the first point at which the novelty threshold is reached for FS1 according to the number of cuts that define the normal condition. When the normal condition is defined using above 200 cuts, the threshold is not reached for the whole data set. However, if 80 cuts are used to define the normal condition, for example, the threshold is reached at between 200 and 250 cuts.

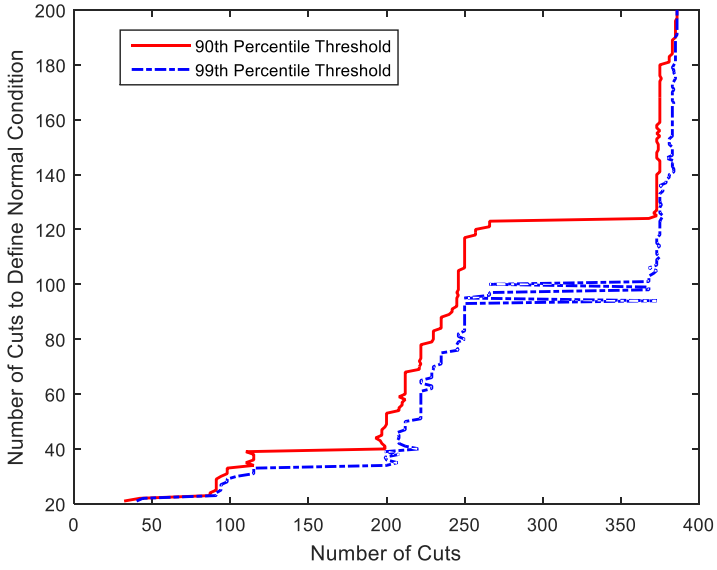

Figure 6-8: Principled novelty threshold limits for FS1

The 90th percentile threshold plots for FS1, FS4 and FS6 are shown in Figure 6-9. It can be seen that for FS6, increasing the number of cuts to define the normal condition from around 100 through to 250, has little effect on the point a novelty is detected.

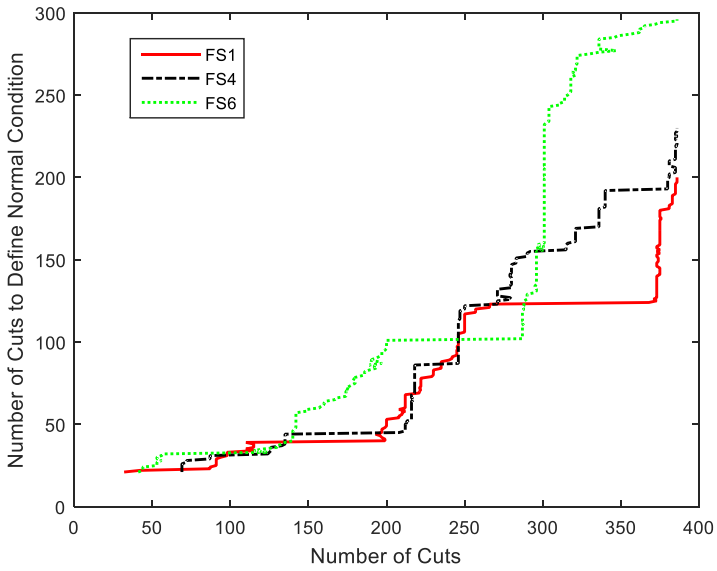

Figure 6-9: 90th Percentile novelty threshold for FS1, FS4 and FS6

Several observations can be made from Figure 6-9, as follows:

- The threshold obtained using FS1 and FS4 classifies a fault in less than 200 cuts when the normal condition data set is less than approximately 50.
- The threshold is not passed for any cut for FS1 and FS4 if more than approximately 200 cuts are used to define the normal condition.
- The threshold is passed at approximately 300 cuts for FS6 where the normal condition data set is between approximately 100 and 250 cuts.

Clearly, the appropriate number of cuts to define the normal condition is dependent on the feature set and the desired tool change point. For subsequent analysis, the first 100 cuts will be used to define the normal condition and the 90th percentile will be used as the novelty threshold.

6.1.3 Detection of Changes to Depth of Cut

In order to validate the novelty detection method described, the variable depth of cut data obtained in Experiment 2 has been evaluated. In all cases, the data from Experiment 2 was classed as a novelty. Figure 6-10 shows the data for Experiment 1 and Experiment 2 for FS1 using only the first two principle components to present the data. Note that the Mahalanobis distance is calculated from the full data set, while the plot only uses two dimensions to present the data. A data set of 100 cuts was used to define the normal condition and the 90th percentile defined the novelty threshold.

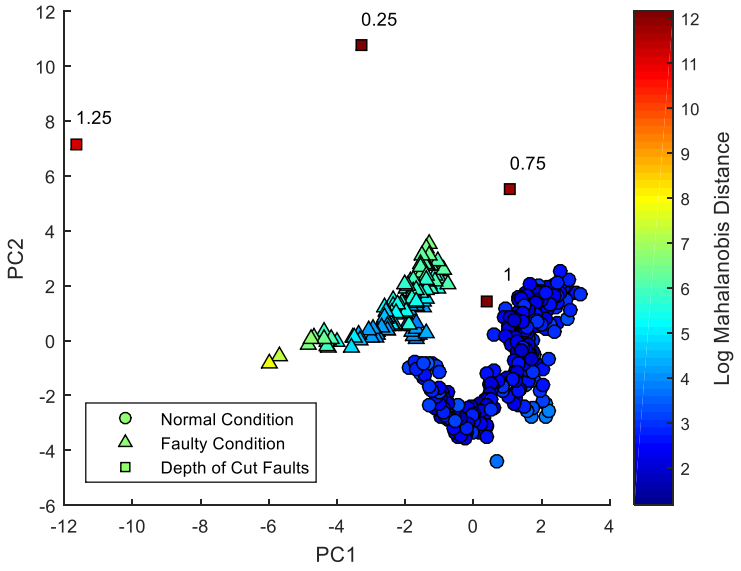

Figure 6-10: Experiment 1 and Experiment 2 data for FS1

For FS1, all data from Experiment 2 had a larger Mahalanobis distance from the normal data set than the highest distance found in Experiment 1 data. However, this was not the case for FS4 and FS6. Figure 6-11 shows the Mahalanobis distance for Experiment 2 for each feature subset. The figure also shows the novelty threshold calculated and the maximum Mahalanobis distance found in Experiment 1.

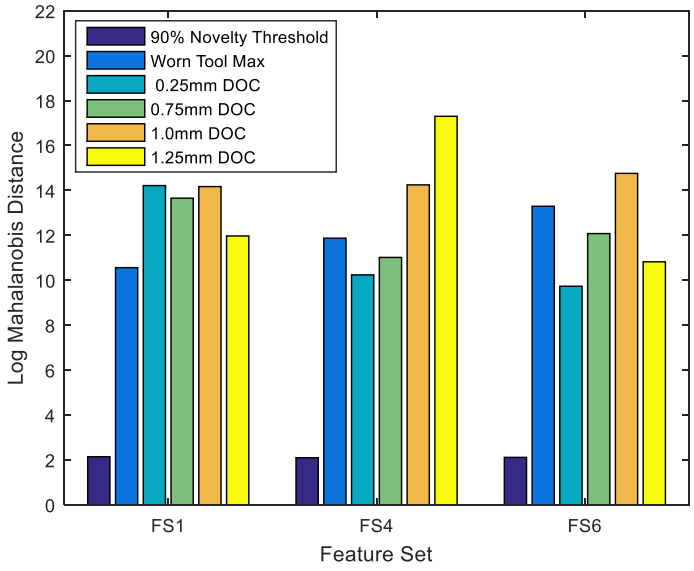

Figure 6-11: Log of Mahalanobis distance for Experiment 2 for each feature set

6.2 Fault Diagnosis

Fault diagnosis is achieved by associating data with a fault type. The literature review has shown that in the vast majority of cases, this has been achieved using supervised learning by training a given system to recognise known, pre-defined faults. The high cost of obtaining fault data has been discussed, and in many cases, it is impractical to re-create fault conditions on a production process. Consequently, this section will present a method for supporting a machine, or operator, in making a diagnosis of a fault type or cause without extensive training requirements.

An unsupervised method for fault diagnosis can be achieved by extending the novelty detection method in the previous section to consider multiple clusters within the data set.

Section 6.2.1 will first show that the data set from Experiment 1 can be modelled using multiple Gaussians, rather than the single normal condition Gaussian shown in section 6. Two applications are then presented, where clustering of the data allows fault types to be distinguished. The first, in section 6.2.1, will evaluate the clusters that are present in the tool life data by using a Gaussian Mixture Model (GMM). The nature of tool wear faults will be considered to differentiate them from other fault types. Section 6.2.3 will then evaluate how new faults can be added to the data set as they are observed in production, then allowing repeat faults to be diagnosed by association to a small number of previous observations.

6.2.1 Describing the Data Set with Multiple Gaussians

A limitation of the novelty detection method described in the previous section is that it relies on the normal state being correctly described by a single Gaussian. In some cases, the normal state may not be a single Gaussian distribution and may be better represented as a number of separate distributions.

The problem of misrepresenting the normal condition is illustrated by the theoretical data set shown in Figure 6-12, where a fault has been incorrectly associated with the normal condition. In Figure 6-13, however, the normal condition is represented as two Gaussians and the fault condition is a clear outlier. Referring back to Figure 6-2, the normal cluster may carry these characteristics, given the normal data on the left of the plot appears to be a

separate distribution. The example presented in the figures has also been seen in the previous data shown in section 6.1.1.

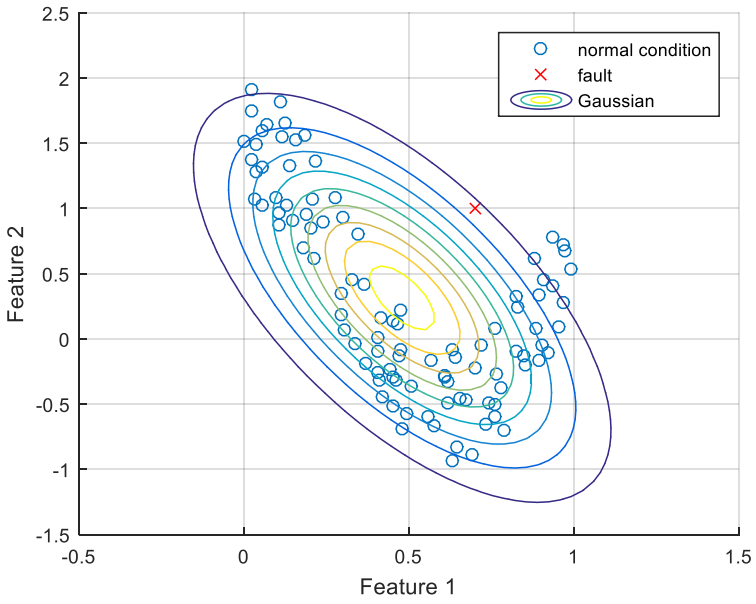

Figure 6-12: Example normal condition represented as one Gaussian

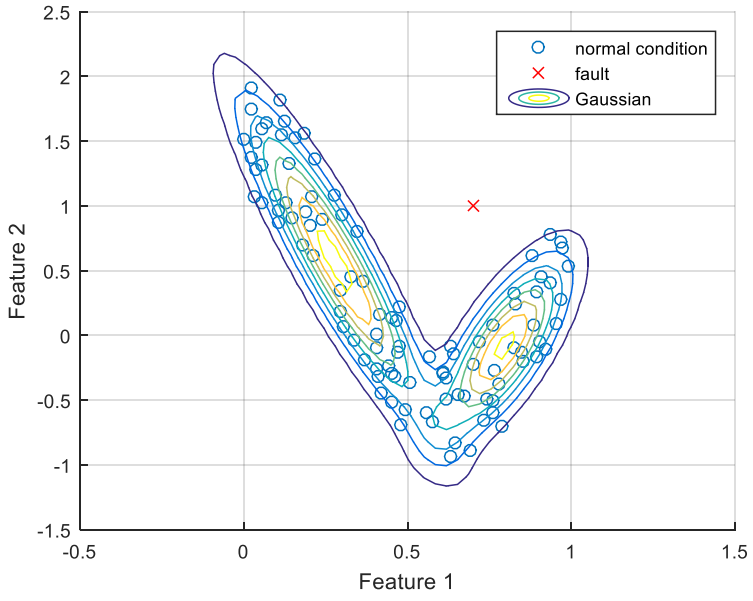

Figure 6-13: Example normal condition represented as two Gaussians

One means of detecting when this issue is arising is to measure when a data set begins to become non-Gaussian, then to use this measure as a threshold for defining new clusters.

Investigation into this has not been carried out in this work, but should be considered in future investigations.

This issue of over simplifying the model that describes the data also applies to fault diagnosis. Gaussian Mixture Models (GMM) can be used to separate the data into an optimum number of clusters and representing each cluster probabilistically using a Gaussian distribution. The different clusters can then be used to define multiple classes of both normal and faulty conditions.

An example of novelty detection from multiple Gaussians is now presented using feature subset FS1. The same method as shown in 6.1.1 (Figure 6-2 and Figure 6-3) is used here, where the cuts that follow cut 266 will be classed as faulty. Data up to and including cut 266 will be evaluated using a GMM to determine the optimum number of clusters that describe this data. Data after cut 266 have been omitted from the GMM given that these points would not be available in a production environment as the process would be halted once a fault is detected.

The optimum number of clusters can be measured using the Silhouette function described in section 5.3.3. In the case of FS1, the optimum number of clusters is found to be 3, as shown by the mean Silhouette for each GMM shown in Figure 6-14.

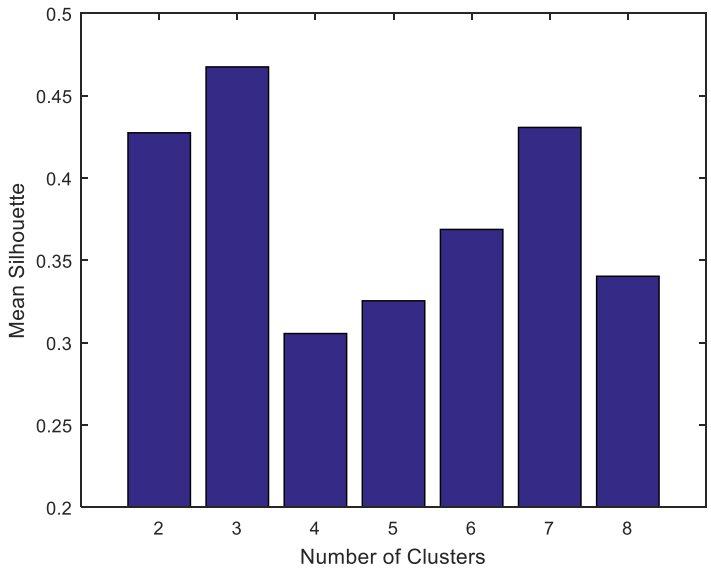

Figure 6-14: Mean Silhouette vs number of clusters for FS1

It can be shown that the natural separation in the data is time dependent. The three cluster model fits the data such that the first cluster is made up of cuts 1-39, the second from cuts 40-159 and the third from cuts 160-266. The probability of each point belonging to a cluster can be extracted from the model and is shown in Figure 6-15.

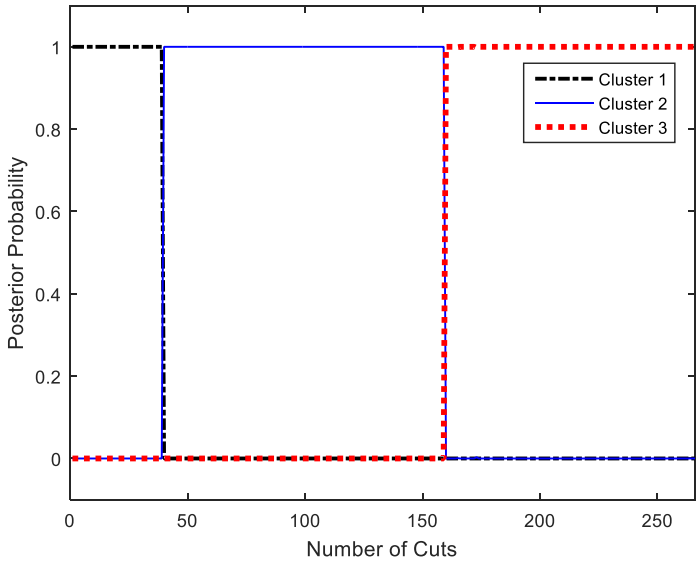

Figure 6-15: Probability of data point belonging to each cluster using the 3 normal clusters GMM for FS1

The three clusters are plotted in Figure 6-16 using the first two principal components of FS1. To emphasise the separation of cluster Normal 1 and Normal 2, the third principle component is added and the data is plotted as a 3D scatter plot in Figure 6-17.

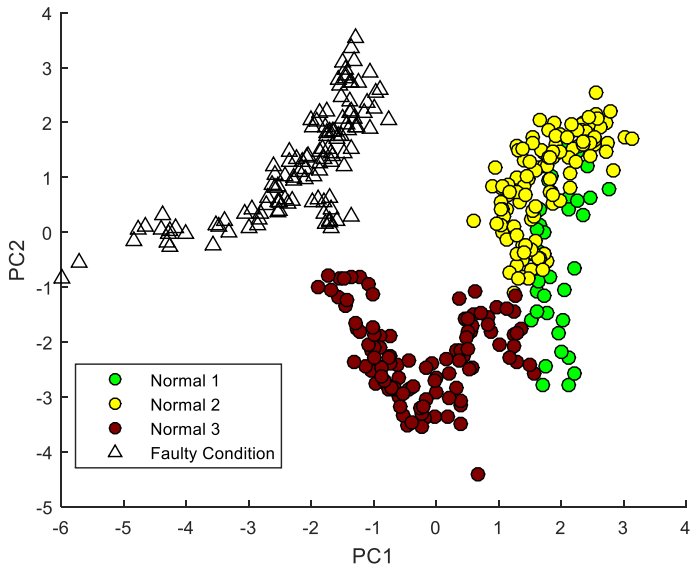

Figure 6-16: First two principle components showing 3 normal clusters for FS1

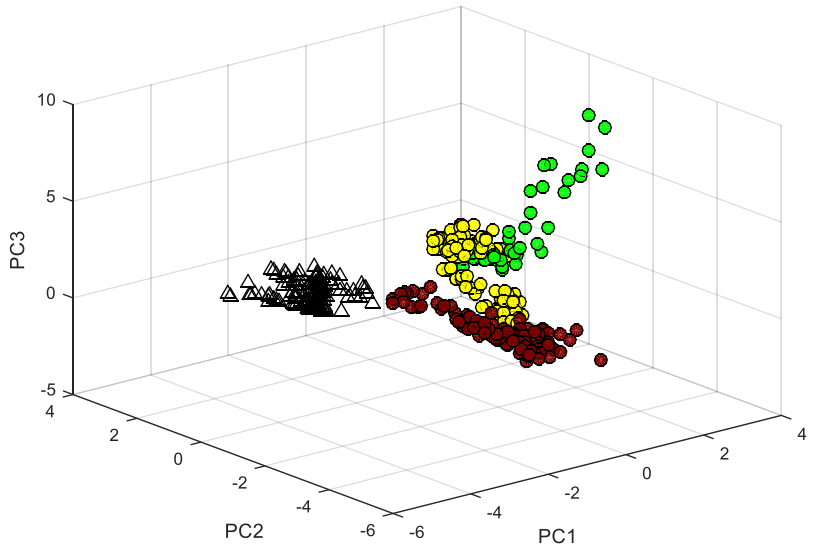

Figure 6-17: First three principle components showing 3 clusters for FS1

The novelty detection method presented in Section 6 can now be used on each cluster found in the data set. Figure 6-18 shows the detection of a novelty from the Normal 1 cluster (cuts 1-39) at cut 110, Figure 6-19 shows the detection of a novelty form the Normal 2 cluster (cuts 40-159) at cut 222, and Figure 6-20 shows the detection of a novelty from the Normal 3 cluster at cut 398. Note that a novelty is where the data does not lie within any of the three

clusters, however, fault warnings could be used where the data does not lie in Normal 1, and again when not in Normal 1 or Normal 2.

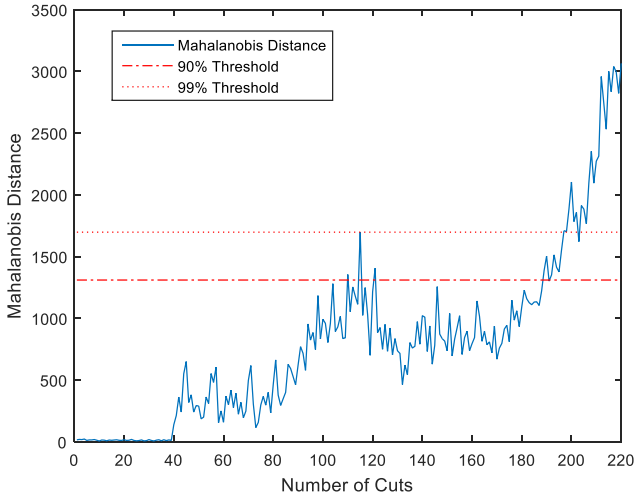

Figure 6-18: Novelty detection on Normal 1 data

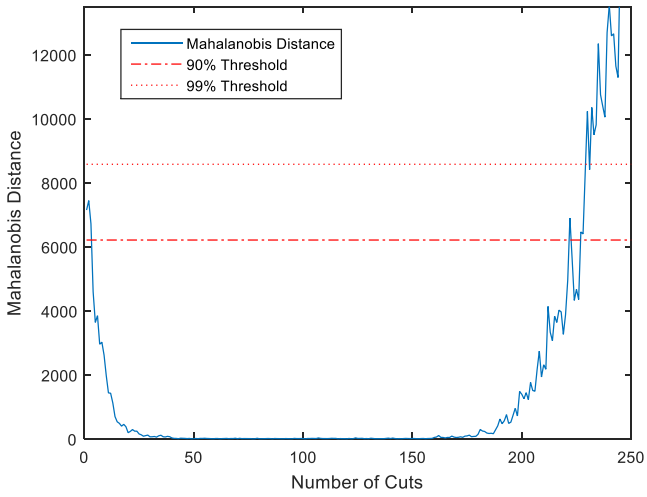

Figure 6-19: Novelty detection on Normal 2 data

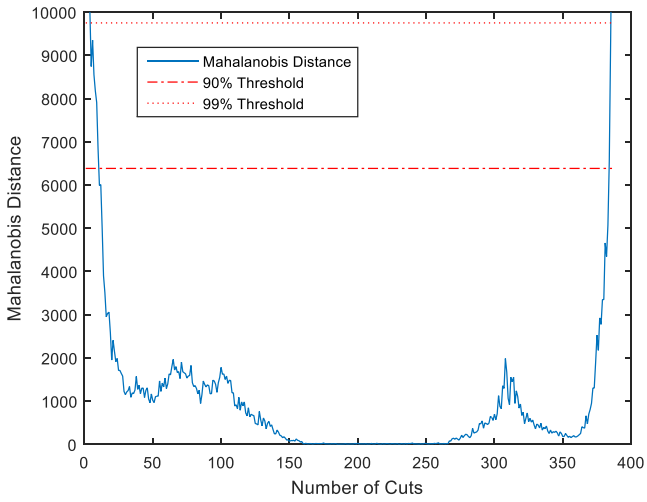

Figure 6-20: Novelty detection on Normal 3 data

The previous plots have shown that novelty detection can be applied when modelling the normal condition, as more than one multivariate Gaussian distribution. In the case presented, the definition of the normal condition provides a closer approximation to the data than using a single Gaussian; therefore, the potential for incorrectly classifying a faulty data point as normal is reduced. This affect was illustrated previously in Figure 6-12 and Figure 6-13. Furthermore, the natural clustering in the data was found to be separated by the number of cuts taken.

6.2.2 Diagnosis of Tool Wear Fault

In comparison to other fault types, tool wear is a gradual effect where the cutting edge transitions from a new condition to a worn condition during its time in cut. The literature review has discussed that tools often pass through one or more different tool wear states before they are considered unusable. Furthermore, the definition of the unusable state is dependent on the specific process requirements. It was also noted in the literature review conclusions that supervised classification of tool wear states is neither practical nor flexible for a production solution, given the inspection and classification of tool wear states requires skilled and time consuming measurements that are only viable in laboratory conditions.

Without training data, the ability to determine whether a fault condition is a result of tool wear can be achieved by determining if there is a pattern in the data that is symptomatic of

tool wear progression. The progression of tool wear has been observed in sensor data in many previous papers discussed in the literature review.

Two methods that support the diagnosis of a worn tool fault are now presented; tool condition clustering and rate of change in cutting conditions.

Tool Condition Clustering

The last section demonstrated that the natural clusters present in the data in Experiment 1 are separated by time in cut. Given the tool condition is the only variable that changes over time in this experiment, each cluster can then be associated with a different condition of the tool as it wears. Figure 6-21 shows the clusters that are found using GMM in feature subset FS1 over the normal condition of the tool (1-266 cuts). The number of clusters must be stated when calculating a GMM; therefore the model is calculated for 2 to 8 clusters. There is a common change in cluster for most the results at around cuts 40, 160 and 220. The data for 3 clusters is consistent with the PCA plot in Figure 6-16. (Note that 10,000 replicates of the GMM fitting were computed and the best fit was chosen).

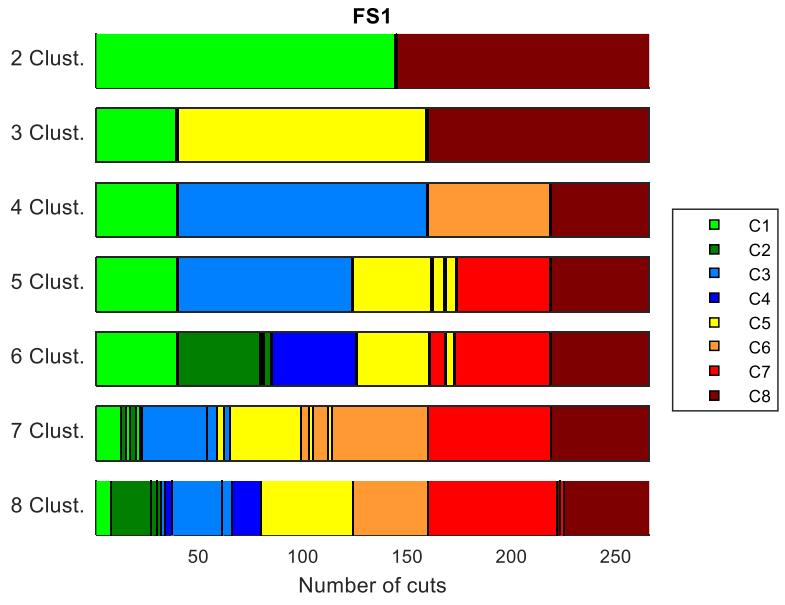

Figure 6-21: Cluster vs number of cuts for 2 to 8 clusters for FS1

Figure 6-22 presents the same data for FS4 (left) and FS6 (right). The patterns are similar and again the clusters are separated by the number of cuts. For example, for FS4, there is a common change in cluster at around cut 60 and cut 120.

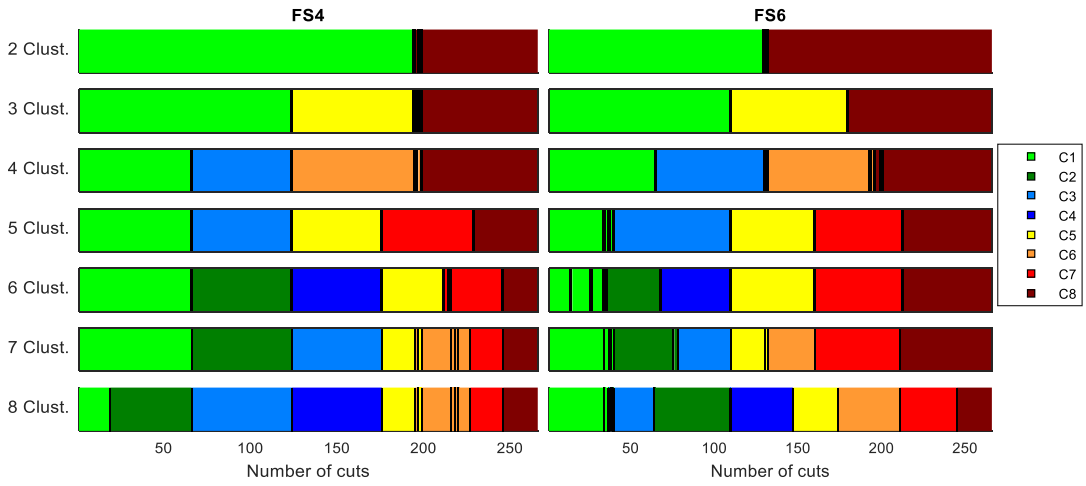

Figure 6-22: Cluster vs number of cuts for 2 to 8 clusters for FS4 (left) and FS6 (right)

Once this data have been obtained on the first tool, subsequent tools can be compared without the need for direct tool wear measurement data. A demonstration of this will be provided later in section 6.3.

Rate of Change of Cutting Conditions

The velocity at which the data travels within the feature space provides a measure of the rate of change of the cutting conditions. As tool wear is generally a gradual effect, the measure of this velocity allows a normal tool wear fault to be distinguished from other fault types that typically cause a more sudden change in cutting conditions.

If the velocity of the feature data is measured using the Euclidean distance travelled between each point, a gradual increase in the rate of change of cutting conditions can be observed over the life of the tool. The Euclidean distance has been used as this can be applied to a data set a small as 2, whereas the Mahalanobis distance requires you to accumulate a number of data points great enough to adequately define a Gaussian.

Figure 6-23 presents the Euclidean distance moved from one point to the next over the course of the tool's life using the data from Experiment 1. Note that the first 100 cuts have been used to define the normal condition, and hence the data has been normalised by these values.

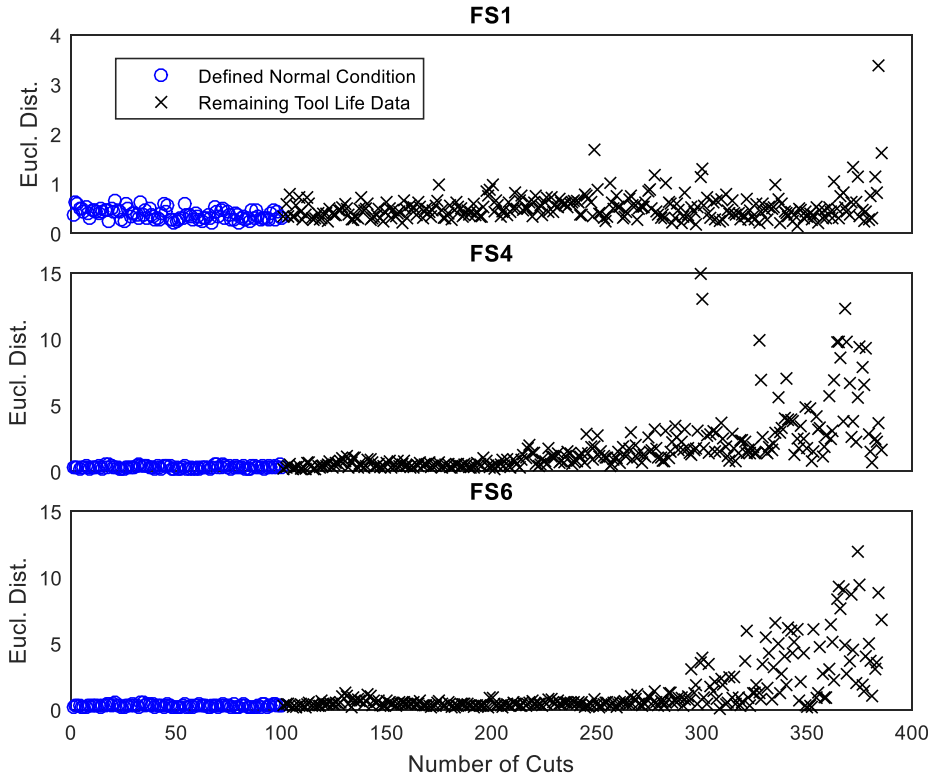

Figure 6-23: Euclidean distance travelled per cut for Experiment 1

It is clear from Figure 6-24 that the distance travelled to reach the depth of cut faults obtained in Experiment 2 is far greater than any movement during tool wear, as the log of the Euclidean distance is required to clearly view the data on the same plot. FS1 data has been used in the figure, though the effect is the same for FS4 and FS6. Two arbitrary thresholds have been proposed as an example to differentiate between the different fault types; a six sigma threshold on the normal condition data set and a x10 threshold, which is 10 times the highest magnitude seen in the normal condition data set. It is perhaps not surprising that the depth of cut data are shown to be outliers as the test is qualitatively different, however it is reassuring that the method can detect this.

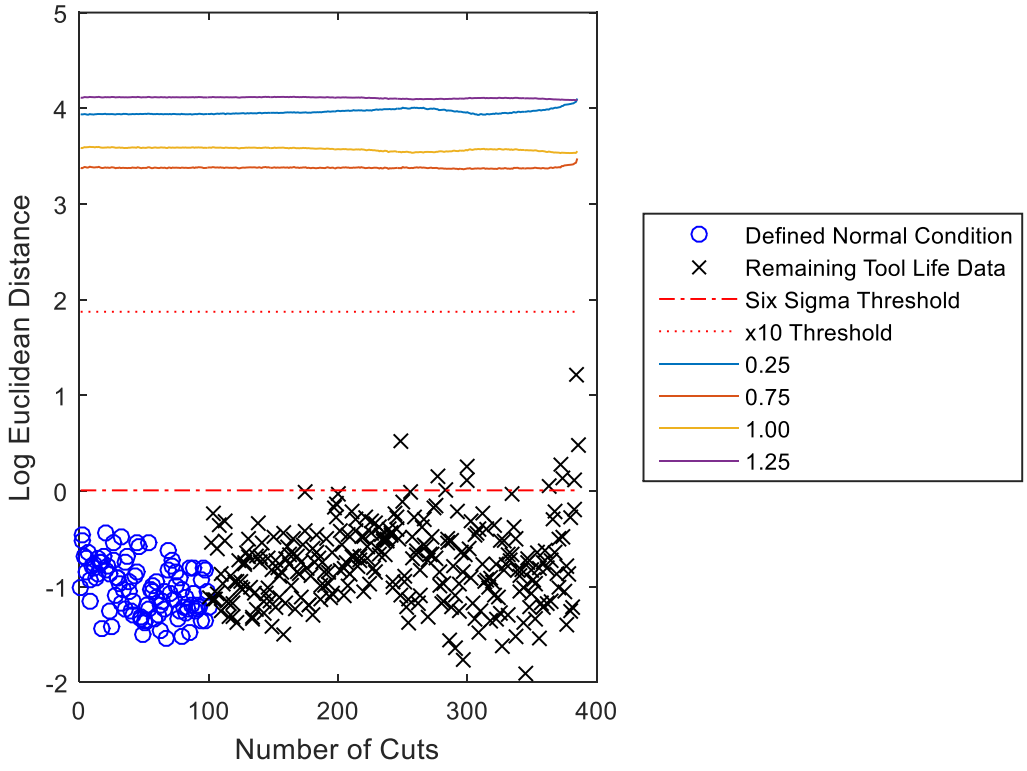

Figure 6-24: Euclidean distance traveled per cut in Experiment 1 compared to distance to Experiment 2 data

A further advantage of using the velocity of the data is that after each tool change the rate of wear of a previous tool can be compared to that of the current tool. This data would further support the diagnosis of the fault conditions, indicating if a given tool is experiencing faster or slower tool wear than previous tool data. A demonstration of this will be provided later in section 6.3.

6.2.3 Diagnosis of New Faults

The high cost of obtaining fault data to define different fault types has already been discussed. When faults are observed in production, it may be possible to recognise repeat faults by associating them with previous data. This section will use the sensor data obtained from Experiments 1 and 2 to demonstrate the ability to associate new data with previous observations.

Nearest Neighbour for Fault Association

Whilst there are many other methods for associating data with previously defined data sets, particularly supervised learning techniques, the fault association problem presented here must associate data with very low numbers of fault data sets, and in many cases just a single fault data point of each type. This is because fault data is very sparse in production and often a result of multiple different processes and causes; clearly the objective of the production process is to avoid faults all together.

The principle of associating new data to previous cuts can be demonstrated using the nearest neighbor criteria. The nearest neighbour will be measured using the Euclidean distance in the feature subset space. Similar to before, the Euclidean distance has been used in place of the Mahalanobis distance as Euclidean distance can be calculated from a data set as small as 2 points.

Section 6.1.3 has already shown that data from Experiment 2 can be distinguished from the normal tool condition from Experiment 1. If we assume that in our production process a tool has been used through to the end of its life (cuts 1-266 from Experiment 1) and subsequently fault data for cuts of 0.25mm, 0.75mm, 1.0mm and 1.25mm DOC is observed (from Experiment 2)], the nearest neighbour for each fault can be used to diagnose similar cuts. Figure 6-25 show the Euclidean distance from the 1.0mm fault to all other data using feature subset FS4. The first three nearest neighbours in increasing distance are the 1.25mm fault, the 0.75mm fault, and cut 113 from the Experiment 1. The 0.25mm fault is the farthest.

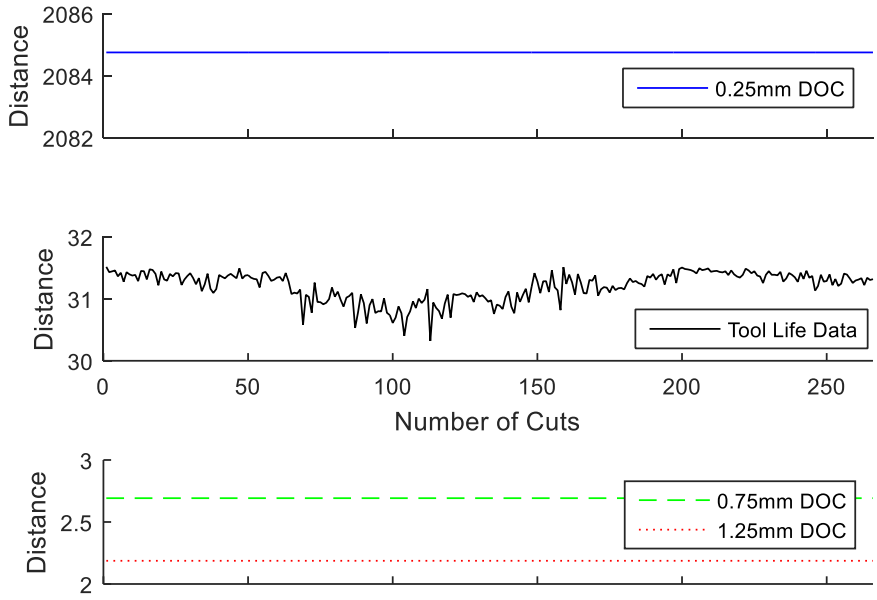

Figure 6-25: Distance from 1.0mm fault for FS4

The previous plot demonstrates that by using the nearest neighbour criteria, new faults can be associated closely with previous faults of a similar type. To evaluate this further, the 4 nearest neighbours to each fault type for each feature subset are listed in Table 6-1. In all but one case the nearest neighbour to each fault is another depth of cut fault. Using FS6, however, 1.0 and 1.25mm faults are closer to the normal condition than they are to the 0.25mm and 0.75mm faults.

Table 6-1: Nearest Neighbours for each feature subset

Feature Subset	n^{th} Nearest	0.25mm	0.75mm	1.0mm	1.25mm
FS1	**1**	**0.75mm**	**1.00mm**	**1.25mm**	**1.00mm**
	2	1.00mm	1.25mm	0.75mm	0.75mm
	3	1.25mm	0.25mm	0.25mm	cut156
	4	cut42	cut49	cut156	cut167
FS4	**1**	**0.75mm**	**1.25mm**	**1.25mm**	**0.75mm**
	2	1.25mm	1.00mm	0.75mm	1.00mm
	3	1.00mm	cut113	cut113	cut113
	4	cut113	cut104	cut104	cut104
FS6	**1**	**0.75mm**	**1.00mm**	**1.25mm**	**cut42**
	2	1.00mm	1.25mm	cut42	cut38
	3	1.25mm	cut42	cut38	cut41
	4	cut42	cut38	cut41	cut46

Note that in cases where there are a sufficient number of faults observed to build a GMM, the method presented in section 6.2.1 can be used for fault classification.

6.3 Case Study

The steps taken to complete the fault detection and diagnosis system, as proposed in the previous sections of this thesis, are briefly summarised in Figure 6-26.

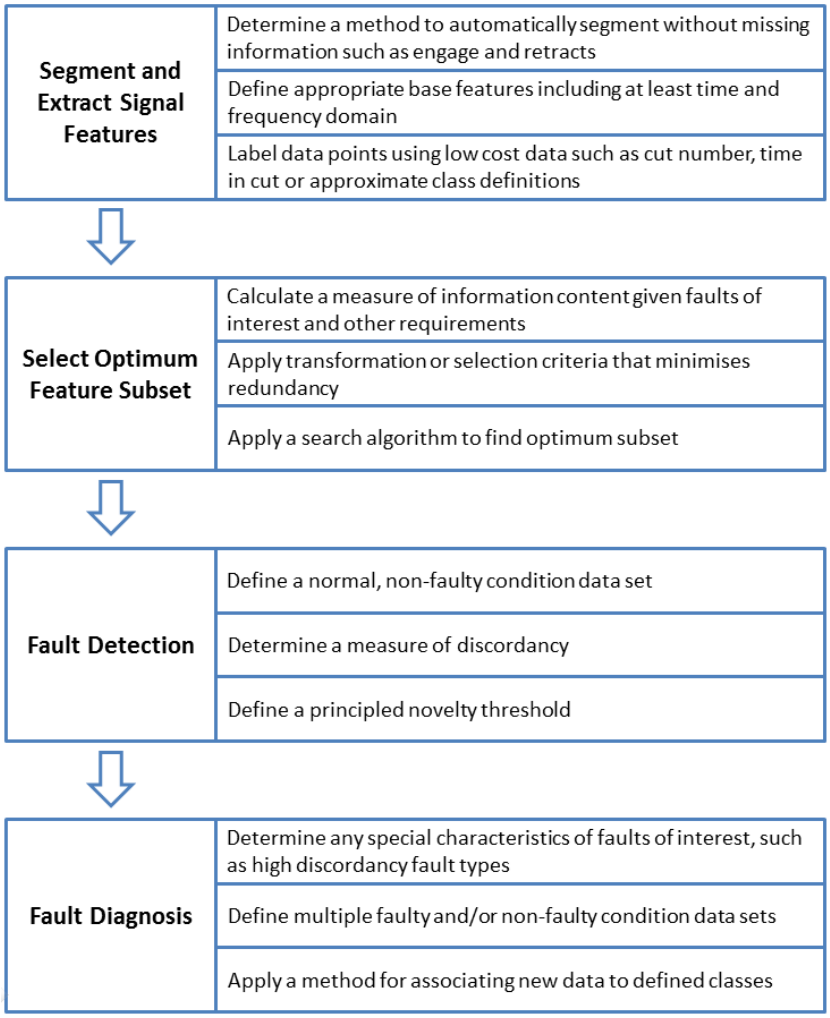

Figure 6-26: Summary of steps taken to develop the proposed fault detection and diagnosis solution

Many of the methods have been applied to data introduced in Section 4.3.3; Experiment 3: Published Case Study Data. In this final section of the thesis, the following steps have been carried out on this data set.

Step 1: Feature extraction and subset selection

Extract 20 features from each sensor signal as described in section 5.2. Using only the first tool's data set, determine a suitable feature subset using polynomial model fitting and the Merit function presented in section 5.3.1.

Step 2: Define the normal condition and novelty threshold

Define the normal operating conditions from the first 100 cuts in the first tool's data set. Consider the option to add the first 100 cuts from each subsequent tool in order to increase the size of the normal definition data set over time. For each revised normal condition data set, select a principled novelty threshold using the Mahalanobis distance, as described in section 6.1.2. Determine the point at which a fault is detected for each of the 6 data sets.

Step 3: Define clusters using GMM and associate future data to the model

Define the optimum number of clusters using the first tools data set by using GMM, as described in section 6.2.1. Re-define the model after each tool has been used with an increased data set. Associate each tool with the GMM clusters defined by the previous tools and determine if intermediate tool wear states can be observed in the data, as described in section 6.2.2.

Step 4: Identify if the velocity of data increases as the tool wears

Calculate the velocity of the data using the Euclidean distance between each point and identify if the onset of tool wear is a result of gradually increasing velocity, as described in section 6.2.2.

6.3.1 Feature Extraction and Subset Selection

140 features have been extracted from the 7 channel data set. We have assumed in this case that the measurement of force data is a viable solution. Forward and reverse sequential feature selection has then been applied to the data and the results are shown in Figure 6-27. The optimum subset is found using reverse sequential feature selection and consists of 8 features (FY.FDf.S, AE.TD.V, FX.TD.S, VZ.TD.S, FY.TD.K, VX.FD.K, FZ.TD.K, AE.FD.M). This subset is then taken forward to the next step.

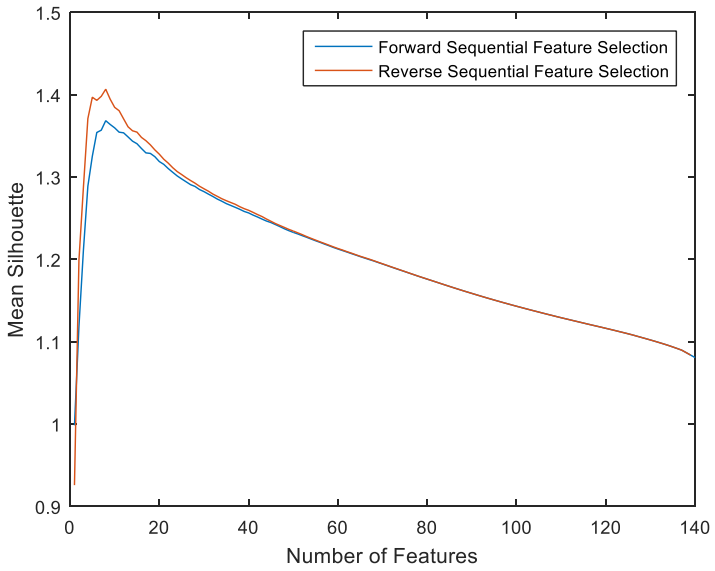

Figure 6-27: Sequential feature selection results

6.3.2 Define Normal Condition and Novelty Threshold

The first 100 cuts of tool 1 data are used to define the normal condition. The data can be plotted using the first two principal components of the feature subset, as shown in Figure 6-28. The colour bar presents the log of the Mahalanobis Distance.

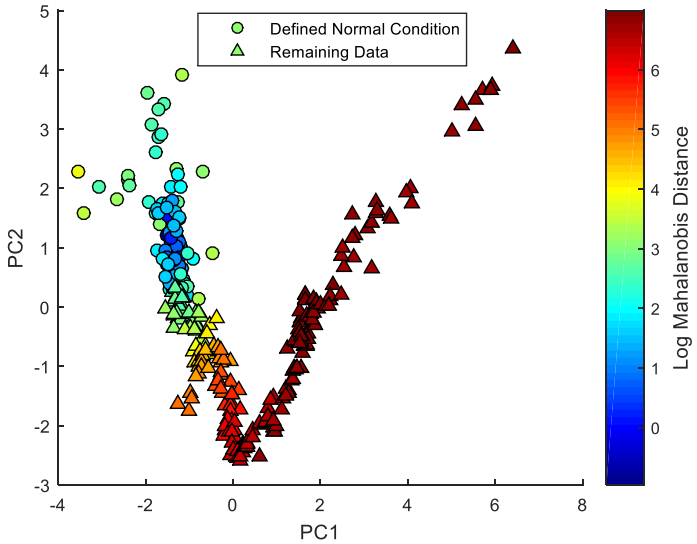

Figure 6-28: 2 dimension PCA plot for tool 1

Figure 6-29 presents the variance explained by each of the five components used to represent the eight features. Note that only 63% of the variance in the data set can be shown in two dimensions, therefore the separation in the data is not fully described by the 2D scatter plot.

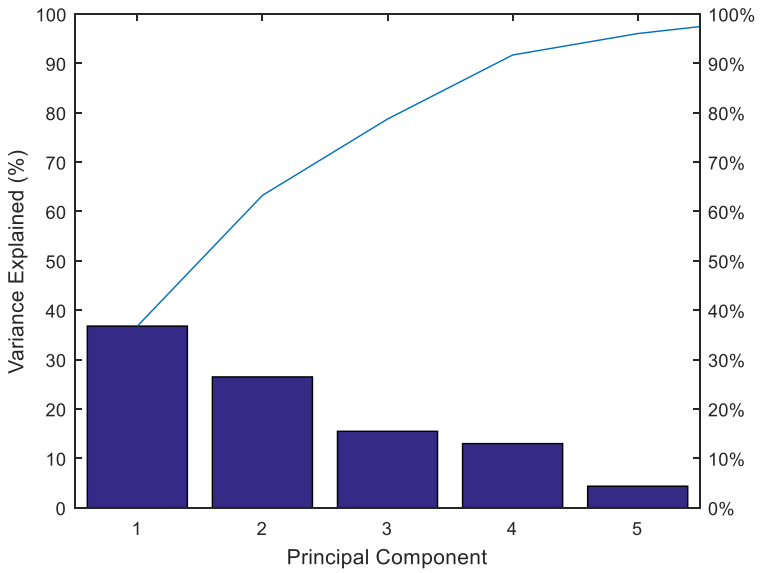

Figure 6-29: Variance explained by each principle component for Tool 1

A 3D scatter plot including the third principle component is shown in Figure 6-30. With this view of the data there is once again evidence of multiple Gaussians, similar to that found in section 6.1.1. There is also an interesting turning point in the direction of the points once the tool reaches a Log Mahalanobis distance of approximately 5.5 that may be indicative in a change in the wear stat of the tool.

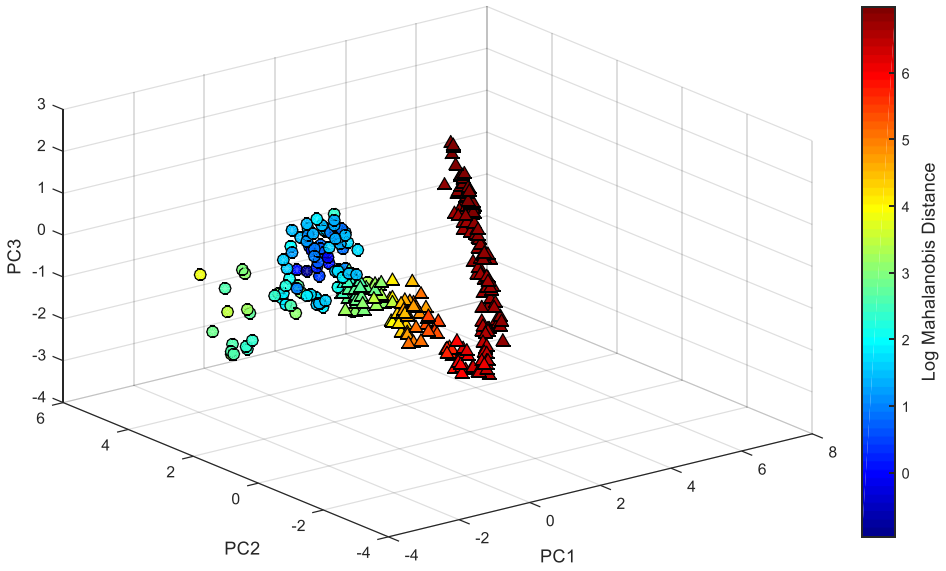

Figure 6-30: 3 dimension PCA plot for tool 1

The Mahalanobis distance correlates well with the number of cuts. A principled novelty threshold can be derived using the Monte Carlo method described in section 6.1.2. The 90th percentile has been used to define this threshold. The Mahalanobis distance for each cut for tool 1 is shown in Figure 6-31. The 90% percentile threshold shows the tool is classed as faulty from cut 186 onward.

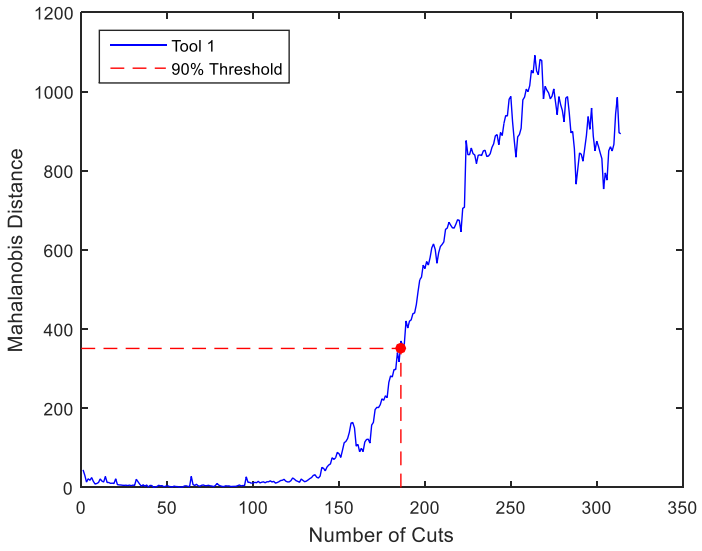

Figure 6-31: Mahalanobis distance and novelty threshold for tool 1

When comparing the first two principle components for all six tools, the common trend in the data can be seen in Figure 6-32. Figure 6-33 shows the first two principle components

for the normal condition data only. Here we can see that Tool 5 has a higher mean value of PC1 for the normal condition and also a greater variance.

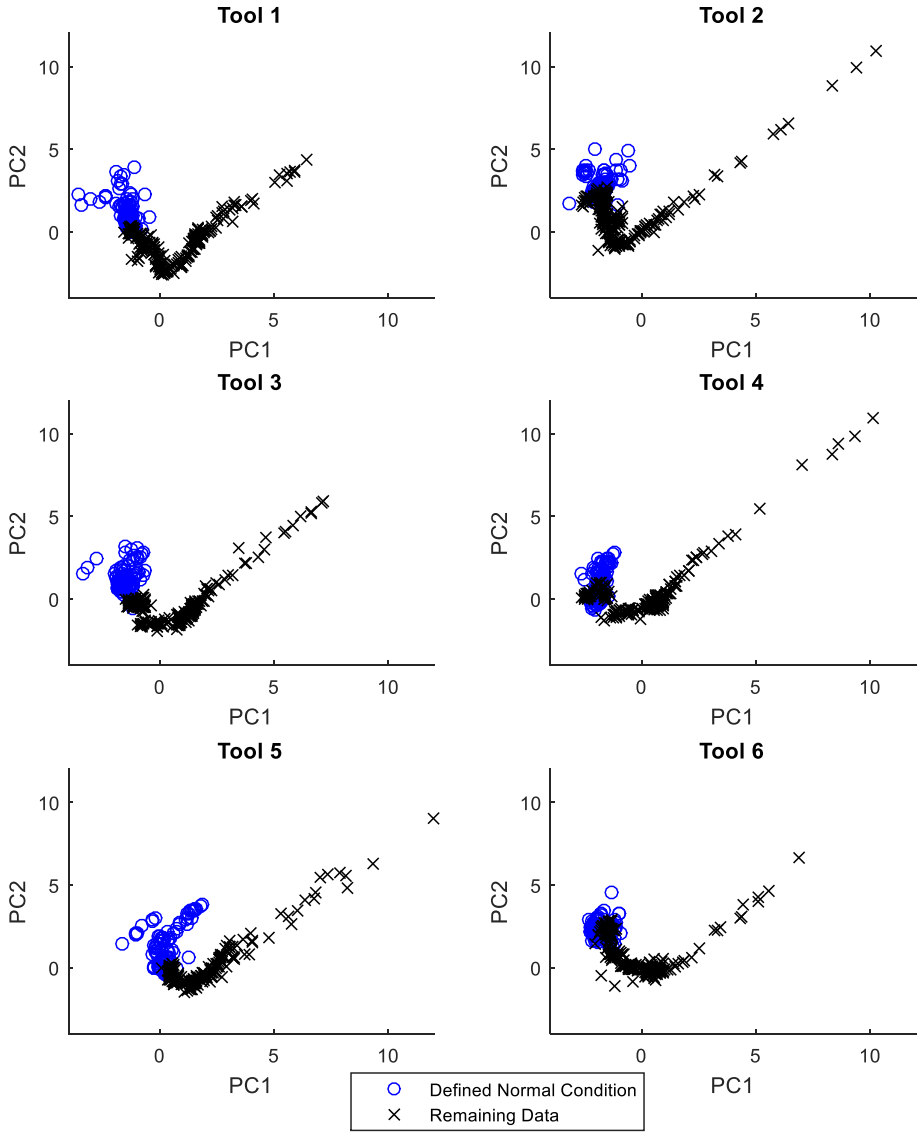

Figure 6-32: PCA plots for each tool using Tool 1 cuts 1-100 to define the principle components

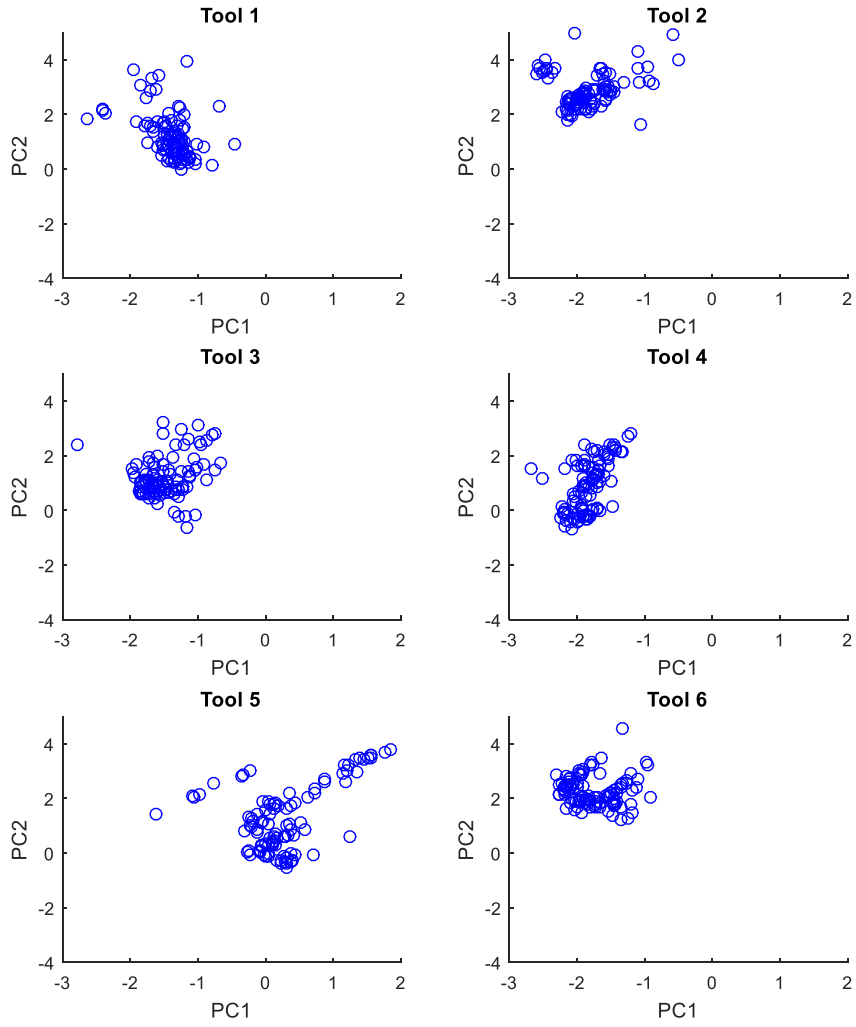

Figure 6-33: 2 dimensional PCA plot of normal condition data for each tool

If the normal condition is to be defined by the current tool in every case, the resultant thresholds and faulty condition points will be as per Figure 6-34. The faulty condition for tools 1-6 are found to be at cuts 186, 224, 161, 201, 197 and 220 respectively. Note that tool 3 exhibits a spike that causes the limit to be reached. This may be a measurement error and therefore it may be practical to wait for several outliers observed in succession before confirming the fault.

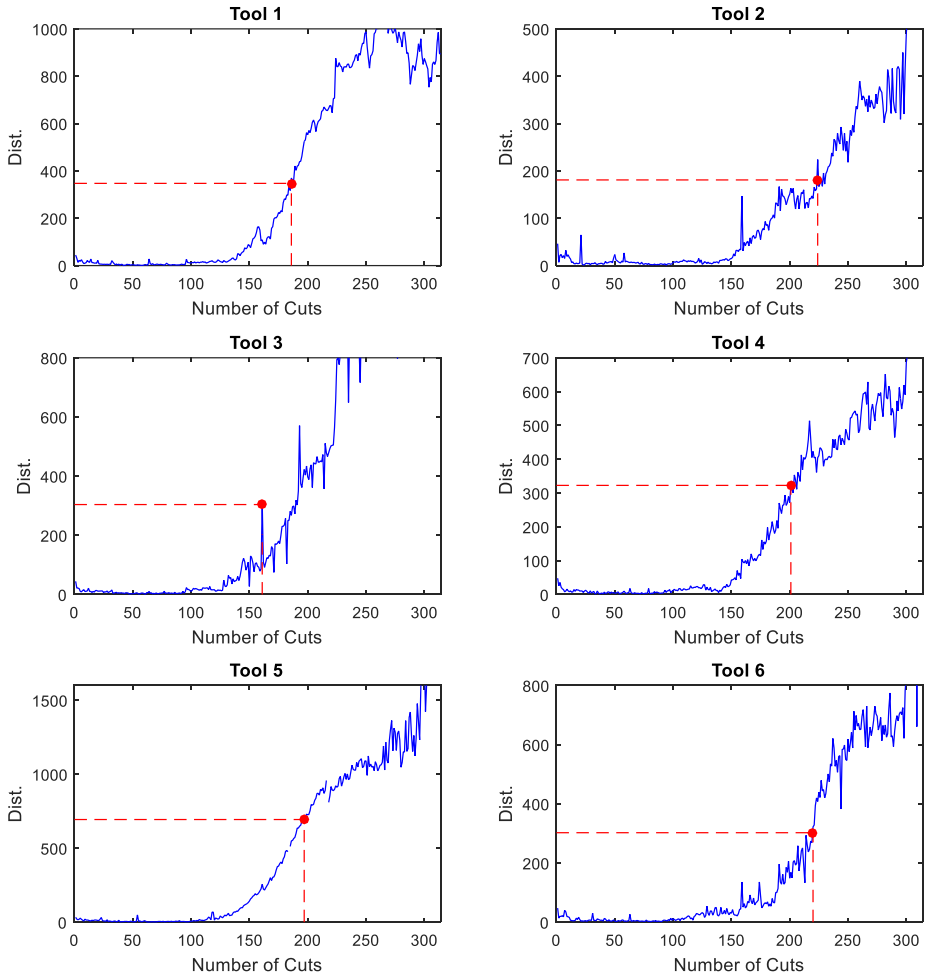

Figure 6-34: Mahalanobis distance and novelty threshold for tools 1-6

The normal condition can also be defined by a number of previous tool data sets in order to establish a broader definition of the acceptable operating conditions. This would also be appropriate if there is a need to validate a data set in order to accept it as a normal operating condition, for example if a tool began the process with partial wear, it would not be appropriate to use it to build the definition of normal. So, for example, when using the 3rd tool, the normal condition can be defined by the first and second tool data, again from cuts 1-100. When using the 4th tool, the normal condition can be defined by the first, second and third tool data, and so on.

The result of this method for tools 3-6 is shown in Figure 6-35. It can be seen that tools 3, 4 and 6 last longer than the previous result, now reaching the faulty condition after 222 (+21), 237 (+40) and 256 (+36) cuts respectively. Tool 5, however, is classed as faulty at cut 9,

indicating that there is something different in this data than that found in tools 1,2, 3 and 4, which have been used to define the normal condition. Note that tool 5 was not considered faulty until cut 197 in the previous result. This observation may be an important one, and therefore a skilled operator may wish to decide if the data for this tool should be added to the normal condition and the process continue, or if the tool is not appropriate for the normal condition definition.

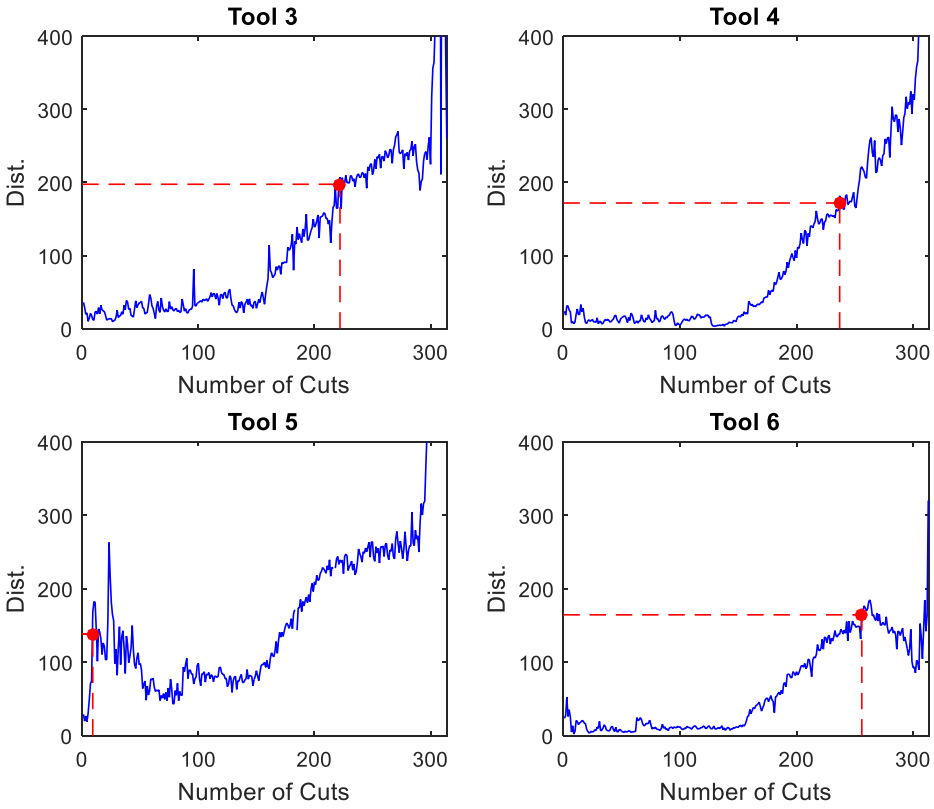

Figure 6-35: Mahalanobis distance and novelty threshold for tools 3-6 using prior normal condition

6.3.3 Define Clusters

The data can be separated into clusters using GMM, as described in section 6.2.1. Figure 6-36 shows that the natural separation in the data for tool 1 is again a result of the number of cuts. For the increasing number of clusters, there is a trend for a cluster separation to appear at approximately cuts 20, 90, and 220.

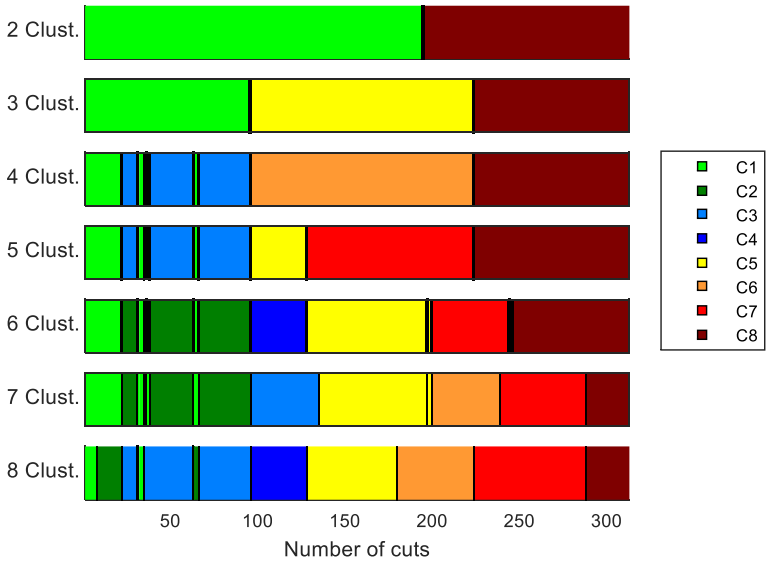

Figure 6-36: Tool 1 clusters against number of cuts

In practice, only the data that precedes the fault detection will be available in production. Therefore the clustering method used here will be applied only to data before the fault detection using the cut number where a fault is detected in Figure 6-34. The clusters are defined from only preceding tools used, so for tool 1 there is no clustering data provided, for tool 2 the clusters are defined by tool 1, for tool 3 they are defined by tools 1 and 2, and so on. The resultant clusters when setting the number of clusters to 7, are shown in Figure 6-37. In the figure, the data ends (coloured white) when the novelty is detected. As a result of poor repeatability from one tool to the next, there is no improvement in the cluster assignment as more tools are added to the data set.

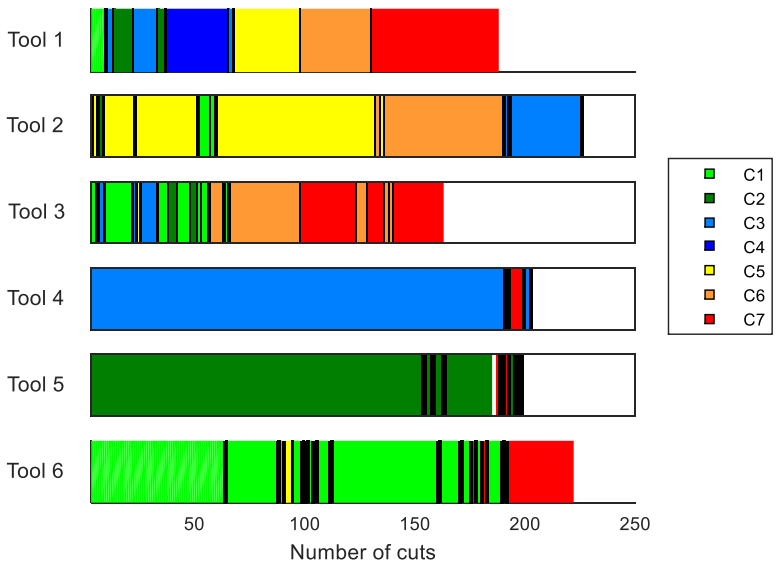

Figure 6-37: Clustering of the normal data set

Figure 6-38 shows all six tools using the first two principle components. Figure 6-39 shows the same data but only up until a novelty is detected, according to Figure 6-34. Whilst there is a common tail in the data towards the end of the tools life in the first figure, the different tools do not overlay well prior to the novelty detection. In particular, tool 5 appears to be offset to the other data sets. This provides an explanation to why it is difficult to describe the data as a common set of clusters for all tools.

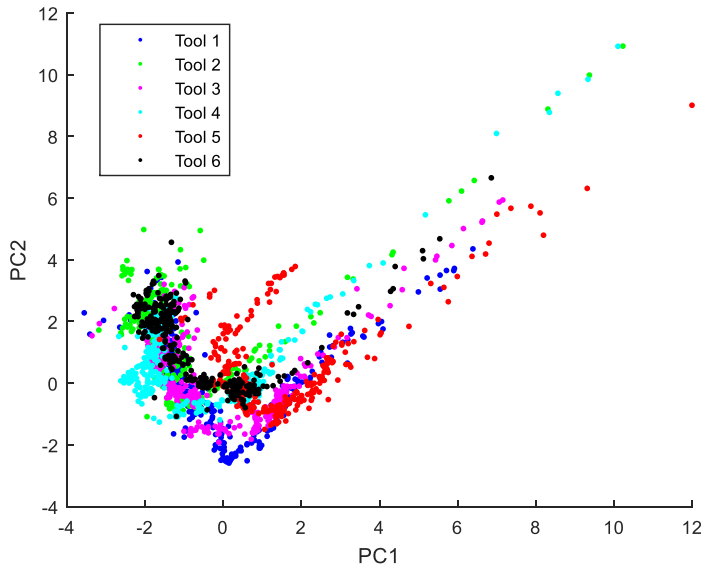

Figure 6-38: PCA plot for all six tools

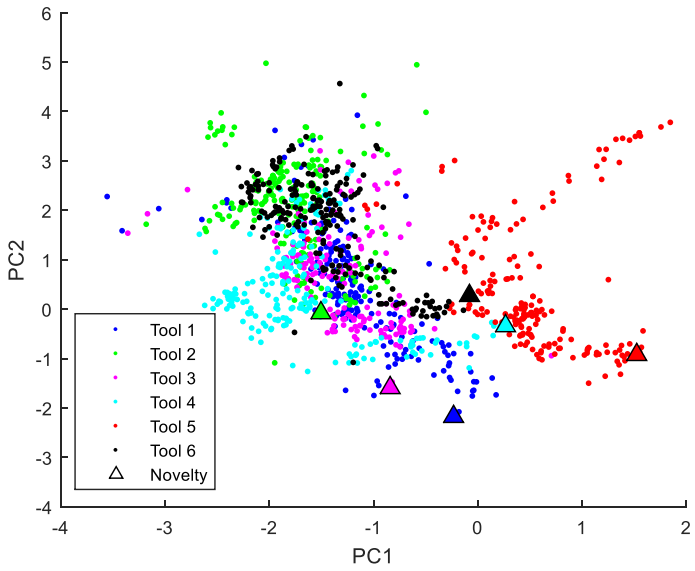

Figure 6-39: PCA plot only up until first novelty is detected

The offset in the data in tool 5 (leading to the difficulty to associate this tool with other tool states) may appear to be a weakness of the technique presented. However, if the change in tool 5 is meaningful, and is not simply down to signal noise, then the detection of this change becomes a useful capability. For example, should the work piece be different to those previously machined, the knowledge of this event may not only help determine tool life, but also machined surface condition that may not otherwise be detected. The observation of these small changes is achievable using the method presented as the data is visually informative.

6.3.4 Evaluate the Velocity of the Data to Determine the Fault Type

It is known that the fault types in this data set are only that of tool wear, therefore the data can only be interrogated to see if the velocity of the data, as described in section 6.2.2, is consistent with gradual tool wear. The distance travelled per cut for tools 1-3 and tools 4-6 are plotted in Figure 6-40 and Figure 6-41, respectively. The 10x threshold shown earlier in Figure 6-24 is also plotted as dotted lines. The velocity remains relatively stable before shooting off over the final 10-30 cuts taken with each tool.

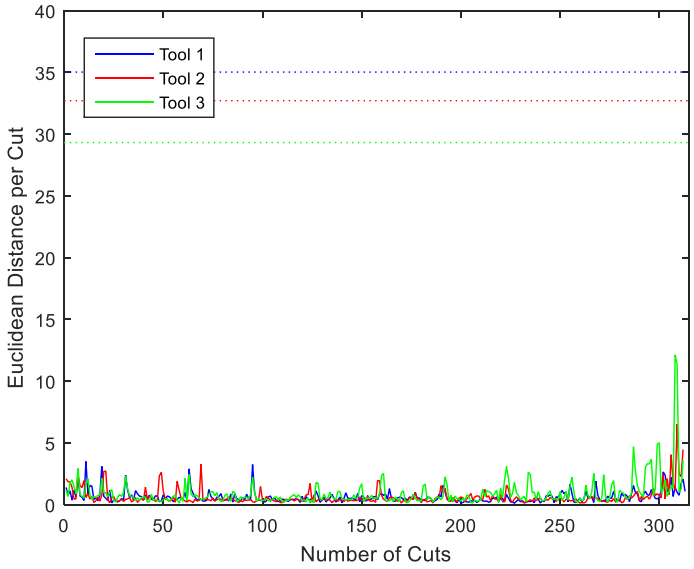

Figure 6-40: Euclidean distance travelled per cut for tools 1-3

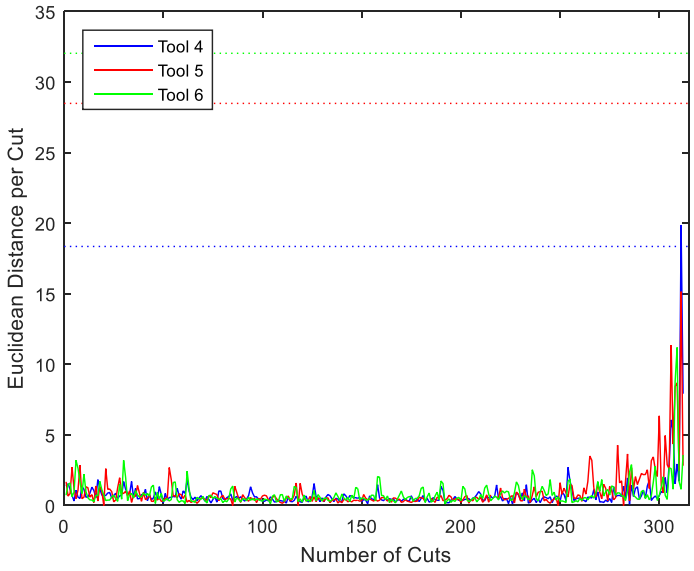

Figure 6-41: Euclidean distance travelled per cut for tools 4-6

7 SUMMARY AND CONCLUSIONS

The main aim of this research was to design and demonstrate a method for monitoring machining processes that can reliably detect and diagnose faulty operating conditions. Much of the work has focused on unsupervised techniques and non-intrusive sensing hardware in order to address the practical limitations that prevent exploitation.

A process failure mode and effect analysis (PFMEA) was carried out at the start of this research in order to drive the functional requirements of a machining process monitoring system. An investigation into the software and hardware design choices followed in Chapters 3 and 4. Most failure modes recorded in the PFMEA could be resolved with current industry technology, however, the detection of undesirable changes to depth of cut, tool condition and material properties could not.

A sensing system has been designed, built and tested for milling applications. This system has allowed a number of signals to be acquired from close to the cutting process without interfering with the normal operation of the machine tool. Spindle power, vibration and acoustic emission data has been collected during milling trials and subsequently analysed to develop methods for fault detection and diagnosis. The hardware developed in this work provides a robust platform for measurement in a lab environment and may also provide a prototype design for future use in production processes.

The first objective set out in Chapter 1 was to identify the suitable sensor signal features available for describing the condition of the machining process. The sensor signal features were obtained by applying multiple time and frequency domain feature extraction techniques. The most useful signal features for interpreting the condition of the cutting process have been found by first fitting polynomial models to the trajectory of each signal feature over the tool life, followed by applying a heuristic equation for scoring feature subsets.

The selection of useful sensor signal features has also been considered by observing transient events in the signals. Spikes in vibration and acoustic emission sensor signals were observed at several intervals over the tool's life may have been a result of tool chipping.

A class separation technique has been proposed where the separation in clusters created from the feature subset data has been used as a measure of the ability to differentiate between multiple tool wear states. Gram-Schmidt orthogonalisation has been evaluated to reduce dimensionality and redundancy in a feature subset. The methods shown for feature selection have been applied previously in structural health monitoring literature, but not to machining applications. This research has shown them to be successful alternatives to those used previously in machining process monitoring literature, ensuring an optimum feature subset with low redundancy and low computational expense. Most significantly to addressing the hypothesis, the methods have shown that feature selection can be carried out by more than one method without supervision or training data.

The second objective was to incorporate a fault detection method into the proposed monitoring system. This required a means for the system to identify fault conditions from sensor data without the need for extensive training data or measured class labels. A novelty detection method has been proposed as the first step in a monitoring system hierarchy. There has been limited application of novelty detection methods in machining process monitoring literature. However, the methods presented in this research have shown promising alternatives to other literature, especially where supervised learning is not viable. The detection of any data point that is an outlier to a defined normal condition has been achieved using the Mahalanobis distance to measure discordancy. A principled novelty threshold has been selected to determine when a data point should be considered a novelty. The method has proven effective to detect worn tools and incorrect depths of cut and has performed well with several different selected feature subsets.

The third objective was to extend this calculation so that fault diagnosis is possible. With minimal training, the system should be able distinguish between more than one fault type. A classification method has been presented for fault diagnosis. A Gaussian Mixture Model has been used to define multiple normal or faulty condition clusters in a data set. The association of a new point to the existing clusters has been done using either the Mahalanobis distance or using the nearest neighbour criteria. The detection of a tool wear fault has also been achieved by measuring the rate of change of the sensor signal features, defined by the Euclidean distance between two points. A tool that gradually moves from the normal condition to a novelty has been assumed to represent a worn tool fault type.

The discussed feature selection, fault detection and diagnosis methods have been tested on a second data set made available by the Prognostics Health Monitoring (PHM) Society and have given good results. It was shown that the normal condition is best defined by the current tool in use, given that there was reasonable drift in the sensor signal data from one tool to the next. Furthermore, given the apparent drift in sensor signal features between tools, the classification of tool wear state was not viable using the proposed Gaussian Mixture Model method.

The fourth objective set out in Chapter 1 was for a system to be designed in a way that it does not obstruct the production environment, thus being a practical solution for industrial exploitation. Both the hardware selection and the emphasis on unsupervised learning algorithms support this aim. Whilst it is accepted that some setup time and configuration of these algorithms is still required, such as the definition of classes, the reliance on training data with class labels has been significantly reduced when compared to supervised learning methods.

Based on the work carried out, a framework for fault detection and diagnosis is set out in Figure 7-1.

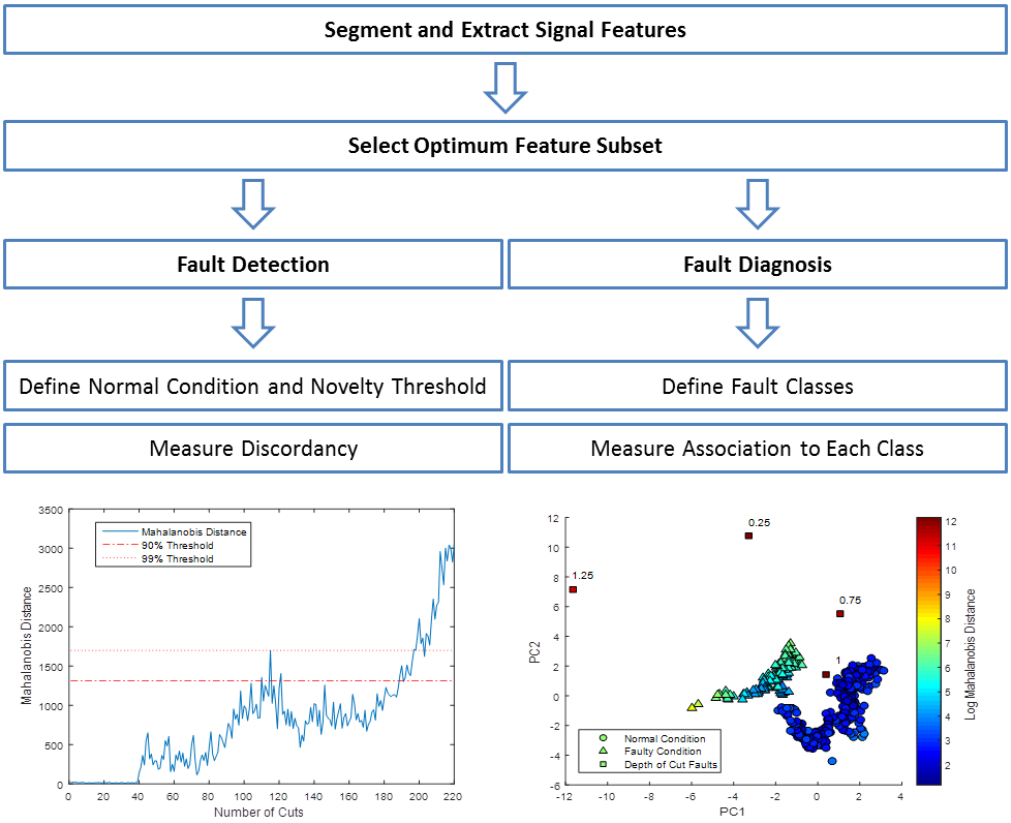

Figure 7-1: Framework for fault detection and diagnosis systems for machining

The application of feature sub-set selection, fault detection and fault diagnosis methods presented in this thesis show a promising solution for machining process monitoring. A method to achieve the aim of this research; monitoring of machining processes to reliably detect and diagnose faulty operating conditions, has been presented. By providing a robust and automatic fault detection solution, cautionary process interventions can be eliminated. Fault diagnosis data can be provided to a machine operator for known faults, reducing the amount of time spent correcting the process. In some cases, the corrective action could be automated through NC code using an event-based control approach. By presenting data in an easily interpretable format, such as the PCA plots used for cluster analysis, a user can quickly observe whether there is an anomaly in the process. New fault types can be defined from new data during production, potentially allowing fault diagnosis capability to improve over time.

7.1 Further Work

This thesis has presented a viable alternative to the commonly used supervised learning techniques for machining process condition monitoring. There is only a relatively small amount of literature that has attempted to apply unsupervised learning to this problem, therefore there remains many more techniques and algorithms available for further exploration than those presented in this thesis. In order to progress the research carried out here, there are a number of key future subject areas described below.

Firstly, the definition of the normal condition for novelty detection has been based on an experiential estimate of the tool life. A principled number of cuts to define the normal condition would be required to remove this experience factor. It was found in Chapter 6 that there was evidence of at least two Gaussians in the defined normal condition. These multiple Gaussians may have a physical meaning, such as the result of an incipient fault. A method for self-clustering, capturing these changes in cutting conditions and reducing the need for experience based class definition would be a useful route for future research.

Analysis of the trajectory of the data over time has not been fully explored in this thesis. Whilst a method for diagnosing tool wear has been proposed by measuring the rate of change of the sensor features, this may not explain the cutting conditions fully. It is proposed that future research explores this further, looking to compare cutting conditions, tool wear types, and chatter vibration issues with the signals and the path they follow over time.

Remaining useful life predictions have been applied to a single sensor feature in Appendix C. The measurement of tool wear was required in order to demonstrate this; however, there are three proposed topics of future research in relation to this; (i) to attempt to actively learn the spindle power trajectory without reliance on the prior information or training data, (ii) to consider multiple sensor signal features into this algorithm in order to improve its accuracy and again predict the data trajectory, and (iii) to investigate the automatic direct measurement of tool wear to reduce the cost of training such systems in production and allow multiple tool wear mechanisms to be quantified and correlated to sensor signal features.

8 REFERENCES

[1] Kappmeyer, G., Hubig, C., Hardy, M., Witty, M., & Busch, M., "Modern machining of advanced aerospace alloys-Enabler for quality and performance." Procedia CIRP 1 (2012): 28-43.

[2] ARTIS tool monitoring company. http://www.artis.de/en/

[3] MARPOSS group. http://www.marposs.com/

[4] Brankamp, the process monitoring company. http://www.brankamp.com/en/

[5] Kistler. http://www.kistler.com/CH_en-ch/49_ProcessMonitoring/Process-Monitoring.html

[6] Prometec. http://www.prometec.com/EN

[7] Montronix monitoring solutions. http://www.montronix.com/in/home.html

[8] Nordmann tool monitoring. http://www.toolmonitoring.com/index.html

[9] Renishaw http://resources.renishaw.com/

[10] Blum Novotest http://www.blum-novotest.de/measuring-components/

[11] TTL adaptive machining solutions. http://www.ttl-solutions.com

[12] Metrology Software Products – NC PerfectPart, http://www.nc-perfectpart.com/

[13] MAG Cincinatti adaptive feed control

[14] Okuma machining Navi spindle speed control. http://www.okuma.co.jp/english

[15] Weck, M., Zenner, K., Tüchelmann, Y., & Zühlke, D. "Concept of integrated data processing in computer controlled manufacturing systems (FMS)" International Journal of Production Research 18.3 (1980): 295-306.

[16] Goldsby, A.F., Haberl, F.J., and Anand, S.K., "Machine Operating Condition Monitoring System" U.S. Patent No. RE29,450. 18 Oct. 1977.

[17] Scott, D., McCullagh, P.J., and Campbell., G.W., "Condition monitoring of gas turbines—an exploratory investigation of ferrographic trend analysis." Wear 49.2 (1978): 373-389.

[18] Teti, R., A Review of Tool Condition Monitoring Literature Database, Annals of the CIRP, 44/2 (1995): 659-666

[19] Teti, R., Jemielniak, K., O'Donnell, G., & Dornfeld, D. "Advanced monitoring of machining operations." CIRP Annals-Manufacturing Technology 59.2 (2010): 717-739.

[20] Leem, C.S., Dornfeld D.A., "Design and implementation of sensor-based tool-wear monitoring systems", Mechanical Systems and Signal Processing 10, (1996): 439–458.

[21] EPSRC Research Strategy, Manufacturing the Future. http://www.epsrc.ac.uk/research/ourportfolio/themes/manufacturingthefuture/

[22] German Federal Ministry for Education and research, Industry 4.0. http://www.bmbf.de/en/19955.php

[23] Technology Strategy Board, High Value Manufacturing Strategy, 2012-2015, https://www.innovateuk.org

[24] UK HIGH VALUE MANUFACTURING FUTURE 'LANDSCAPE', A study conducted by University of Cambridge Institute for Manufacturing, Education and Consulting Services. Version 1, Draft 2.10, January 2011.

[25] European Commission, Research and Innovation, Call for Factories of the Future, H2020-FoF-2014, http://ec.europa.eu

[26] Foresight (2013). "The Future of Manufacturing: A new era of opportunity and challenge for the UK", The Government Office for Science, London. http://www.bis.gov.uk/foresight

[27] Byrne, G., Dornfeld, D., Inasaki, I., Ketteler, G., König, W., & Teti, R. "Tool Condition Monitoring (TCM) — The Status of Research and Industrial Application." CIRP Annals-Manufacturing Technology 44.2 (1995): 541-567.

[28] Rehorn, A.G., Jiang, J., Orban, P.E., "State-of-the-art methods and results in tool condition monitoring: a review." The International Journal of Advanced Manufacturing Technology 26.7-8 (2005): 693-710.

[29] Liang, S.Y., Hecker, R.L., Landers, R.G., "Machining process monitoring and control: The state-of-the-art." Journal of manufacturing science and engineering 126.2 (2004): 297-310.

[30] Quintana, G., Garcia-Romeu, M.L., Ciurana, J., "Surface roughness monitoring application based on artificial neural networks for ball-end milling operations." Journal of Intelligent Manufacturing 22.4 (2011): 607-617.

[31] Marinescu, I., Axinte., D.A., "An automated monitoring solution for avoiding an increased number of surface anomalies during milling of aerospace alloys." International Journal of Machine Tools and Manufacture 51.4 (2011): 349-357.

[32] Quintana, G., Ciurana, J., "Chatter in machining processes: A review," International Journal of Machine Tools & Manufacture, vol. 51, pp. 363-376, May 2011

[33] Lu, X., Chen, F., Altintas, Y. "Magnetic actuator for active damping of boring bars." CIRP Annals-Manufacturing Technology 63.1 (2014): 369-372.

[34] Budak, E., Comak, A., Ozturk E., "Stability and high performance machining conditions in simultaneous milling." CIRP Annals-Manufacturing Technology 62.1 (2013): 403-406.

[35] Bhuiyan, M. S. H., Choudhury, I. A., Nukman. Y., "An innovative approach to monitor the chip formation effect on tool state using acoustic emission in turning." International Journal of Machine Tools and Manufacture 58 (2012): 19-28.

[36] Rehorn, A.G., Sejdić, E., Jiang, J., "Fault diagnosis in machine tools using selective regional correlation." Mechanical Systems and Signal Processing 20.5 (2006): 1221-1238.

[37] Martin, K. F. "A review by discussion of condition monitoring and fault diagnosis in machine tools." International Journal of Machine Tools and Manufacture 34.4 (1994): 527-551.

[38] Abellan-Nebot, J.V., Subirón., F.R.,"A review of machining monitoring systems based on artificial intelligence process models." The International Journal of Advanced Manufacturing Technology 47.1-4 (2010): 237-257.

[39] Worden, K., Manson, G., "The application of machine learning to structural health monitoring." Philosophical Transactions of the Royal Society A: Mathematical, Physical and Engineering Sciences 365.1851 (2007): 515-537.

[40] Dey, S., Stori, J. A. "A Bayesian network approach to root cause diagnosis of process variations ." International Journal of Machine Tools and Manufacture 45.1 (2005): 75-91.

[41] Morgan, G., Cheng, R.Q., Altintas, Y. and Ridgway, K., "An expert troubleshooting system for the milling process." International Journal of Machine Tools and Manufacture 47.9 (2007): 1417-1425.

[42] Aliustaoglu, C., Ertunc, H.M., Ocak, H., "Tool wear condition monitoring using a sensor fusion model based on fuzzy inference system." Mechanical Systems and Signal Processing 23.2 (2009): 539-546.

[43] Kerrigan, K., O'Donnell, G.E., "Temperature Measurement in CFRP Milling Using a Wireless Tool-Integrated Process Monitoring Sensor." Journal ref: International Journal of Automation Technology 7.6 (2013): 742-750.

[44] Chung, T.K., Lee, H., Tseng, C.Y., Lo, W.T., Wang, C.M., Wang, W.C., Tu, C.J., Tasi, P.Y. and Chang, J.W., "Self-powered wireless vibration-sensing system for machining monitoring." SPIE Smart Structures and Materials+ Nondestructive Evaluation and Health Monitoring. International Society for Optics and Photonics, 2013.

[45] Stoney, R., O'Donnell, G.E., Geraghty, D., "Dynamic wireless passive strain measurement in CNC turning using surface acoustic wave sensors." The International Journal of Advanced Manufacturing Technology69.5-8 (2013): 1421-1430.

[46] Al-Sulaiman, F.A., Baseer, M.A., Sheikh, A.K., "Use of electrical power for online monitoring of tool condition," Journal of Materials Processing Technology, vol. 166 (2005): 364-371.

[47] Axinte, D., Gindy, N., "Assessment of the effectiveness of a spindle power signal for tool condition monitoring in machining processes," International Journal of Production Research, vol. 42, (2004): 2679-2691.

[48] Shao, H., Shi, X., Li, L., "Power signal separation in milling process based on wavelet transform and independent component analysis," International Journal of Machine Tools & Manufacture, vol. 51, (2001): 701-710.

[49] Kim, D., Jeon, D., "Fuzzy-logic control of cutting forces in CNC milling processes using motor currents as indirect force sensors," Precision Engineering-Journal of the International Societies for Precision Engineering and Nanotechnology, vol. 35, (2011): 143-152.

[50] Vijayaraghavan, A., Dornfeld, D., "Automated energy monitoring of machine tools," Cirp Annals-Manufacturing Technology, vol. 59, (2010): 21-24.

[51] Park, S.S., Altintas, Y., "Dynamic compensation of spindle integrated force sensors with kalman filter." Journal of Dynamic Systems, Measurement, and Control 126.3 (2004): 443-452.

[52] Klocke, F., O. Adams, T. Auerbach, S. Gierlings, S. Kamps, S. Rekers, D. Veselovac et al. "New concepts of force measurement systems for specific machining processes in aeronautic industry." CIRP Journal of Manufacturing Science and Technology 9 (2015): 31-38.

[53] Yaldız, S., Ünsaçar, F., Sağlam, H. and Işık, H., "Design, development and testing of a four-component milling dynamometer for the measurement of cutting force and torque."Mechanical Systems and Signal Processing 21.3 (2007): 1499-1511.

[54] O'Donnell, G., Young, P., Kelly, K., Byrne, G., "Towards the improvement of tool condition monitoring systems in the manufacturing environment," Journal of Materials Processing Technology, vol. 119, (2001): 133-139.

[55] Teti, R., Jawahir, I.S., Jemielniak, K., Segreto, T., Chen, S. and Kossakowska, J., "Chip form monitoring through advanced processing of cutting force sensor signals." *CIRP Annals-Manufacturing Technology* 55.1 (2006): 75-80.

[56] Klocke, F., Keitzel, G.,Veselovac, D., "Innovative Sensor Concept for Chip Transport Monitoring of Gun Drilling Processes." *Procedia CIRP* 14 (2014): 460-465.

[57] Jang, D.Y., Choi, Y.G., Kim, H.G., Hsiao, A., "Study of the correlation between surface roughness and cutting vibrations to develop an on-line roughness measuring technique in hard turning," International Journal of Machine Tools & Manufacture, vol. 36, (1996): 453-464.

[58] Altintas, Y., Manufacturing automation: metal cutting mechanics, machine tool vibrations, and CNC design. Cambridge university press, 2012.

[59] Benardos, P. G., Vosniakos, G-C., "Predicting surface roughness in machining: a review." International Journal of Machine Tools and Manufacture43.8 (2003): 833-844.

[60] Abouelatta, O. B., Madl, J., "Surface roughness prediction based on cutting parameters and tool vibrations in turning operations." Journal of Materials Processing Technology 118.1 (2001): 269-277.

[61] Konig, W., Kutzner, K., Schehl, U., "Tool Monitoring of Small Drills with Acoustic-Emission," International Journal of Machine Tools & Manufacture, vol. 32, (1992): 487-493.

[62] Lee, D.E., Hwang, I., Valente, C.M.O., Oliveira, J.F.G., Dornfeld, D.A., "Precision manufacturing process monitoring with acoustic emission," International Journal of Machine Tools & Manufacture, vol. 46, (2006): 176-188.

[63] Li, X.L., "A brief review: acoustic emission method for tool wear monitoring during turning," International Journal of Machine Tools & Manufacture, vol. 42, (2002): 157-165.

[64] Marinescu, I., Axinte, D.A., "A critical analysis of effectiveness of acoustic emission signals to detect tool and workpiece malfunctions in milling operations," International Journal of Machine Tools & Manufacture, vol. 48, (2008): 1148-1160.

[65] A. Araujo, S. J. Wilcox, and R. L. Reuben, "Investigation of the role of dislocation motion in the generation of acoustic emission from metal cutting," Proceedings of the Institution of Mechanical Engineers Part B-Journal of Engineering Manufacture, vol. 223, (2009): 1507-1518.

[66] Basti, A., Obikawa, T., Shinozuka, J., "Tools with built-in thin film thermocouple sensors for monitoring cutting temperature." International Journal of Machine Tools and Manufacture 47.5 (2007): 793-798.

[67] Karaguzel, U., Bakkal, M., Budak, E., "Modeling and Measurement of Cutting Temperatures in Milling." Procedia CIRP 46 (2016): 173-176.

[68] Abouridouane, M., Klocke, F., Lung, D., Veselovac, D., "The Mechanics of Cutting: In-situ Measurement and Modelling." Procedia CIRP 31 (2015): 246-251.

[69] Byrne, G., "Thermoelectric signal characteristics and average interfacial temperatures in the machining of metals under geometrically defined conditions." International Journal of Machine Tools and Manufacture 27.2 (1987): 215-224.

[70] O'Sullivan, D., Cotterell, M., "Temperature Measurement in Single Point Turning," Materials Processing Technology, vol. 118, (2001): 301-308.

[71] Lin, J., Liu, C.Y., "Measurement of cutting tool temperature by an infrared pyrometer." Measurement science and technology 12.8 (2001): 1243.

[72] Actarus SAS tool mounted temperature measurement http://www.actarus-sas-88.com/

[73] http://www.testandmeasurementtips.com/test-equipment/communication-test/test-and-measurement-basics-of-microphones/

[74] Shure PG81 Microphone; http://cdn.shure.com/specification_sheet/upload/67/us_pro_pg81_specsheet.pdf

[75] Okuma machining Navi spindle speed control. http://www.okuma.co.jp/english

[76] Harmonizer chatter avoidance http://www.mfg-labs.com/mfg-labs/Harmonizer/index.html

[77] Ghosh, N., Ravi, Y.B., Patra, A., Mukhopadhyay, S., Paul, S., Mohanty, A.R. and Chattopadhyay, A.B., "Estimation of tool wear during CNC milling using neural network-based sensor fusion." Mechanical Systems and Signal Processing 21.1 (2007): 466-479.

[78] Delio, T., Tlusty, J., Smith, S., "Use of audio signals for chatter detection and control." Journal of Manufacturing Science and Engineering 114.2 (1992): 146-157.

[79] Piezoelectric accelerometers; http://www.pcb.com/TechSupport/Tech_Accel

[80] Shahbazian, E., Blodgett, D.E, Labbé, P., "The extended OODA model for data fusion systems." Proceedings of the International Conference on Information Fusion, (2001): FrB1-19—FrB1-25.

[81] Jemielniak, K. "Commercial tool condition monitoring systems." The International Journal of Advanced Manufacturing Technology 15.10 (1999): 711-721.

[82] Rytter, A. "Vibrational based inspection of civil engineering structures". PhD Thesis, (1993).

[83] Cross, E. "On structural health monitoring in changing environmental and operational conditions." PhD Thesis (2012).

[84] Bedworth, M., O'Brien, J., "The Omnibus model: a new model of data fusion?." IEEE Aerospace and Electronic Systems Magazine 15.4 (2000): 30-36.

[85] Hall, D.L., Llinas, J., "An introduction to multisensor data fusion." Proceedings of the IEEE 85.1 (1997): 6-23.

[86] Steinberg, A.N., Bowman, C.L., "Rethinking the JDL data fusion levels." NSSDF JHAPL (2004): 22.

[87] Segreto, T., Simeone, A., Teti, R., "Multiple Sensor Monitoring in Nickel Alloy Turning for Tool Wear Assessment via Sensor Fusion." Procedia CIRP 12 (2013): 85-90.

[88] Cherkassky, V., Mulier, F.M., "Learning from data: concepts, theory, and methods." Wiley. com, 2007.

[89] Farrar, C.R., Worden, K. "Structural health monitoring: a machine learning perspective". John Wiley & Sons, 2012.

[90] Bishop, C.M., "Neural networks for pattern recognition". Oxford university press, 1995.

[91] Marinescu, I., Axinte, D., "A time–frequency acoustic emission-based monitoring technique to identify workpiece surface malfunctions in milling with multiple teeth cutting simultaneously." International Journal of Machine Tools and Manufacture 49.1 (2009): 53-65.

[92] Li, X., Dong, S., Yuan. Z., "Discrete wavelet transform for tool breakage monitoring." International Journal of Machine Tools and Manufacture 39.12 (1999): 1935-1944.

[93] Cho, S.Y., Binsaeid, S., Asfour, S., "Design of multisensor fusion-based tool condition monitoring system in end milling," International Journal of Advanced Manufacturing Technology, vol. 46, (2010): 681-694

[94] Budak, E., Altintas. Y., "Analytical prediction of chatter stability in milling—part I: general formulation." Journal of Dynamic Systems, Measurement, and Control 120.1 (1998): 22-30.

[95] Bi, Y., Guan, J., Bell, D., "The combination of multiple classifiers using an evidential reasoning approach." Artificial Intelligence 172.15 (2008): 1731-1751.

[96] Jemielniak, K., Urbański, T., Kossakowska, J. and Bombiński, S., "Tool condition monitoring based on numerous signal features." The International Journal of Advanced Manufacturing Technology 59.1-4 (2012): 73-81

[97] Cohen, L. "Time-frequency distributions-a review." Proceedings of the IEEE77.7 (1989): 941-981.

[98] Antoni, J. "Cyclostationarity by examples." Mechanical Systems and Signal Processing 23.4 (2009): 987-1036.

[99] Antoni, J., Bonnardot, F., Raad, A. and El Badaoui, M., "Cyclostationary modelling of rotating machine vibration signals." Mechanical systems and signal processing 18.6 (2004): 1285-1314.

[100] Lamraoui, M., Thomas, M., El Badaoui, M., "Cyclostationarity approach for monitoring chatter and tool wear in high speed milling." Mechanical Systems and Signal Processing 44.1 (2014): 177-198.

[101] Bechhoefer, E., Kingsley, M., "A review of time synchronous average algorithms." Annual conference of the prognostics and health management society. Vol. 23. (2009).

[102] Antoni, J., Randall, R.B., "The spectral kurtosis: application to the vibratory surveillance and diagnostics of rotating machines." Mechanical Systems and Signal Processing 20.2 (2006): 308-331.

[103] Kohavi, R., John, G.H., "Wrappers for feature subset selection." Artificial intelligence 97.1 (1997): 273-324.

[104] ISO11381-1:2004 (en), “Condition monitoring and diagnostics of machines -- Prognostics -- Part 1: General guidelines”

[105] Venkatasubramanian, V., Rengaswamy, R., Yin, K. and Kavuri, S.N., "A review of process fault detection and diagnosis: Part I: Quantitative model-based methods." Computers & chemical engineering 27.3 (2003): 293-311.

[106] Tobon-Mejia, D. A., Medjaher, K., Zerhouni, N., "CNC machine tool's wear diagnostic and prognostic by using dynamic Bayesian networks."Mechanical Systems and Signal Processing 28 (2012): 167-182.

[107] Si, X.S., Wang, W., Hu, C.H. and Zhou, D.H., "Remaining useful life estimation–A review on the statistical data driven approaches." European Journal of Operational Research 213.1 (2011): 1-14.

[108] Zaidan, M.A., Mills, A.R., Harrison, R.F., "Bayesian framework for aerospace gas turbine engine prognostics." Aerospace Conference, IEEE, 2013.

[109] Sick, B. "On-line and indirect tool wear monitoring in turning with artificial neural networks: a review of more than a decade of research." Mechanical Systems and Signal Processing 16.4 (2002): 487-546.

[110] Kohonen T, “Self-organisation and Associative Memory”, Springer-Verlag, Berlin (1989).

[111] Silva, R.G., Reuben, R.L., Baker, K.J., Wilcox, S.J., “Tool wear monitoring of turning operations by neural network and expert system classification of a feature set generated from multiplevsensors”. Mech Syst. Signal Process 12 (1998): 319–332.

[112] Burke, L.I., Rangwala, S., "Tool condition monitoring in metal cutting: a neural network approach." Journal of Intelligent Manufacturing 2.5 (1991): 269-280.

[113] Jammu, V. B., Danai, K., Malkin, S., Unsupervised neural network for tool breakage detection in turning. Ann. CIRP, 42 (1), (1993): 67.

[114] Dimla, D.E., Lister, P.M., Leighton, N.J., "Neural network solutions to the tool condition monitoring problem in metal cutting—a critical review of methods." International Journal of Machine Tools and Manufacture 37.9 (1997): 1219-1241.

[115] Ko, T.J, Cho, D.W., Jung, M.J., “On-line monitoring of tool breakage in face milling using self-organized neural network”, Journal of Manufacturing Systems 14 (2) (1995): 80–90.

[116] Li, S., Elbestawi, M.A., “Fuzzy clustering for automated tool condition monitoring in machining”, Mechanical Systems and Signal Processing 10, (1996): 533–550.

[117] Niu, Y.M., Wong, Y.S., Hong G.S., Liu, T.I., “Multi-category classification of tool conditions using wavelet packets and ART2 network”, Journal of Manufacturing Science and Engineering, Transactions of the ASME 120, (1998): 807–816..

[118] Özel, T., Karpat, Y., "Predictive modeling of surface roughness and tool wear in hard turning using regression and neural networks." International Journal of Machine Tools and Manufacture 45.4 (2005): 467-479.

[119] Worden, K., Staszewski, W.J., Hensman, J.J., "Natural computing for mechanical systems research: A tutorial overview." Mechanical Systems and Signal Processing 25.1 (2011): 4-111.

[120] Alaeddini, A., Dogan, I., "Using Bayesian networks for root cause analysis in statistical process control." Expert Systems with Applications 38.9 (2011): 11230-11243.

[121] Lewis, R.W., Ransing, R.S., "A semantically constrained Bayesian network for manufacturing diagnosis." International journal of production research 35.8 (1997): 2171-2188

[122] Ransing, R.S., Srinivasan, M.N., Lewis, R.W., "ICADA: Intelligent computer aided defect analysis for castings." Journal of Intelligent Manufacturing 6.1 (1995): 29-40.

[123] Liu, T.I., Anantharaman, K.S., "Intelligent classification and measurement of drill wear." Journal of engineering for industry 116.3 (1994): 392-397.

[124] Abu-Mahfouz, I. "Drilling wear detection and classification using vibration signals and artificial neural network." International Journal of Machine Tools and Manufacture 43.7 (2003): 707-720.

[125] Dimla Sr, D.E., Lister, P.M., "On-line metal cutting tool condition monitoring: II: tool-state classification using multi-layer perceptron neural networks." International Journal of Machine Tools and Manufacture 40.5 (2000): 769-781.

[126] Siddhpura, A., Paurobally, R., "A review of flank wear prediction methods for tool condition monitoring in a turning process." The International Journal of Advanced Manufacturing Technology 65.1-4 (2013): 371-393.

[127] Rousseeuw, P.J., "Silhouettes: a graphical aid to the interpretation and validation of cluster analysis." Journal of computational and applied mathematics 20 (1987): 53-65.

[128] Guyon, I., Elisseeff, A., "An introduction to variable and feature selection." The Journal of Machine Learning Research 3 (2003): 1157-1182.

[129] Li, X., Lim, B.S., Zhou, J.H., Huang, S., Phua, S.J., Shaw, K.C. and Er, M.J., "Fuzzy neural network modelling for tool wear estimation in dry milling operation.", Annual conference of the prognostics and health management society. (2009): 1-11.

9 APPENDICES

Appendix A PFMEA

Process Step	Process Details	Potential Failure Mode	Potential Effect(s) of Failure	SEV	Potential Cause(s) of Failure	OCC	Current Process Controls		DET	RPN
							Prevention of Failure mode escape	Detection of Failure cause		
10	Assemble tool	Wrong holder used	geometric part error, surface finish error, delay, machine damage, tool damage	7	tooling documentation wrong	4	None	IPT3, technical sign off	5	140
					tooling documentation not followed	3	None	Double sign off	6	126
		Holder not clamped correctly	geometric part error, surface finish error, delay, machine damage, tool damage	8	failure of tool holder	3	Tooling maintenance	None	10	240
					incorrect tool used for setting	3	Tooling control and specification	Double sign off	6	144
					correct tool clamping procedure not followed	4	Tooling control and specification	Double sign off	6	192
		Wrong tool used	geometric part error, surface finish error, delay, machine damage, tool damage	7	tooling documentation wrong	4	None	IPT3, technical sign off	5	140
					tooling documentation not followed	3	None	Double sign off	6	126
		Wrong inserts used	geometric part error, surface finish error, delay, machine damage, tool damage	7	tooling documentation wrong	3	None	IPT3, technical sign off	5	105
					tooling documentation not followed	5	None	Double sign off	6	210
		Insert not clamped correctly	geometric part error, surface finish error, delay, machine damage, tool damage	7	failure of tool holder	3	Tooling maintenance	None	10	210
					incorrect tool used for setting	3	Tooling control and specification	Double sign off	6	126
20	Load Tool	Tool loaded to wrong pot	geometric part error, surface finish error, delay, machine damage, tool damage	7	tooling documentation wrong	4	None	IPT3, technical sign off	5	140
					tooling documentation not followed	2	None	Double sign off	6	84
		Tool loaded backwards (turning)	geometric part error, surface finish error, delay, machine damage, tool damage	7	tooling documentation wrong	4	None	IPT3, technical sign off	5	140
					tooling documentation not followed	3	None	Double sign off	6	126
		Tool not correctly locked in position in pot	machine damage, delay, tool damage	6	Machine issue	2	machine maintenance	None	10	120
					loading not done correctly	3	Tooling control and specification	None	10	180
		Wrong tool loaded	geometric part error, surface finish error, delay, machine damage, tool damage	7	tooling documentation wrong	5	None	IPT3, technical sign off	5	175
					tooling documentation not followed	5	None	Double sign off	6	210
		Offsets written to wrong tool number in machine control	geometric part error, surface finish error, delay, machine damage, tool damage	7	documentation not followed	3	None	Double sign off	6	126
		Offsets not written	geometric part error, surface finish error, delay, machine damage, tool damage	7	documentation not followed	3	None	Double sign off	6	126
		Wrong offsets written to machine control	geometric part error, surface finish error, delay, machine damage, tool damage	7	documentation not followed	3	None	Double sign off	6	126

Process Step	Process Details	Potential Failure Mode	Potential Effect(s) of Failure	SEV	Potential Cause(s) of Failure	OCC	Current Process Controls		DET	RPN
							Prevention of Failure mode escape	Detection of Failure cause		
30	Assemble Fixture	Wrong parts used in assembly	geometric part error, surface finish error, delay, machine damage, tool damage, injury,	8	fixture documentation wrong	4	None	IPT3, technical sign off	5	160
					fixture documentation not followed	3	None	Double sign off	5	120
		Assembled parts not at correct torque	geometric part error, surface finish error, delay, machine damage, tool damage, injury,	8	fixture documentation wrong	5	None	IPT3, technical sign off	5	200
					fixture documentation not followed	4	None	Double sign off	5	160
		Assembled parts not aligned correctly/sufficiently accurate	geometric part error, surface finish error, delay, machine damage, tool damage, injury,	8	fixture documentation wrong	6	None	IPT3, technical sign off	5	240
					fixture documentation not followed	6	None	Double sign off	5	240
		Parts missing from assembly	geometric part error, surface finish error, delay, machine damage, tool damage, injury,	8	fixture documentation wrong	5	None	IPT3, technical sign off	4	160
					fixture documentation not followed	4	None	Double sign off	4	128
40	Load Fixture	Fixture too heavy for machine	Damage to machine, program feed/speed not achieved, delay	7	Wrong specification of fixture/machine	2	Design/FEA	IPT Review	4	56
		Fixture too large for machine	Damage to machine, fixture, tool, delay	7	Wrong specification of fixture/machine	2	Design/FEA	IPT Review	4	56
		Wrong fixture loaded	Unable to load part, wrong datum used, collision, geometric part error, surface finish error, delay	8	fixture documentation wrong	4	None	IPT3, technical sign off	4	128
					fixture documentation not followed	5	None	Double sign off	4	160
					Fixture/parts not marked correctly	7	None	Complete documentation	4	224
		Fixture not/cannot be loaded	Delay	4	Wrong specification of fixture/machine	5	Design/FEA	IPT Review	4	80
					fixture documentation wrong	4	None	IPT3, technical sign off		0
					fixture documentation not followed	4	None	Double sign off		0
					Not planned/actioned	4	None	project management	3	48
		Fixture not securly attached	Injury, damage to fixture, machine, geometric part error, surface finish error, delay, machine damage, tool damage,	10	fixture documentation wrong	4				0
					fixture documentation not followed	4				0
					Bolts not torqued correctly/Torque wrench or tooling failure	4				0
		Loading equipment not suitable	Injury, damage to fixture, damage machine, delay, damage loaded equipment, damage other shop equipment	10	Wrong specification of loading equipment/ not fit for purpose	6				0
					equipment not maintained	4				0
		Fixture position incorrect	geometric part error, surface finish error, delay, machine damage, tool damage, fixture damage	8	fixture documentation wrong	6				0
					fixture documentation not followed	5				0
					DTI not adequate for location accuracy	4				0

Process Step	Process Details	Potential Failure Mode	Potential Effect(s) of Failure	SEV	Potential Cause(s) of Failure	OCC	Current Process Controls		DET	RPN
							Prevention of Failure mode escape	Detection of Failure cause		
50	Align/locate fixture	Fixture not flat	geometric part error, surface finish error, delay	8	fixture not flat	5				0
					fixture deflected	4				0
		Fixture not positioned concentric	geometric part error, surface finish error, delay	8	fixture positioned incorrectly	5				0
		Fixture not positioned square	geometric part error, surface finish error, delay	8	part mating face not square/parralel to fixture mating face	5				0
					Machine bed not square	4				0
					fixture positioned incorrectly	5				0
60	Load part	Part too heavy for machine								
		Part too small/large for fixture								
		Wrong part used								
		Part not loaded								
70	Clamp part	Wrong torque/wrench used								
		Wrong hydraulic pressure applied								
		Bolts too long								
		Bolts too short								
		Part not clocked true correctly								
		Part/fixture wrong size								
		Tooling not available								
		Fixture clamping components missing								
		not clamped								
80	Load program	Wrong program loaded								
		Program partially loaded								
		No program loaded								

Process Step	Process Details	Potential Failure Mode	Potential Effect(s) of Failure	SEV	Potential Cause(s) of Failure	OCC	Current Process Controls		DET	RPN
							Prevention of Failure mode escape	Detection of Failure cause		
110	Run milling program	Part vibration	geometric part error, machine damage, tool damage, delay,	7	Part not clamped correctly	5	None	Double sign off	4	140
					Part condition has changed	6	None	Operator observation/ CoC	6	252
					Material condition changed	5	None	CoC	8	280
					Fixture assembly incorrect	4	None	Double sign off	5	140
					Cutting parameters too aggressive	6	None	Double sign off	5	210
					Spindle speed excites part vibration mode	5	None	Tap test	8	280
					Wrong tool used	4	Tooling control and specification	Double sign off	5	140
					Wrong cutting parameters used	7	None	Double sign off	5	245
					Tool is worn or damaged	6	Tooling control and specification	Double sign off	5	210
					Part position error causing depth of cut change	5	None	Double sign off	7	245
					Tool length error causing depth of cut change	5	None	Double sign off	7	245
					Tool not clamped correctly	4	None	Double sign off	6	168
					Excessive cutting force	5	None	Operator observation	8	280
					part stiffness insufficient	5	None	Tap test	7	245
		Tool vibration	geometric part error, machine damage, tool damage, delay,	7	Part condition has changed	6	None	Operator observation/ CoC	6	252
					Material condition changed	5	None	CoC	8	280
					Cutting parameters too aggressive	6	None	Double sign off	5	210
					Spindle speed excites part vibration mode	5	None	Tap test / harmoniser	8	280
					Wrong tool used	4	Tooling control and specification	Double sign off	5	140
					Wrong cutting parameters used	7	None	Double sign off	5	245
					Tool is worn or damaged	6	Tooling control and specification	Double sign off	5	210
					Part position error causing depth of cut change	5	None	Double sign off	7	245
					Tool length error causing depth of cut change	5	None	Double sign off	7	245
					Tool not clamped correctly	4	None	Double sign off	6	168
					Excessive cutting force	5	None	Operator observation	8	280
					Tool stiffness insufficient	6	None	Tap test / harmoniser	7	294

Process Step	Process Details	Potential Failure Mode	Potential Effect(s) of Failure	SEV	Potential Cause(s) of Failure	OCC	Current Process Controls		DET	RPN
							Prevention of Failure mode escape	Detection of Failure cause		
110	Run milling program	Excessive tool wear	geometric part error, tool damage, delay,	7	Part condition has changed	6	None	Operator observation/ CoC	6	252
					Material condition changed	5	None	CoC	8	280
					Cutting parameters too aggressive	6	None	Double sign off	5	210
					Spindle speed excites part vibration mode	5	None	Tap test	8	280
					Wrong tool used	4	Tooling control and specification	Double sign off	5	140
					Wrong cutting parameters used	6	None	Double sign off	5	210
					Tool is worn or damaged	5	Tooling control and specification	Double sign off	5	175
					Part position error causing depth of cut change	4	None	Double sign off	7	196
					Tool length error causing depth of cut change	4	None	Double sign off	7	196
					Tool not clamped correctly	4	None	Double sign off	6	168
					Excessive cutting force	5	None	Operator observation	8	280
					chatter due to tool stiffness	6	None	Operator observation	7	294
					chatter due to part stiffness	5	None	Operator observation	7	245
					Insufficient coolant flow	6	None	Operator observation	7	294
					Incorrect coolant mix	4	None	operator observation	6	168
		Tool breakage	geometric part error, tool damage, delay,	8	Part condition has changed	6	None	Operator observation/ CoC	6	288
					Material condition changed	5	None	CoC	8	320
					Cutting parameters too aggressive	6	None	Double sign off	5	240
					Spindle speed excites part vibration mode	5	None	Tap test / harmoniser	8	320
					Wrong tool used	4	Tooling control and specification	Double sign off	5	160
					Wrong cutting parameters used	6	None	Double sign off	5	240
					Tool is worn or damaged	5	Tooling control and specification	Double sign off	5	200
					Part position error causing depth of cut change	4	None	Double sign off	7	224
					Tool length error causing depth of cut change	4	None	Double sign off	7	224
					Tool not clamped correctly	4	None	Double sign off	6	192
					Excessive cutting force	5	None	Operator observation	6	240
					chatter due to tool stiffness	6	None	Operator observation	6	288
					chatter due to part stiffness	5	None	Operator observation	6	240
					Collision	4	None	Operator observation	6	192
					Insufficient coolant flow	6	None	Operator observation	6	288
					Incorrect coolant mix	4	None	operator observation	6	192

Process Step	Process Details	Potential Failure Mode	Potential Effect(s) of Failure	SEV	Potential Cause(s) of Failure	OCC	Current Process Controls		DET	RPN
							Prevention of Failure mode escape	Detection of Failure cause		
110	Run milling program	Collision	geometric part error, machine damage, tool damage, delay,	8	Wrong tool used	5	Tooling control and specification	Double sign off	5	200
					Part condition has changed	5	None	Operator observation/ CoC	6	240
		coolant delivery failure	geometric part error, tool damage, delay,	8	Wrong tool/collet used	5	Tooling control and specification	Double sign off	5	200
					Coolant pump/line failure	4	None	Machine sensor	5	160
		Wrong coolant type/concentration	geometric part error, tool damage, delay,	7	Coolant checking procedure not followed	5	None	Operator observation	6	210
		Tool pull out	geometric part error, tool damage, delay,	8	Part condition has changed	6	None	Operator observation/ CoC	6	288
					Material condition changed	5	None	CoC	8	320
					Cutting parameters too aggressive	6	None	Double sign off	5	240
					Spindle speed excites part vibration mode	5	None	Tap test / harmoniser	8	320
					Wrong tool used	4	Tooling control and specification	Double sign off	5	160
					Wrong cutting parameters used	6	None	Double sign off	5	240
					Tool is worn or damaged	5	Tooling control and specification	Double sign off	5	200
					Part position error causing depth of cut change	4	None	Double sign off	7	224
					Tool length error causing depth of cut change	4	None	Double sign off	7	224
					Tool not clamped correctly	4	None	Double sign off	6	192
					Excessive cutting force	5	None	Operator observation	6	240
					chatter due to tool stiffness	6	None	Operator observation	6	288
					chatter due to part stiffness	5	None	Operator observation	6	240
		Wrong program run	geometric part error, machine damage, tool damage, delay,	8	fixture documentation wrong	5	None	IPT3, technical sign off	5	200
					fixture documentation not followed	4	None	Double sign off	5	160
		Machine alarm	geometric part error, machine damage, tool damage, delay,	8	-					
		NC code alarm	geometric part error, tool damage, delay,	8	-					
		Incorrect tool called	geometric part error, machine damage, tool damage, delay,	8	-					
		Incorrect cutting parameters	geometric part error, tool damage, delay, tool vibration	8	-					
		Max spindle power reached	geometric part error, tool damage, delay,	8	-					
		Max spindle torque reached	geometric part error, tool damage, delay, machine stall	8	-					
		Max spindle RPM reached	geometric part error, tool damage, delay, tool vibration	8	-					
		Excessive tool run out	geometric part error, tool damage, delay,	8	-					
		Dry run turned on	geometric part error, machine damage, tool damage, delay,	8	-					
		Feed and speed overide not at 100%	geometric part error, tool damage, delay,	8	-					

Appendix B Further Sensor Signal Data

The following tables list the R-squared value for each sensor signal feature and their best fit polynomial models. Each sensor signal feature is also given a unique reference number in the first column entitled '#'.

Table B.1 – X-axis vibration signal feature R-squared values

#	(604B31) X-Axis Accelerometer						
	Feature Type		R-squared for Polynomial Models				
			1st Order	2nd Order	3rd Order	4th Order	5th Order
1	Time Domain	RMS	0.6282	0.9339	0.9485	0.9635	0.9846
2		Variance	0.6165	0.9439	0.9776	0.9816	0.9955
3		Kurtosis	0.2795	0.4293	0.4295	0.5878	0.7042
4		Skew	0.0045	0.7429	0.7770	0.7770	0.7871
5		Peak-to-Peak	0.4702	0.8342	0.8427	0.8438	0.8840
6		Crest Factor	0.1899	0.1927	0.2057	0.2947	0.3051
7		Peak	0.4508	0.8176	0.8249	0.8256	0.8655
8	Original Power Spectrum	Mean	0.6223	0.9376	0.9732	0.9792	0.9953
9		Variance	0.7120	0.9495	0.9558	0.9738	0.9842
10		Kurtosis	0.8045	0.8093	0.8397	0.8547	0.8562
11		Skew	0.7718	0.7767	0.8318	0.8435	0.8436
12		Sum TPF	0.8028	0.9284	0.9298	0.9754	0.9826
13	Filtered Power Spectrum	Mean	0.6051	0.9319	0.9725	0.9779	0.9952
14		Variance	0.5675	0.9015	0.9780	0.9781	0.9876
15		Kurtosis	0.0023	0.4313	0.4332	0.6019	0.6176
16		Skew	0.0189	0.5127	0.5130	0.6665	0.6983
17	Band of Power Spectrum	Mean	0.6246	0.9607	0.9742	0.9845	0.9885
18		Variance	0.7060	0.8623	0.9017	0.9018	0.9029
19		Kurtosis	0.4265	0.4409	0.4421	0.4588	0.4767
20		Skew	0.4844	0.5478	0.5517	0.5661	0.5737

Table B.2 – Y-axis vibration signal feature R-squared values

#	(604B31) Y-Axis Accelerometer						
	Feature Type		R-squared for Polynomial Models				
			1st Order	2nd Order	3rd Order	4th Order	5th Order
21	Time Domain	RMS	0.8439	0.8536	0.8739	0.9808	0.9873
22		Variance	0.8467	0.8488	0.8607	0.9674	0.9851
23		Kurtosis	0.1299	0.6175	0.6189	0.8576	0.8635
24		Skew	0.1089	0.2521	0.3270	0.7309	0.7396
25		Peak-to-Peak	0.1838	0.4357	0.4671	0.7534	0.7551
26		Crest Factor	0.1828	0.4092	0.4101	0.5446	0.5492
27		Peak	0.1876	0.4232	0.4528	0.7343	0.7369
28	Original Power Spectrum	Mean	0.8375	0.9027	0.9127	0.9843	0.9916
29		Variance	0.5292	0.6150	0.6218	0.8329	0.9122
30		Kurtosis	0.8234	0.9084	0.9231	0.9831	0.9843
31		Skew	0.8484	0.9090	0.9205	0.9803	0.9803
32		Sum TPF	0.1936	0.5597	0.5697	0.6129	0.6354
33	Filtered Power Spectrum	Mean	0.8373	0.8999	0.9101	0.9837	0.9913
34		Variance	0.6624	0.6763	0.6901	0.8633	0.9326
35		Kurtosis	0.0000	0.0067	0.0081	0.0081	0.0156
36		Skew	0.0180	0.3240	0.3383	0.3727	0.4637
37	Band of Power Spectrum	Mean	0.7760	0.9768	0.9894	0.9925	0.9955
38		Variance	0.5967	0.7604	0.7839	0.7839	0.8013
39		Kurtosis	0.0000	0.2034	0.2327	0.4646	0.4742
40		Skew	0.0073	0.2224	0.2468	0.4560	0.4625

Table B.3 – Z-axis vibration signal feature R-squared values

#	(604B31) Z-Axis Accelerometer						
	Feature Type		R-squared for Polynomial Models				
			1st Order	2nd Order	3rd Order	4th Order	5th Order
41	Time Domain	RMS	0.9013	0.9755	0.9804	0.9874	0.9942
42		Variance	0.8494	0.9712	0.9856	0.9929	0.9960
43		Kurtosis	0.0841	0.4377	0.4412	0.8463	0.8551
44		Skew	0.8957	0.9069	0.9460	0.9483	0.9491
45		Peak-to-Peak	0.4694	0.4917	0.4931	0.6956	0.7023
46		Crest Factor	0.1200	0.3008	0.3009	0.4786	0.4788
47		Peak	0.4224	0.4380	0.4404	0.6328	0.6374
48	Original Power Spectrum	Mean	0.7995	0.9764	0.9902	0.9931	0.9957
49		Variance	0.7647	0.9428	0.9440	0.9673	0.9738
50		Kurtosis	0.7202	0.9022	0.9075	0.9342	0.9496
51		Skew	0.7194	0.9166	0.9241	0.9451	0.9595
52		Sum TPF	0.8199	0.9403	0.9403	0.9707	0.9753
53	Filtered Power Spectrum	Mean	0.7508	0.9421	0.9699	0.9921	0.9939
54		Variance	0.6421	0.9146	0.9737	0.9797	0.9820
55		Kurtosis	0.0214	0.3130	0.3169	0.3449	0.3567
56		Skew	0.0488	0.3967	0.4069	0.4186	0.4566
57	Band of Power Spectrum	Mean	0.8529	0.9918	0.9943	0.9959	0.9967
58		Variance	0.7256	0.8907	0.9013	0.9016	0.9054
59		Kurtosis	0.0177	0.2659	0.3210	0.4217	0.4308
60		Skew	0.0409	0.3649	0.4052	0.5112	0.5135

Table B.4 – High frequency vibration signal feature R-squared values

#	(352A60) High Frequency Accelerometer						
	Feature Type		R-squared for Polynomial Models				
			1st Order	2nd Order	3rd Order	4th Order	5th Order
61	Time Domain	RMS	0.6484	0.6544	0.7109	0.8157	0.8586
62		Variance	0.6334	0.6436	0.6888	0.7965	0.8578
63		Kurtosis	0.6123	0.6618	0.7413	0.7870	0.8338
64		Skew	0.8187	0.8674	0.9288	0.9527	0.9581
65		Peak-to-Peak	0.0764	0.0779	0.1780	0.2982	0.3905
66		Crest Factor	0.2070	0.2070	0.2147	0.2158	0.2504
67		Peak	0.0728	0.0733	0.1544	0.2477	0.3378
68	Original Power Spectrum	Mean	0.4900	0.5750	0.5786	0.7356	0.7925
69		Variance	0.7643	0.9425	0.9436	0.9672	0.9737
70		Kurtosis	0.2262	0.3324	0.4133	0.5705	0.6327
71		Skew	0.2304	0.3368	0.4184	0.5789	0.6387
72		Sum TPF	0.8247	0.9420	0.9421	0.9709	0.9757
73	Filtered Power Spectrum	Mean	0.3460	0.4087	0.4131	0.6460	0.7263
74		Variance	0.1289	0.2540	0.2996	0.6028	0.7020
75		Kurtosis	0.1670	0.1843	0.2008	0.3942	0.4365
76		Skew	0.0617	0.1335	0.2040	0.4024	0.4599
77	Band of Power Spectrum	Mean	0.8219	0.9819	0.9827	0.9911	0.9918
78		Variance	0.7582	0.8959	0.8977	0.9099	0.9114
79		Kurtosis	0.1468	0.1608	0.1864	0.2454	0.3205
80		Skew	0.1823	0.2539	0.2680	0.3138	0.3895

Table B.5 – 378C01 microphone signal feature R-squared values

#	(378C01) Microphone						
	Feature Type		R-squared for Polynomial Models				
			1st Order	2nd Order	3rd Order	4th Order	5th Order
81	Time Domain	RMS	0.8246	0.8975	0.9236	0.9603	0.9609
82		Variance	0.8113	0.8934	0.9172	0.9574	0.9586
83		Kurtosis	0.8308	0.8983	0.9017	0.9326	0.9358
84		Skew	0.7360	0.7578	0.7594	0.7624	0.7779
85		Peak-to-Peak	0.5539	0.6268	0.6661	0.7130	0.7152
86		Crest Factor	0.4209	0.4354	0.4411	0.4437	0.4560
87		Peak	0.4708	0.5262	0.5527	0.5922	0.5960
88	Original Power Spectrum	Mean	0.8082	0.8874	0.9122	0.9525	0.9531
89		Variance	0.7912	0.9042	0.9153	0.9556	0.9585
90		Kurtosis	0.1887	0.2168	0.2507	0.2975	0.3027
91		Skew	0.1616	0.2172	0.2903	0.3547	0.3569
92		Sum TPF	0.7994	0.8899	0.9140	0.9546	0.9564
93	Filtered Power Spectrum	Mean	0.2871	0.2871	0.3201	0.3644	0.3744
94		Variance	0.0094	0.0630	0.0836	0.0915	0.1422
95		Kurtosis	0.0012	0.0450	0.0737	0.0746	0.1401
96		Skew	0.0005	0.0444	0.0611	0.0615	0.1214
97	Band of Power Spectrum	Mean	0.2752	0.2752	0.3091	0.3535	0.3638
98		Variance	0.0103	0.0643	0.0846	0.0924	0.1432
99		Kurtosis	0.0014	0.0450	0.0737	0.0746	0.1400
100		Skew	0.0003	0.0437	0.0604	0.0608	0.1205

Table B.6 – H378B02 microphone signal feature R-squared values

#	(H378B02) Microphone						
	Feature Type		R-squared for Polynomial Models				
			1st Order	2nd Order	3rd Order	4th Order	5th Order
101	Time Domain	RMS	0.8281	0.9050	0.9274	0.9618	0.9626
102		Variance	0.8152	0.9022	0.9222	0.9597	0.9610
103		Kurtosis	0.8073	0.8793	0.8843	0.9221	0.9248
104		Skew	0.7808	0.8115	0.8128	0.8231	0.8333
105		Peak-to-Peak	0.5868	0.6506	0.6744	0.6945	0.6947
106		Crest Factor	0.3780	0.3898	0.3952	0.4134	0.4141
107		Peak	0.4806	0.5432	0.5629	0.5786	0.5812
108	Original Power Spectrum	Mean	0.8132	0.8994	0.9185	0.9563	0.9572
109		Variance	0.7906	0.9063	0.9164	0.9566	0.9598
110		Kurtosis	0.6610	0.6648	0.7126	0.7133	0.7133
111		Skew	0.6973	0.7122	0.7372	0.7373	0.7377
112		Sum TPF	0.8127	0.9119	0.9283	0.9619	0.9646
113	Filtered Power Spectrum	Mean	0.0463	0.0522	0.0808	0.1195	0.1359
114		Variance	0.0317	0.0732	0.0750	0.0962	0.1334
115		Kurtosis	0.0001	0.0327	0.0337	0.0354	0.0798
116		Skew	0.0010	0.0279	0.0286	0.0323	0.0712
117	Band of Power Spectrum	Mean	0.0459	0.0522	0.0809	0.1195	0.1362
118		Variance	0.0323	0.0738	0.0756	0.0967	0.1338
119		Kurtosis	0.0002	0.0327	0.0336	0.0353	0.0797
120		Skew	0.0009	0.0276	0.0284	0.0321	0.0710

Table B.7 – Spindle power signal feature R-squared values

#	Spindle Power						
	Feature Type		R-squared for Polynomial Models				
			1st Order	2nd Order	3rd Order	4th Order	5th Order
121	Time Domain	Mean	0.8060	0.8279	0.8351	0.8791	0.8792
122		RMS	0.8053	0.8274	0.8347	0.8788	0.8789
123		Variance	0.0001	0.0001	0.0041	0.0047	0.0049
124		Kurtosis	0.0063	0.0088	0.0094	0.0172	0.0172
125		Skew	0.0014	0.0014	0.0016	0.0020	0.0029
126		Peak-to-Peak	0.0011	0.0022	0.0034	0.0036	0.0036
127		Crest Factor	0.4213	0.4213	0.4214	0.4347	0.4353
128		Peak	0.1774	0.1909	0.1962	0.2131	0.2134
129	Original Power Spectrum	Mean	0.0027	0.0040	0.0099	0.0100	0.0115
130		Variance	0.0131	0.0139	0.0401	0.2099	0.2449
131		Kurtosis	0.0720	0.1301	0.2295	0.3114	0.3373
132		Skew	0.0394	0.0892	0.1874	0.2848	0.3133
133	Band of Power Spectrum	Mean	0.0030	0.0092	0.0171	0.0493	0.0585
134		Variance	0.0550	0.0819	0.1909	0.3622	0.4362
135		Kurtosis	0.0029	0.0390	0.1106	0.1458	0.1757
136		Skew	0.0023	0.0431	0.1212	0.1630	0.1965

Table B.8 – Acoustic Emission signal feature R-squared values

#	Acoustic Emission						
	Feature Type		R-squared for Polynomial Models				
			1st Order	2nd Order	3rd Order	4th Order	5th Order
137		RMS	0.4408	0.8145	0.8732	0.8911	0.9150
138		Variance	0.4306	0.8008	0.8556	0.8800	0.9022
139		Kurtosis	0.2908	0.2932	0.4415	0.4606	0.5593
140		Skew	0.0498	0.0721	0.0822	0.1068	0.1111
141		Peak-to-Peak	0.3030	0.3949	0.4860	0.5001	0.5118
142		Crest Factor	0.0077	0.0457	0.0753	0.0774	0.0779
143		Peak	0.2862	0.3700	0.4602	0.4790	0.4875
144	Original Power Spectrum	Mean	0.4295	0.8669	0.8697	0.9152	0.9154
145		Variance	0.2017	0.6795	0.6801	0.6817	0.6818
146		Kurtosis	0.0842	0.1373	0.1375	0.3079	0.3112
147		Skew	0.0741	0.1387	0.1399	0.3721	0.3751
148	Band of Power Spectrum	Mean	0.3092	0.8465	0.8565	0.8833	0.8839
149		Variance	0.1880	0.6506	0.6512	0.6513	0.6513
150		Kurtosis	0.1072	0.1482	0.1497	0.2872	0.2917
151		Skew	0.1021	0.1431	0.1431	0.3427	0.3495

Table B.9 – Favored model order by avoiding overfitting for each feature, listed by feature

#	Ord.	#	Ord.	#	Ord.	#	Ord.	#	Ord..	#	Ord.	#	Ord.
1	5	23	5	45	5	67	5	89	5	111	3	133	5
2	5	24	5	46	4	68	5	90	5	112	5	134	5
3	5	25	5	47	5	69	5	91	5	113	5	135	5
4	5	26	5	48	5	70	5	92	5	114	5	136	5
5	5	27	5	49	5	71	5	93	5	115	5	137	5
6	5	28	5	50	5	72	5	94	5	116	5	138	5
7	5	29	5	51	5	73	5	95	5	117	5	139	5

8	5	30	5	52	5	74	5	96	5	118	5	140	5
9	5	31	4	53	5	75	5	97	5	119	5	141	5
10	5	32	5	54	5	76	5	98	5	120	5	142	3
11	4	33	5	55	5	77	5	99	5	121	4	143	5
12	5	34	5	56	5	78	5	100	5	122	4	144	5
13	5	35	1	57	5	79	5	101	5	123	1	145	2
14	5	36	5	58	5	80	5	102	5	124	1	146	5
15	5	37	5	59	5	81	5	103	5	125	1	147	5
16	5	38	5	60	5	82	5	104	5	126	1	148	5
17	5	39	5	61	5	83	5	105	4	127	4	149	2
18	5	40	5	62	5	84	5	106	4	128	4	150	5
19	5	41	5	63	5	85	5	107	5	129	1	151	5
20	5	42	5	64	5	86	5	108	5	130	5		
21	5	43	5	65	5	87	5	109	5	131	5		
22	5	44	5	66	5	88	5	110	4	132	5		

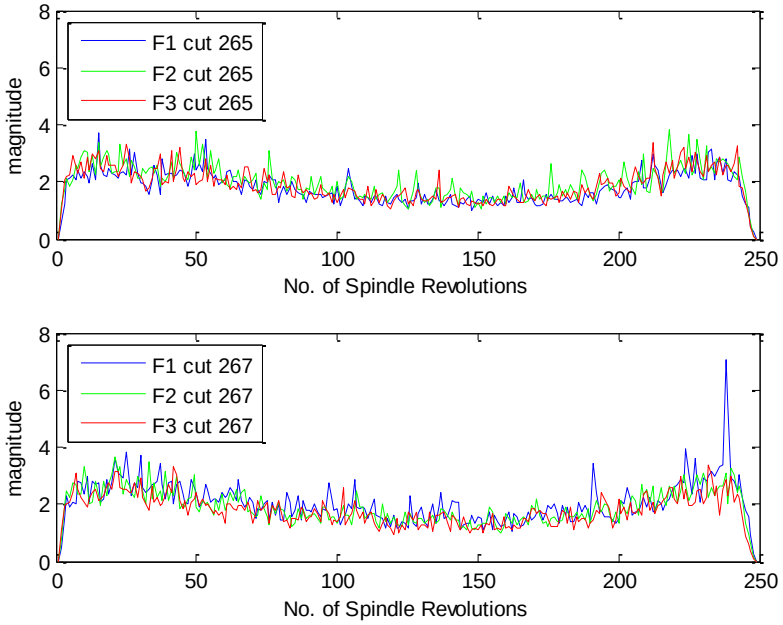

Figure B.1: HF Vibration peak for cut 265 and 267 vs spindle revolution

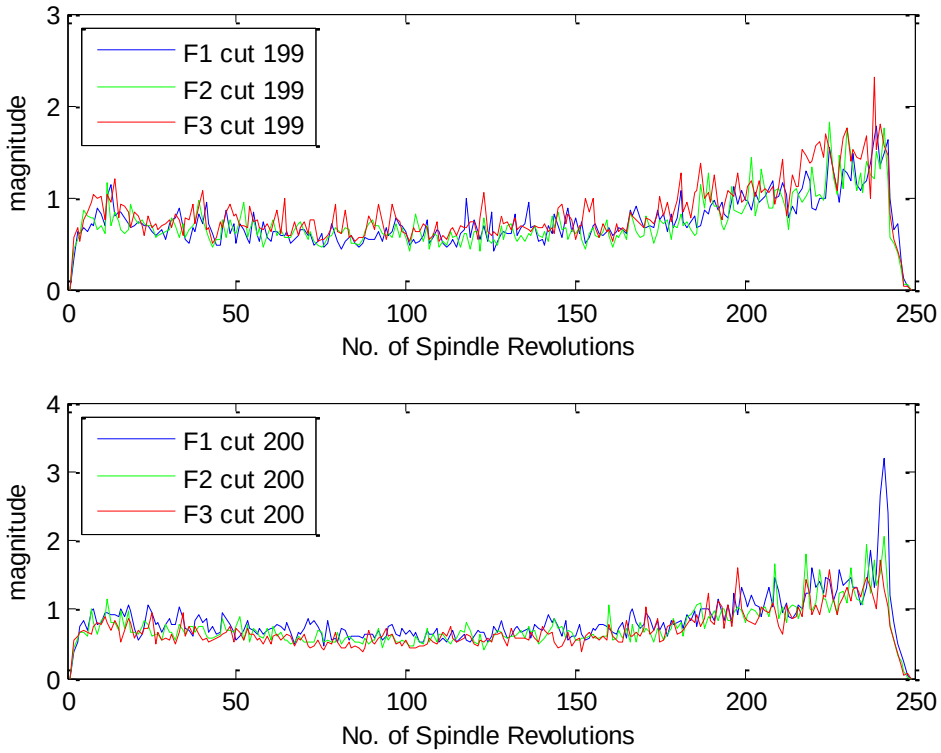

Figure B.2: Z-axis vibration peak for cut 199 and 200 vs spindle revolution

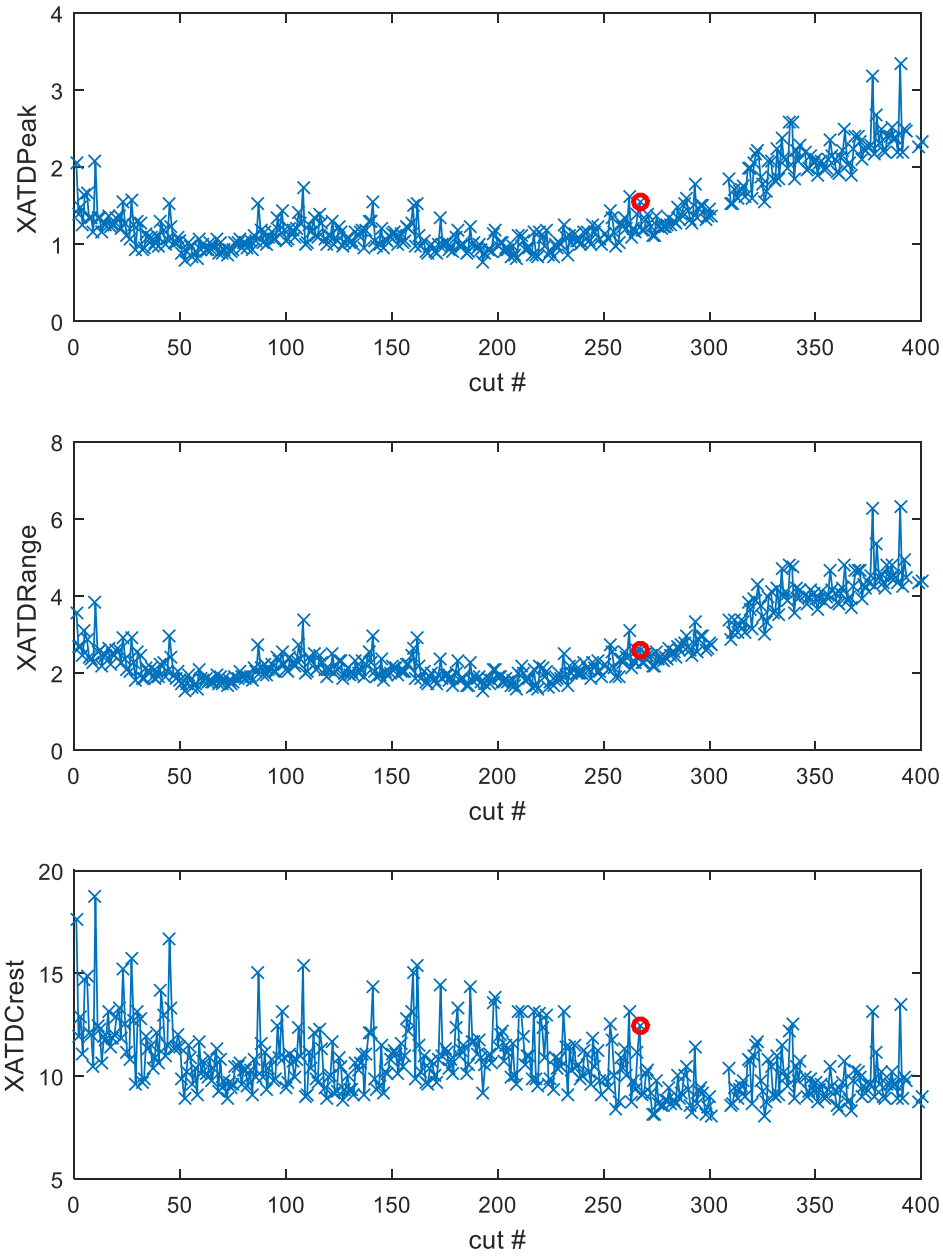

Figure B.3: X-axis vibration TD peak, range and crest factor for all cuts with cut 267 data points circled

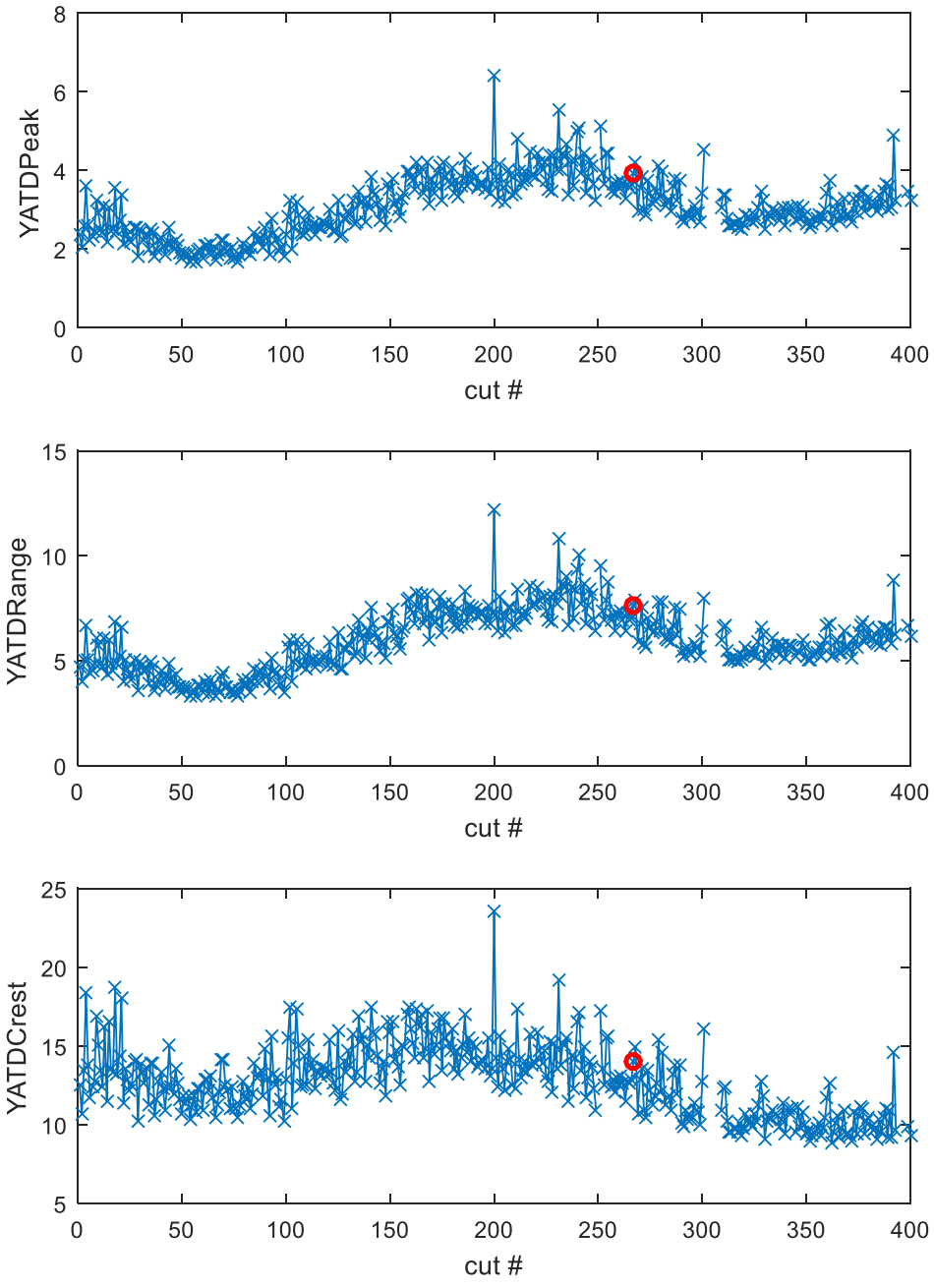

Figure B.4: Y-axis vibration TD peak, range and crest factor for all cuts with cut 267 data points circled

Appendix C Prognosis; Remaining Useful Tool Life

The main body of this thesis has based the methods on the assumption that the data is randomly found to be faulty or in a number of different classes. Another way of looking at the data is to consider it to have trajectory, therefore the extrapolation can allow the time to a fault to be assessed. For the following analysis, we will assume that we have the ability to affordably collect response data from a tool wear trial in order to understand the tool wear progression, and therefore the tool life. This section will present a method for predicting the remaining useful life (RUL) of a tool based on a single feature by using the measurement of flank wear width to define the tools condition.

It has already been discussed that the life of a cutting tool varies due to the stochastic nature of the cutting process, therefore prognosis of the end of a tools life can be difficult to achieve. Uncertainty in tool life can be a result of many process variables, such as material property, depth of cut and coolant behaviour. Given the inherent uncertainty, a tools life is therefore appropriately represented as a probability distribution.

Bayesian inference can allow us to model the uncertainty in a tools life and update this as new information is obtained. Let the prior distribution of an uncertain event, A, be $P(A)$. The likelihood of obtaining an experimental result, B, given that event A has occurred is then $P(B|A)$. The probability of observing the experimental result, B, without knowing whether A has occurred is $P(B)$. Bayes rule can be used to determine the posterior belief about an event A, following experimental results, as shown by equation (20).

$$\mathrm{P}(A|B) = \frac{P(A)P(B|A)}{P(B)} \tag{20}$$

An important consideration when applying Bayes rule is how to form the prior distribution of the tools life before any experimental observation has been made. The initial prediction should be as accurate as possible and may be obtained from a combination of expert opinion and previous experimental results. Where multiple experimental observations are made, the posterior belief following the first observation becomes the prior belief for the second calculation, and so on for all observations.

Additional tool wear tests have been conducted to assess the feasibility of using Bayes rule to predict the RUL of a cutting tool using only spindle power data. The experimental setup is similar to that presented in Chapter 4, however in this case a 4 flute, 10mm diameter end mill was used with a cutting speed of 115m/min, feed rate of 0.06mm/tooth, radial depth of 2.5mm and axial depth of 2mm. Through tool coolant at 50bar pressure was used to ensure that the dominant tool wear mechanism was abrasive and to be consistent with most production processes of this type. The RMS power was sampled over a 6 second period of cutting for each pass. Each pass was approximately 13 seconds in cut. The tool wear was measured on each flute after every six passes. Three tools were worn until the tool wear in each case exceeded 0.3mm flank wear width. The point at which tool wear reaches 0.3mm will be considered to be the end of the tools life. The spindle RMS data has been normalised to be presented as a % of the first cut taken with each tool. This is consistent with many commercial spindle power monitoring systems such as ARTIS CTM [2] and removes some of the signal noise observed from the signal from one tool to another.

Both flank wear width and RMS of spindle power increase over the tools life, as shown in the results for the first tool in Figure 9-1 and Figure 9-2 respectively. The end of the tools life is reached at 22 minutes where the flank wear width exceeds 0.3mm on at least one of the flutes. Spindle power reaches 119% at 22 minutes in cut.

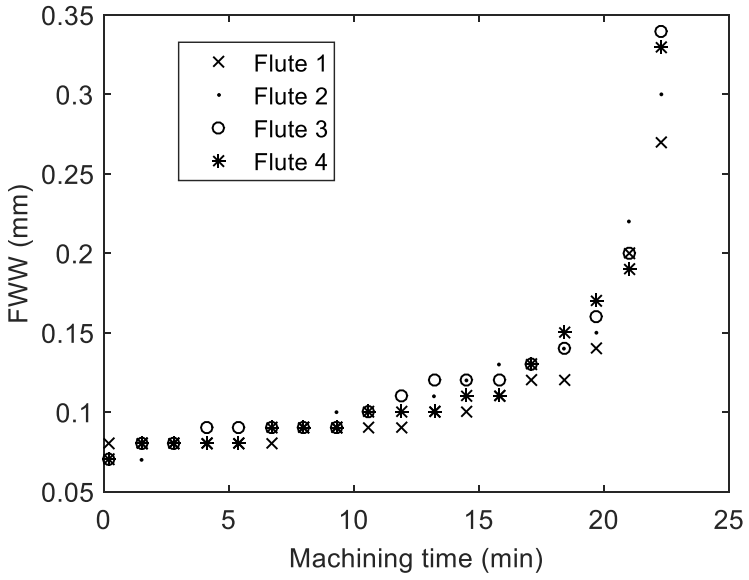

Figure 9-1: Flank wear width measurements for tool 1

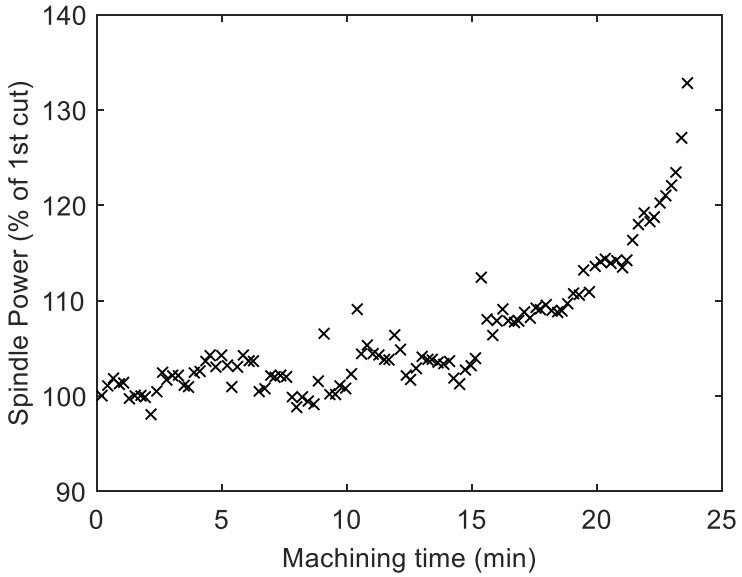

Figure 9-2: RMS spindle power for tool 1

An approximation of the spindle power curve can be made by fitting a 2nd order power curve to the data. The uncertainty in the spindle power growth as a function of time can then be represented by constructing a number of different sample paths, where each has some probability. These sample paths will initially represent the prior, where in the first instance each path has equal probability. After each observation, the probability of each sample path can be updated using Bayes rule. This is shown in equation (21), with the normalising constant $P(B)$ omitted (the product of all curves should be normalised so that the sum is equal to 1).

$$\mathrm{P}(path = true|test\ result) \propto P(path = true) \times P(test\ result|path = true) \qquad (21)$$

Where $P(path = true)$ is the prior probability that a given path is the true spindle power growth curve, $\mathrm{P}(path = true|test\ result)$ is the posterior that the path is the true spindle power curve and $P(test\ result|path = true)$ is referred to as the likelihood.

To test this hypothesis, 1000 sample curves have been constructed by selecting three points and fitting a 2nd order power curve in each case. The three points are selected from random distributions as follows:

- The first point is selected at the start of the tools life (t=0). A normal distribution with a mean of 100% and a standard deviation of 3%, N(100,3), is used to determine the spindle power at time 0, where N denotes a normal distribution.
- The second point will be selected at the end of the initial wear stage. In the first tool, the tool wear begins to increase more rapidly between 10 and 15 minutes. A uniform distribution between these values will be used to define the time at which the initial wear stage ends, denoted by U(10,15). Additionally, the spindle power value at this point will be N(102,3); a normal distribution with mean 102% and standard deviation 3%.
- The final point is selected at the end of the tools life. The tool life is assumed to have a mean of 22 minutes and a standard deviation of 3 minutes, based on the result from the first tool. The distribution is then denoted as N(22,3). Additionally, the spindle power value at the end of the tool life will be assumed to be equally likely to be between 110% and 120%, therefore the uniform distribution, U(110,120), is used to select this point.

The construction of each curve from the three points can be summarised in Figure 9-3.

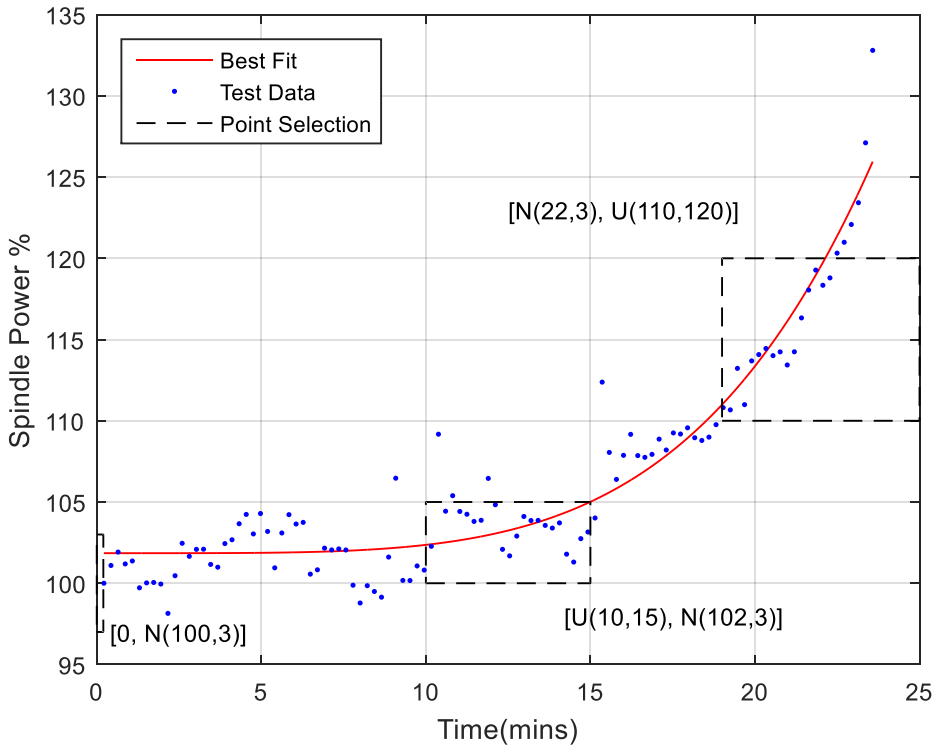

Figure 9-3: Construction of prior from three randomly selected points

The first 100 curves generated are shown in Figure 9-4 and the prior cumulative distribution function (CDF) is shown in Figure 9-5.

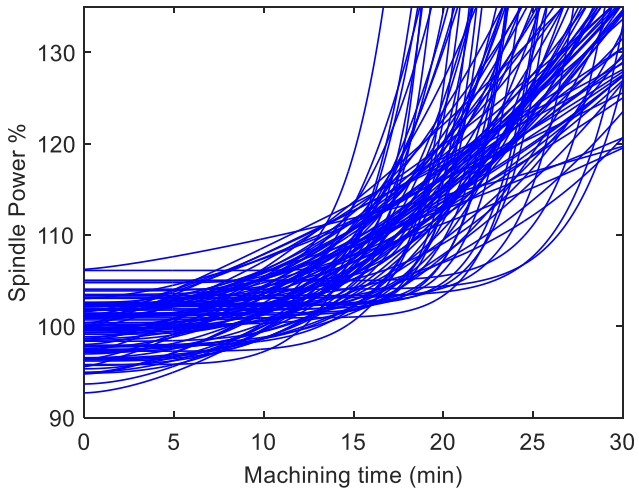

Figure 9-4: 100 randomly generated curves using a 2nd Order power model

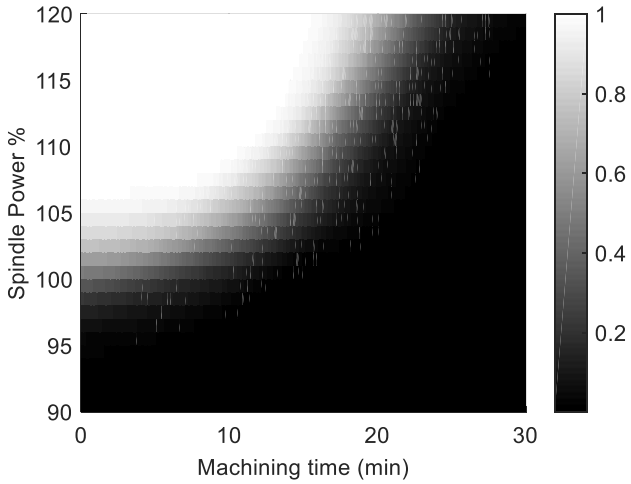

Figure 9-5: Prior CDF of the spindle power. The colour bar denotes the probability that the tool is worn.

After each measurement, the posterior CDF is calculated by applying Equation (21) to each curve. The likelihood used in this study was a Gaussian distribution of the following form:

$$\mathrm{l} = e^{\frac{-(p-pm)^2}{2\sigma^2}} \tag{22}$$

Where l is the likelihood, p is the power at a given time according to the curve in question and pm is the measured power at that time. A standard deviation of $\sigma = 3\%$ has been used

for this study. A more conservative estimate of tool life can be achieved by increasing this value.

The RUL of the tool can be calculated using the CDF once you have selected (i) the true spindle power % at the end of the tool life, Pt, and (ii) the probability of failure, Pf. Figure 9-6 shows the prior probability that the tool is worn for Pt = 110% and Pt = 120%. The RUL is calculated as 16.8 minutes for Pf=0.05, and Pt=120%. It has been assumed, however, that at the point of tool failure it is equally likely for Pf to be between 110% and 120%. The RUL is therefore calculated as an average between these values. The prior estimate of the RUL is then calculated to be 15.2 minutes.

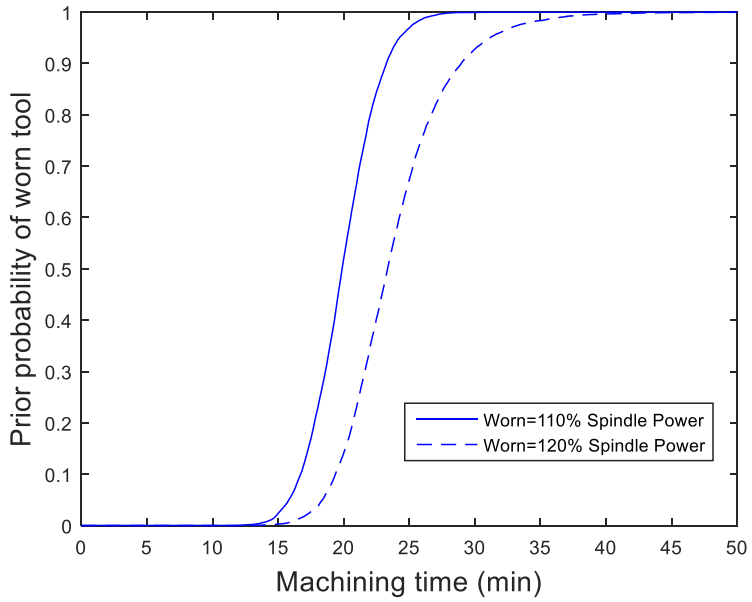

Figure 9-6: Probability of worn tool for 110% and 120% spindle power

Figure 9-7 shows the result of calculating the RUL after each observation for Tool1. The predicted life is underestimated and becomes more accurate towards the end of the tools life.

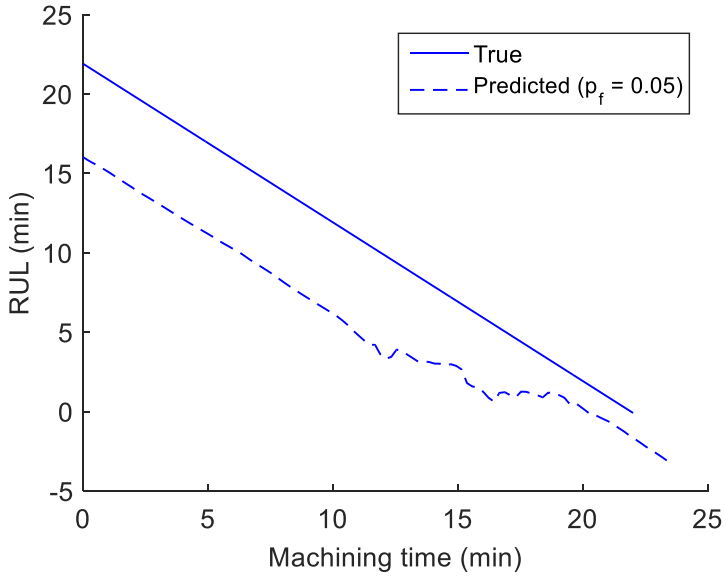

Figure 9-7: Remaining useful life with Pf=0.05

Two further tests have been conducted to test the method with new data. Tool 2 resulted in 17.7 minutes in cut before at least one flute showed above 0.3mm of flank wear. The spindle power is shown in Figure 9-8 and at 17.7 minutes it was only 108%, far lower than the 119% observed for tool 1. Recall that it has been assumed that the end of tool life is equally likely to be reached between 110% and 120% spindle power. This may explain why Figure 9-9 presents a RUL curve that is less conservative in its estimation of tool life when compare to tool 1, though it is underestimating the life for most of the observations.

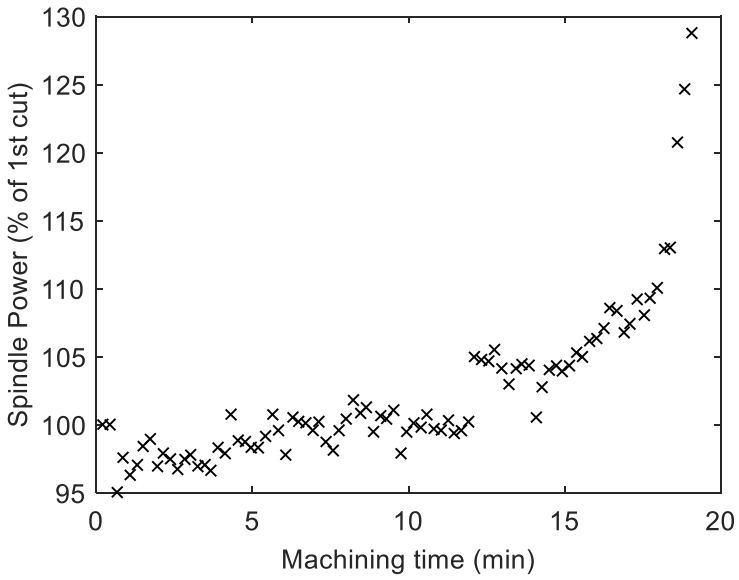

Figure 9-8: Spindle power measurements for tool 2

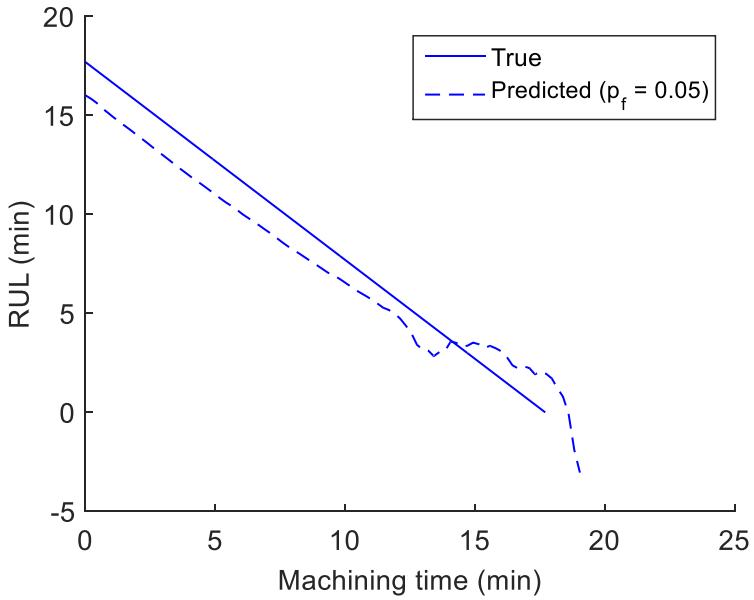

Figure 9-9: RUL estimates for tool 2

The spindle power and RUL data for tool 3 is presented in Figure 9-10 and Figure 9-11 respectively. The RUL is again underestimating when using a conservative value for Pf of 0.05. An high magnitude outlier is seen in this data of around 125% spindle power and 10 minutes machining time. This data point is believed to be an anomaly due to an error in the testing depth of cut. The outcome of this single outlier has a minor impact on the RUL estimate, demonstrating the methods resilience to outliers in the data set.

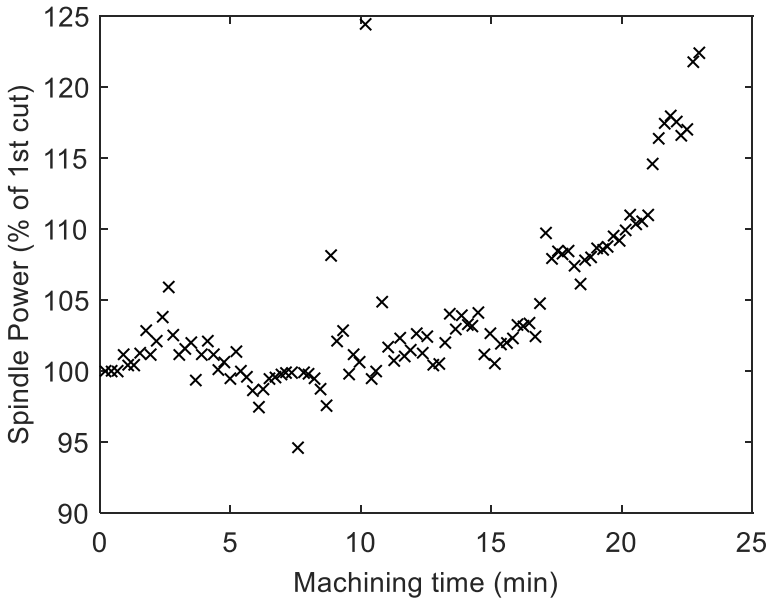

Figure 9-10: Spindle power measurements for tool 3

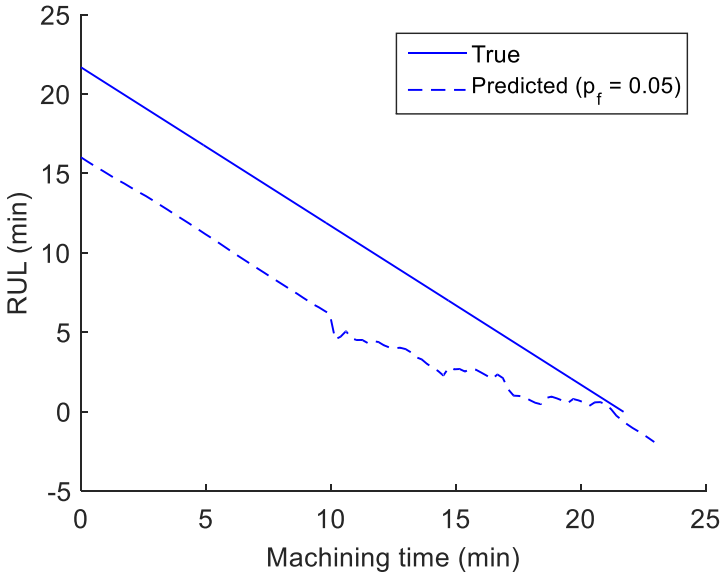

Figure 9-11: RUL estimates for tool 3

The approach presented in this chapter has allowed a prior estimate of tool life and spindle power failure threshold to be defined from either experiential knowledge or a training experiment. The prediction accuracy of the RUL has shown to improve with time in cut by using the Bayesian updating of the degradation model. A limitation of this method is that the failure threshold for the spindle power is defined by experiential knowledge and is not updated according to the process, however the system could be developed further to incorporate an adaptive threshold from observed tool life.

Appendix D Matlab and LabView Code Extracts

Polynomial Model Fitting, Merit Function and Sequential Feature Subset Selection

```
clearvars -except e_num ii
%% Load the complete list of extracted features, as generated by
LabView prior to subset selection, for each of the 8 sensors:
file_list{1}='C:\Users\me1tem\Desktop\PhD\Signal Analysis and
LabView Dec 2014\data\Matlab\MAT Files\604B31-X Accel v2.mat';
Sensor{1}='XA ';
file_list{2}='C:\Users\me1tem\Desktop\PhD\Signal Analysis and
LabView Dec 2014\data\Matlab\MAT Files\604B31-Y Accel v2.mat';
Sensor{2}='YA ';
file_list{3}='C:\Users\me1tem\Desktop\PhD\Signal Analysis and
LabView Dec 2014\data\Matlab\MAT Files\604B31-Z Accel v2.mat';
Sensor{3}='ZA ';
file_list{4}='C:\Users\me1tem\Desktop\PhD\Signal Analysis and
LabView Dec 2014\data\Matlab\MAT Files\352A60-Z Accel v2.mat';
Sensor{4}='HF ';
file_list{5}='C:\Users\me1tem\Desktop\PhD\Signal Analysis and
LabView Dec 2014\data\Matlab\MAT Files\378C01 Mic v2.mat';
Sensor{5}='M1 ';
file_list{6}='C:\Users\me1tem\Desktop\PhD\Signal Analysis and
LabView Dec 2014\data\Matlab\MAT Files\HT378B02 Mic v2.mat';
Sensor{6}='M2 ';
file_list{7}='C:\Users\me1tem\Desktop\PhD\Signal Analysis and
LabView Dec 2014\data\Matlab\MAT Files\Spindle Power v2.mat';
Sensor{7}='SP ';
file_list{8}='C:\Users\me1tem\Desktop\PhD\Signal Analysis and
LabView Dec 2014\data\Matlab\MAT Files\AE Sensor v2.mat';
Sensor{8}='AE ';
FEAT={};
NAMES={};
%% Sort the complete feature list into two arrays - feature array
FEAT and names array NAMES.
for k=1:8
    load(file_list{k})
    TDCrest=TDPeak./TDRMS;    % Add crest factor to feature list
    TD_feats={TDMean; TDRMS; TDVar; TDKurt; TDSkew; TDRange;
TDCrest; TDPeak}; % Setup feature cell arrays (file by whole cut)
    TD_feats_str={'TDMean'; 'TDRMS'; 'TDVar'; 'TDKurt'; 'TDSkew';
'TDRange'; 'TDCrest'; 'TDPeak'};
    for i=1:size(TD_feats) % replace NaN to 0 for all TD features
        feature=TD_feats{i};
        feature(feature==0)=NaN;
        TD_feats{i}=feature;
    end
    FD_feats={FDMean; FDVar; FDKurt; FDSkew; Sum5TPFs};% FDPeakFreq
removed
    FD_feats_str={'FDMean'; 'FDVar'; 'FDKurt'; 'FDSkew';
'Sum5TPFs'};% FDPeakFreq removed
    for i=1:size(FD_feats)  % replace NaN to 0 for all FD features
        feature=FD_feats{i};
        feature(feature==0)=NaN;
        FD_feats{i}=feature;
    end
    FD_feats_filt={FDMean_filt; FDVar_filt; FDKurt_filt;
FDSkew_filt};% FDPeakFreq_filt removed
```

```
    FD_feats_filt_str={'FDMean filt'; 'FDVar filt'; 'FDKurt filt';
'FDSkew filt'};% FDPeakFreq_filt removed
    for i=1:size(FD_feats_filt)  % replace NaN to 0 for all FD filt
features
        feature=FD_feats_filt{i};
        feature(feature==0)=NaN;
        FD_feats_filt{i}=feature;
    end
    FD_feats_band={FDMean_band_filt; FDVar_band_filt;
FDKurt_band_filt; FDSkew_band_filt};% FDPeakFreq_band_filt removed
    FD_feats_band_str={'FDMean band'; 'FDVar band'; 'FDKurt band';
'FDSkew band' };% FDPeakFreq_band_filt removed
    for i=1:size(FD_feats_band) % replace NaN to 0 for all FD band
features
        feature=FD_feats_band{i};
        feature(feature==0)=NaN;
        FD_feats_band{i}=feature;
    end
    features=[TD_feats; FD_feats; FD_feats_filt; FD_feats_band];
    features_str=[TD_feats_str; FD_feats_str; FD_feats_filt_str;
FD_feats_band_str];
    for j=1:21
        features_str{j}=strcat(Sensor{k},features_str{j});
    end
    FEAT{k}=features;
    NAMES{k}=features_str;
    clearvars -except features features_str k FEAT NAMES file_list
Sensor ii e_num
end
%% Convert the feature data cell array to the double array/matrix, X
names=NAMES';
xx=[FEAT{1}; FEAT{2}; FEAT{3}; FEAT{4}; FEAT{5}; FEAT{6};  FEAT{7};
FEAT{8}];
NAMES=[NAMES{1}; NAMES{2}; NAMES{3}; NAMES{4}; NAMES{5}; NAMES{6};
NAMES{7}; NAMES{8}];
n=numel(xx);
for i=1:n
x=xx{i};
x=x(1:400)';
xx{i}=x;
end
X=cell2mat(xx);
X=X';
clear x xx i k n features features_str file_list nn N Sensor xx FEAT
%% Delete omitted features
n=[164, 163, 162, 161, 160, 143, 142, 141, 140, 139];
N=numel(n);
for i=1:N
nn=n(i);
X(:,nn)=[];
NAMES(nn)=[];
end
clear nn n i N names
%% Delete Vibration, Mic and AE Means
n=[1 22 43 64 85 106 143];
n=fliplr(n);
N=numel(n);
for i=1:N
```

```
    nn=n(i);
    X(:,nn)=[];
    NAMES(nn)=[];
end
clear i n N nn
num_feat=size(NAMES);num_feat=num_feat(1,1);
t=linspace(1,400,400)';
%% Delete missing data points: 250, 302-308, 344, 394-398
n=[250, 302, 303, 304, 305, 306, 307, 308, 344, 394, 395, 396, 397,
398];
N=numel(n);
for i=1:N
nn=n(i)-i+1;
X(nn,:)=[];
t(nn)=[];
end
clear nn n i N
%% Convert X so that each feature has zero mean and unit variance
for i=1:num_feat
mu=mean(X(:,i));
stdev=std(X(:,i));
X(:,i)=X(:,i)-mu;
X(:,i)=X(:,i)/stdev;
end
clear mu stdev i
%% create a random set of training cuts of length nnn
%rng(0,'twister');
nnn=100;
r = randi([1 386],1,nnn);
u=unique(r);
nn=nnn-numel(u);
while nn>0
    r = [u randi([1 386],1,nn)];
    u=unique(r);
    nn=nnn-numel(u);
end
clear nn nnn r i N
%% split X into a training and a testing data set for the polynomial
model fitting that follows
Pointer=zeros(1,386);
Pointer=dec2bin(Pointer);
Pointer=Pointer=='1';
Pointer=Pointer';
for i=1:386
    TRU=u(u==i);
    if numel(TRU)==1
        Pointer(i)=1;
    end
end
X_test=X(Pointer,:);
t_test=t(Pointer);
X_train=X(~Pointer,:);
t_train=t(~Pointer);
clear i TRU
%% generate polynomial models from the training data and measure the
R-sqaured with the test data
for i=1:num_feat
% Prepare data
```

```
    TEST=X_test(:,i);
    TRAIN=X_train(:,i);
    name=NAMES(i);
    [xData, yData] = prepareCurveData( t_train, TRAIN );
    [xData2, yData2] = prepareCurveData( t_test, TEST );
% Set up fittype and options.
    ft1 = fittype( 'poly1' );
    ft2 = fittype( 'poly2' );
    ft3 = fittype( 'poly3' );
    ft4 = fittype( 'poly4' );
    ft5 = fittype( 'poly5' );
    opts.Lower = [-Inf -Inf -Inf];
    opts.Robust = 'LAR';
    opts.Upper = [Inf Inf Inf];
% Poly1
    opts = fitoptions( ft1 );
    [fitresult1, gof1] = fit( xData, yData, ft1, opts );
    COEF=coeffvalues(fitresult1);
    for j=1:numel(TEST)
    TEST_mod(j)=COEF(1)*t_test(j)+COEF(2);
    end
    poly1_er=TEST-TEST_mod';
    poly_error(i,1)=rms(poly1_er);
% Poly2
    opts = fitoptions( ft2 );
    [fitresult2, gof2] = fit( xData, yData, ft2, opts );
    COEF=coeffvalues(fitresult2);
    for j=1:numel(TEST)
    TEST_mod(j)=COEF(1)*t_test(j)^2+COEF(2)*t_test(j)+COEF(3);
    end
    poly2_er=TEST-TEST_mod';
    poly_error(i,2)=rms(poly2_er);
% Poly3
    opts = fitoptions( ft3 );
    [fitresult3, gof3] = fit( xData, yData, ft3, opts );
    COEF=coeffvalues(fitresult3);
    for j=1:numel(TEST)

TEST_mod(j)=COEF(1)*t_test(j)^3+COEF(2)*t_test(j)^2+COEF(3)*t_test(j
)+COEF(4);
    end
    poly3_er=TEST-TEST_mod';
    poly_error(i,3)=rms(poly3_er);
% Poly4
    opts = fitoptions( ft4 );
    [fitresult4, gof4] = fit( xData, yData, ft4, opts );
    COEF=coeffvalues(fitresult4);
    for j=1:numel(TEST)

TEST_mod(j)=COEF(1)*t_test(j)^4+COEF(2)*t_test(j)^3+COEF(3)*t_test(j
)^2+COEF(4)*t_test(j)+COEF(5);
    end
    poly4_er=TEST-TEST_mod';
    poly_error(i,4)=rms(poly4_er);
% Poly5
    opts = fitoptions( ft5 );
    [fitresult5, gof5] = fit( xData, yData, ft5, opts );
    COEF=coeffvalues(fitresult5);
```

```
    for j=1:numel(TEST)

TEST_mod(j)=COEF(1)*t_test(j)^5+COEF(2)*t_test(j)^4+COEF(3)*t_test(j
)^3+COEF(4)*t_test(j)^2+COEF(5)*t_test(j)+COEF(6);
    end
    poly5_er=TEST-TEST_mod';
    poly_error(i,5)=rms(poly5_er);
%build R2 array for each of the first 5 polynomial orders
    R2(i,1)=gof1.rsquare;
    R2(i,2)=gof2.rsquare;
    R2(i,3)=gof3.rsquare;
    R2(i,4)=gof4.rsquare;
    R2(i,5)=gof5.rsquare;
[min_size min_element]=min(poly_error(i,:));
elements(i)=min_element;
R2_opt(i)=R2(i,min_element); %this is the optimum R squared value
selected from the first 5 order polynomials
end
%%

%% subset scoring
subS=zeros(1,148);
subS(1)=1;
subS_temp=subS;
load('feature_polyfit_data.mat')
subSrfc=fifthOrd;%secondOrd; %using the 2nd order polynomial model
data in this case

    %get first merit with only 1 feature
    k=1;
    subS_temp=dec2bin(subS_temp);
    subS_temp=subS_temp=='1';
    subS_temp=subS_temp';
    X_temp=X;
    FeatsubS=X_temp(:,subS_temp);
    subSrfc_temp=subSrfc(subS_temp,:);
    % Calculate Mean Feature-Feature Correlation
    FeatCorr=zeros(k,k);
    for i=1:k
        featA=X(:,i);
        for j=1:k
        featB=X(:,j);
        FeatCorr(i,j)=corr(featA,featB);
        end
    end
    % Calculate Merit.s (merit.s=(k*rfc)/sqrt((k+(k*(k-1)*rff))
    %k=number of features in subset
    %rfc=mean feature-class correlation
    %rff=mean feature-feature correlation
    rfc=mean(subSrfc_temp);
    rff=mean2(FeatCorr);
    merit(1)=(k*rfc)/(k+(k*(k-1)*rff)^0.5);

k=148;
for ii=2:148
    subS_temp(ii)=1;
    subS_temp=dec2bin(subS_temp);
    subS_temp=subS_temp=='1';
```

```
        subS_temp=subS_temp';
        X_temp=X;
        FeatsubS=X_temp(:,subS_temp);
        subSrfc_temp=subSrfc(subS_temp,:);
        % Calculate Mean Feature-Feature Correlation
        FeatCorr=zeros(k,k);
        for i=1:k
            featA=X(:,i);
            for j=1:k
                featB=X(:,j);
                FeatCorr(i,j)=corr(featA,featB);
            end
        end
        % Calculate Merit.s (merit.s=(k*rfc)/sqrt((k+(k*(k-1)*rff))
        %k=number of features in subset
        %rfc=mean feature-class correlation
        %rff=mean feature-feature correlation
        rfc=mean(subSrfc_temp);
        rff=mean2(FeatCorr);
        merit(ii)=(k*rfc)/(k+(k*(k-1)*rff)^0.5);
    end
```

Silhouette and Gram-Schmidt

```
%% Gram Schmidt and Silhouette Feature Selection
clear all
%close all
% Load the feature data file containting:
% 'C:\Users\me1tem\Desktop\PhD\Matlab
2015\GramSchmidt\Feat_Data_GS.mat'
% m = the number of data points in a feature, N = the number of
features
% Containing C = 1 by N double of class data, F = m by N matrix of
feature data
% Names = N by 1 cell array of strings for the names of each of the
features
load('C:\Users\me1tem\Desktop\PhD\Matlab
2015\GramSchmidt\Feat_Data_GS.mat')
C=C4;%selected which class data set
%% initialise a feature subset pointer, subS
subS=zeros(1,N);
subS=dec2bin(subS);
subS=subS=='1';
subS=subS';

index=0;
h = waitbar(0,'Initializing waitbar...');
for k=1:N % Loops every time a new feature is SELECTED
    for ii=1:N % Loops every time a new feature is TESTED with the
currently SELECTED feature set

        TRU=any(index==ii);
        if TRU==1;% Do not repeat on a feature already selected
            Sil(k,ii)=-1;

        else
            subS_temp=subS;% Copy the current set of selected
features
            subS_temp(ii)=1;% Add a pointer to feature ii
            K=sum(subS_temp(:));% K is the number of features in
current subset
            A=[];
            for iii=1:K-1%sort AA to inculde all selected features
in order they have been selected
                A=[A,F(:,index(iii))];
            end
            A=[A,F(:,ii)];
            % Calculate the GRAM-SCHMIDT
            for j=1:K%K is the number of features in the current
subset
                v=A(:,j);
                for i=1:j-1
                    R(i,j)=Q(:,i)'*A(:,j);
                    v=v-R(i,j)*Q(:,i);
                end
                R(j,j)=norm(v);   %R is the square matrix that
satisfies A=QR
                Q(:,j)=v/R(j,j);  %Q is the new data set (F'*)
            end
```

```
            % Calculate Silhouette for Q
            S = silhouette(Q,C);
            Sil(k,ii)=mean(S);% Add the mean Silhouette to the
record matrix
        end
        clear v A R Q S i j TRU
        messge=strcat('%d%% k = ',num2str(k), ' of 158');
        perc=round(100*(ii/148));
        waitbar(perc/100,h,sprintf(messge,perc))
    end

    Sil_temp=Sil;
    Sil_temp(:,subS)=-1;
    [max_value(k), index(k)] = max(Sil_temp(k,:));
    Selected{k}=Names{index(k)};
    subS(index(k))=1;

    Last_max=max_value(k);
    FeatsubS=F(:,subS);
    S = silhouette(FeatsubS,C);
    S_C(k,1)=sum(S(1:100))/386;
    S_C(k,2)=sum(S(101:200))/386;
    S_C(k,3)=sum(S(201:266))/386;
    S_C(k,4)=sum(S(267:end))/386;
end
close(h)
```

Gaussian Mixture Models for Classification

```
%% INITIALISE
% close all
clear all
load('C:\Users\me1tem\Desktop\PhD\Matlab 2015\Feature
Selection\Features158_data.mat')
% load('C:\Users\me1tem\Desktop\PhD\Matlab 2015\DoC testing
data\ALL_DoC_Data.mat')
% load('C:\Users\me1tem\Desktop\PhD\Matlab 2015\Feature
Selection\feature_polyfit_data.mat')
% load('C:\Users\me1tem\Desktop\PhD\Matlab 2015\Feature
Selection\feature_corr_data.mat')
%% DELETE VIBRATION, MIC AND AE TD MEAN
num_feat2=[1 22 43 64 85 106 143];
num_feat2=fliplr(num_feat2);
N=numel(num_feat2);
for i=1:N
    nn=num_feat2(i);
    X(:,nn)=[];
    NAMES(nn)=[];
end
clear i n N nn
num_feat=numel(NAMES);
%% DEFINE CLASS
CLASS1=ones(1,100);%100
% CLASS2=ones(1,99);%+1;%199
% CLASS3=ones(1,67);%+2;%266
% CLASS4=ones(1,44)+1;%+3;%300
% CLASS5=ones(1,76)+1;%+4;%386
% CLASS=[ones(1,267) ones(1,133)+1];% use this for 2 class problem
(1-267, 268-end)
CLASS=[CLASS1 CLASS1+1 CLASS1+2 CLASS1+3];%Use this for 4 class
problem
clear CLASS1
%% DELETE NaN ROWS FROM X AND CLASS(250, 302-308, 344, 394-398)
num_feat2=[250, 302, 303, 304, 305, 306, 307, 308, 344, 394, 395,
396, 397, 398];
num_feat2=fliplr(num_feat2);
N=numel(num_feat2);
for i=1:N
nn=num_feat2(i);
X(nn,:)=[];
CLASS(nn)=[];
end
clear i nn N n

%% ZERO MEAN AND UNIT VARIANCE FOR X
for i=1:num_feat
mu=mean(X(:,i));
stdev=std(X(:,i));
X(:,i)=X(:,i)-mu;
X(:,i)=X(:,i)/stdev;
end
clear mu stdev i
%% SELECT FEATURE SUBSET
```

```
subs_all{1}=[41 31 121 30 57 3 42 21 12 32 72 10 45 63 22 71 61
83];% 1st order Poly MERIT
subs_all{2}=[14 25 3 13 32];% 3rd order Poly MERIT
subs_all{3}=[61 43 71 139 16 62 134 70 136 24 74 94 76];% 30]
removed because of gm computation error;% 5th order Poly MERIT
subs_all{4}=[5 6 7 45 46 47 65 66 67];% Transient Feature Set
subs_all{5}=[89 109 112 92 108 102 52 88 72 82];% 2-Class Cluster
Seperation
subs_all{6}=[41 42 57 30 37 77 144 31 61 148];% 4-Class Cluster
Seperation
subs_all{7}=[41 30 77 144 61];% 4-Class Cluster Seperation -
Duplicates Removed
subs_all{8}=[41 30];% test

%---SELECT HERE---
subs=subs_all{6};
%-----------------
num_feat2=numel(subs);
for i=1:num_feat2
    n=subs(i);
    X_2(:,i)=X(:,n);
end
clear i n subs_all
%% CLASSIFICATION
CLASS_DATA=[CLASS' X_2];
%% SELF CLUSTERING using GMM
figure
for num_c=2:8 %number of clusters
    rng('default');  % For reproducibility %rng(1)%;
    options = statset('MaxIter',1000);
    try

gm=fitgmdist(X_2,num_c,'Options',options,'RegularizationValue',0.001
);
    catch exception
    disp('There was an error fitting the Gaussian mixture model')
    error = exception.message
    end

%   P= posterior(gm,X_2);
    idx = cluster(gm,X_2);
    idx_reserve=idx;

    % score clustering method using silhoette and my own method
    s(:,num_c-1)=silhouette(X_2,idx);
    s_mean(num_c-1)=mean(s(:,num_c-1));

        idx_score=0;
    for i=2:numel(idx)
        if idx(i)==idx(i-1)
        else
            idx_score=idx_score+1;
        end
    end
    idx_s(num_c-1)=idx_score-(num_c-1);

    if num_c==2
```

```
    idx(idx==1)=[10];
    idx(idx==2)=[80];
elseif num_c==3
    idx(idx==1)=[80];
    idx(idx==2)=[60];
    idx(idx==3)=[10];
elseif num_c==4
    idx(idx==1)=[60];
    idx(idx==2)=[80];
    idx(idx==3)=[70];
    idx(idx==4)=[10];
elseif num_c==5
    idx(idx==1)=[10];
    idx(idx==2)=[50];
    idx(idx==3)=[60];
    idx(idx==4)=[70];
    idx(idx==5)=[80];
elseif num_c==6
    idx(idx==1)=[70];
    idx(idx==2)=[10];
    idx(idx==3)=[30];
    idx(idx==4)=[50];
    idx(idx==5)=[60];
    idx(idx==6)=[80];
elseif num_c==7
    idx(idx==1)=[50];
    idx(idx==2)=[80];
    idx(idx==3)=[20];
    idx(idx==4)=[70];
    idx(idx==5)=[30];
    idx(idx==6)=[10];
    idx(idx==7)=[60];
elseif num_c==8
    idx(idx==1)=[80];
    idx(idx==2)=[10];
    idx(idx==3)=[60];
    idx(idx==4)=[70];
    idx(idx==5)=[50];
    idx(idx==6)=[20];
    idx(idx==7)=[30];
    idx(idx==8)=[40];
else
    'error line 147';
    return
end

c1 = (idx == 1);
c2 = (idx == 2);
c3 = (idx == 3);
c4 = (idx == 4);
c5 = (idx == 5);
c6 = (idx == 6);
c7 = (idx == 7);
c8 = (idx == 8);
% Clusters vs Time plot
idx2=[idx idx]';
% figurefig
subplot(7,1,(num_c-1))
```

```
    contourf(idx2)
end



%%
col1=[0 1 0];%green
col2=[1 1 0];%yellow
col3=[1 0.6 0.2];%orange
col4=[0 1 1];%cyan
col5=[1 0 1];%magenta
col6=[1 0 0];%red
col7=[0 0.4 1];%blue
col8=[0.4 0 0.75];%purple
colm=[col1;col2;col3;col4;col5;col6;col7;col8];
% colm=colm(1:num_c,:);
colormap(colm)


%% plot axis edits
for i=1:7
subplot(7,1,i)
set(gca,'ytick',[]);
ylabel('1 Cluster','rot',0);
ylabh = get(gca,'YLabel');
label_y=[num2str(i+1),' Clust.'];
ylabel(label_y,'rot',0,'Position',get(ylabh,'Position') - [20 .5
0]);
end
xlabel('Number of Cuts');
for i=1:6
subplot(7,1,i)
set(gca,'xtick',[])
end

%% Plot PCA 2D
[wcoeff,score,latent,tsquared,explained] =pca(X_2);
C=idx;%_reserve;
x=score(:,1);
y=score(:,2);

c1=10;
c2=20;
c3=30;
c4=40;
c5=50;
c6=60;
c7=70;
c8=80;

figure()
scatter(x(C==c1),y(C==c1),'o','MarkerEdgeColor','k','MarkerFaceColor
',colm(1,:));
hold on
scatter(x(C==c2),y(C==c2),'o','MarkerEdgeColor','k','MarkerFaceColor
',colm(2,:));
```

```
scatter(x(C==c3),y(C==c3),'o','MarkerEdgeColor','k','MarkerFaceColor
',colm(3,:));
scatter(x(C==c4),y(C==c4),'o','MarkerEdgeColor','k','MarkerFaceColor
',colm(4,:));
scatter(x(C==c5),y(C==c5),'o','MarkerEdgeColor','k','MarkerFaceColor
',colm(5,:));
scatter(x(C==c6),y(C==c6),'o','MarkerEdgeColor','k','MarkerFaceColor
',colm(6,:));
scatter(x(C==c7),y(C==c7),'o','MarkerEdgeColor','k','MarkerFaceColor
',colm(7,:));
scatter(x(C==c8),y(C==c8),'o','MarkerEdgeColor','k','MarkerFaceColor
',colm(8,:));
xlabel('1st Principal Component')
ylabel('2nd Principal Component')

%% not using pca for plot
x=X_2(:,1);
y=X_2(:,2);
figure()
scatter(x(C==c1),y(C==c1),'o','MarkerEdgeColor','k','MarkerFaceColor
',colm(1,:));
hold on
scatter(x(C==c2),y(C==c2),'o','MarkerEdgeColor','k','MarkerFaceColor
',colm(2,:));
scatter(x(C==c3),y(C==c3),'o','MarkerEdgeColor','k','MarkerFaceColor
',colm(3,:));
scatter(x(C==c4),y(C==c4),'o','MarkerEdgeColor','k','MarkerFaceColor
',colm(4,:));
scatter(x(C==c5),y(C==c5),'o','MarkerEdgeColor','k','MarkerFaceColor
',colm(5,:));
scatter(x(C==c6),y(C==c6),'o','MarkerEdgeColor','k','MarkerFaceColor
',colm(6,:));
scatter(x(C==c7),y(C==c7),'o','MarkerEdgeColor','k','MarkerFaceColor
',colm(7,:));
scatter(x(C==c8),y(C==c8),'o','MarkerEdgeColor','k','MarkerFaceColor
',colm(8,:));
xlabel('1st Principal Component')
ylabel('2nd Principal Component')


%% Plot PCA 2D
[wcoeff,score,latent,tsquared,explained] =pca(X_2);
C=idx;%_reserve;
x=score(:,1);
y=score(:,2);
z=score(:,3);

c1=10;
c2=20;
c3=30;
c4=40;
c5=50;
c6=60;
c7=70;
c8=80;

figure()
```

```
scatter3(x(C==c1),y(C==c1),z(C==c1),'o','MarkerEdgeColor','k','Marke
rFaceColor',colm(1,:));
hold on
scatter3(x(C==c2),y(C==c2),z(C==c2),'o','MarkerEdgeColor','k','Marke
rFaceColor',colm(2,:));
scatter3(x(C==c3),y(C==c3),z(C==c3),'o','MarkerEdgeColor','k','Marke
rFaceColor',colm(3,:));
scatter3(x(C==c4),y(C==c4),z(C==c4),'o','MarkerEdgeColor','k','Marke
rFaceColor',colm(4,:));
scatter3(x(C==c5),y(C==c5),z(C==c5),'o','MarkerEdgeColor','k','Marke
rFaceColor',colm(5,:));
scatter3(x(C==c6),y(C==c6),z(C==c6),'o','MarkerEdgeColor','k','Marke
rFaceColor',colm(6,:));
scatter3(x(C==c7),y(C==c7),z(C==c7),'o','MarkerEdgeColor','k','Marke
rFaceColor',colm(7,:));
scatter3(x(C==c8),y(C==c8),z(C==c8),'o','MarkerEdgeColor','k','Marke
rFaceColor',colm(8,:));
xlabel('1st Principal Component')
ylabel('2nd Principal Component')
zlabel('3rd Principal Component')
```

LabView Segmentation and Feature Extraction Code

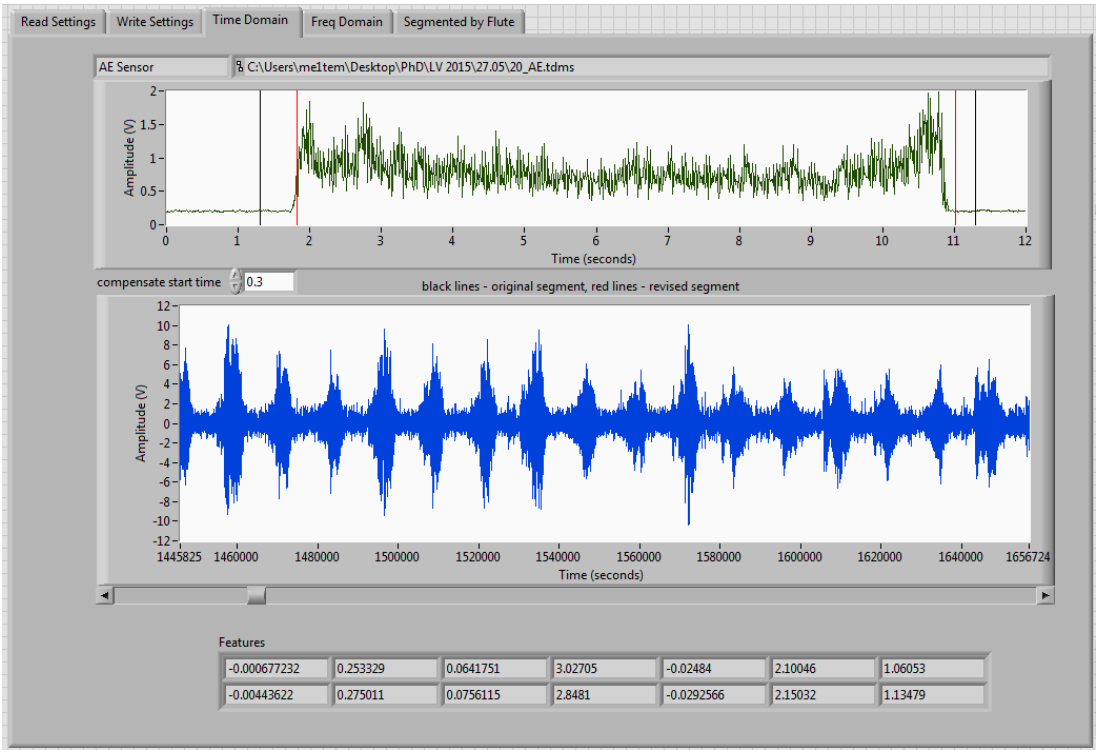

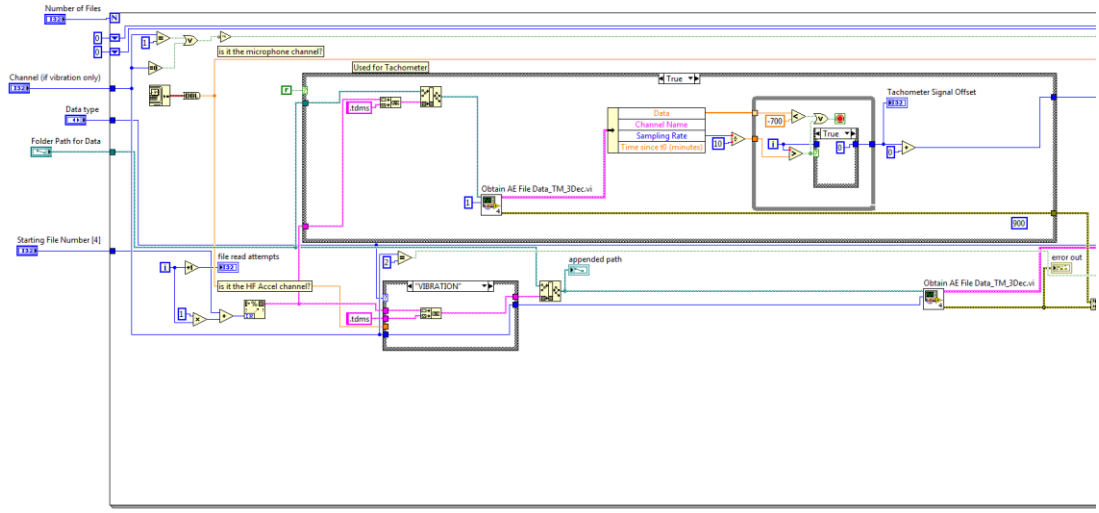

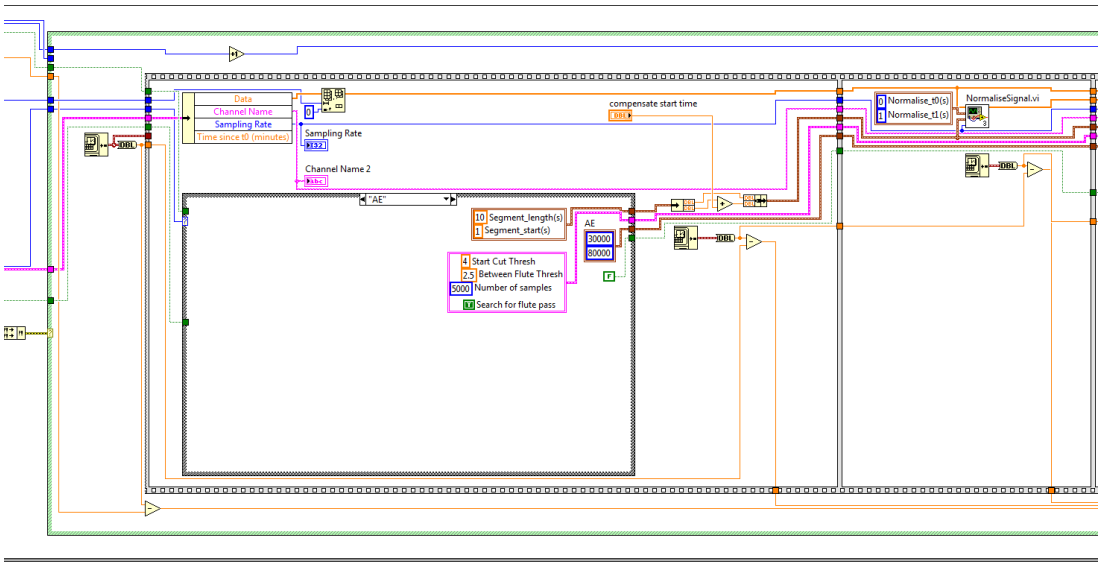
Data
Channel Name
Sampling Rate
Time since t0 (minutes)
Sampling Rate
Channel Name 2
"AE"
compensate start time
Segment_length(s)
Segment_start(s)
AE
30000
80000
Start Cut Thresh
Between Flute Thresh
5000
Number of samples
Search for flute pass
Normalise_t0(s)
Normalise_t1(s)
NormaliseSignal.vi

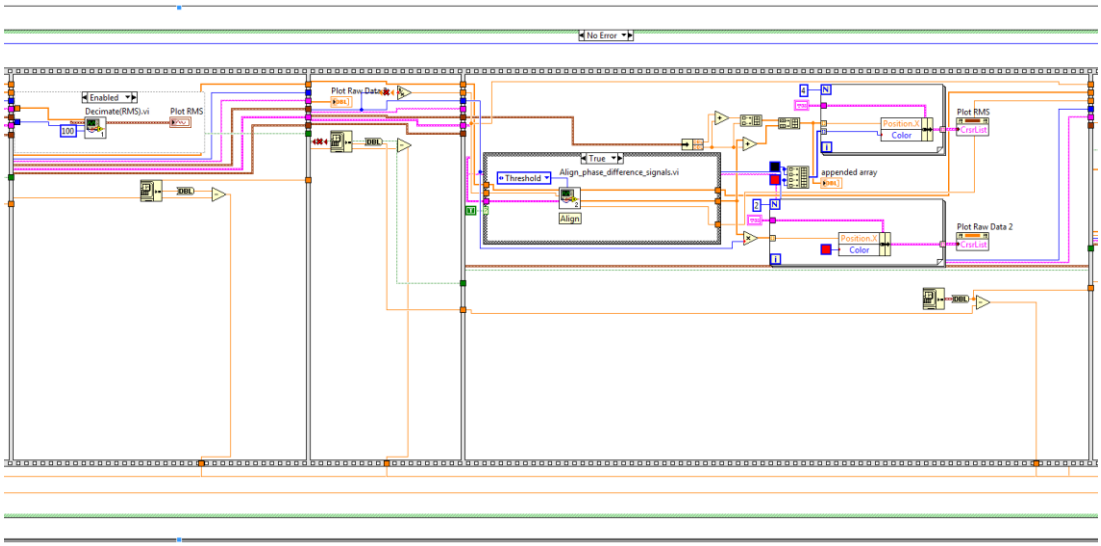
No Error
Enabled
Decimate(RMS).vi
Plot RMS
Plot Raw Data
True
Threshold
Align_phase_difference_signals.vi
Align
appended array
Position.X
Color
Plot RMS
Plot Raw Data 2

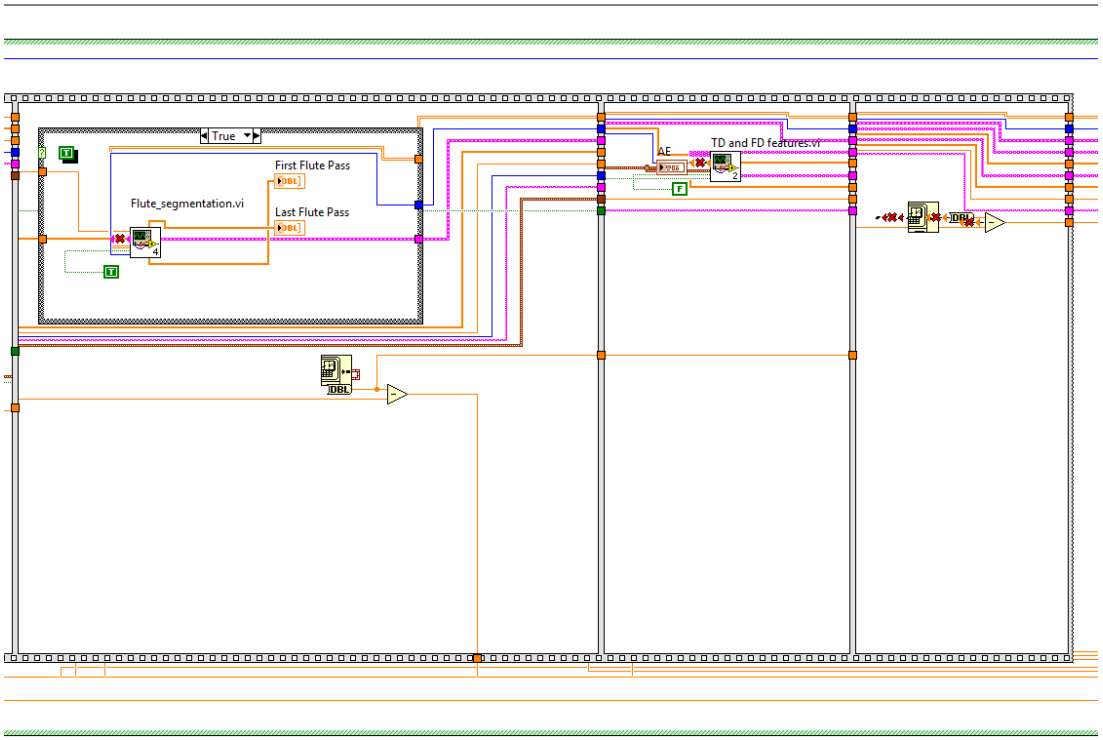
True
First Flute Pass
Flute_segmentation.vi
Last Flute Pass
AE
TD and FD features.vi
DBL

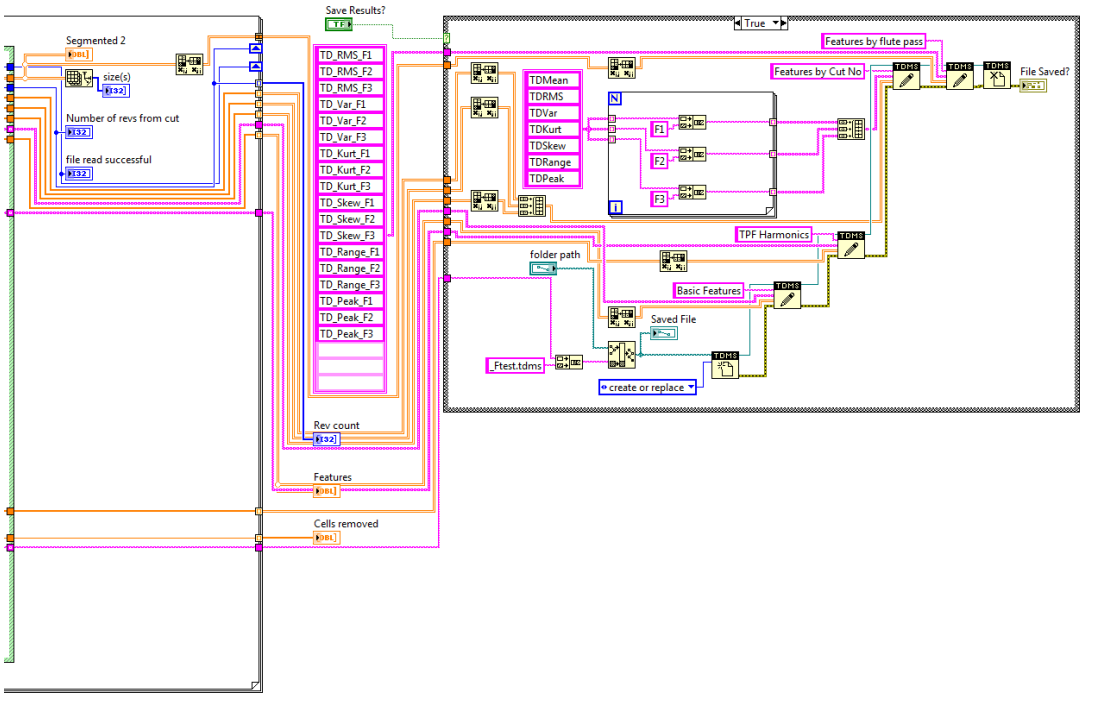
Save Results?
Segmented 2
size(s)
Number of revs from cut
file read successful
TD_RMS_F1
TD_RMS_F2
TD_RMS_F3
TD_Var_F1
TD_Var_F2
TD_Var_F3
TD_Kurt_F1
TD_Kurt_F2
TD_Kurt_F3
TD_Skew_F1
TD_Skew_F2
TD_Skew_F3
TD_Range_F1
TD_Range_F2
TD_Range_F3
TD_Peak_F1
TD_Peak_F2
TD_Peak_F3
Rev count
Features
Cells removed
True
Features by flute pass
Features by Cut No
File Saved?
TDMean
TDRMS
TDVar
TDKurt
TDSkew
TDRange
TDPeak
F1
F2
F3
TPF Harmonics
folder path
Basic Features
Saved File
Ftest.tdms
create or replace
TDMS